

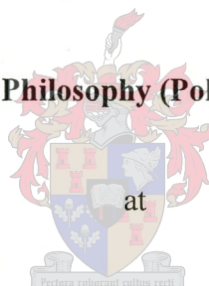
**ETHYLENE AND PROPYLENE COPOLYMERS  
UTILIZING FISCHER-TROPSCH  $\alpha$ -OLEFINS**

by

Dawid Johannes Joubert

Dissertation presented for the degree

**Doctor of Philosophy (Polymer Science)**



The University Of Stellenbosch

Promotor:

Dr. A.J. van Reenen

December 2000

## **DECLARATION**

I, the undersigned hereby declare that the work contained in this dissertation is my own original work and has not previously, in its entirety or in part, been submitted at any University for a degree.

## ABSTRACT

From the Sasol Fischer-Tropsch process, a variety of different  $\alpha$ -olefins are produced. Sasol recently started presenting these  $\alpha$ -olefins to polymer producers. To demonstrate the application possibilities of these  $\alpha$ -olefins as comonomers for ethylene and propylene polymerization, it was necessary to first synthesize catalysts having a combination of high activity and good comonomer incorporation, and in the case of propylene copolymers, also sufficient stereospecificities.

Different methods to produce catalysts conforming to these requirements were investigated and it was found that catalysts produced from a  $\text{MgCl}_2$ -support activated by a combination of chemical and mechanical means produced suitable catalysts. The amount of alcohol used during the support activation step and the time allowed for alkylation of the active centers were important. No clear correlation between total titanium content and activity was observed. The degree to which active sites are protected was evaluated from the amount of comonomer present in the final copolymer based on the amount added to the reaction. Cyclopentadiene was used to selectively deactivate the unprotected active sites to determine the ratio between protected and "open" active sites. High activity catalysts are not suitable for gas-phase copolymerization and were consequently "diluted" by dispersion in a pre-formed polymer powder and by prepolymerization. Catalyst activity based on titanium content was substantially decreased, but comonomer incorporation was not.

Catalysts for producing crystalline polypropylene require the presence of both an internal and external electron donor. It was shown that isotacticity increased linearly with an increase in external modifier at the expense of catalyst activity and that a double treatment of the support or catalyst before the final  $\text{TiCl}_4$  fixation was more effective at increasing stereospecificity. The less stereospecific sites are more capable

of accepting bulky comonomers in the coordination complex and thus by decreasing the amount of less-stereospecific active sites, the overall capability of the catalyst to incorporate comonomer was decreased.

Comonomer sequence distributions and average lamellar thicknesses of different ethylene /  $\alpha$ -olefin copolymers were calculated from CH<sub>2</sub> dyad concentrations determined by <sup>13</sup>C NMR spectroscopy. Ethylene sequences in the 1-butene containing copolymers are generally longer than those where a higher  $\alpha$ -olefin was used as comonomer which indicates that a more random comonomer distribution is obtained when the higher  $\alpha$ -olefins are used. It was shown that an inverse relationship exists between branch size and density. For density, no effect resulting from the comonomer type was observed. This same inverse relationship was also observed for tensile strength. Modulus, hardness and impact strength, on the other hand, did show an effect resulting from the comonomer type. Modulus and hardness were not depressed as much and impact strength improved more than what was expected from calculations based on branch size. Homogeneous copolymers have broad melting peaks. It was shown that at sufficiently high comonomer content, peak broadening occurs when the higher  $\alpha$ -olefins are used as comonomer, which also indicates that more random comonomer distributions are obtained with the higher  $\alpha$ -olefins. From the chain propagation probabilities calculated it was observed that two types of active sites are present. Those responsible for producing mainly polyethylene have an alternating character while the sites capable of incorporating comonomer have a blocky character.

It was expected that the additional introduction of a third  $\alpha$ -olefin during ethylene / 1-pentene copolymerization will produce a terpolymer with density and related properties similar to the mathematical average between those of the relevant copolymers. This was only observed for the terpolymers containing 1-heptene, 1-octene and 1-nonene. The 1-butene containing terpolymers have densities well *below* the expected values while the 1-hexene containing terpolymers have values very similar to that of the ethylene / 1-hexene copolymer densities, but still below the expected values. Properties related to density, such as tensile strength and modulus, follow this same trend. It is believed that the presence of 1-pentene breaks up the

tendency of the lower  $\alpha$ -olefins to cluster which results in improved randomness. Compared to the copolymers, 1-butene and 1-hexene containing terpolymers seem to reach the impact strength maximum at a lower total comonomer content than that of the 1-pentene copolymers which also indicates an enhanced effect from the combined use of 1-pentene with these  $\alpha$ -olefins. No substantial difference between impact strengths of co- and terpolymers prepared with higher  $\alpha$ -olefins was observed.

In general, the melting temperatures of the terpolymers are slightly lower and spread over a wider temperature range than those of the copolymers which can be realized if the comonomer units are less clustered and thus more randomly distributed. Decrease in melting temperature was, however, not as much as for the metallocene catalyzed terpolymers.

From sequence length calculations from  $^{13}\text{C}$  NMR spectroscopy it was found that the crystallizable ethylene sequences of 1-butene containing terpolymers were shorter than those of the corresponding copolymers, which confirms the notion that the introduction of a third comonomer resulted in an increase in randomness. Crystallizable sequence lengths became gradually shorter when higher  $\alpha$ -olefins were used in co- and terpolymers and those of the terpolymers are generally shorter.

From the different types of active centers present on a Ziegler-Natta catalyst, it was reasoned that three main types of polymer chains can be present in the terpolymers: (a) ethylene homopolymer, (b) ethylene / lower  $\alpha$ -olefin copolymer and (c) ethylene / lower  $\alpha$ -olefin / higher  $\alpha$ -olefin terpolymer. The ratio between these components in the final terpolymer depends primarily on the size of the higher  $\alpha$ -olefin. The larger the third  $\alpha$ -olefin becomes, the more active sites will reject it, resulting in a higher amount of ethylene / lower  $\alpha$ -olefin copolymer. It was thus suggested that the large decrease in density and the associated change in related properties observed for ethylene / 1-pentene / 1-butene terpolymers can be related to the combined result of improved random comonomer incorporation together with the decrease in the amount of ethylene homopolymer.

The possibilities of using the higher  $\alpha$ -olefins having uneven carbon numbers were investigated in random propylene copolymers. Similar to that observed for the ethylene copolymers, less of the higher  $\alpha$ -olefins was necessary to achieve a certain level of crystallinity. A good agreement was observed between tensile properties and comonomer type and content and the size of the branch and the resulting defect it causes in the crystal structure is the primary factor affecting tensile strength. For impact strength a close correlation between the size of the comonomer side chain and comonomer content was observed. It was shown that the effect of the heptyl branch derived from a 1-nonene unit was 2.3 times that of the propyl group derived from the 1-pentene unit.

Properties of block copolymers can not be related directly to 1-pentene content as is the case with random copolymers, mainly due to the heterogeneity of the block copolymers. The activating effect of hydrogen on catalyst activity was observed. It was also observed that the amount of 1-pentene incorporated in the copolymer as well as the copolymer yield were higher in the presence of hydrogen than when the reaction was carried out in the absence of hydrogen.

By using DSC it was possible to identify different crystalline phases in the propylene / 1-pentene block copolymers due to the differences in their crystallization kinetics. A connection between the low-temperature peak and impact strength was observed. It was found that the presence of the low-temperature peak resulting from thin lamellae formed by chain containing many defects was undesirable when high impact strength is required. It was not possible to quantify the extent to which the intensity of this peak affected mechanical properties of the block copolymers. However, from sequence length calculations it was found that the ratio between the propylene and 1-pentene sequence lengths could be related quantitatively to impact strength, modulus, hardness and tensile strength of the polymers investigated.

## OPSOMMING

'n Verskeidenheid van verskillende  $\alpha$ -olefiene word in die Sasol Fischer-Tropsch proses vervaardig. Sasol het onlangs begin om hierdie  $\alpha$ -olefiene aan polimeervervaardigers te bied. Om die toepassingsmoontlikhede van hierdie  $\alpha$ -olefiene as komonomere vir etileen en propileen polimerisasie te demonstreeer was dit nodig om eerstens 'n katalis met 'n kombinasie van hoë aktiwiteit en goeie komonomeer invoeging te sintetiseer. In die geval van propileen word voldoende stereospesifisiteit ook vereis.

Verskillende metodes om kataliste wat aan hierdie vereistes voldoen te vervaardig is ondersoek. Daar is gevind dat kataliste waarvan die  $MgCl_2$  basis deur 'n kombinasie van chemiese- en meganiese metodes geaktiveer is, die vereiste eienskappe besit. Die hoeveelheid alkohol gebruik tydens die basis aktivering stap en die tyd toegelaat vir die alkilering van die aktiewe spesies was belangrik. Geen duidelike verband tussen totale titaan inhoud en aktiwiteit is waargeneem nie. Die mate waartoe aktiewe spesies beskerm is, is bepaal vanaf die hoeveelheid komonomeer teenwoordig in die finale kopolimeer in verhouding met die hoeveelheid bygevoeg tydens die reaksie. Siklopentadien is gebruik om onbeskermdde aktiewe spesies selektief te deaktiveer om die verhouding tussen beskermdde en oop aktiewe spesies te bepaal. Hoë-aktiwiteit kataliste is nie geskik vir gasfase kopolimerisasie nie en is gevolglik verdun deur dit te versprei in 'n voorafgevormde polimeer poeier en deur prepolimerisasie. Katalis aktiwiteit gebaseer op titaan inhoud was aansienlik laer maar komonomeer invoeging was nie merkbaar beïnvloed nie.

Kataliste vir die vervaardiging van kristallyne polipropileen vereis die teenwoordigheid van beide interne- en eksterne elektron donors. Daar is gewys dat isotaktisiteit liniêr verhoog met 'n toename in eksterne modifiseerder ten koste van

katalis aktiwiteit en dat 'n dubbele behandeling van die basis of katalis, voor die finale titaan fiksering, meer effektief was om stereospesifisiteit te verhoog. Die spesies met laer stereospesifisiteit is meer bevoeg om bonkige komonomere in die koördinasie kompleks toe te laat en deur dus die konsentrasie van hierdie spesies te verlaag is die bevoegdheid van die katalis om bonkige komonomeer te inkorporeer, verlaag.

Komonomeer reeksverspreiding en gemiddelde lamellêre dikte van verskillende etileen /  $\alpha$ -olefien kopolimere is bereken vanaf  $\text{CH}_2$  diad konsentrasie bepaal deur KMR spektroskopie. Etileen reekse in die kopolimere wat 1-buteen bevat is oor die algemeen langer as dié waarin 'n hoër  $\alpha$ -olefien as komonomeer gebruik was, wat aandui dat 'n meer egalige komonomeer verspreiding verkry word as hoër  $\alpha$ -olefiene gebruik word. Daar is getoon dat 'n inverse verhouding tussen die grootte van die vertakking en digtheid bestaan. Geen effek komende van die komonomeer tipe kon waargeneem word nie. Hierdie soortgelyke inverse verhouding was ook waargeneem vir treksterkte. Modulus, hardheid en impaksterkte aan die ander kant, hét 'n effek komende van die komonomeer tipe getoon. Modulus en hardheid was nie soveel verlaag, en impak sterkte soveel verhoog as wat verwag is vanaf berekeninge gebaseer op vertakking grootte nie. Homogene kopolimere toon breë smeltpieke. Daar is gewys dat by voldoende komonomeer inhoud 'n verbreding van die pieke voorgekom het wanneer hoër  $\alpha$ -olefiene as komonomere gebruik is, wat ook aandui dat 'n meer egalige komonomeer verspreiding met hierdie  $\alpha$ -olefiene verkry kan word. Vanaf berekening van die ketting voortplantingsmoontlikhede is waargeneem dat twee tipes aktiewe spesies teenwoordig is. Die verantwoordelik vir die vorming van polietileen het 'n alternerende karakter terwyl die sentra wat komonomeer kan inkorporeer 'n blokagtige karakter het.

Daar is verwag dat die addisionele byvoeging van 'n derde  $\alpha$ -olefien tydens etileen / 1-penteen kopolimerisasie, 'n terpolimeer met digtheid en verwante eienskappe soortgelyk aan die wiskundige gemiddelde tussen dié van die relevante kopolimere tot gevolg sal hê. Dit was egter slegs waargeneem vir terpolimere wat 1-hepteen 1-okteen en 1-noneen bevat. Die 1-buteen bevattende terpolimere het digthede ver onder die verwagte waardes terwyl die 1-hekseen bevattende terpolimere waardes soortgelyk aan die etileen / 1-hekseen kopolimeer digthede het' wat steeds onder die



verwagte waardes is. Eienskappe verwant aan digtheid, soos treksterkte en modulus, volg dieselfde neiging. Dit word geglo dat die teenwoordigheid van 1-penteen die neiging van die laer  $\alpha$ -olefiene om saam te bondel opbreek wat 'n verbeterde egaligheid in komonomeerverspreiding tot gevolg het. Vergeleke by die kopolimere blyk dit dat die terpolimere wat 1-buteen en 1-hekseen bevat, die impaksterkte maksimum by 'n laer totale komonomer inhoud bereik as dié van die 1-penteen polimere. Dit dui ook op 'n verbeterde effek as gevolg van die gekombineerde gebruik van 1-penteen met ander  $\alpha$ -olefiene. Geen duidelike verskil tussen die impaksterktes van ko- en terpolimere, wat met die hoër  $\alpha$ -olefiene berei was, is waargeneem nie.

In die algemeen is die smeltingstemperature van die terpolimere effens laer, en versprei oor 'n wyer temperatuurgebied as dié van die kopolimere wat verklaar kan word as komonomere minder saamgebondel is en dus meer homogeen versprei is. Die afname in smelt temperatuur was egter nie soveel as dié van die metalloseen-gekataliseerde terpolimere nie.

Vanaf reekslengte berekeninge met behulp van KMR spektroskopie is daar gevind dat die kristalliseerbare etileen reekse van die 1-buteen bevattende terpolimere korter was as dié van die ooreenkomstige kopolimere, wat die gevoel dat die byvoeging van 'n derde komonomeer 'n verbeterde komonomeerverspreiding tot gevolg het, bevestig.

Vanaf die verskillende aktiewe spesies teenwoordig in 'n Ziegler-Natta katalis is daar geredeneer dat drie hooftypes polimeerkettings in die terpolimere teenwoordig kan wees: (a) etileen hompolimeer, (b) etileen / laer  $\alpha$ -olefiën kopolimeer en (c) etileen / laer  $\alpha$ -olefiën / hoër  $\alpha$ -olefiën terpolimeer. Die verhouding tussen hierdie komponente in die finale terpolimeer hang primêr van die grootte van die hoër  $\alpha$ -olefiën af. Hoe groter die derde  $\alpha$ -olefiën is, deur hoe meer van die aktiewe spesies sal dit verwerp word wat 'n groter hoeveelheid etileen / laer  $\alpha$ -olefiën kopolimeer tot gevolg sal hê. Daar word dus voorgestel dat die groot afname in digtheid en die geassosieerde veranderinge in die toepaslike eienskappe waargeneem vir etileen / 1-penteen / 1-buteen terpolimeere, herlei kan word na die gekombineerde effek van

verbeterde komonomeerverspreiding tesame met die afname in die hoeveelheid etileen homopolimeer.

Die moontlikheid om hoër  $\alpha$ -olefiene met onewe koolstofgetalle te gebruik in homogene propileen kopolimere is ondersoek. Soortgelyk aan dit wat waargeneem is vir die etileen kopolimere, was minder van die hoër  $\alpha$ -olefiene nodig om 'n spesifieke vlak van kristalliniteit te bereik. 'n Goeie ooreenkoms tussen trek-eienskappe en komonomeer tipe- en inhoud is waargeneem en die grootte van die vertakking en die gevolglike defek wat dit veroorsaak in die kristal struktuur is die primêre faktor wat treksterkte beïnvloed. Vir impaksterkte is 'n noue verband tussen die grootte van die vertakking en komonomeer inhoud waargeneem. Daar is aangetoon dat die effek van die heptiel vertakking vanaf die 1-noneen eenheid 2.3 keer dié van die propiel groep van die 1-penteen eenheid is.

Eienskappe van blok kopolimere kan nie direk na 1-penteen inhoud herlei word soos die geval met die homogene kopolimere was nie, hoofsaaklik as gevolg van die heterogeniteit van die blok kopolimere. Die aktiverende effek van waterstof op katalis aktiwiteit is waargeneem. Daar is ook gesien dat die hoeveelheid 1-penteen geïnkorporeer in die kopolimeer, sowel as die kopolimeer opbrengs, hoër was in die teenwoordigheid van waterstof as wanneer die reaksie sonder waterstof uitgevoer is.

Deur DSC te gebruik was dit moontlik om verskillende kristallyne fases in die propileen / 1-penteen blok kopolimere vanaf die verskille in hulle krisallisasië kinetika, te identifiseer. 'n Verbintenis tussen die lae-temperatuur piek en impaksterkte is waargeneem. Daar is gevind dat die teenwoordigheid van die lae-temperatuur piek, komende van die dun lamellas gevorm, deur kettings wat baie defekte bevat, ongewens is wanneer hoë impaksterkte vereis word. Dit was nie moontlik om die bereik waartoe die intensiteit van hierdie piek die meganiese eienskappe van die blok kopolimere affekteer, te kwantifiseer nie. Vanaf reekslengte bepalings is daar gevind dat die verhouding tussen die propileen en 1-penteen reekslengtes kwantitatief herlei kan word na impaksterkte, modulus, hardheid en treksterkte van die ondersoekte polimere.

This thesis is dedicated to my parents, Joe and Hester, for their unwavering confidence and the unselfish support over the years, to my wife Lizelle, for her patience and encouragement during the write-up, to André and Janine for providing a lively commotion in the house, and to the rest of my family for their support.

## ACKNOWLEDGEMENTS

I would like to thank the following people and institutions for their contributions:

**Dr. A.J. van Reenen**, my study leader, for his advice and guidance throughout this study.

**Dr. I. Tincul**, my mentor and friend from Sasol Technology, for invaluable advice and many hours of fruitful discussions.

**Drs. C. Reynecke, G. Rall and D. Young**, from Sasol Technology, for their support of the projects and the opportunity to undertake into this study.

**Dr N. Emslie**, from Instrumental Techniques at Sasol Technology, for assistance with scheduling and outsourcing of analyses.

**Dr. H Retief, Mrs. H. Assumption and M. Kirk**, from Instrumental Techniques at Sasol Technology, for NMR and XRD work.

**Mr. D Bryssinck**, from Instrumental Techniques at Sasol Technology, for compositional analysis of the catalysts.

**Miss R Snyman**, from Instrumental Techniques at Sasol Technology, for IR analysis.

**Miss. G. ter Stege**, from Basic Catalyst Research at Sasol Technology for taking the SEM photos.

**Mrs. V Bezuidenhout**, from Basic Catalyst Research at Sasol Technology, for surface area and pore volume analyses of the catalysts.

**Mrs. G. Wells, N. Naidoo and N. Gurupersaad**, from Wax Research at Schümann-Sasol, for thermal analysis.

**Mrs. R. Strachan and Messrs. L Zulu and W Mokoena**, from Polymer Research at Sasol Technology, for their assistance with the autoclaves, sample preparation and analyses of mechanical properties.

**Messrs. J. Labuschagne and W. Louw**, from the Sasol Technical Library for their assistance with literature searches.

**Mrs. S Roux and S. van Vuuren**, from the Sasol Technical Library for their assistance in obtaining literature.

**Mr. P. Roberts**, formerly from AECl, and **Mrs. S. Rhodes** and **A. de Raedt** from the CSIR for NMR work.

**SASOL**, for sponsoring this work.

## CONTENTS

### 1. INTRODUCTION AND OBJECTIVES

1.1	Introduction	1
1.2	Objectives	2
1.2.1	Ziegler-Natta Catalysts	2
1.2.2	Polyethylenes	3
1.2.3	Polypropylenes	4

### 2. OLEFIN POLYMERIZATION CATALYSTS

2.1	Historical Overview	6
2.1.1	Early Developments	6
2.1.2	High-Pressure Free-Radical Polymerization of Ethylene	6
2.1.3	Low-Pressure Polymerization Of $\alpha$ -Olefins - The Initial Discoveries of Ziegler and Natta	9
2.1.4	Medium-Pressure Polymerization by Transition Metal Oxides	11
2.1.5	Development of the Ziegler-Natta Catalyst	12
2.1.5.1	First Generation Ziegler-Natta Catalysts – In Situ and Preformed Catalysts	12
2.1.5.2	Second Generation Ziegler-Natta Catalysts – Donor Modified Preformed Catalysts	14
2.1.5.3	Third Generation Ziegler-Natta Catalysts – Supported Catalysts	16
2.1.5.4	Fourth Generation Ziegler-Natta Catalysts – Catalyst Architecture	20

2.1.6	Homogeneous Vanadium Catalysts	22
2.2	Overview of the Theory of Ziegler-Natta Polymerization	23
2.2.1	Mechanisms of Ziegler-Natta Polymerization of Olefins	23
2.2.1.1	Early Mechanisms	23
A.	Insertion Mechanisms of Ziegler and Natta	23
B.	Radical Mechanisms	23
C.	Anionic Mechanisms	24
2.2.1.2	Bimetallic Mechanisms	24
A.	The Uelzmann Mechanism	24
B.	The Natta and Mazzanti Mechanism	24
C.	The Patat and Sinn Mechanism	25
2.2.1.3	Monometallic Mechanisms	26
A.	The Cossee-Arlman Mechanism	26
B.	The Trigger Mechanism	27
2.2.1.4	Stereoregulation with Heterogeneous Catalysts	28
A.	Propagation Errors	28
B.	Internal and External Electron Donors	29
2.2.1.5	Kinetic Models	30
A.	Early Models	30
B.	Model of Böhm	36
C.	Adsorption Models	36
2.2.1.6	Influence of Electronic and Steric Factors on Olefin Reactivity	37
2.3	Single Site Catalysts	39
2.3.1	Metallocenes	39
2.3.2	Post-Metallocene Single-Site Catalysts	44
2.3.2.1	Dow Constrained Geometry Catalysts	45
2.3.2.2	Brookhart-Gibson Catalysts	46
2.3.2.3	Mitsui FI Catalyst	48
2.3.3.	Possibilities with Single-Site Catalysts	48
2.3.4	Mechanisms for Single-Site Polymerization of Olefins	50
2.3.4.1	Kaminsky's Model	50
2.3.4.2	Corradini's Model	50
2.3.5	Stereoregulation with Homogeneous Catalysts	50

2.3.5.1	Pino's Model	51
2.3.5.2	Corradini's Model	51
2.3.5.3	Brintzinger's Model	52
2.3.6	Kinetic Models	53
2.3.6.1	Ewen's Model	53
2.3.6.2	Chien's Model	53
2.4	References	55

### **3. POLYOLEFINS**

3.1	Global Production Capacities	65
3.1.1	Polyethylene	65
3.1.2	Polypropylene	69
3.2	Polymerization Processes	71
3.2.1	Polyethylene	71
3.2.1.1	LDPE	71
3.2.1.2	HDPE	73
3.2.1.3	LLDPE	78
3.2.2	Polypropylene	79
3.2.2.1	Early Processes	81
3.2.2.2	Current Processes	81
3.3	Polymer Properties	83
3.3.1	Polyethylene	83
3.3.1.1	LDPE	84
3.3.1.2	HDPE	86
3.3.1.3	LLDPE	87
3.3.2	Polypropylene	90
3.4	Applications	92
3.4.1	Polyethylene	92
3.4.1.1	LDPE	92
3.4.1.2	HDPE	94
3.4.1.3	LLDPE	96
3.4.2	Polypropylene	98
3.5	References	101



## 4. EXPERIMENTAL

4.1	Polymerization	105
4.1.1	Materials and Equipment	105
4.1.2	Polyethylene	107
4.1.3	Polypropylene	107
4.2	Polymer Characterization	108
4.2.1	Mechanical Properties	108
4.2.1.1	Tensile Properties	108
4.2.1.2	Impact Strength	108
4.2.1.3	Hardness	108
4.2.2	Physical Properties	109
4.2.2.1	Melt Flow Index	109
4.2.2.2	Density	109
4.2.2.3	Crystallinity	109
4.2.2.4	Composition and Microstructure	110
A	Polyethylene	110
B	Polypropylene	120
4.2.2.5	Molecular Weight	124
4.2.2.6	Scanning Electron Microscopy	125
4.2.3	Thermal Properties	125
4.3	References	126

## 5. ZIEGLER-NATTA CATALYSTS

5.1	Introduction	127
5.2	Experimental	129
5.2.1	Materials and Equipment	129
5.2.2	Analyses	129
5.2.2.1	X-Ray Diffraction	129
5.2.2.2	Surface Area and Pore Size	130
5.2.2.3	Titanium Oxidation States	130
5.2.2.4	Catalyst Composition	130

5.2.2.5	Copolymer Composition	131
5.2.3	Polyethylene Catalyst Preparation	131
5.2.4	Polyethylene Catalyst Activity	132
5.2.5	Polypropylene Catalyst Preparation	133
5.2.6	Propylene / 1-Pentene Copolymerization	133
5.2.7	Catalyst Kinetics	134
5.3	Polyethylene Catalysts	135
5.3.1	Crystallographic Changes	135
5.3.2	Catalyst Activity	138
5.3.3	Comonomer Incorporation	143
5.3.4	Prepolymerization	149
5.4	Polypropylene Catalysts	151
5.4.1	Kinetics	154
5.4.2	Comonomer Incorporation	156
5.5	Conclusions	159
5.6	References	161
<b>6.</b>	<b>ETHYLENE COPOLYMERS</b>	
6.1	Introduction	163
6.2	Experimental	169
6.3	Results and Discussion	171
6.3.1	Comonomer Sequence Distributions	172
6.3.2	Density	175
6.3.3	Mechanical Properties	178
6.3.3.1	Tensile Strength	178
6.3.3.2	Tensile Strength: The Effect of Comonomer Type	179
6.3.3.3	Tensile Strength: The Effect of Density.	181
6.3.3.4	Modulus	182
6.3.3.5	Impact Strength	184
6.3.4	Thermal Properties	187
6.4	Conclusions	195
6.5	References	197

**7. ETHYLENE / 1-PENTENE / LINEAR  $\alpha$ -OLEFIN TERPOLYMERS**

7.1	Introduction	200
7.2	Experimental	202
7.3	Results and Discussion	205
7.3.1	Density	205
7.3.2	Mechanical Properties	211
7.3.2.1	Tensile Strength	212
7.3.2.2	Young's Modulus	214
7.3.2.3	Impact Strength	217
7.3.3	Thermal Properties	219
7.3.3.1	Ethylene / 1-Pentene / 1-Butene Terpolymers	220
7.3.3.2	Ethylene / 1-Pentene / 1-Hexene Terpolymers	225
7.3.3.3	Ethylene / 1-Pentene / Higher $\alpha$ -Olefin Terpolymers	227
7.3.4	Microstructure	229
7.4	Conclusion	233
7.5	References	236

**8. PROPYLENE /  $\alpha$ -OLEFIN RANDOM COPOLYMERS**

8.1	Introduction	238
8.2	Experimental	239
8.3	Results and Discussion	241
8.3.1	Mechanical Properties	241
8.3.1.1	Tensile Strength	242
8.3.1.2	Impact Strength	244
8.3.2	Thermal Properties	248
8.4	Conclusions	256
8.5	References	258

**9. PROPYLENE / 1-PENTENE BLOCK COPOLYMERS**

9.1	Introduction	260
-----	--------------	-----

9.2	Experimental	265
9.3	Results and Discussion	267
9.3.1	Polymer Yield - The Effect of Hydrogen	268
9.3.2	Polymer Yield - The Effect of Comonomer	269
9.3.3	Mechanical Properties	272
9.3.4	Thermal Properties	273
9.3.5	Relationship Between Impact Strength and Melting Curve Profile	277
9.3.6	Fracture Surfaces	280
9.3.7	Microstructure	281
9.4	Conclusions	285
9.5	References	287

## LIST OF TABLES

### CHAPTER 3

3.1	Density Range for Different Polyethylenes.	83
3.2	Blown Film Properties of LDPE.	84
3.3	Properties of Typical Commercial LDPE Grades.	85
3.4	Typical Properties of Commercial HDPE.	86
3.5	Difference in LLDPE Properties Resulting From Uniform and Non-uniform Comonomer Distribution.	88
3.6	Properties of Commercial LLDPE Film with Non-uniform Comonomer Distribution.	89
3.7	Typical Properties of Commercial LLDPE Including Uniform and Non-uniform Composition Distributions.	89
3.8	Typical Property Range of Commercial, Mainly Isotactic Polypropylene Grades.	90
3.9	Properties of Polypropylene Films.	91
3.10	Major Fields of Application for LDPE.	93
3.11	Volumes of Major Fields of Application for HDPE.	95
3.12	Volumes of Major Fields of Application for LLDPE.	97
3.13	Volumes of Major Fields of Application for Polypropylene.	99

### CHAPTER 4

4.1	Comparison of Observed and Calculated Chemical Shifts of Ethylene / $\alpha$ -Olefin Copolymers.	111
4.2	Chemical Shift Prediction for Ethylene / ( $\alpha$ -Olefin) Copolymers Utilizing the Grant and Paul Additivity Rules.	115

4.3	Grant and Paul Chemical Shift Prediction for Poly( $\alpha$ -Olefins).	117
4.4	$^{13}\text{NMR}$ $\alpha$ -Carbon Peak Assignments of the Indicated Dyad Sequences for Copolymers of Ethylene with Higher $\alpha$ -Olefins.	118
4.5	Chemical Shift Prediction for Propylene / ( $\alpha$ -Olefin) Copolymers Utilizing the Grant and Paul Additivity Rules.	122
4.6	$^{13}\text{NMR}$ $\alpha$ -Carbon and Branching Carbon Peak Assignments of the Indicated Dyad Sequences for Copolymers of Propylene with Higher $\alpha$ -Olefins.	123

## CHAPTER 5

5.1	Preparation Methods of Different $\text{MgCl}_2$ -Supported Catalysts.	139
5.2	Properties of $\text{MgCl}_2$ -Supported Ziegler-Natta Catalysts.	141
5.3	Properties of Differently Prepared Catalysts Comparing Activities with Titanium Composition.	142
5.4	Comonomer Incorporation for Different Catalysts During Co- and Terpolymerization with Ethylene.	144
5.5	Gas-Phase Terpolymerization of Ethylene and Two Higher $\alpha$ -Olefins Using Modified Catalysts.	150
5.6	Summary of Different Preparation Methods for Catalysts Suitable for Isospecific Copolymerization of Propylene and Higher $\alpha$ -Olefins.	159
5.7	Comonomer Incorporation Ratios of Different Catalysts Used for Co- and Terpolymerization of Propylene with Higher $\alpha$ -Olefins.	157

## CHAPTER 6

6.1	Comparison Between LLDPE Grades of Similar Density Containing Different Comonomers.	165
6.2	Relative Reactivities of $\alpha$ - Olefins.	167

6.3	Properties of Ethylene / $\alpha$ -Olefin Copolymers.	171
6.4	Comonomer Sequence Distribution of Ethylene / $\alpha$ -Olefin Copolymers.	173
6.5	$^{13}\text{NMR}$ $\alpha$ -Carbon Peak Assignments of the Indicated Dyad Sequences for Copolymers of Ethylene with Higher $\alpha$ -Olefins.	174
6.6	Observed <i>vs.</i> Calculated Comonomer Content at a Fixed Density of $\rho = 0.930 \text{ g/cm}^3$ .	177
6.7	Observed <i>vs.</i> Calculated Comonomer Content at a Fixed Tensile Strength of 13 MPa.	181
6.8	Observed <i>vs.</i> Calculated Comonomer Content at a Fixed Young's Modulus of 500 MPa.	183
6.9	Observed <i>vs.</i> Expected Slopes of Impact Curves of Different Ethylene / $\alpha$ -Olefin Copolymers.	185
6.10	Thermal Properties of Ethylene / $\alpha$ -Olefin Copolymers.	188
6.11	Thermal Properties of Copolymers Prepared with Metallocene Catalysts.	189
6.12	Chain Propagation Probabilities.	191

## CHAPTER 7

7.1	Properties of Solution Phase Metallocene Catalyzed Ethylene / 1-Pentene / $\alpha$ -Olefin Terpolymers.	206
7.2	Properties of Ethylene / 1-Pentene / $\alpha$ -Olefin Terpolymers Obtained with a Conventional Ziegler-Natta Catalyst.	207
7.3	Thermal Properties of Metallocene- and Ziegler-Natta Catalyzed Ethylene / 1-Pentene / 1-Butene Terpolymers.	220
7.4	Thermal Properties of Metallocene- and Ziegler-Natta Catalyzed Ethylene / 1-Pentene / 1-Butene Terpolymers Cooled at a Rate of $0.3^\circ\text{C/min}$ .	223
7.5	Thermal Properties of Metallocene- and Ziegler Natta Catalyzed Ethylene / 1-Pentene / 1-Hexene Terpolymers.	225

7.6	Thermal Properties of Metallocene- and Ziegler-Natta Catalyzed Ethylene / 1-Pentene / 1-Hexene Terpolymers Crystallized at 0.3°C/min.	227
7.7	Thermal Properties of Metallocene- and Ziegler-Natta Catalyzed Ethylene / 1-Pentene / Higher $\alpha$ -Olefin Terpolymers.	228
7.8	Comonomer Sequence Distribution of Ziegler-Natta Catalyzed Ethylene / 1-Pentene / $\alpha$ -Olefin Terpolymers.	230

## CHAPTER 8

8.1	Mechanical Properties of Propylene / $\alpha$ -Olefin Copolymers.	241
8.2	Calculated vs. Observed Comonomer Content to Obtain an Impact Strength of 15 kJ/m <sup>2</sup> .	247
8.3	Thermal Properties of Propylene / $\alpha$ -Olefin Copolymers.	250

## CHAPTER 9

9.1	Polymerization Parameters and Fundamental Properties of Propylene / 1-Pentene Block Copolymers.	267
9.2	Effect of Introduced Comonomer on Copolymer Yield.	269
9.3	Mechanical and Thermal Properties of Propylene / 1-Pentene Block Copolymers.	272
9.4	Observed and Calculated Chemical Shifts of a Propylene / 1-Pentene Block Copolymer.	282
9.5	Propylene and 1-Pentene Sequence Lengths.	283
9.6	Mechanical Properties as Related to Propylene / 1-Pentene Sequence Length Ratio.	284



**LIST OF FIGURES****CHAPTER 2**

2.1	Different Polymerization Kinetics Illustrated through different Yield / Time and Rate / Time Curves	31
-----	---	----

**CHAPTER 3**

3.1	Global LDPE Capacities by Country	65
3.2	Global HDPE Capacities by Country	66
3.3	Global LLDPE Capacities by Country	68
3.4	Top 10 Global Polyethylene Producers	68
3.5	Global Polypropylene Capacities per Country	69
3.6	Top 10 Global Polypropylene Producers	70
3.7	High Pressure Polymerization of Ethylene	73
3.8	Du Pont Solution Process	74
3.9	Phillips Loop Reactor Process	76
3.10	Union Carbide Gas-Phase Process	77
3.11	Novolen Gas-Phase Process	81

**CHAPTER 4**

4.1	$^{13}\text{C}$ NMR DEPT Spectrum of Ethylene / 1-Butene Copolymer	112
4.2	$^{13}\text{C}$ NMR DEPT Spectrum of Ethylene / 1-Pentene Copolymer	113
4.3	$^{13}\text{C}$ NMR DEPT Spectrum of Ethylene / 1-Hexene Copolymer	113
4.4	$^{13}\text{C}$ NMR DEPT Spectrum of Ethylene / 1-Heptene Copolymer	114
4.5	$^{13}\text{C}$ NMR DEPT Spectrum of a Propylene / 1-Pentene Copolymer	120
4.6	$^{13}\text{C}$ NMR DEPT Spectrum of a Propylene / 1-Heptene Copolymer	121

4.7	IR Spectrum of Propylene / 1-Pentene Copolymer	124
-----	--	-----

## CHAPTER 5

5.1	X-Ray Diffractogram of MgCl <sub>2</sub> Containing 1.5% Water.	136
5.2	X-Ray Diffractogram of MgCl <sub>2</sub> Containing 5% Water.	136
5.3	X-Ray Diffractogram of MgCl <sub>2</sub> Containing 5% Water Treated with Tri-Ethyl Aluminum.	137
5.4	X-Ray Diffractogram of Reaction Products Obtained from Different Steps During Catalyst Preparation.	138
5.5	Effect of Different Amounts of Alcohols and Alcohol Mixtures on Catalyst Activity.	139
5.6	Activity vs. Ageing Time for Catalyst 2.	140
5.7	Temperature Profiles for Different $\alpha$ -Olefin Homopolymerizations.	146
5.8	Ethylene / 1-Octene Copolymer Yields Obtained Using Different Amounts of Cyclopentadiene as Catalyst Deactivator.	147
5.9	Tacticity and Activity of the Non-Stereospecific Catalyst A as Function of External Modifier Content.	151
5.10	Effect of Titanium Loading Time on Catalyst Activity and Titanium Content.	152
5.11	Increase in Copolymer Yield with Reaction Time Using Different Catalysts.	155
5.12	Rate / Time Profiles for Copolymerizations Using Different Catalysts.	155
5.13	Change in 1-Pentene Concentration with Time Using Different Catalysts.	156

**CHAPTER 6**

6.1	Sasol Fischer-Tropsch Process.	164
6.2	Olefins Obtained from the Fischer-Tropsch Process.	165
6.3	Decrease in Density with Different $\alpha$ -Olefins.	175
6.4	Relationship between Tensile Strength and Young's Modulus for Ethylene / $\alpha$ -Olefin Copolymers.	178
6.5	Comparison of Tensile Strength of Different Ethylene / $\alpha$ -Olefin Copolymers.	180
6.6	Dependence of Tensile Strength at Yield on Density.	181
6.7	Comparison of Young's Modulus of Different Ethylene / $\alpha$ -Olefin Copolymers.	182
6.8	Notched Izod Impact Strength of Ethylene / $\alpha$ -Olefin Copolymers.	184
6.9	Deviation of Slopes of the Actual Impact Curves from the Expected Values.	186
6.10	Melting Curves for Heterogeneous Ethylene / $\alpha$ -Olefin Copolymers.	193
6.11	Heats of Fusion of Different Ethylene / $\alpha$ -olefin Copolymers.	193

**CHAPTER 7**

7.1	Densities of Terpolymers of Ethylene, 1-Pentene and a Third $\alpha$ -Olefin.	205
7.2	Densities of Ethylene / 1-Pentene / 1-Butene Terpolymers Containing Different Ratios of the Comonomers.	208
7.3	Densities of Ethylene / 1-Pentene / 1-Hexene Terpolymers Containing Different Ratios of the Comonomers.	209
7.4	Densities of Ethylene / 1-Pentene / Higher $\alpha$ -Olefin Terpolymers Containing Different Ratios of the Comonomers.	210
7.5	Relationship Between Tensile Strength and Modulus.	211
7.6	Tensile Strength of Ethylene / 1-Pentene / 1-Butene Terpolymers Containing Different Ratios of the Comonomers.	212

7.7	Tensile Strength of Ethylene / 1-Pentene / 1-Hexene Terpolymers Containing Different Ratios of the Comonomers.	213
7.8	Tensile Strength of Ethylene / 1-Pentene / Higher $\alpha$ -Olefin Terpolymers Containing Different Ratios of the Comonomers.	213
7.9	Young's Modulus of Ethylene / 1-Pentene / 1-Butene Terpolymers Containing Different Ratios of the Comonomers.	215
7.10	Young's Modulus of Ethylene / 1-Pentene / 1-Hexene Terpolymers Containing Different Ratios of the Comonomers.	215
7.11	Young's Modulus of Ethylene / 1-Pentene / Higher $\alpha$ -Olefin Terpolymers Containing Different Ratios of the Comonomers.	216
7.12	Notched Izod Impact Strength of Ethylene / 1-Pentene / 1-Butene Terpolymers Containing Different Ratios of the Comonomers.	217
7.13	Notched Izod Impact Strength of Ethylene / 1-Pentene / 1-Hexene Terpolymers Containing Different Ratios of the Comonomers.	218
7.14	Notched Izod Impact Strength of Ethylene / 1-Pentene / Higher $\alpha$ -Olefin Terpolymers Containing Different Ratios of the Comonomers.	219
7.15	Comparison of the Melting Curves of Metallocene- and Ziegler-Natta Catalyzed Ethylene / 1-Pentene / 1-Butene Terpolymers.	222
7.16	Comparison of DSC Curves of Metallocene and Ziegler-Natta Catalyzed Terpolymers Cooled at Different Rates.	224
7.17	Comparison of the Melting Curves of Metallocene- and Ziegler-Natta Catalyzed Ethylene / 1-Pentene / 1-Hexene Terpolymers.	226
7.18	Comparison of the Melting Curves of Metallocene- and Ziegler-Natta Catalyzed Ethylene / 1-Pentene / 1-Octene Terpolymers.	228
7.19	Comparison Between Ethylene Sequence Length of 1-Butene and 1-Octene Containing Co- and Terpolymers.	231

**CHAPTER 8**

8.1	Relationship Between Tensile Strength at Yield and Young's Modulus for Co- and Terpolymers.	242
8.2	Relationship Between Tensile Strength at Yield and Comonomer Type and Content.	243
8.3	Hardness vs. Modulus Showing Independence on Comonomer Type.	244
8.4	Impact strength of Different Copolymers as a Function of Modulus.	245
8.5	Dependence of Impact Strength on Comonomer Type and Content.	246
8.6	Relationship Between Molecular Weight and Melt Flow Index.	248
8.7	Melting Temperatures of Different Propylene / $\alpha$ -Olefin Copolymers.	251
8.8	Melting and Crystallization Curves for Propylene / 1-Pentene Copolymers. Magenta=2.6%, Blue=3.4%, Green=3.8%, Red=4.6%.	252
8.9	Melting and Crystallization Curves for Propylene / 1-Heptene Copolymers. Magenta=0.8%, Blue=1.0%, Green=2.8%, Red=4.0%.	253
8.10	Melting and Crystallization Curves for Propylene / 1-Nonene Copolymers. Magenta=0.4%, Blue=1.8%, Green=2.0%, Red=3.0%.	253
8.11	Fusion Enthalpy as a Function of Comonomer Content	254

**CHAPTER 9**

9.1	Crazes Around a Vertically Stretched Rubber Particle.	262
9.2	Active Site with Monomer Unit Co-ordinated such that a 2,1-Misinsertion will Occur, Leading to a Dormant, Sterically Hindered Site.	268
9.3	Plot of 1-Pentene Introduced vs. Mole % 1-Pentene Found in the Copolymer. High Molecular Weight Polymers Contain Less 1-Pentene.	271
9.4	Comparison of Melting- and Crystallization Curves of Low Molecular Weight Copolymers with Different Impact Properties.	278
9.5	Comparison of Melting- and Crystallization Curves of High Molecular Weight Copolymers with Different Impact Properties.	179
9.6	Fracture Surface of Low Impact Strength Block Copolymer.	280
9.7	Fracture Surface of Low Impact Strength Block Copolymer.	280
9.8	Fracture Surface of High Impact Strength Block Copolymer.	281

9.9	NMR Spectrum of Propylene / 1-Pentene Block Copolymer.	282
9.10	Dependence of Impact Strength on the Number Average Propylene : 1-Pentene Sequence Length Ratio.	284

**LIST OF ABBREVIATIONS**

$A$	Cross sectional area of tensile sample
ABS	Acrylonitrile / butadiene / styrene graft copolymer
aPP	Atactic polypropylene
BNP	<i>n</i> -Propyl benzoate
Br	Branching carbon
Bu	Butyl
C	Comonomer
$C^*$	Active center concentration
[C]	Comonomer concentration
(CC)	Comonomer-comonomer dyad concentration
$C_I^*$	Active centers being initiated
CIR	Comonomer incorporation ratio
Cp	Cyclopentadiene
Cp*	Penta methyl cyclopentadienyl
$C_p^*$	Propagating active centers
C <sub>4</sub>	1-Butene
C <sub>5</sub>	1-Pentene
C <sub>6</sub>	1-Hexene
C <sub>7</sub>	1-Heptene
C <sub>8</sub>	1-Octene
C <sub>9</sub>	1-Nonene
DBE	Di-butyl ether
DEPT	Distortionless enhancement by polarization transfer
DIBP	Di- <i>iso</i> -butyl phthalate
DEAC	Di-ethyl aluminum chloride
DSC	Differential scanning calorimetry
E	Young's modulus

(E)	Ethylene
EB	Ethyl benzoate
(EE)	Ethylene-ethylene dyad concentration
(EC)	Ethylene-comonomer dyad concentration
EPDM	Ethylene / propylene / diene terpolymer
EPM	Ethylene / propylene rubber
EPR	Ethylene / propylene rubber
Et	Ethyl
$F$	Force needed to extend tensile sample
GC	Gas chromatography
GPC	Gel permeation chromatography
HDPE	High density polyethylene
$\Delta H_f$	Fusion enthalpy
$\Delta H_{fc}$	Crystalline fusion enthalpy
$\Delta H_u$	Heat of fusion of the repeat unit
ICP	Inductively coupled plasma
Ind	Indenyl
IR	Infra red spectroscopy
$k_t^{Al}$	Chain transfer constant with cocatalyst
$k_t^{H_2}$	Chain transfer constant with hydrogen
$k_t^m$	Chain transfer constant with monomer
$k_t^p$	Chain transfer constant with polymer
$k_p$	Propagation rate constant
$k_I$	Rate constants for initiation after a transfer reaction
$L$	Original length of tensile sample
$\Delta L$	Change in length of tensile sample
LDPE	Low density polyethylene
LLDPE	Linear low density polyethylene
MAO	Methyl aluminoxane
$m$	<i>Meso</i> stereosequences
MD	Machine direction
$M_n$	Number average molecular weight
MDPE	Medium density polyethylene



Met	Metallocene
MFI	Melt flow index
MW	Molecular weight
$M_w$	Weight average molecular weight
MWD	Molecular weight distribution
$M_x$	Molecular weight of monomer x
$m_x$	Weight of monomer x
NMR	Nuclear magnetic resonance spectroscopy
$\bar{n}_p$	Number-average propylene sequence length
$\bar{n}_E$	Number-average ethylene sequence length
$\bar{n}_C$	Number-average comonomer sequence length
Oct	1-Octene
(P)	Propylene
PE	Polyethylene
$P_{EE}$	Chain propagation probability
$P_{EC}$	Preferred addition probability of comonomer
$P_C$	Advantage of comonomer over ethylene to add to the chain
$P_{CE}$	Preferred addition probability of ethylene
(PC)	Propylene-comonomer dyad concentration
$P_n$	Degree of polymerization
ppm	Parts per million
Ph	Phenyl
PP	Polypropylene
(PP)	Propylene-propylene dyad concentration
PVC	Poly(vinyl chloride)
$\rho$	Density
$\rho_c$	Crystalline density
$\rho_a$	Amorphous density
$R$	Universal gas constant
$r$	Racemic stereosequences
$r_E$	Relative reactivity of ethylene
$r_C$	Relative reactivity of comonomer
$R_p$	Rate of polymerization

SBS	Styrene / butadiene / styrene block copolymer
SEM	Scanning electron microscopy
sPP	Syndiotactic polypropylene
sPS	Syndiotactic polystyrene
SHAC	Shell High Activity Catalyst
$\sigma$	Tensile strength at yield
TEA	Tri-ethyl aluminum
TBP	2,2'-thio- <i>bis</i> (6- <i>t</i> -butyl-4-methylphenoxy)
TD	Transverse direction
THF	Tetrahydro furan
$T_m$	Equilibrium melting temperature
$T_m^0$	Melting temperature of linear polyethylene
TREF	Temperature rising elution fractionation
UHMWPE	Ultra high molecular weight polyethylene
VLDPE	Very low density polyethylene
$W_a$	Weight in air
$W_w$	Weight in water
$w^c$	Weight percent crystallinity
$x$	Ethylene / comonomer mole ratio
$X_E$	Mole fraction of the crystallizable unit
XRD	X-Ray diffraction

## LIST OF RELEVANT PUBLICATIONS

### Conference Poster Presentations

1. Joubert D.J., Tincul I., **Propylene / 1-Pentene Copolymers**, 6<sup>th</sup> *SPSJ International Polymer Conference*, Society of Polymer Science, Kusatsu, Japan, 259, Oct. 20-24 (1997)
2. Joubert D.J., Tincul I. Moss J.R., **Contribution to the Development of Ziegler-Natta Catalysts**, *Inorganic '99*, South African Chemical Institute, Stellenbosch, SA, 49, Jan. 17-20 (1999)
3. Joubert D.J., Tincul I., van Reenen A.J., **Prepolymerized Ziegler-Natta Catalyst for Gas-Phase Production of LLDPE**, *Unesco Conf. Proc.*, Mar. (1999)

### Conference Presentations

1. Joubert D.J., Tincul I., Potgieter A.H., **Propylene / 1-Pentene Random Copolymers**, *MSSA Proceedings*, (1998)
2. Tincul I., Joubert D.J., Potgieter A.H., **Impact Fracture Toughness of Propylene / 1-Pentene Random Copolymers**, *PMSE Proceedings*, ACS Fall Meeting, 79, 190 (1998)
3. Tincul I., Joubert D.J., Potgieter A.H., **1-Pentene Copolymers with Ethylene and Propylene**, *Polymer '98*, European Polymer Federation, Brighton, UK, 23, Sep. 9-11 (1998)
4. Tincul I., Joubert D.J., **Thermoanalysis of 1-Pentene Copolymers with Ethylene and Propylene**, *ESTAC 7*, Hungarian Chemical Society, Balatonfüred, Hungary, 291, Aug. 30 – Sep 4 (1998)
5. Tincul I., Joubert D.J., **Advances in Polyolefins II, A New Family of Polyolefins With Fischer-Tropsch Olefins: Terpolymers of Ethylene / 1-Pentene and a Third  $\alpha$ -Olefin**, ACS, Napa, CA, Oct 24 – 27 (1999)

6. Tincul I., Joubert D.J., **Polymers with Fischer-Tropsch Olefins. – Part 1**, *Unesco Conf. Proc.*, Apr. (2000)

### **Patents**

1. Tincul I., Joubert D.J., Potgieter I.H., *PCT Int. Appl. WO 97/45460*, Sasol Technology R&D, Dec. 4 (1997)
2. Tincul I., Joubert D.J., Potgieter I.H., *PCT Int. Appl. WO 97/45454*, Sasol Technology R&D, Jun. 2 (1997)
3. Joubert D.J., Potgieter I.H., Tincul I. Young D.A., *PCT/GB99/00241*, Sasol Technology R&D, Jan 25 (1999)
4. Joubert D.J., Tincul I. Young D.A., *RSA Appl. 98/6441*, Sasol Technology R&D, Jul. 20 (1999)
5. Joubert D.J., Potgieter A.H., Potgieter I.H., Tincul I., *PCT Int. Appl. WO99/01485*, Sasol Technology R&D, (1998)
6. Joubert, D.J., Potgieter A.H., Potgieter I.H., Tincul I., *PCT Int. Appl. WO 96/24623*, Sasol Technology, R&D, 30 Jan (1996)
7. Joubert D.J., Potgieter A.H., Potgieter I.H., Tincul I., Young D.A., *RSA Appl. 97/8887*, Sasol Technology R&D, Oct. 3 (1997)

## CHAPTER 1

### INTRODUCTION AND OBJECTIVES

#### 1.1 INTRODUCTION

From the chance finding of a small amount of white material in a high-pressure autoclave in 1933, polyolefins have developed into the most versatile and widely used commodity plastic in use today. In the past, polyolefin producers relied heavily on process- and catalyst developments to gain an advantage over their competition. For ethylene polymers, 1-butene was initially employed as comonomer, but later 1-hexene and 1-octene were also used. These comonomers are produced by ethylene oligomerization and only even-numbered compounds can therefore be obtained. It is clear that the role of the comonomer was very much neglected as to the contribution it could make to polymer properties, presumably due to its unavailability up to now. In the Sasol Fischer-Tropsch process, unique  $\alpha$ -olefins including 1-pentene, 1-heptene and 1-nonene compounds are produced. Sasol recently started production of 1-hexene and 1-octene, but the odd-numbered  $\alpha$ -olefins can become available in a short period of time if sufficient demand exists. Of the uneven carbon number linear  $\alpha$ -olefins, the production of polymerization-grade 1-pentene and 1-heptene have already been demonstrated.

## 1.2 OBJECTIVES

### 1.2.1 ZIEGLER-NATTA CATALYSTS

In order to demonstrate the possibilities offered by these new comonomers, it was necessary to first develop catalysts which are capable of incorporating sufficient amounts of these  $\alpha$ -olefins in polyethylene and polypropylene. Ziegler-Natta catalysts have a heterogeneous distribution of active sites with different accessibilities and activities which is responsible for the wide molecular weight distribution and comonomer distributions usually observed. To be able to incorporate the higher  $\alpha$ -olefins such as 1-octene and 1-nonene, catalyst active sites should thus be “open” enough to allow these bulky monomers to be inserted into the polymer chains. If the active sites are protected, the bulky monomers will not be able to come close enough to these active sites to be inserted into the polymer chain, resulting in mainly linear chains. Supporting  $\text{TiCl}_4$  on an inert support such as  $\text{MgCl}_2$  decreases the amount of transition metal residues left in the polymer, leading to better color- and oxidative stability and thus improved product quality. In addition, catalyst activities of the supported catalysts are much improved compared to the “self-supported” first and second generation catalysts, and is believed to result from increased separation between active centers which improve their accessibility.

Catalysts for producing crystalline polypropylene should not only have accessible active sites, but monomer placement in the chain should be regular, *i.e.* the monomer should only enter the coordination complex with a specific orientation of its alkyl group. The active sites should therefore also be able to regulate the coordination of the monomer to ensure a regular chain with as little stereo defects as possible.

The ideal catalyst should therefore have accessible active sites, be capable of incorporating bulky comonomers in the ethylene and propylene chains, have high catalytic activity and, in the case of polypropylene, also sufficiently high isotacticity. The different methods used and the properties of these catalysts are discussed in Chapter 5.

### 1.2.2 POLYETHYLENES

The properties of polyethylene are directly related to its crystallinity. Short branches present in the polyethylene backbone are mostly rejected from the crystal which results in decreased lamellar thickness and less perfect crystals and, as a consequence, decreased density. Properties can clearly be affected by the concentration of these branches. By changing the length of the short-chain branches, the effect it has is similarly changed, thereby introducing a further dimension by which polymer properties can be tailored.

The higher  $\alpha$ -olefins are less reactive and insertion into the polyethylene chain becomes increasingly more difficult as their side chain lengths increase. The ethylene /  $\alpha$ -olefin feed ratio should thus be decreased which will result in a decreased polymerization rate. However, because the effect resulting from the long branches of the higher  $\alpha$ -olefins is larger, the amount of comonomer needed to obtain a certain density should therefore be less. A consequence of having less comonomer present in a chain is that less clustering of the co-units will occur, thereby making the disruptive effect of the comonomer on crystallinity more effective. In addition, by decreasing clustering, a more homogeneous distribution of comonomer is expected.

Changing to a different comonomer may, however, have a profound impact, not only on the production process, but also on conversion processes and end-use. In general, therefore, it is not an option for polymer producers to change between the different available even-numbered comonomers as the investment costs of changing the side-chain length by two carbons may prove inhibitive. Changes in branch length of one carbon atom made possible by the introduction of odd-numbered  $\alpha$ -olefins may therefore prove more viable.

In order to decrease the effect of a different comonomer even further, a third monomer can be introduced during polymerization to “dilute” the effect of the primary comonomer, thereby only slightly modifying some properties of the polymer without substantial

changes to the polymerization process. Terpolymerization may therefore be employed to further diversify the product portfolio of a polymer producer. However, terpolymerization not only introduces small modifications to polymer properties. If required, substantial changes can also be made to polymer properties by introducing larger amounts of the third monomer.

It is in this light that the study regarding the effect of different comonomers in ethylene /  $\alpha$ -olefin co- and terpolymers presented in Chapters 6 and 7, was undertaken.

### 1.2.3 POLYPROPYLENES

Polypropylene has the highest production volume of all the olefin polymers that amounts to 29 million tons in the current world market with the copolymers taking a large share of this market. Similar to polyethylene, developments mainly focussed on improving processes and catalyst performance while very little attention was, until now, given to the role of the comonomer. In the polypropylene family, ethylene and 1-butene are commonly employed as comonomers although 1-hexene was also described. Application of the odd-numbered  $\alpha$ -olefins in the polypropylene family was, until recently, totally neglected. Propylene / 1-pentene copolymers exhibit exciting application possibilities and as an extension of this study, the properties of random copolymers of propylene with the higher  $\alpha$ -olefins, having uneven carbon numbers, was investigated and results are presented in Chapter 8.

Polypropylene is a very versatile polymer with many outstanding properties. One drawback it does have is low impact resistance at low temperatures. Random copolymers do have increased impact resistance when compared to the homopolymer but crystallinity is lower and consequently the melting- and softening temperature, tensile strength, modulus, dimensional stability and hardness decrease. For many applications, such as external automotive trim, parts should be as thin as possible while retaining sufficient impact strength and stiffness over a wide temperature range. Food containers on the other hand are typically exposed to temperature extremes. For both these applications,



articles should be able to withstand low temperature impact as well as being dimensionally stable at elevated temperatures. These demands cannot be simultaneously met by PP random copolymers.

Propylene is typically copolymerized with ethylene in a two step cascade process where propylene is homopolymerized in one reactor, transferred to a second reactor and copolymerized with ethylene to form the so-called block- or impact copolymers. These copolymers are not true block copolymers, but rather a heterogeneous reactor blend of (a) a polypropylene homopolymer continuous phase to provide stiffness, (b) a dispersed ethylene / propylene rubber phase functioning as stress concentrators for dissipating stresses in the matrix and (c) a number of chains containing long runs of both propylene and EPR to provide adhesion between the homopolymer and rubber phases. Following on from the results obtained from random copolymers, where ethylene was substituted for 1-pentene, the possibilities of using 1-pentene in the rubber phase of block copolymers was investigated and the findings are presented in Chapter 9.

## CHAPTER 2

### OLEFIN POLYMERIZATION CATALYSTS

#### 2.1 HISTORICAL OVERVIEW

##### 2.1.1 EARLY DEVELOPMENTS

Von Pechmann [1] observed as early as 1898 that a solution of diazomethane in ether, on standing, yields a white substance which could be recrystallized from chloroform. In 1900, Bamberger *et al.* [2] determined the melting temperature to be 128°C, and that the structure corresponded to (CH<sub>2</sub>)<sub>n</sub>. This material was called polymethylene. The formation of the polymer presumably took place according to:



The Fischer-Tropsch reduction of carbon monoxide with hydrogen generally yields low molecular weight products [3] but by proper choice of a reaction conditions and catalyst such as the metal tungstite described by Arnold *et al.* [4] high molecular weight polyethylene with a melting temperature of 133°C could be prepared.

Reduction of poly(vinyl chloride), dissolved in tetrahydrofuran or decahydronaphtalene, with lithium aluminum hydride under pressure above 100°C, gave reaction products with the formula (CH<sub>2</sub>)<sub>n</sub> and properties the same as those of polyethylene [5]. These products were all insoluble and crosslinked as noted previously by Staudinger [6].

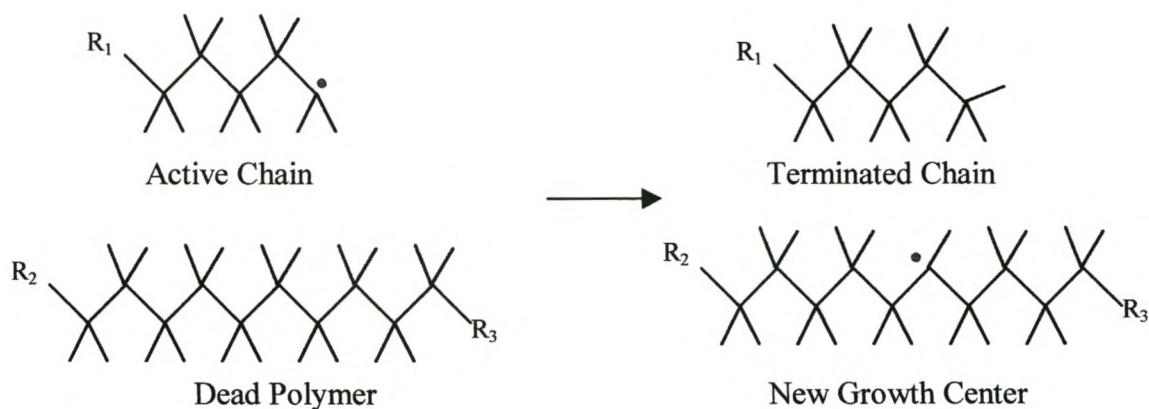
##### 2.1.2 HIGH-PRESSURE FREE-RADICAL POLYMERIZATION OF ETHYLENE

During a study in March 1933 conducted by Imperial Chemical Industries on the high-pressure chemistry of organic compounds, polyethylene was discovered as a

trace of white powder in a reactor vessel. This discovery, first reported by Fawcett and Gibson in 1934 [7] resulted in the basic patent [8] for the high-pressure production of polyethylene. Commercialization was delayed as the process involved numerous technical problems. The highly exothermic free-radical polymerization of ethylene required precise control and extensive safety procedures. In spite of this, experimental lengths of submarine cables insulated with polyethylene were produced from material obtained from a continuously running pilot plant constructed by ICI. The first commercial plant was ready for production in 1939 but with the advent of World War II it was decided to double capacity and an entirely new plant was erected which was in full production early in 1942 [9]. During the war the polyethylene produced was exclusively for military use, particularly for cable insulation in high frequency applications, because of its unique combination of properties. Despite numerous early patents, commercialization of copolymers of ethylene produced by the high-pressure polymerization was a slow process and only in 1961 were ethylene / ethyl acrylate and ethylene / vinyl acetate copolymers introduced.

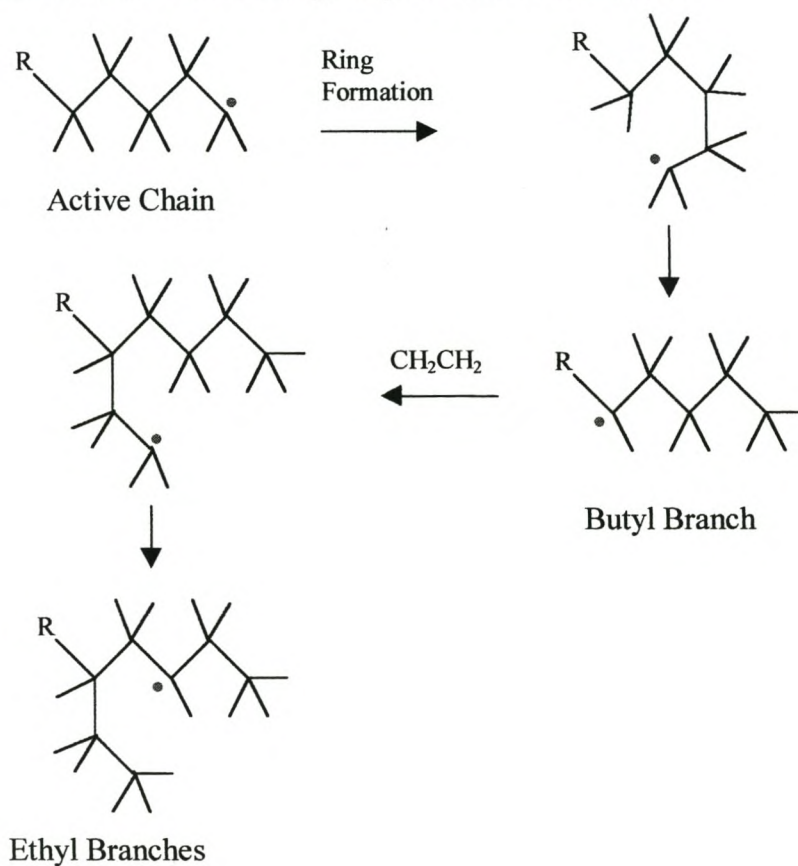
After ICI started production, licenses were granted to Union Carbide and Du Pont and today this peroxide-initiated highly branched polymer, called low-density polyethylene (LDPE) is manufactured under pressures up to 3 000 bar and temperatures between 100 and 300°C, preferably in continuous fashion in stirred autoclaves or tubular reactors with diameters less than 25 mm and lengths up to 30 meters, utilizing bulk or solution processes [10].

Because of extensive branching the crystallinity of LDPE is low, resulting in relatively low densities. By varying the reaction conditions, commercial grades with densities between 0.915 and 0.940 g/cm<sup>3</sup> can be obtained [11]. Two types of branches have been identified. Long chain branching arises from an *intermolecular* chain transfer reaction such as that shown in Scheme 1 where the active chain end extracts a hydrogen from a neighboring chain, thereby initiating a growth center for a new branch and itself becoming terminated. Short chain branching - identified through studies of infrared absorption and degradation under bombardment with high energy radiation - results from *intramolecular* transfer reactions shown in Scheme 2.



**Scheme 1. Branching via Intermolecular Transfer**

When the active chain end extracts a hydrogen from its parent chain through a mechanism known as backbiting, butyl branches are formed.



**Scheme 2. Butyl- and Ethyl Branches through Intramolecular Transfer.**

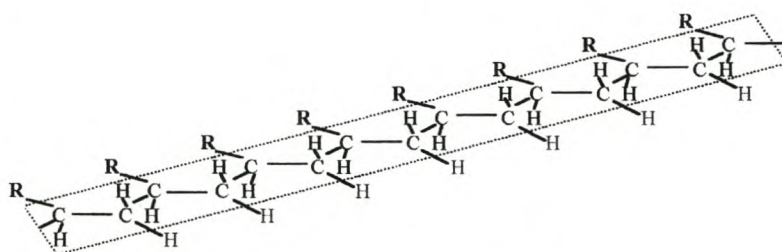
When further transfer occurs with the hydrogen on the butyl branch directly after ethylene was added to this active site, ethylene branches result [10].

Major uses of LDPE are in the manufacture of film, toys and housewares, wire and cable coverings, coating with hot solutions, melts or emulsions [12].

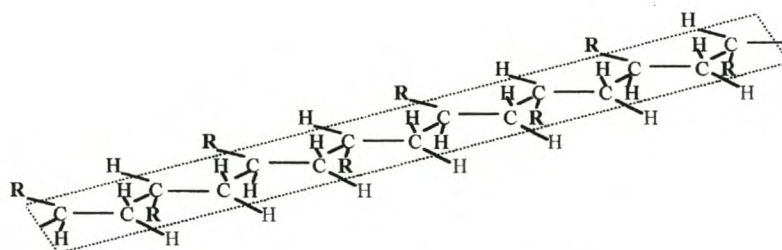
### 2.1.3 LOW-PRESSURE POLYMERIZATION OF ETHYLENE AND $\alpha$ -OLEFINS – THE INITIAL DISCOVERIES OF ZIEGLER AND NATTA

In 1930, Friedrich and Marvel reported that ethylene was polymerized to low molecular weight products in the presence of lithium alkyls [13]. After World War II, Ziegler reinitiated a program based on the lithium alkyls in order to synthesize high molecular weight products. This was however proven to be an unsuitable initiator because of the formation of LiH which precipitates early in the reaction [14]. By reacting  $\text{LiAlH}_4$  with ethylene,  $\text{LiAlEt}_4$  was obtained as the lithium alkyl source. Both LiEt and  $\text{AlEt}_3$  polymerized ethylene,  $\text{AlEt}_3$  even more efficiently than LiEt [15]. Because of experimental advantages, Ziegler and Gellert switched to  $\text{AlEt}_3$  but molecular weight remained in the range 3 000 to 30 000 g/mol, depending on reaction conditions. One day, instead of polyethylene, predominantly 1-butene was found in the reactor, its presence being traced back to a nickel contaminant from a previous hydrogenation experiment and it was speculated that the chain transfer reaction which forms AlH was catalyzed by the nickel [16]. A series of transition metal salts were then examined. Holzkamp found in one reaction that when a combination of  $\text{AlEt}_3$  and zirconium acetylacetonate was used, a small amount of a solid white precipitate was formed. In later experiments this material was found to be high molecular weight polyethylene with the most active catalyst prepared by a combination of  $\text{AlEt}_3$  with  $\text{TiCl}_4$  [17,18]. In effect, a solid catalyst was prepared *in situ* from a soluble transition metal halide (e.g.  $\text{TiCl}_4$ ) and an aluminum alkyl. The polymer was characterized and found to consist of essentially linear chains with high molecular weight. Before informing the scientific community of his work, Ziegler disclosed his findings to Montecatini. Professor Gulio Natta, at that time consultant to Montecatini was studying the kinetics of ethylene addition to aluminum alkyls. Natta started investigating Ziegler's catalyst in 1952 [19]. Two years later, Natta's group successfully synthesized regular, linear, head-to-tail polymers of  $\alpha$ -olefins [20] with increased crystallinity. This was achieved by using preformed titanium chlorides in

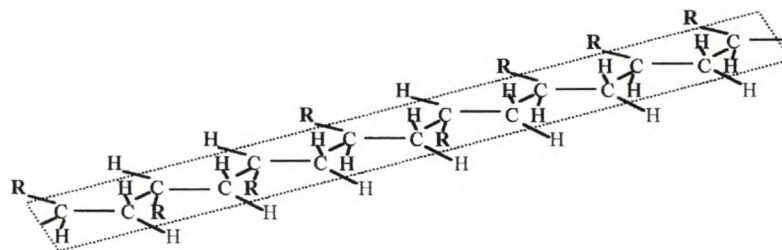
lower valence states in stead of the Ziegler catalyst which contains the transition metal in the highest valence state [18], in this case  $TiCl_4$ . Natta thus realized the advantages of using *performed* transition metal halides, usually in lower valence states. In 1953, Natta produced EPM, the rubbery copolymer of propylene and ethylene. Polymerization of propylene, particularly with the  $AlEt_3 - TiCl_3$  system yields two types of polymer: a soft rubbery soluble fraction and a hard, insoluble, crystalline material with a high melting temperature. Crystallographic investigations led to the concept of tacticity. The soft rubbery material having an irregular structure was labeled *atactic* and the crystalline material with the regular structure labeled *isotactic* [21].



**Isotactic**



**Syndiotactic**



**Atactic**

**Polypropylene Stereoisomers**

The contribution of Professor Gulio Natta to the original work of Professor Karl Ziegler, led to the type of catalyst known today as Ziegler-Natta catalysts. These two pioneers were awarded the Nobel Prize for Chemistry in 1963 by the *Royal Academy of Science* of Sweden for these groundbreaking discoveries which initiated this new and diverse field of science.

#### 2.1.4 MEDIUM-PRESSURE POLYMERIZATION BY TRANSITION METAL OXIDES

At about the same time as Ziegler's discoveries, two other methods for polymerizing ethylene and higher  $\alpha$ -olefins were developed by Standard Oil of Indiana and Phillips Petroleum.

*Molybdenum Catalysts.* The catalysts developed by Standard Oil were based on molybdenum oxide on  $\gamma$ -alumina [22] calcined in air at 500 to 600°C before activation with a reducing gas such as hydrogen or CO at temperatures between 430 to 480°C [23,24]. These catalysts were also found to polymerize propylene but the yields were low and the polymers were described as high molecular weight, rubbery polymers [25]. However, catalyst activities could not be improved satisfactorily and this approach was discontinued. No commercial polyethylene process in use today employs supported molybdenum oxide catalysts [26].

*Chromium Catalysts.* In the late 1940s Phillips, having large amounts of feedstock that could be cracked into olefins, initiated a project dealing with the catalytic di- and trimerization of specifically ethylene and propylene. Initially, this oligomerization was achieved with a nickel oxide on silica-alumina catalyst. Due to difficulties with catalyst lifetimes, Hogan and Banks, who were assigned to this project, added a chromium salt to this catalyst to extend its lifetime. Reaction with propylene resulted in the formation of a solid white powder, which was found to be polypropylene and after an extensive patent dispute involving the patent granted to Natta [27], the U.S. patent office concluded that their patent [28] was valid. When ethylene was passed over a chromium salt on silica-alumina catalyst, polyethylene was formed. Their patent application filed in 1953 [28] described this catalyst system which eventually

became the preferred catalyst for the production of HDPE in continuous single-stage loop reactors worldwide [29].

## 2.1.5 FURTHER DEVELOPMENT OF THE ZIEGLER-NATTA CATALYST

### 2.1.5.1 First Generation Ziegler-Natta Catalysts – In Situ and Preformed Catalysts

Once the discoveries of Ziegler and Natta were made public, worldwide interest in the new Ziegler-Natta catalysts for low-pressure polymerization of ethylene and other  $\alpha$ -olefins resulted in a frenzy of research activity, both in new catalysts and new polymers. The polyethylene produced was stiffer, less branched, more crystalline and thus of higher density and melting temperature than the high-pressure LDPE and for the first time highly crystalline polymers from propylene, styrene and 1-butene could easily be synthesized [30]. The initial  $\text{TiCl}_4 - \text{AlEt}_3$  catalyst system for the production of this new linear, high-density polyethylene (HDPE) was licensed to Petrochemicals, Hoechst, Montecatini and Hercules [29].

One of the problems experienced with these catalysts was the inability to control transfer reactions, this time to decrease the molecular weight of the products. Diethyl zinc was used as transfer agent [31] but it was soon realized that hydrogen offered a much better method of molecular weight control. In mid-1954, Hercules acquired a license to Ziegler's new low-pressure ethylene polymerization method and in 1955 both Hercules and Montecatini filed patents demonstrating control of molecular weight by means of hydrogen [32,33].

Natta found that titanium trichloride could be prepared in four crystalline forms. The brown, chainlike  $\beta$  form [34] was the main product from the low temperature reduction method in hydrocarbon solvent and produced polypropylene containing about 35 to 40 % of polypropylene insoluble in boiling *n*-heptane [35] i.e. the isotactic index of the polymer was 35 to 40. The  $\alpha$ -form prepared by the reduction of  $\text{TiCl}_4$  with hydrogen at temperatures between 400 and 800°C [36] yielded polypropylene



with isotacticities between 80 and 90%. This made the development of the first industrial process by Montecatini of the production of polypropylene possible [37].

A major drawback of these early Ziegler-Natta catalysts was their low polymerization activity. Typically 5 kg polyethylene per gram of transition metal was produced resulting in titanium residues in the polymer as high as 100 ppm. Correspondingly, chlorine levels were also high resulting in excessive corrosion and thermo-oxidative stability problems. This necessitated the removal of these catalyst residues through expensive washing procedures [26]. Higher catalyst activities gives increased production and, more importantly, it leads to fewer catalyst residues in the polymers, leading in turn to higher quality products.

Reducing  $\text{TiCl}_4$  with aluminum or soluble aluminum compounds, resulted in some aluminum left in the structure. This cocrystallized  $\text{TiCl}_3 \cdot x\text{AlCl}_3$  material showed increased activity together with an increase in the isotactic PP fraction. X-ray analyses of the reaction product of  $\text{TiCl}_4$  and ethylaluminum dichloride ( $\text{EtAlCl}_2$ ) mentioned by Vandenberg [38,39] gave no evidence of crystalline  $\text{AlCl}_3$  but showed new patterns related to that of the known purple  $\alpha$  form which Natta *et al.* [36] reported as the  $\delta$  form. Even better results were obtained with the catalyst prepared using a 1:3 ratio of triethyl aluminum ( $\text{AlEt}_3$ ) and  $\text{TiCl}_4$ , resulting in  $\text{TiCl}_3 \cdot 0.33\text{AlCl}_3$  with a crystal structure identical to the  $\gamma$  form reported by Natta *et al.* [36]. The specific method of reduction therefore, determines the composition and the crystal structure of the titanium catalyst. The catalytic activity of the  $\alpha$ - and  $\gamma$  forms is lower than that of the  $\delta$  form and as mentioned earlier, propylene polymerized with the  $\beta$  form is generally amorphous with a low isotactic content [34]. They also showed that the type of cocatalyst and reaction temperature have profound effects on the tacticity of the polypropylene produced. Reactions carried out at  $15^\circ\text{C}$  generally have higher isotactic content than those prepared at  $70^\circ\text{C}$  and the alkyl aluminum halides persistently gave higher isotacticities than triethylaluminum with diethyl aluminum iodide the preferred cocatalyst. Although catalysts containing a beryllium alkyl performed better, alkyl aluminum compounds were preferred because of their availability and lower toxicity when compared to the beryllium compounds. From the discussion by Vandenberg [38] regarding the early development of polypropylene

catalysts at Hercules, it seems that the highest polymerization activity and tacticity were achieved by using a stoichiometric ratio for the reaction between  $\text{TiCl}_4$  and  $\text{AlEt}_3$ . However, Natta *et al.* [34] found no stereoregulating effect from the alloyed aluminum in the  $\alpha$ -,  $\gamma$ - or  $\delta$   $\text{TiCl}_3$  catalysts, but catalytic activity was significantly increased.

Tornqvist *et al.* [40,41] discovered that ball-milling of the  $\alpha$ ,  $\gamma$  and  $\delta$  forms of titanium resulted in even higher polymerization activities and that both the  $\alpha$  and  $\gamma$  forms are converted to the  $\delta$  form [42]. This crystalline modification takes place as a result of a sliding of the Cl-Metal-Cl layers, resulting in stacking faults. They also showed that the activating effect was the direct consequence of extensive size reduction because of the layered structure. Activity increased until the crystallite size reached 50Å. Further reduction led to a less active catalyst that was suggested to be caused by the tendency for such small crystals to change their structure to the less active  $\beta$  form.

#### 2.1.5.2 Second Generation Ziegler-Natta Catalysts – Donor Modified Preformed Catalysts

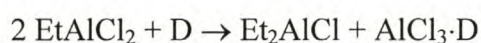
A further improvement in catalyst stereospecificity was achieved by the introduction of aliphatic and aromatic esters, ethers, amides, amines, ketones, phosphorous compounds etc. to the Ti/Al mixture. These materials are generally considered to be catalyst poisons. These compounds are often ball-milled together with the  $\delta$ - $\text{TiCl}_3 \cdot 0.33\text{AlCl}_3$  and because factors like mode of addition, temperature, concentration and the nature of the donor all influence catalyst performance, most companies have their own recipes [43]. Coover *et al.* [44,45] reported that high crystallinity polypropylene can be obtained by including an electron donor in the preparation of the preformed  $\text{TiCl}_3$  catalysts. Mitsubishi demonstrated an increase in stereospecificity by the addition of an electron donor such as a carboxylic acid ester [46]. Activity often decreases when catalysts are prepared in the presence of electron donors [43] but Coover and Joyner [47] found an increase in activity when controlled amounts of donors are introduced. They observed that the catalyst with a hexamethyl

phosphoric triamide / EtAlCl<sub>2</sub> ratio of 1:0.7 displayed optimum polymerization activity and at a 1:0.6 ratio, stereospecificity was optimum at 96%.

The mechanism of modification of these donors was formulated by Tait [43]:

- Complexation of the donor with active centers leads to hindered or completely blocked active centers. The mechanism believed to operate in many donor-modified systems is that of the donor complexing with exposed, less stereospecific centers which increases stereospecificity.
- Complexation with a metal alkyl leads to a decrease in the ability of the metal alkyl to reduce the transition metal as well as a decrease in transfer reactions to the metal alkyl.
- Strong complexation with metal alkyl dihalide poisons formed during alkylation of the transition metal, leads to increased activity.
- Catalyst modification such as removal of AlCl<sub>3</sub> from δ-TiCl<sub>3</sub>·0.33AlCl<sub>3</sub> type catalysts assists catalyst break-up during polymerization and consequently to increased activity.

Zambelli *et al.* [48] reported that the EtAlCl<sub>2</sub> is converted to Et<sub>2</sub>AlCl by the reaction:



The first successful commercial second-generation catalyst was developed by Solvay in 1973 [49] using diisoamyl ether as donor and Et<sub>2</sub>AlCl as cocatalyst. The preparative method used in their initial invention included reaction of TiCl<sub>4</sub> with Et<sub>2</sub>AlCl at about 0°C in hydrocarbon solvent to form aluminum complexed β-TiCl<sub>3</sub>. This complex is then reacted with diisoamyl ether at 35°C to extract many of the aluminum compounds, resulting in a porous matrix that assists catalyst breakup during polymerization. This resulting solid was then reacted with TiCl<sub>4</sub> at 65°C for 2 hours to yield the more active α-TiCl<sub>3</sub> containing both diisoamyl ether and an ethylaluminum chloride. The best results were obtained with the complex catalyst α-TiCl<sub>3</sub>·EtAlCl<sub>2</sub>·donor. The preparation of a catalyst entailing a prepolymerization step before ether treatment (as internal modifier) and using a combination of Et<sub>2</sub>AlCl and

one or more external modifiers as cocatalyst was later described [50]. This introduced a further *in situ* modification step during active site formation before polymerization commenced.

Although the activities of these second generation catalysts were high enough to allow the commercialization of bulk and gas-phase propylene polymerization processes, catalyst residues were still high with Ti and Cl contents above the target levels of 10 and 40 ppm respectively. This resulted in the production of poor quality materials [51,52,53]. Natta [54] and Rodriguez *et al.* [55] observed that only a small percentage (<1%) of the titanium on the catalyst surface located on the lateral faces and edges and along crystal defects were active. The rest of the matrix acted as a support for these active titanium species. It was realized that better product quality should be obtained if the titanium could be supported on appropriate matrices.

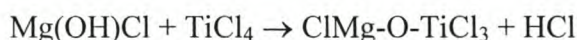
### 2.1.5.3 Third Generation Ziegler-Natta Catalysts – Supported Catalysts

The next significant improvement in Ziegler-Natta catalyst development came with the invention of supported titanium compounds, either co-milled in the presence of the support material, or linked to a chemically activated support, together with stereoregulators if isotactic polymers are to be obtained. In the absence of electron donors,  $\text{MgCl}_2 / \text{TiCl}_4$  catalysts are up to 200 times more active than  $\text{TiCl}_3$ -based catalysts, but polypropylene isotacticities are low - between 20 and 50% [56]. Incorporation of  $\text{TiCl}_4$  onto a support having a large surface area and internal pore volume resulted in isolation of these titanium centers. This increased the population of accessible active sites when compared to the conventional unsupported materials. This is the main reason why the activities attainable with supported catalysts are so much higher than those of the unsupported catalysts [57].

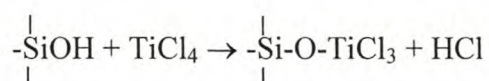
The use of supports was not new at the time. Many research laboratories had demonstrated the advantages of using various supports for the active centers. The 1953 discovery by Hogan and Banks [28] of the chromium catalyst supported on silica is an example of the use of a support. Many compounds, including OH containing  $\text{SiO}_2$  and  $\text{Al}_2\text{O}_3$ , and magnesium alkoxides were extensively investigated.

These support materials will be described in general terms.  $\text{MgCl}_2$ , which was found to be the most promising, will be discussed in more detail below.

*Hydroxyl-Containing Supports.* As mentioned above, one of the most well known catalysts prepared with this type of support is the Phillips chromium oxide based catalyst for polyethylene production. By heat- and/or chemical treatment with, for example, carbon monoxide (CO) or triethyl aluminum (TEA), the amount of surface hydroxyls that can chemically anchor the transition metal to the surface through an O-M bond, can be precisely controlled. Union Carbide developed the chromocene-based  $(\eta^5\text{-C}_5\text{H}_5)_2\text{Cr}$  catalysts, chemically linked to the  $\text{SiO}_2$  surface [58]. Reaction of  $\text{Mg}(\text{OH})\text{Cl}$  with titanium give a particularly suitable support in which Ti was chemically linked to Mg as shown in the reaction:



This procedure yielded a high activity catalyst, but the isotactic content of the polypropylenes prepared were generally low [59]. Fairly high crystallinities were obtained with some of these catalysts [60]. This suggests that either small  $\text{TiCl}_3$  crystallites are present or that the surface of  $\text{Mg}(\text{OH})\text{Cl}$  at the center has the required geometry to give isotactic insertion of the monomer [61]. The Cabot catalyst [62,63] utilizes silica as the support with the titanium fixed via the reaction:



Cabot, ICI, Union Carbide, Solvay, Mitsui, B.F. Goodrich, Montecatini and Hoechst filed a series of patents dealing with catalysts supported on compounds containing surface hydroxyl groups [26,43].

*Magnesium Alkoxide Supports.* While the transition metals are chemically bound to the hydroxyl-containing supports discussed above, it was found that catalysts need not be anchored to the support to be active. These catalysts are produced by reaction of magnesium alkoxides with transition metal halides [26]. This reaction forms a mixture consisting of magnesium chloride, magnesium alkoxide,

magnesium(alkoxy)halide and magnesium-titanium complexes such as  $\text{Mg}(\text{TiCl}_n)(\text{OR})_m$  where  $n + m = 6$  [64]. During preparation of these catalysts, the crystal structure of the magnesium alkoxide is completely destroyed [65], leading to an increased surface area. This material could be further modified by the introduction of complex magnesium alkoxides such as  $\text{Li}_2[\text{Mg}(\text{OC}_2\text{H}_5)_4]$  or by carrying out the reaction in the presence of an acid halide such as  $\text{SnCl}_4$  [26]. Böhm [66] described an amorphous, porous catalyst with a surface area of  $60 \text{ m}^2/\text{g}$  prepared from  $\text{Mg}(\text{OEt})_2$  and  $\text{TiCl}_4$  using  $\text{AlEt}_3$  as cocatalyst. From analysis of the polymerization kinetics using this catalyst Böhm concluded that up to 75% of all titanium atoms are active during polymerization. In a later study Böhm [67] determined that the optimum fraction of active titanium to be 75% for reactions performed at reaction temperatures between 65 and 85°C. During polymerization these porous structures disintegrate completely resulting in very small residual catalyst particle sizes. Hoechst, Solvay & Cie., Standard Oil, Shell and Phillips, amongst others, hold patents on catalysts based on the reaction products between magnesium alkoxides and transition metal compounds [26].

*Magnesium Chloride Supports:* Judged from the vast amount of academic and patent literature on supported polyolefin catalysts, magnesium compounds are probably the most extensively studied of all support materials. Some of the best catalysts for polypropylene manufacture are derived from  $\text{MgCl}_2$  [68]. The main reasons for the success of  $\text{MgCl}_2$  as a catalyst support are summarized below [57]:

- $\text{MgCl}_2$  has crystalline forms similar to  $\text{TiCl}_3$  [68].
- $\text{MgCl}_2$  has desirable morphology as a support. The structure can resist particle break-up during handling but is still weak enough to disintegrate during polymerization.
- $\text{MgCl}_2$  has a lower electronegativity as compared to other metal halides. According to Soga [69] this will increase ethylene polymerization productivity.
- $\text{MgCl}_2$  is inert to chemicals used for polymerization and can be left in the polymer without necessitating deashing.

Early patents by Shell [70], Mitsui Petrochemicals [71,72] and Montecatini-Edison [73] described the preparation of high yield catalysts exhibiting good stereocontrol. These initial patents describe two distinct routes for catalyst preparation. Typically, dried, anhydrous  $\text{MgCl}_2$  is ball-milled for 20 hours at about  $5^\circ\text{C}$  in the presence of an electron donor such as ethyl benzoate prior to  $\text{TiCl}_4$  treatment at 80 to  $120^\circ\text{C}$ . After washing with n-heptane, the catalyst contains between 1 and 5 % Ti and 5 to 20 % ethyl benzoate (Mitsui). Alternatively, a complex such as  $\text{TiCl}_4$ ·ethyl benzoate is ball-milled with dried, anhydrous  $\text{MgCl}_2$  followed by washing with n-heptane (Montedison). Both these types of catalysts contain the electron donor *in* the catalyst structure, (an *internal donor*) and both are used with a combination of  $\text{AlEt}_3$  and an *external donor* such as ethyl benzoate, *p*-ethyl anisate *etc.* Ball-milling in the presence of ethyl benzoate for example, stabilizes the small  $\text{MgCl}_2$  crystallites to prevent re-aggregation by complexing with the freshly cleaved surfaces [74]. Crystal break-up occurs in the Cl-Mg-Cl double layer, similar to  $\text{TiCl}_3$ , by these layers sliding over each other as a result of the shear forces during milling. This results in the formation of stacking faults [75] which provides sites for  $\text{TiCl}_4$  attachment. Montedison was the first [26] to disclose the use of  $\text{MgCl}_2$  in an active form in these types of catalyst [76] and optimization of the preparation method using the most suitable stereomodifiers led to the discovery of highly active and stereospecific catalysts supported on  $\text{MgCl}_2$  [77]. The polyolefin did not require the expensive catalyst residue removal step. Barbé *et al.* [68] mentioned that earlier results [78,79,80,81] demonstrated the following principal features:

- The catalysts displayed very high initial activity followed by rapid decay to reach a stationary state of much lower activity
- Maximum productivity occurred at a reaction temperature of  $60^\circ\text{C}$
- An increase in isotacticity index with temperature reached a maximum at  $70^\circ\text{C}$
- Stereospecificity was inversely related to productivity
- Reversible variation of catalyst activity and stereospecificity was achieved by varying the aluminum alkyl / donor ratio
- An absence of monomer diffusion phenomena was noted

These results were rationalized by assuming chemical deactivation of some of the centers. At least two types of species should be present on the catalyst surface *viz.* i.) unstable isospecific centers and ii) more stable slightly specific centers. It is thus clear that the decay in polymerization rate must be the result of chemical deactivation of the active centers. Keii and Doi [80,81] theorized on a bimolecular disproportionation reaction between active species with a consequent reduction by the cocatalyst of  $Ti^{3+}$  to  $Ti^{2+}$ .  $Ti^{2+}$  is inactive in the polymerization of propylene. Spitz [78,79] on the other hand found strong correlations between deactivation and donor concentration and type. It follows from various studies that the deactivation kinetics cannot be related to a single model according to a simple first and second order relationship. The kinetics seem to follow a more complicated behavior due to different sites having different stabilities, activities and stereospecificities decaying at different rates. It has been reported that different internal and external electron donors reduce the catalyst rate decay [82]. Replacing ethyl benzoate as internal donor with dialkyl phthalates such as diisobutyl- or diisooctyl phthalate and replacing of *p*-ethyl anisate as external donor with silane compounds such as phenyltriethoxysilane in combination with the cocatalyst was found to result in more stable rate-time profiles. The activity and stereospecificity of a catalyst system is however, not the only criteria making it commercially viable. New and sophisticated requirements in terms of process and product quality raised the performance expected from the catalyst in terms of its ability to allow control over polydispersity, stereoregularity, branching, particle shape, size and distribution, comonomer incorporation and distribution *etc.*

#### 2.1.5.4 Fourth Generation Ziegler-Natta Catalysts – Catalyst Architecture

It has long been known that the polymer particle mimics the shape and size distribution of the catalyst particles and the replication factor of the conventional catalysts is between 7 and 10. Sometimes, when the catalyst activity is very high, exploded popcorn-like particles are produced [53]. Arzoumanidis found that low-yield propylene polymerization using these high activity catalysts gave a prepolymerized catalyst in which the purple  $Ti^{3+}$  particles inside the polymer particles can be observed under polarized light.



The key discovery in the development of high activity third generation catalysts was the recognition of the importance of initiator system architecture. This is an intricate combination of the chemical ingredients together with the physical properties of the support itself, which mutually influence the type and amount of active sites, crystal dislocations, accessibility of monomer and selectivity of these active sites [37]. The importance of a delicate balance between the chemical and physical properties of these catalysts can be realized.

The three-dimensional shape of the initiator particle can be duplicated by the growing polymer particle if the monomer has equal access to any active site, on the surface as well as on the inside of the particle. As monomer reaches an initiator particle, polymer starts growing from the most accessible sites, not only on the surface but also on the inside of the particle, causing the particle to expand. For true replication, the activity of the active sites should be in balance with the mechanical strength of the particle. If the structure is too weak, the forces generated by the growing polymer chains shatter the initiator particles into a fine powder. If the structure is too strong, growth is hampered by the volume restrictions of the polymer chains growing inside the particle. The requirements for this super-active initiator system was summarized by Galli and Haylock [37]:

- High surface area
- High porosity with a large number of cracks evenly distributed throughout the mass of the particle
- Mechanical strength high enough to withstand mechanical processing but low enough to allow the forces developed by the growing polymer chains to break down the granule into microscopic particles that remain entrapped and dispersed in the expanding polymer granule
- Homogeneous distribution of active sites
- Free access of monomers to the innermost regions of the initiator particle

Preparation of the high activity phthalate based catalysts may involve the usual ball-milling procedures but precipitation [83,84,85] or spray-drying [86,87] of magnesium chloride-alcoholate supports offers a distinct advantage. In this process uniform,

spherical initiator granules can be produced. In this regard, Himont developed the *Reactor Granule Technology* processes for polypropylene (Spheripol) and polyethylene (Spherilene) which produce large (up to 5 mm) uniform, spherical polymer particles directly in the reactor with a replication factor of up to 50 [37,88]. By changing porosity and active site distribution, mass and heat transfer can be controlled such that different polymerization rates (and indeed different copolymers if a further monomer is introduced during polymerization) can be obtained in the interior and on the surface of the catalyst particle. With this type of catalyst it is thus possible to produce the usual sticky high comonomer content copolymers such as high rubber content impact polypropylene or very low and ultra low density polyethylenes in the form of free-flowing particles without equipment fouling. It is thus possible to handle these resins in gas-phase processes and because of simplified solvent separation, entire sections of the polymerization process could become obsolete in slurry processes using this technology.

#### 2.1.6 HOMOGENEOUS VANADIUM CATALYSTS

Many vanadium compounds are active polymerization catalysts for olefins and the catalyst have found widespread application for the production of ethylene / propylene rubbers (EPR) and sulfur vulcanizable ethylene / propylene / diene (EPDM) terpolymers. The rubber is cross-linked through its built-in unsaturation. Between 3 and 9% non-conjugated dienes such as 1,4-hexadiene can be introduced as a third monomer. EPDM is extensively used in the automotive industry e.g. for window seals, radiator hoses, weather strips and basically any non-tire application [89]. Small quantities of EPR blended with an isotactic propylene homopolymer results in a dramatic increase in polymer low temperature flexibility properties [90]. Due to their saturation, these rubbers are cross-linked through free-radical initiators

Syndiotactic polypropylene can be produced with  $VCl_4$  using  $AlEt_3$ ,  $AlEt_2Cl$  or  $AlEt_2Cl$ /anisole as cocatalyst. Similar results can be obtained with the catalyst system  $V(\text{acetylacetonate})_3 / AlEt_2Cl$ . The catalyst components should be reacted at low temperatures, typically well below  $-40^\circ C$  with the ratio  $Al:V = 3-10:1$  for  $VCl_4$  [43].

## 2.2 OVERVIEW OF THE THEORY OF ZIEGLER-NATTA POLYMERIZATION

### 2.2.1 MECHANISMS OF ZIEGLER-NATTA POLYMERIZATION OF OLEFINS

#### 2.2.1.1 Early Mechanisms

##### A. Insertion Mechanisms of Ziegler and Natta

After his discovery of the ethylene polymerization reaction Ziegler proposed a mechanism involving the role for tri-ethyl aluminum. Ziegler suggested the olefin “aufbau” reaction in which a polarized ethylene molecule is inserted in stepwise fashion at an anionic aluminum-carbon bond [91]. Natta’s earliest mechanism was in essence an extended version of the “aufbau” reaction applied to propylene [92] but the configuration of the inserting propylene molecule was not outlined. He considered two very important transfer mechanisms; Firstly a  $\beta$ -hydrogen elimination from the polymer chain to form a metal hydride and an unsaturated chain end and secondly,  $\beta$ -hydrogen transfer to an incoming monomer, which released an unsaturated polymer chain from the metal center.

##### B. Radical Mechanisms

Nenitzescu *et al.* [93] proposed a mechanism in which a chlorine atom is displaced from the  $\text{TiCl}_4$  by an alkyl group from the aluminum alkyl. The reaction entailed reduction of titanium from an oxidation state of  $\text{Ti}^{4+}$  to  $\text{Ti}^{3+}$  while the released alkyl radical was believed to polymerize ethylene. Friedlander and Oita [94] considered the effects of the catalyst surface on the insertion reaction and proposed a mechanism whereby an electron is released from the transition metal surface to a chemisorbed olefin molecule which in turn transferred another electron to an adjacent molecule. Polymer growth therefore was proposed to take place via bound radicals, thereby replicating the shape of the catalyst particle.

### C. Anionic Mechanisms

Gilchrist [95] proposed an anionic mechanism in which transfer of an alkyl group from the adsorbed metal alkyl to an adsorbed olefin resulted in an anionic olefin-alkyl molecule. The unbound anion continuously added to adsorbed olefin molecules on the surface. Both anionic and radical mechanisms have now been discounted because evidence from three crucial experiments have indicated that the monomer is inserted into a metal-alkyl bond [96]:

- $^{14}\text{C}$ -labelled aluminum alkyls gave polymers containing labeled carbon atoms
- Quenching reactions using *e.g.* tritiated methanol introduced tritium into the polymer
- Chain transfer reactions involving deuterium or tritium yielded the appropriate label in the polymer

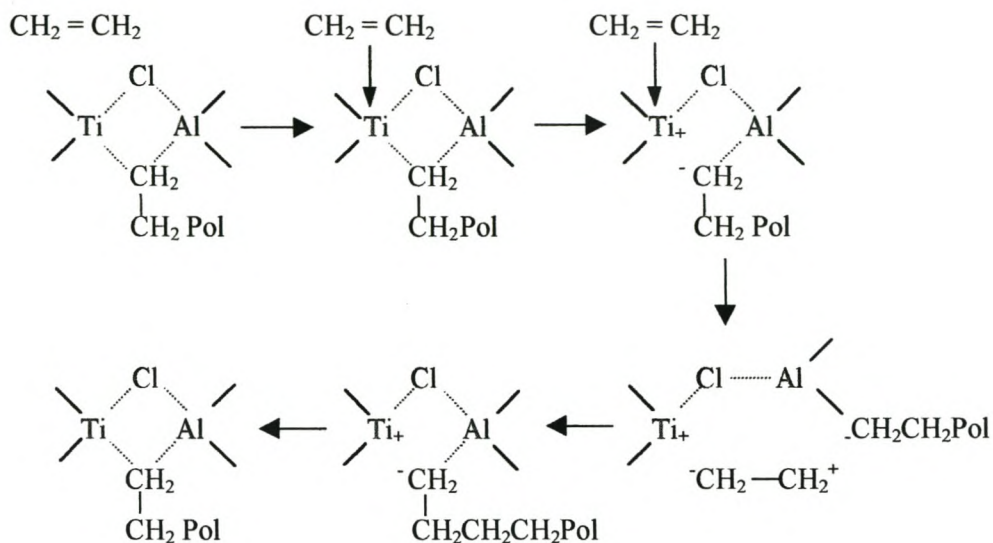
#### 2.2.1.2 Bimetallic Mechanisms

##### A. The Uelzmann Mechanism

In Uelzmann's [97,98] bimetallic mechanism, reaction between  $\text{TiCl}_3$  and an aluminum alkyl forms the  $(\text{TiCl}_2)^+(\text{AlR}_3\text{Cl})^-$  ion pair. The titanium attracts an olefin molecule which subsequently aligns itself along the Ti-Al axis and inserts into an Al-R bond.

##### B. The Natta and Mazzanti Mechanism

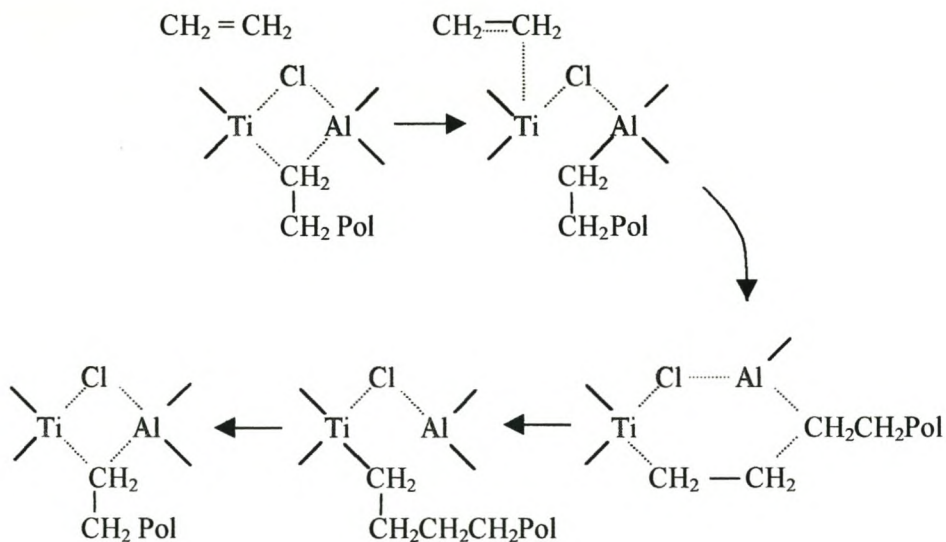
The mechanisms of Natta and Mazzanti [99] and Patat and Sinn [100] are essentially similar. In these mechanisms the titanium, halogen, aluminum and methylene from one of the alkyl groups (or the polymer chain) form a four-membered ring that is opened up at the Ti-C bond when an olefin coordinates with the titanium, forming a six-membered configuration which allows insertion of the olefin before reverting back to the four-membered ring.



### Olefin Polymerization Mechanism According to Natta and Mazzanti

In Natta's mechanism, the olefin forms a  $\pi$ -bond with the titanium and simultaneously assists with cleaving of the Ti-C bond. Thereafter the olefin is polarized in a six-membered configuration before being inserted into the Al-C bond.

#### C. The Patat and Sinn Mechanism



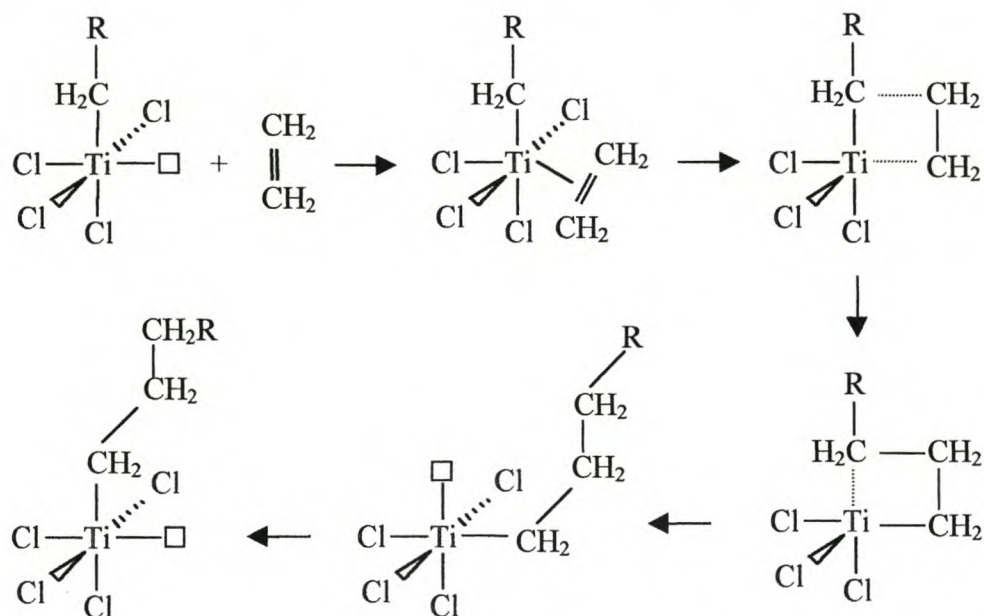
### Olefin Polymerization Mechanism According to Patat and Sinn

In the mechanism proposed by Patat and Sinn the coordinated olefin in the six-membered ring forms a  $\sigma$ -bond with the methylene in the Al-C bond, the latter breaking and reforming a partial bond with the carbon attached to the titanium.

### 2.2.1.3 Monometallic Mechanisms

#### A. The Cossee-Arlman Mechanism

Mechanisms proposed by Nenitzescu *et al.* [93], Carrick [101] and Breslow *et al.* [102] were developed by Cossee [103,104,105] and supported with molecular orbital calculations. The mechanism devised by Cossee [103], with a contribution by Arlman [106], is currently the most widely accepted mechanism explaining olefin insertion into a transition metal-carbon bond. Arlman realized that a vacancy must exist on the surface of the  $\text{TiCl}_3$  crystal. Cossee developed this idea further into a model in which the active center in titanium has an octahedral arrangement of four chlorine atoms, one alkyl group from the alkyl aluminum and a vacant site.



#### Olefin Polymerization Mechanism According to Cossee and Arlman

An olefin coordinates at the vacant site thereby forming a four-membered transition state with the titanium and the methylene of the Ti-C bond. Thereafter the latter bond

breaks and new Ti-C and C-C  $\sigma$ -bonds form between titanium, the last inserted monomer and the previously attached alkyl group. This process regenerates the vacancy, but it is then situated in the position previously occupied by the alkyl group. In order to explain the formation of isotactic polyolefins from these (heterogeneous) types of catalysts, migration of the (new) alkyl group is required in the last step to restore the original configuration of the active site.

## **B. The Trigger Mechanism**

Even though the back-flip of the polymer chain is considered a weakness in the Cossee-Arlman mechanism, it has been widely accepted. However, many other observations can not be explained through this mechanism [107]:

- The free, acidic coordination site is not attacked by Lewis bases
- The isospecific propagation rate is higher than the aspecific propagation rate
- Stereoregularity of the first inserted monomer is lower than the subsequent insertions
- The polymerization rate order relative to monomer is higher than 1

Ystenes [108] proposed the trigger mechanism where the insertion of a complexed monomer molecule is triggered by an incoming monomer. In this mechanism the coordination site is always occupied by a coordinated monomer which will insert only when the next monomer is ready to coordinate. Attack from Lewis bases is thus not possible. Stereochemical discrimination occurs when the next monomer enters the complex and is controlled by the interactions between the complexed and incoming monomer and the other ligands in the complex. In this mechanism, complexation of the first monomer is much more difficult and active center formation requires the action of a monomer unit. Thus, the number of active centers are dependent on the monomer concentration.

### 2.2.1.4 Stereoregulation With Heterogeneous Catalysts

#### A. Propagation Errors

Stereospecific polymerization with typical Ziegler-Natta catalysts produce polymers that are not totally regular [109]. One of the propagation errors that may occur, apart from the normal 1,2 or head-to-tail addition of monomer units is 2,1 and 1,3 regioirregular insertions. A 2,1-misinsertion leads to a dormant active site which may be reactivated through the incorporation of the defect into the chain, but in the presence of hydrogen, will almost always lead to chain transfer rather than further propagation [110].

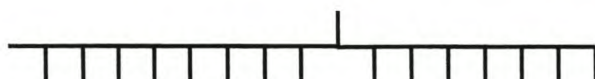
Even highly isotactic chains, insoluble in boiling heptane contain between 1-5% steric defects. These types of stereo errors may be caused by two types of control mechanisms acting on the growing chain [111]. The first type of stereo error, originating from the chain end itself (chain end control), results in the switching of the side group from the one side to the other side of the chain:



This can happen if the placement of the next monomer unit is controlled by the chirality of the last inserted monomer. If the last inserted monomer was erroneously placed (by some unspecified mechanism) with its side-group on the opposite side of the chain, placement of subsequent monomer units continue with this trend.

Another mechanism which is more in line with the mechanism proposed for heterogeneous catalyst systems concerns the reattachment of a growing chain to a catalytic site with opposite chirality.

A second type of stereo error may result in a single misplaced monomer:





In this case, the chirality of the active site controls the placement of each monomer and any misinsertion is automatically corrected during the next addition step. Numerous experimental data from  $^1\text{H}$  and  $^{13}\text{C}$  NMR spectroscopic analysis of polypropylene and poly(1-butene) demonstrated that this “enantiomorphous control” mechanism operates during isospecific polymerization with heterogeneous Ziegler-Natta catalysts. For the above sequences, standard NMR notation is *mmmmrmmmm* and *mmmmrrmmmm* respectively. At triad level, for chain end control, no *rr* sequences should be present whilst for enantiomorphous control, both *rr* and *mr* triads should be present and in a 1 : 2 ratio. It was shown that the *rr* and *mr* triads exist in polypropylene [112] and poly(1-butene) [113] in a 1 : 2 ratio [114]. Further evidence based on  $^{13}\text{C}$  NMR analysis of isotactic polypropylene with low amounts of copolymerized ethylene confirmed the enantiomorphous control. If steric control was due to the chirality of the last inserted monomer, insertion of a propylene unit following insertion of an achiral ethylene molecule would be non-stereospecific [115].

## **B. Internal and External Electron Donors**

Natta and coworkers found that stereospecificities of polypropylene prepared with the Ziegler catalyst were in the range 20 – 40 % depending on reaction conditions [116]. Dramatic improvement in tacticity up to 95% was achieved by using  $\alpha$ ,  $\gamma$  or  $\delta$  crystal modifications of  $\text{TiCl}_3$  together with trialkyl aluminums or dialkyl aluminum halides [117,118]. The tacticities of heptane insoluble fractions were found to be highly stereoregular which suggested that there were two main types of catalytic sites present in different proportions, the one which produced atactic polymer and the other which produced isotactic polymer. It was thus realized that the route to highly isotactic polymers was to selectively poison the aspecific sites. Consequently, many electron-rich compounds including ethers, esters, amines, aldehydes, alcohols, ketones, organic acids *etc.* [30] were found to be effective at increasing tacticity. The second generation self-supported  $\text{TiCl}_3$  catalysts were used with one or more internal (added as part of the catalyst preparation steps) and/or external (added in combination with the aluminum alkyl) modifiers such as diisoamyl ether used in the Solvay catalyst [49] as third component. Some of the advantages of using an electron donor include

increased isotactic content of the polymers produced, together with increased activity [119]. It was suggested [120] that the activating effect observed was due to the deactivation of the known catalyst poison ethyl aluminum dichloride which forms by reaction between diethyl aluminum chloride and  $\text{TiCl}_3$ . Above a certain concentration, an electron donor can poison [121] or block [122] the active site, leading to a decrease in activity.

Although catalyst activities up to 200 times higher were obtained by supporting the active titanium species on magnesium dichloride, tacticities were between 20 and 50% [56]. Simply adding electron donors to the catalyst system did increase isotacticity but catalyst activity was severely affected. In contrast, with  $\text{TiCl}_3$  it was found that  $\text{MgCl}_2$ -supported catalysts required the use of both internal and external electron donors [123] to obtain high isotacticity without seriously decreasing catalyst activity [124]. Catalyst preparation includes treatment of the  $\text{MgCl}_2$  with the electron donor during support preparation before  $\text{TiCl}_4$  treatment to yield a catalyst containing an internal donor. Together with triethyl aluminum, these catalysts exhibit activities 20 times higher than conventional  $\delta\text{-TiCl}_3$  but isotacticity index is about 50%. By using this catalyst with a 3:1 mixture of triethyl aluminum : donor, isotacticities of up to 98% have been obtained [125].

Donors also have a great influence on composition distribution and comonomer content. Sacchi *et al.* [126] found through fractionation experiments of propylene / 1-butene copolymers that the internal donors selectively poison the least stereospecific sites while cooperation between internal and external donors produce new active sites that are more selective towards the incoming monomer. Xu *et al.* [127] showed through TREF analyses of low 1-butene content propylene copolymers that internal and external donors enhance tacticity differently and that comonomer content is reduced by both internal and external donors.

### 2.2.1.5 Kinetic Models

#### A. Early Models

The kinetic behavior of a catalyst can be depicted in terms of the conversion of monomer to polymer during a certain period of time. Such curves typically present polymerization rate vs. time, derived from the amount of polymer formed during certain time intervals. Catalysts can thus be classified according to the type of kinetic rate-time curve it produces during polymerization of a specific monomer under specified conditions. These curves consist essentially of three periods *viz.* acceleration, steady state and decay periods. Factors that may influence the type of kinetic behavior displayed include cocatalyst used, monomer, monomer pressure, polymerization temperature and polymerization medium [128].

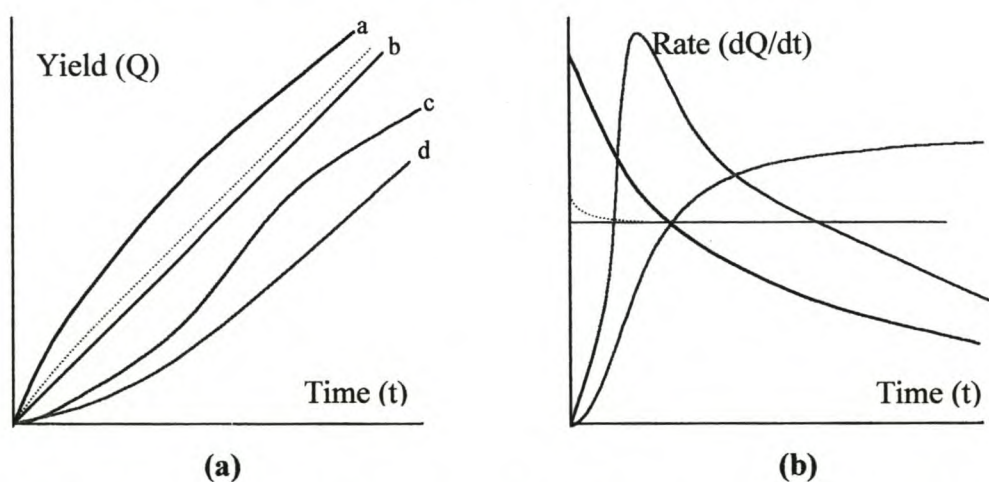


**Figure 2.1. Different Polymerization Kinetics Illustrated through different Yield / Time and Rate / Time Curves**

Type (a) behavior exhibits decay-type kinetics and is shown by many high-activity catalysts such as  $\text{MgCl}_2\text{-EB-TiCl}_4$ . In this case the initial polymerization rate is high or a high activity is rapidly achieved, followed by a rapid decrease in polymerization rate [128].

Type (b) behavior shows a situation where polymerization activity is constant with time or settles to constant activity very soon after the start of polymerization. This

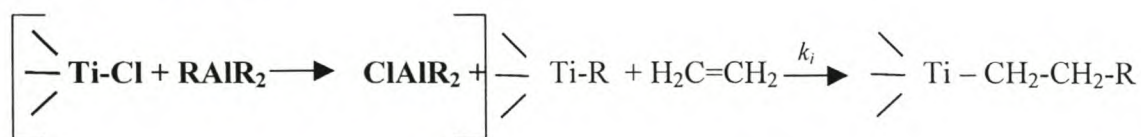
behavior is shown by  $\text{Cp}_2\text{TiCl}_2$ -MAO for ethylene polymerization [129] and by a  $\delta$ - $\text{TiCl}_3$ - $\text{AlEt}_2\text{Cl}$  catalyst used for polymerization of 4-methyl-1-pentene [130].

Type (c) behavior can be observed when trialkyl aluminum is used as cocatalyst [96] with a catalyst such as the  $\delta$ - $\text{TiCl}_3 \cdot \frac{1}{3}\text{-AlCl}_3 \cdot \frac{1}{3}\text{BNP}$  /  $\text{AlHexyl}_3$  (BNP = *n*-propyl benzoate), used for the polymerization of 3-methyl-1-butene [131]. The catalyst activity increases to a maximum after which it decreases throughout the polymerization.

Type (d) behavior is shown by many first generation catalysts using diethyl aluminum chloride as cocatalyst. This profile shows an acceleration period after which a steady state is reached. It was established that the number of active sites increase during polymerization through breakdown of the solid catalyst matrix. This exposes fresh titanium atoms on the newly formed surfaces which are then activated and then participate in the polymerization reaction, thus increasing the polymerization rate until no further breakdown occurs [132].

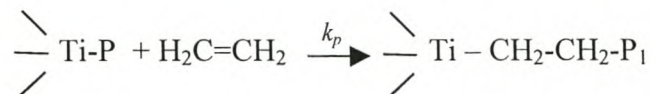
Several steps have been identified in Ziegler-Natta catalyzed olefin polymerization reactions *viz.* initiation, propagation, transfer and termination.

*Chain Initiation:* This step concerns the insertion of the first monomer unit into the metal-carbon bond of an active, alkylated titanium polymerization site at a specific rate  $k_i$  according to:



The rate constant for subsequent initiation after chain transfer, where an active site which had already formed polymer was reinitiated, may be different from that of the virgin site [133]. All active sites may not be immediately available and this can be observed in the acceleration period which may have a duration of a few minutes up to several hours [134].

*Chain Propagation:* The subsequent insertions of monomer units into a metal-carbon bond proceeds at a rate  $k_p$  according to:

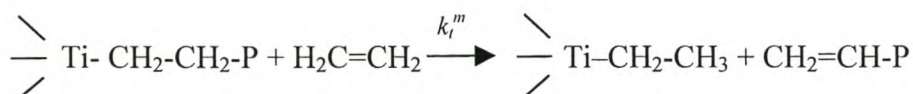


It is known that all centers are not equally active and the activity depends on the location of the site on the catalyst surface, shielding of the sites by modifiers etc. The propagation rate is therefore considered to be the average of the propagation rates of all active species.

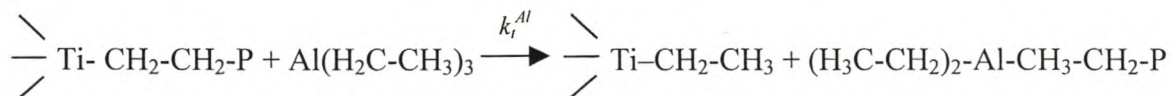
*Chain Termination:* This is the process where a growing polymer chain is detached from the metal center. This can occur through various transfer reactions including monomer, alkyl aluminum, polymer, added transfer agents such as  $\text{H}_2$  and, less important, spontaneous transfer [96].

Some examples include:

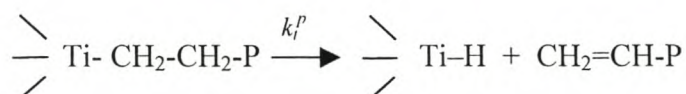
With monomer, resulting in terminal unsaturation:



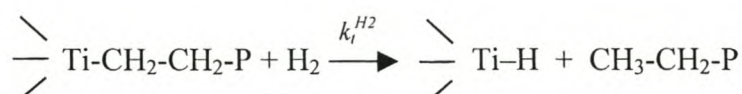
With alkyl aluminum:



Via  $\beta$ -Hydrogen elimination from the polymer chain to give terminal unsaturation:



With  $\text{H}_2$ :



The maximum molecular weight attainable with a specific catalyst system can be estimated along the lines followed by Kissin [134]. The concentration of all active centers ( $C^*$ ), proportional to the amount of catalyst, is the sum of propagating centers ( $C_p^*$ ) and centers being initiated ( $\sum_j C_I^*$ ).

$$C^* = C_p^* + \sum_j C_I^* \quad (2.1)$$

Under steady state conditions, the rate of initiation is equal to the rate of transfer which in turn is equal to the sum of all transfer reactions. As no initiation reaction can take place in the absence of monomer, it is clear that initiation reactions are dependent on monomer concentration. Thus, for transfer reactions with monomer, alkyl aluminum, polymer and hydrogen respectively:

$$k_i' C_i' [M] = k_t^m C_p^* [M] \quad (2.2)$$

$$k_i'' C_i'' [M] = k_t^{Al} C_p^* [Al] \quad (2.3)$$

$$k_i''' C_i''' [M] = k_t^P C_p^* [P] \quad (2.4)$$

$$k_i'''' C_i'''' [M] = k_t^{H_2} C_p^* [H_2] \quad (2.5)$$

where  $k_i'$ ,  $k_i''$  etc. are the rate constants for initiation after each individual type of transfer reaction. From Equation 2.4 (transfer reaction with polymer) it can be seen that the concentration of polymer equivalent to the number of chains bonded to a metal center is therefore equal to the concentration of propagating active centers. It can be shown that:

$$C_p^* = C^* (1 + k_t^m / k_i' + k_t^{Al} [Al] / k_i'' [M] + k_t^P [P] / k_i''' [M] + k_t^{H_2} [H_2] / k_i'''' [M])^{-1} \quad (2.6)$$

In the presence of hydrogen and at high monomer concentrations, transfer reactions to polymer and alkyl aluminum become insignificant, leading to:

$$C_p^* = C^* (1 + k_t^{H_2} [H_2] / k_i'''' [M])^{-1} \quad (2.7)$$

The rate of polymerization depends on catalyst and monomer concentration and the steady state polymerization rate, hence:

$$R_p = k_p C_p^* [M] \quad (2.8)$$

and by substitution of  $C_p^*$  from Equation 2.7:

$$R_p = k_p C^* [M] / (1 + k_t^m / k_i + k_t^{H_2} [H_2] / k_i [M]) \quad (2.9)$$

*i.e.* the rate of polymerization is directly proportional to the monomer concentration and amount of catalyst and inversely proportional to the amount of hydrogen present.

The degree of polymerization is given by:

$$P_n = k_p / (k_t^m [M] + k_t^{H_2} [H_2]) \quad (2.10)$$

However, transfer reactions to polymer and alkyl aluminum are significant, and when the reciprocal of the degree of polymerization is taken, Equation 2.10 becomes:

$$P_n^{-1} = [M]^{-1} [(k_t^{Al} [Al] / k_p) + (k_t^p [P] / k_p) + (k_t^{H_2} [H_2] / k_p)] + k_m / k_p \quad (2.11)$$

which is a straight line representing an inverse degree of polymerization versus inverse monomer concentration having an intercept at  $k_m / k_p$  with slope depending on the rate constants and concentration of the various transfer agents. At high monomer concentrations, the contributions of transfer reactions other than monomer becomes less significant and the equation can be reduced to  $P_n = k_p / k_m$ , *i.e.* the degree of polymerization becomes independent on other polymerization variables. When decay type kinetics operate, these steady state kinetic expressions cannot be applied. Factors which take into account the dynamic nature of active center formation and decay, possible diffusion limitation phenomena need also to be considered.

## B. Model of Böhm

Böhm [135] produced a kinetic model which claimed to include all relevant reactions in heterogeneous and homogeneous Ziegler-Natta polymerization reactions [96]. Some of the features of this model, noted by Tait and Watkins, are:

- Complexation between olefin and active site is assumed to be reversible
- Polymer is formed through subsequent insertion reactions
- $\beta$ -Hydrogen elimination takes place via a 6-membered transition state
- Active centers and alkyl aluminum interact reversibly, therefore transfer reactions may result
- Spontaneous transfer to generate a M-H bond is permitted
- Transfer with hydrogen is permitted and may explain the rate decrease sometimes observed in the presence of hydrogen
- An expression relating degree of polymerization to monomer and alkyl aluminum concentration can also be formulated
- An important equation, from which the number of active centers can be derived from molecular weight data, can be obtained

## C. Adsorption Models

As described earlier, many studies were concerned with describing the polymerization reaction by means of adsorption mechanisms. It was suggested by Cossee [136] that under steady state conditions, the rate determining step is the insertion of the monomer into the transition metal-carbon bond. This can be expressed as follows:

$$R_p = (k_1 k_3 / k_2) [M] \{ [MP] + [P] \} \quad (2.12)$$

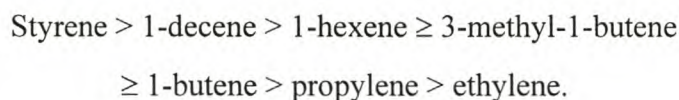
$k_1$  and  $k_2$  are the rate constants for the reversible monomer coordination steps,  $k_3$  is the rate constant for monomer insertion and  $[MP]$  is the concentration of the polymerizing sites to which are attached both a polymer molecule and a coordinated monomer. As the term  $k_1 k_3 / k_2$  actually includes the complete propagation step it is equal to  $k_p$  and  $[MP] + [P]$  is the concentration of active sites participating ( $C_p^*$ ), this equation reduce to Equation 2.8.



### 2.2.1.6 Influence of Electronic and Steric Factors on Olefin Reactivity

In general it is accepted that monomer reactivities in a specific polymerization reaction are compared through their reactivity ratios  $r_1$  and  $r_2$ . A good correlation with the propagation rate constants  $k_p$  exists for copolymerization with heterogeneous Ziegler-Natta catalysts and the reactivities of the different olefins vary over a wide range [137]. By evaluating the influence of the polymer chain on the polymerization activity it was found that  $k_{ii} \neq k_{ij}$  where  $i$  and  $j$  are different last inserted monomer units. Therefore, the reactivity of an active center does not have a constant value, but depends on the structure of the last inserted monomer. Data on the inductive Taft parameters ( $\sigma^*$ ) [138] do not differ substantially and the effect of variation in  $k_{ii} / k_{ij}$  for polymer chains with different last inserted monomer units can be attributed mostly to the steric influence of the last inserted monomer unit. Chains with bulky R groups  $\beta$  to the end- $\text{CH}_2$  group inhibit insertion of the next monomer unit, but no significant effect of the electronic properties of the last inserted unit was found. When styrene derivatives were compared, electronic effects were found to be of greater importance than the steric effects.

If the steric properties of the olefin molecule is neglected, or it is for the moment accepted to be very similar, its donor-acceptor interaction with the active site and last inserted monomer unit in the polymer chain should determine its reactivity. The order of reactivity in this case should be:



The real order found experimentally is the reverse. For the branched olefins reactivity depends strongly on the position and bulkiness of the branch and decrease as the branch comes closer to the double bond. Comparison of the electronic and steric parameters for different linear and branched alkyl groups showed that their  $\sigma^*$  are very similar ranging from  $-0.1$  to  $-2.1$  [139]. Correlation between olefin reactivity and electronic properties of their alkyl groups is meaningless [140]. Although data on steric parameters are scattered, the main tendency observed was that an increase of the bulkiness of the alkyl group in the olefin molecule results in a significant decrease in

its reactivity. It was thus concluded that the steric effects mask any possible electronic influence.

## 2.3 SINGLE SITE CATALYSTS

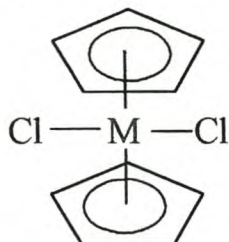
### 2.3.1 METALLOCENES

These catalysts are often referred to as homogeneous Ziegler-Natta catalysts because all the catalyst components are soluble in aromatic hydrocarbon solvents. However, based on the polymerization process and narrow comonomer and molecular weight distributions of the (co)polymers produced, they are generally referred to as single-site catalysts. Metallocene catalysts have been known for a long time. Natta *et al.* [141] showed that a dark red solution is obtained when bis(cyclopentadienyl) titanium dichloride with diethylaluminum chloride were reacted together in aromatic solvents. This solution changed color through green to blue on standing. With triethyl aluminum, the color change to blue is almost instantaneous. The blue compounds obtained from the reaction of bis(cyclopentadienyl) titanium dichloride with alkyl aluminum compounds do polymerize ethylene but with very low activity. For example, the yield of polyethylene produced from reaction at 95°C at a pressure of 40 bar was only 7g/g cat. after 8 hours. A good polymerization rate was obtained by Breslow *et al.* [142] when trace amounts of oxygen was present.

Although the silica supported chromocene catalyst disclosed by Karol *et al.* [58] and commercialized in the '70s by Union Carbide for the production of HDPE, can be considered a metallocene catalyst, unlike the conventional metallocenes, it is inactive if not supported and is very selective towards ethylene and does not incorporate comonomers. The chromocenes will therefore be disregarded in this discussion on metallocenes, which are mostly based on the group IV transition metals.

Water has always been considered a catalyst poison for Ziegler-Natta catalyst systems [143] although a considerable increase in activity was observed for the  $(\eta^5\text{-C}_5\text{H}_5)_2\text{Ti}(\text{C}_2\text{H}_2)\text{Cl}-(\text{C}_2\text{H}_2)\text{AlCl}_2$  catalyst system when water was added in a 1:5 Al:H<sub>2</sub>O ratio. An early investigation by Grogorjan *et al.* [144] showed that the reaction between water and trimethyl aluminum results in the formation of cyclic oligomeric species with a repeat unit  $[-\text{O}-\text{Al}(\text{Me})-]_n$ . By using this methyl aluminoxane (MAO) as cocatalyst with bis(cyclopentadienyl)dimethyltitanium

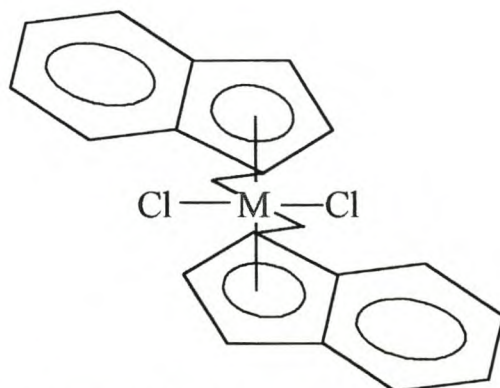
( $\text{Cp}_2\text{TiMe}_2$ ), productivity for ethylene was found to be almost  $10^6$  g/g Ti [64], although the molecular weight was low and the catalysts were aspecific. Atactic polypropylene was produced and the tacticity was related to the active center having  $\text{C}_{2v}$  symmetry, *i.e.* no preferred orientation of the incoming monomer was possible.



**Aspecific –  $\text{C}_{2v}$ -symmetry**

Reaction rate is expected to decrease as steric congestion increases as was demonstrated by the use of pentamethylcyclopentadienyl ( $\text{Cp}^*$ ) ring systems [145]. However, it was found that both electronic effects (though release of electrons into the ring) and steric effects regulate the catalyst activity. Ewen observed an increase in activity and molecular weight with methyl monosubstitution of the Cp rings of a titanium based metallocene catalyst, but by using a bulkier ethyl group, activity decreased. Molecular weight is dependent on chain termination reactions. By releasing electrons into the ring system, the Lewis acidity of the active cationic alkylmetallocenium ion is decreased, thereby decreasing its tendency for termination via  $\beta$ -hydride eliminations [146].

In 1984, Ewen [147] described the use of a chiral homogeneous catalyst to produce partially isotactic polypropylene.

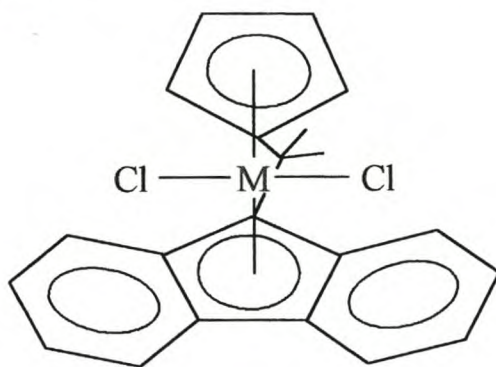


**Isospecific –  $\text{C}_2$  symmetry**

Brintzinger and coworkers synthesized zirconium and titanium derivatives with racemic ethylene-bridged bis(indenyl)- and racemic ethylene-bridged bis(4,5,6,7-tetrahydroindenyl ligands [148,149]. After activation with MAO, these materials catalyzed the highly stereospecific polymerization of propylene, the first time this was achieved with a homogeneous system.

In these cases, the ligand system is such ( $C_2$  symmetry) that the orientation of the incoming monomer is directed by the spatial orientation of the ligands which illustrates the stereochemical control exerted by the ligands. By using a one-atom bridge such as  $Me_2Si$ , the coordination gap aperture is widened resulting in a more active catalyst [150]. Coupled to this decreased steric effect is also an electronic effect, and the combined action brings about changes in reactivity, molecular weight, comonomer incorporation capability and polymer microstructure [151].

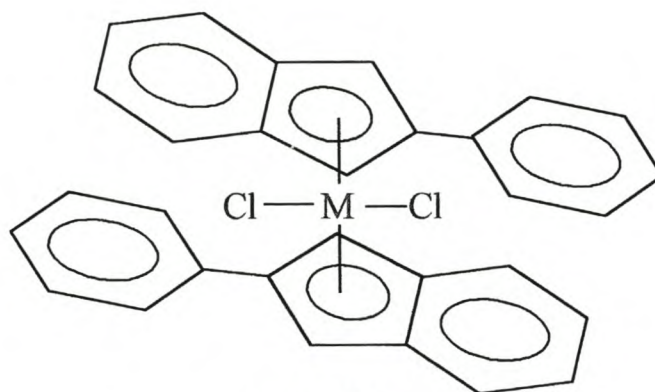
Since these discoveries, many different ligand systems with different ring substituents and bridging groups have been investigated, each having unique catalytic activity and stereoregulating properties.



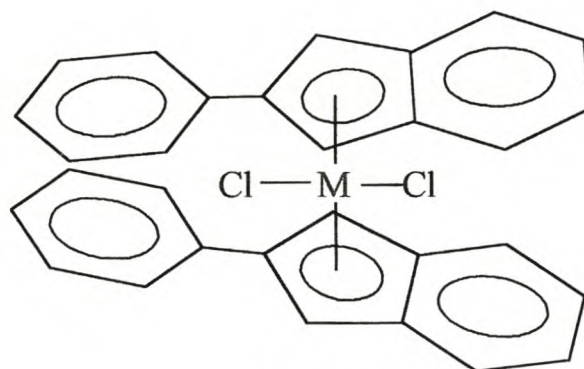
**Syndiospecific –  $C_s$  symmetry**

Syndiospecific polypropylene is normally produced by catalysts having  $C_s$ -symmetry [152]. An example is shown above. By introducing a methyl group onto the cyclopentadienyl ring, the  $C_s$  symmetry is lost and the catalyst forms hemi-isotactic polypropylene where every second methyl group in the chain is aspecifically arranged [153]. Introduction of a bulky group such as a *t*-butyl group instead of methyl leads to the production of isotactic polypropylene.

One very interesting system involves a catalyst containing the unbridged bis(2-phenyl indenyl) ligand which, through ligand rotation, produces both atactic and isotactic blocks [154]. By controlling the rate of rotation by increased or decreased ligand size or polymerization temperature, it is possible to control the sequence lengths of these blocks.



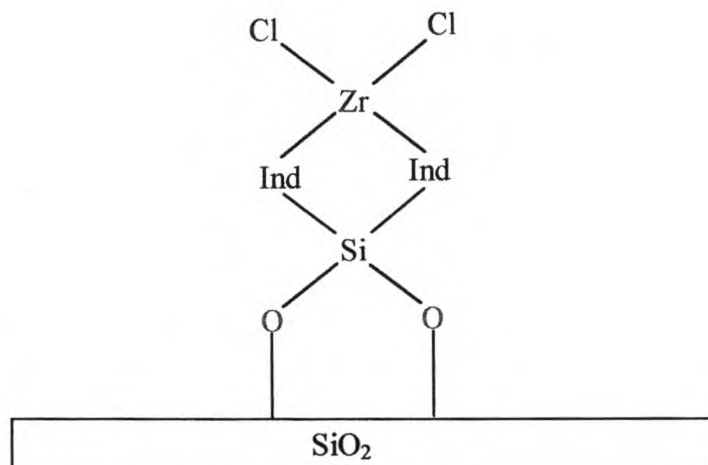
**Isospecific**



**Aspecific**

The amount of MAO used in these metallocene polymerizations are extremely high and it has been shown that the aluminum : metal ratio can range between 400 and 20,000 depending on metallocene type and reaction conditions [155]. Both activity and molecular weight increase with an increase in Al : M ratio [156]. For obvious reasons, this makes the catalyst system prohibitively expensive, which led to developments towards decreasing initiator system costs. One solution that has been fairly successful entails heterogenization of the metallocene complex on a support.

Typically a partially calcined silica is used as support. Heterogenization of the catalyst on a support calcined at 260°C produced a catalyst twice as active as one where the silica was calcined at 460°C [157]. Additional MAO treatment increased catalyst activity even further. A typical example of a metallocene supported on silica is shown below:



**SiO<sub>2</sub>-Supported Bis-Indenyl Zirconium Dichloride Catalyst**

Ziegler-Natta catalysts display broad comonomer and molecular weight distributions because of the presence of different types of active species. The homogeneity of the active sites in single site catalysts results in very narrow comonomer and molecular weight distributions. By supporting different types of single site catalysts at different ratios on the same support (e.g. see Soares *et al.* [158]) it is possible to produce (co)polymers exhibiting narrow to broad and bimodal molecular weight distributions. As the geometries and electronic environments differ between different catalysts, cosupported catalysts also display differences in comonomer incorporation behavior, resulting in non-homogeneous comonomer distributions. By supporting the metallocene complex the aluminum : metal ratio could be reduced to between 50 and 400 [159]. Supported metallocene catalysts are generally less active, probably because of less effective active site formation, but the molecular weight is very high and active sites are much more stable [160]. When Lewis acidic compounds such as Al<sub>2</sub>O<sub>3</sub> or MgCl<sub>2</sub> are used as supports, the resulting supported catalysts can be activated using ordinary trialkyl aluminums. With MgCl<sub>2</sub> as support, the molecular weight distribution also becomes broader [161]. In some cases however, catalyst activities, polymer properties, comonomer incorporation capability and microstructure

are not affected by heterogenization [162]. The key to complete elimination of the use of expensive MAO is to find a cocatalyst that will alkylate the metallocene, stabilize the cationic center in an ion-pair interaction but only weakly coordinate so as not to prevent olefin coordination [156]. In 1986, Jordan *et al.* [163] demonstrated the polymerization of ethylene by the zirconium complex  $[\text{Cp}_2\text{ZrCH}_3(\text{THF})]^+[\text{BPh}_4]^-$ . A most promising example of the stabilized cationic metallocene systems is the  $[\text{Et}(\text{Ind})_2\text{Zr}(\text{CH}_3)]^+[\text{B}(\text{C}_6\text{F}_5)_4]^-$  system developed by Chien *et al.* [164].

### 2.3.2 POST-METALLOCENE SINGLE-SITE CATALYSTS

Giannetti *et al.* [165] reported that the addition of MAO to  $\text{Zr}(\text{CH}_2\text{Ph})_4$  initiated ethylene polymerization with activity similar to conventional metallocene systems. Pellechia *et al.* [166] reported that the active species in compounds such as  $\text{Zr}(\text{CH}_2\text{Ph})_4$ , as well as their monocyclopentadienyl derivatives, are cationic complexes analogous to those of metallocene-based systems; they successfully isolated the  $[\text{Zr}(\text{CH}_2\text{Ph})_3]^+[\text{B}(\text{CH}_2\text{Ph})(\text{C}_6\text{F}_5)_3]^-$  catalytic species. The catalyst activity for ethylene and propylene polymerization is 250 and 1.5 kg mol  $\text{Zr}^{-1}\text{h}^{-1}\text{atm}^{-1}$  respectively and produces a PP containing 20% isotactic polymer.

Another non-metallocene catalyst for ethylene, propylene and styrene polymerization is based on transition metal alkoxides activated with MAO. Titanium complexes with a 2,2'-thio-*bis*(6-*t*-butyl-4-methylphenoxy) (TBP) ligand such as  $(\text{TBP})\text{Ti}(\text{OPr})_2$  is extremely active and produces atactic PP, highly syndiotactic polystyrene (sPS), highly alternating ethylene / styrene copolymers and is active towards dienes and conjugated dienes [167].

Ewen *et al.* [168] reported on catalysts for propylene polymerization where 5-membered heterocyclic compounds are fused to the Cp rings. These heterocenes are stable, highly stereospecific for propylene polymerization with MAO and have activities up to 865 kg PP mol  $\text{Zr}^{-1}\text{h}^{-1}$ .

Xu and Ruckenstein recently reported on a 2-methylbenz(*e*)indenyl-based *ansa*-monocyclopentadienylamido catalyst [169] which was used for ethylene / 1-octene copolymerization. Both high activities and 1-octene incorporation were reported.

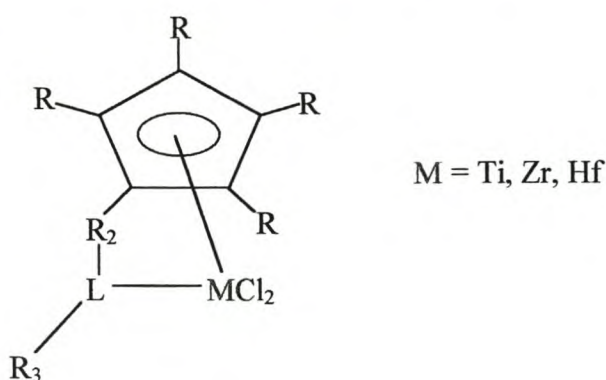


Schaffer *et al.* [170] reported on a  $\text{Me}_2\text{Si}(\text{Cp}^*)\text{cyclodecylamidodimethyl}$  titanium catalyst activated with dimethylanilinium tetrakis(pentafluorophenyl)borate, triphenylmethyl tetrakis(pentafluorophenyl) borate or MAO. This catalyst was used for ethylene / iso-butylene copolymerization. iso-Butylene incorporation up to 45% and activities up to  $400 \text{ kg polymer mol Ti}^{-1}\text{hr}^{-1}$  were claimed.

Miyake [171] reported double bridged metallocenes of the form  $(\text{Me}_2\text{Si})_2\{\eta^5\text{-C}_5\text{H}_3\text{-}(\text{CHMe}_2)\text{-5-Me}\}_2\text{-MCl}_2$  ( $\text{M}=\text{Zr, Ti}$ ). The zirconocenes polymerize propylene to sPP, while the titanocene produces only aPP.

### 2.3.2.1 Dow Constrained Geometry Catalysts

Another class of metallocene catalysts is the so-called constrained geometry catalysts. Shapiro *et al.* were the first to describe scandium based complexes of this type [172]. Stevens *et al.* at DOW developed similar monocyclopentadienyl complexes of titanium, which have been commercialized as INSITE™ Technology [173,174]. This technology is used for the production of polyolefin plastomers, containing <20% 1-octene, and polyolefin elastomers, containing >20% 1-octene.



#### Dow Constrained Geometry Catalyst

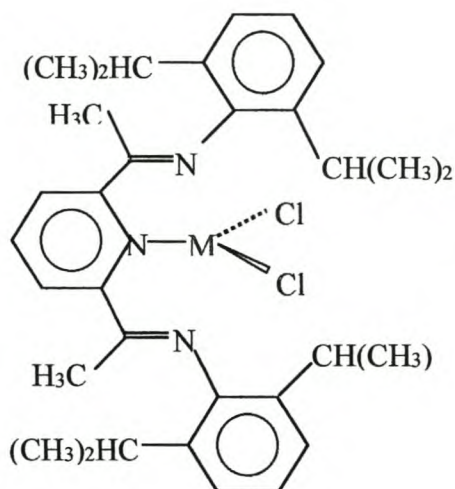
The key features of this type of catalyst are shown in the structure above. In this structure, R and  $\text{R}_3$  are substituents which may be hydrogen, alkyl, aryl or silyl substituents. L is a donor ligand – amide, phosphide, alkoxide - which electronically

stabilizes the metal.  $R_2$  is a bridging group - alkyl, aryl, silyl - which pulls the donor ligand away from its normal position, thereby providing access to monomers at the metal. The open structure does not allow for steric control and these catalysts which can be used with MAO or  $B(C_6F_5)_3$  generally produce atactic to slightly syndiotactic polymers[175]. Used with MAO, the effect of different R groups on ethylene / 1-octene elastomer productivity has been discussed by Stevens [174]. When a silane bridged cyclopentadienyl titanium complex containing an amide donor ligand, methyl ring substituents and a *t*-butyl ligand substituent is used an activity of 150 000 g polymer / g titanium is obtained. By using an ethyl bridge, activity increased to 560 000 g / g Ti. By replacing the Cp ring with a fluorenyl ring and using a *t*-butyl substituent on the amide donor ligand of a Zr-based half-sandwiched catalyst, highly isotactic PP could be obtained [160].

Recently an exciting new system was reported which was produced from a combination of the Dow catalyst and boratobenzene metallocene mimic [176]. This system produced a branched polyethylene. Activities were in the region of 1 200 kg PE mol. Zr<sup>-1</sup>hr<sup>-1</sup>.

#### 2.3.2.2 Brookhart-Gibson Catalysts

A new family of cheap, easy to make catalysts based on chromium and iron was recently discovered independently by the team of Professor Vernon Gibson at Imperial College in London and that of Professor Maurice Brookhart at the University of North Carolina in Chapel Hill [177,178,179]. Based on earlier work with Pd(II) and Ni(II) diimine catalyst systems, Brookhart's team recently reported that these new catalysts based on tridentate pyridine bisimine ligands, containing bulky ortho-substituted aryl rings produced high polymerization activity [180,181]. The complexes, activated with MAO, showed activities similar to that of metallocenes under similar reaction conditions. Branched polyethylenes were obtained. A typical complex is shown below:



### Brookhart-Gibson Catalyst

Development of this new family of catalysts have produced new catalysts which have been characterized by structural analysis. Polymerization behavior with other monomers has been investigated and termination and growth mechanisms by the Brookhart and British teams have been proposed. An ongoing program to explore the commercial advantages of these catalysts is in place.

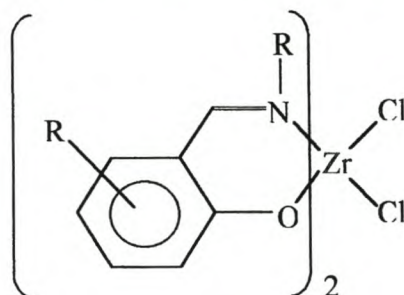
Kim *et al* [182] also reported on Ni(II) and Pd(II) catalysts that produced hyperbranched polyethylenes. Unlike the claim by Brookhart, it was noted that bulky substituents were not necessary to produce branched PE. Unobstructed metal catalysts such as [Ni( $\pi$ -methallyl)Br]<sub>2</sub> or Pd(1,5 cyclooctadiene)(Me)(Cl) together with an excess of an aluminum compound such as AlCl<sub>3</sub> or AlEt<sub>3</sub> were used to obtain highly branched polyethylenes of very low molecular weight (400 – 1 000 g/mole).

True living polymerization of  $\alpha$ -olefins was demonstrated by Brookhart *et al.* [183] using a Ni<sup>2+</sup>- $\alpha$ -diimide catalyst where the molecular weight of polypropylene was shown to increase linearly during the course of the reaction while molecular weight distribution remained constant. True block copolymerization with Ziegler-Natta and conventional metallocene catalysts was previously not possible at common polymerization temperatures [184,185,186] because of rapid chain transfer reactions

[187]. The living character of this catalyst now allows for the development of the first true block copolymerization process for poly( $\alpha$ -olefins).

### 2.3.2.3 Mitsui FI Catalyst

Mitsui Chemicals announced that they succeeded in developing an entirely new ethylene polymerization catalyst of the type shown below [188].



**Mitsui FI Catalyst**

This phenoxyimine complex activated by MAO is highly active and with zirconium as central metal at 25°C and atmospheric pressure its activity is more than ten times that of conventional metallocenes. By changing the ligand structure, polymers from low- to ultra high molecular weight can be produced. Mitsui has suggested that production of novel high polymers via copolymerization of ethylene with polar monomers such as methyl methacrylate and acrylonitrile is possible. It is also mentioned that the catalyst production cost is one-tenth that of metallocene catalysts.

### 2.3.3 POSSIBILITIES WITH SINGLE-SITE CATALYSTS

Homo- and copolymerization with a range of (co)monomers has been made possible by metallocene and single-site catalyst technology [189]. The range of (co)monomers include the following:

- Linear  $\alpha$ -olefins up to C<sub>18</sub>
- Branched  $\alpha$ -olefins such as 4-methyl-1-pentene and 3-methyl-1-butene
- Dienes including 1,3-butadiene and 1,4 dodecadiene
- Aromatics such as styrene, *o*-, *m*- and *p*-methylstyrene, indene
- Cyclic olefins and diolefins such as cyclopentene, dicyclopentene and tetracyclododecene
- Polar monomers including methyl methacrylate, acrylonitrile, acrylic acid, vinyl silane and more recently also 10-undecen-1-ol [190,191,192].

From the preceding description of the properties of the metallocene and single site-catalysts it can be inferred that the main advantages of these catalysts over Ziegler-Natta catalysts include:

- Very high, sustained activities
- Control over different stereospecificities
- Controlled comonomer distribution
- High comonomer incorporation
- Copolymerization with polar comonomers
- Block copolymerization

Disadvantages (with possible solutions) include:

- |  |  |
|--|--|
| • Sometimes extremely laborious preparation procedures | • New catalysts are being developed                |
| • High cost of the catalyst system                     | • New catalysts, processes to decrease MAO content |
| • Poor control over polymer morphology                 | • Supported catalysts                              |
| • Incompatibility with slurry and gas-phase processes  | • Supported catalysts                              |
| • Narrow molecular weight distribution                 | • Co-support of different catalysts                |

## 2.3.4 MECHANISMS FOR SINGLE-SITE POLYMERIZATION OF OLEFINS

### 2.3.4.1 Kaminsky's Model

Based on electron-deficient, penta-coordinated bimetallic complexes, Kaminsky and Steiger [193] proposed that in a  $\text{Cp}_2\text{ZrCl}_2/\text{MAO}$  catalyst, electron density is pulled away from the zirconium atom through a Zr – MAO bond. In the presence of ethylene, it will form a  $\pi$ -complex with the metal, and this will be followed by an insertion reaction. If no ethylene is present, the  $\beta$ -hydrogen of the polymer chain, weakly held through an agostic hydrogen bond, may be eliminated, resulting in chain transfer.

### 2.3.4.2 Corradini's Model

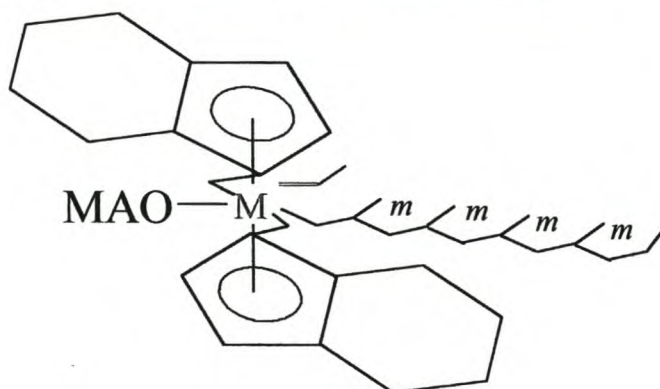
Corradini and Guerra [194] proposed a monometallic mechanism where a metal-carbocationic complex is the active species. In this model polymerization involves coordination of the olefin at the active site and while the  $\gamma$ -hydrogen is held close to the metal through an agostic interaction, the monomer is inserted into the metal-carbon bond through *cis* opening.

## 2.3.5 STEREOREGULATION WITH HOMOGENEOUS CATALYSTS

From the above discussions it was noted that various types of stereospecificities can be obtained with single-site catalysts. The stereospecificity depends on the configuration or type of symmetry of the ligands prior to and after attachment to the metal atom. The effect is believed to arise primarily from steric interaction between the incoming monomer and the ligands. Electronic factors cannot however be ignored. Stereoselectivities of these catalysts are therefore mostly controlled by the catalyst site itself. With achiral catalysts, chain end control is responsible for the formation of stereoblock *iso*-PP observed at low temperatures [147] where the chirality attained through olefin insertion determines the most favored enantioface of the coordinated olefin to be inserted, thereby perpetuating any stereo error.

### 2.3.5.1 Pino's Model

In the model proposed by Pino [195] it was suggested that bonds between MAO, the Zr atom and the last carbon from the growing polymer chain should exist. In the *ansa* Et(H<sub>4</sub>Ind)<sub>2</sub>ZrCl<sub>2</sub>/MAO system the cyclohexenyl group of the indenyl ligand together with the large MAO macromolecule present a large steric hindrance to the incoming monomer. In combination with the low steric effect of the CH group from the Cp groups of the opposite indenyl ligand, a chiral "hole" is presented to the incoming monomer. Olefin coordination favors 1,2 insertion in this picture.



#### Coordination of Propylene to the Metal Center for 1,2-Insertion

Coordination of the prochiral propylene molecule with its methyl group directed away from the cyclohexenyl group is energetically favored, resulting in *meso* (*m*) stereosequences, *i.e.* isotactic polymer. Stereoregulation is thus chiral site controlled. The *meso* catalyst complex, where the two cyclohexenyl groups are situated on top of each other, cannot direct the methyl group of an incoming propylene molecule, resulting in the random formation of *meso* and racemic (*r*) sequences *i.e.* atactic polymer.

### 2.3.5.2 Corradini's Model

On the basis of non-bonded interaction calculations done by Corradini *et al.* [123] and Cavallo *et al.* [196] it was found that Zr could not bond to two  $\pi$ -bonded ligands and three more ligands. Therefore they assumed that only the growing chain and the

coordinating monomer were present in the complex in the stage preceding the monomer insertion. This is possible if the complex has an ionic nature [194]. In this model the ligand framework does not have a direct influence on the coordination of the propylene molecule. Instead, there is a strong interaction between the ligands and the polymer chain which forces the chain to adopt the position of lowest energy. The interaction of the chain with the methyl group of the incoming monomer causes the energy difference between *si* and *re* coordination and hence, the methyl group is always trans to the growing polymer chain [197]. For an (R,R) complex, the incoming monomer is forced to present its *re* face during coordination.

Similar to the case of 2,1-misinsertions with heterogeneous catalysts it was found that when such a regioirregular insertion does occur - as high as 2-3% with zirconium complexes [198] - subsequent insertion becomes difficult. These 2,1-insertion products are relatively long-lived and renders the active site temporarily dormant. It can only be resolved by  $\beta$ -H elimination followed by isomerization and further chain growth or chain transfer to start a new chain. Up to 90% of the zirconium atoms may become dormant as a result of 2,1-misinsertions. This may explain the apparent paradox observed that some sterically congested complexes are more active, and produce polymer with much higher molecular weights and much better stereoregularities [199,200].

### 2.3.5.3 Brintzinger's Model

Brintzinger and coworkers [201,150] proposed a model based on the size and shape of the gap presented by the metal. The angle that two planes touching the inner ligand van der Waal's surfaces of the ligands make with each other is called the *coordination gap aperture* and is determined mainly by the bridging unit and  $\beta$ -substituents on the Cp rings. The intersection of these planes lie at an angle relative to the centroid-M-centroid plane called the *coordination gap obliquity* which, for *ansa*-metallocenes, can be either positive or negative, and is equivalent to *S*- or *R*- configurations. Brintzinger assumed that the transition state has a 4-membered geometry consisting of the metal with the two  $\alpha$ -carbons of the last inserted monomer and the inserting monomer is attached, and the  $\beta$ -carbon of the incoming monomer completing the ring.



The angle formed by two planes through the metal center, touching the van der Waal's spheres of the reaction complex, consisting of the detaching last inserted monomer and the incoming monomer, was named the *reaction complex aperture*. The angle made by the intersection of these planes with a plane through the centers of the metal and the two  $\alpha$ -carbons define the *reaction complex obliquity*. Thus, the catalyst activity and its success at stereoregulating the coordination of the incoming monomer is determined by how well the reaction complex fits into the opening in front of the metal. A tight fit of the reaction complex wedge into the coordination gap aperture will therefore result in decreased activity but increased stereoregulating abilities. On the other hand, if the reaction complex fits loosely into the gap, stereoregulation is decreased together with increased activity for *1,2 insertion*. It should be remembered that 2,1-coordination will render the site temporarily dormant, resulting in decreased activity.

### 2.3.6 KINETIC MODELS

#### 2.3.6.1 Ewen's Model

Ewen [147] proposed the first kinetic model for polymerization of propylene with a  $\text{Cp}_2\text{Ti}$ -based catalyst. The rate of polymerization, expressed in terms of monomer-transition metal (or active center) and MAO concentrations can be written as:

$$R_p = k_p K_M K_{MAO} C_p^* [M][MAO] \quad (2.13)$$

where  $K_M$  and  $K_{MAO}$  is the adsorption constants for propylene and MAO respectively.

#### 2.3.6.2 Chien's Model

The model proposed by Chien *et al.* [146,202] assumes the existence of multiple active species and transfer reactions by  $\beta$ -hydrogen elimination and transfer to MAO. The rate of polymerization, expressed in terms of the concentration of monomer and the sum of the different active sites is given by:

$$R_p = \sum_i k_{p,i} C_i^* [M] \quad (2.14)$$

Assuming first order deactivation kinetics, the total productivity is expressed as:

$$P(t) = [M] \sum_i k_{p,i} [C_i^*]_0 (1 - \exp(-k_{d,i} t)) \quad (2.15)$$

where  $[C_i^*]_0$  is the initial concentration of the  $i^{\text{th}}$  active species. The degree of polymerization can be calculated according to:

$$P_n^{-1} = [M]^{-1} (k_t^{MAO} [MAO] + k_t^{\beta-H}) / k_p \quad (2.16)$$

The plot of  $P_n^{-1}$  vs.  $[M]^{-1}$  gives a straight line with intercept at the origin and a slope depending on transfer reactions with MAO and  $\beta$ -hydride elimination.

## 2.4 REFERENCES

1. Von Pechmann H., *Ber.*, **31**, 2643 (1898)
2. Bamberger E., Tschirner F., *Ber.*, **33**, 955 (1900)
3. Storch H.H., Columbic N., Anderson R.B., *The Fischer-Tropsch and Related Synthesis*, Wiley and Sons, New York (1951)
4. Arnold H.R., Herrick E.C., *US Patent 2,726,218*, E.I. duPont de Nemours & Co., Dec. 6, (1955)
5. Hahn W., Müller W., *Macromol. Chem.*, **16**, 71 (1955)
6. Staudinger H., *Angew. Chem.*, **64**, 155 (1952)
7. Fawcett E.W., Gibson R.O., *J. Chem. Soc.*, 386 (1934)
8. Fawcett E.W., Gibson R.O., Perrin M.W., Paton J.G., Williams E.G., *Brit. Patent 471,590*, Imperial Chemical Industries, Sept. 6 (1937)
9. Raff R., Lyle E., *Historical Developments in Crystalline Olefin Polymers Part I*, Ed. Raff R.A.V., Doak K.W., John Wiley & Sons, New York, 1 (1965)
10. Billmeyer H., *Textbook of Polymer Science*, Second Edition, John Wiley & Sons, New York, 379 (1971)
11. Whelan T., *Polymer Technology Dictionary*, Chapman & Hall, London, 230 (1994)
12. Ulrich H., *Introduction to Industrial Polymers*, Carl Hanser Verlag, München, 48 (1982)
13. Friedrich M.E.P., Marvel C.S., *J. Am. Chem. Soc.*, **52**, 376 (1930)
14. Ziegler K., Gellert H.G., *Justus Liebigs Ann. Chem.*, **567**, 195 (1950)
15. Ziegler K., *Angew. Chem.*, **64**, 323 (1952)
16. Holzkamp E., *Thesis, Technische Hochschule, Aachen*, May 21 (1954)
17. Ziegler K., Holzkamp E., Breil H., Martin H., *Angew. Chem.*, **67**, 426 (1955)
18. Ziegler K., Holzkamp E., Breil H., Martin H., *Angew. Chem.*, **67**, 541 (1955)
19. Natta G., Pino P., Farina M., *Ricerca Sci.*, **25A**, 120 (1955)
20. Natta G., *J. Polym. Sci.*, **16**, 143 (1955)
21. Natta G., Pino P., Corradini P., Danusso F., Mantica E., Mazzanti G., Moraglio G., *J. Polym. Sci.*, **77**, 1708 (1955)
22. Peters E.F., Evering B.L., *U.S. Patent 2,692,261*, Standard Oil of Indiana, Oct. 19 (1954)

23. Friedlander H.N., *Mechanism of Polymerization on Transition Metal Oxide Solid Catalysts.*, in *Crystalline Olefin Polymers Part I*, Ed. Raff R.A.V., Doak K.W., John Wiley & Sons, New York, 215 (1965)
24. Boor J., *Ziegler-Natta Catalysts and Polymerization*, Academic Press, New York, 279 (1979)
25. Zletz A., *U.S Patent 2,692,257*, Standard Oil, (1954)
26. Welch M.B., Hsieh H.L., *Olefin Polymerization Catalyst Technology in Handbook of Polyolefins*, Vasile C., Seymour R.B., Eds., Marcel Dekker, New York, 21 (1993)
27. Natta G., *et al.*, *U.S. Pat.*, 3,715,324, Montecatini (1973)
28. Hogan, J.P., Banks R.L., *U.S. Patent 2,825,721*, Phillips Petroleum, (1958)
29. Seymour R.B., *History of Polyolefins in Handbook of Polyolefins*, Vasile C., Seymour R.B., Eds., Marcel Dekker, New York, 1 (1993)
30. Boor J., *Ziegler-Natta Catalysts and Polymerization*, Academic Press, New York, 19 (1979)
31. Natta G., Giachetti E., Pasquon I., Pajaro G., *Chim. Ind.*, **42**, 10, 1091 (1960)
32. Vandenberg E.J., *U.S. Patent 3,051,690*, Hercules Powder Company, Aug. 28 (1962)
33. Ettore B., Luciano L., *Italian Patent 554,013*, Montecatini, Jan. 5 (1957)
34. Natta G., Pasquon I., Zambelli A., Gatti G., *J. Polym. Sci.*, **51**, 387 (1961)
35. Farina M., *Forty Years After: the Everlasting Youth of Stereospecific Polymerization*, TRIP, **2**, 3, 80 (1994)
36. Natta G., Corradini, P., Allegra G., *J. Polym. Sci.*, **51**, 399 (1961)
37. Galli P., Haylock J.C., *Macromol. Chem., Macromol. Symp.*, **63**, 19 (1992)
38. Vandenberg E.J., *Catalysis: Key to Advances in Applied Polymer Science*, American Chemical Society, 2, (1992)
39. Vandenberg E.J., *U.S. Patent 3,058,963*, Hercules Inc., Oct. 16 (1962)
40. Tornqvist E.G.M., Seelback C.W., Langer A.W., *U.S. Patent 3,128,252*, Esso Research and Engineering, Apr. 7, (1964)
41. Tornqvist E.G.M., Langer A.W., *U.S. Patent 3,032,510*, Esso Research and Engineering, (1962)
42. Wilchinsky Z.W., Looney R.W., Tornqvist E.G.M., *J. Catal.*, **28**, 352 (1973)

43. Tait P.J.T., *Monoalkene Polymerization: Ziegler-Natta and Transition Metal Catalysts in Comprehensive Polymer Science*, Sir Geoffrey Allen, Chairman - Ed. Board, Pergamon Press, **4(1)** 1 (1989)
44. Coover H.W. Jr., *J. Polym. Sci.*, Part C **4**, 1511 (1964)
45. Coover H.W. Jr., McConnell R.L., Joyner F.B., *Macromol. Rev.*, **1**, 91 (1966)
46. *Brit. Pat. 1,092,390*, Mitsubishi Petrochemical Co., Apr 27, (1966)
47. Coover H.W. Jr., Joyner F.B., *J. Polym. Sci.*, Part A **3**, 2407 (1965)
48. Zambelli A., DiPietro J., Gatti G., *J. Polym. Sci.*, Part A, **1**, 403 (1963)
49. Hermans J.P., Henriouille P., *U.S. Patent 3,769,233*, Solvay & Cie, (1973)
50. Hermans J.P., Henriouille P., *U.S. Patent 4,210,738*, Solvay & Cie, (1980)
51. Hsieh H.L., *Polym. J.*, **12**, 597 (1980)
52. Hsieh H.L., *Catal. Rev.-Sci. Eng.*, **26**, 631 (1984)
53. Arzoumanidis G.G., Karayannis N.M., Kheghatian H.M., Lee S.S., *Catalysis Today*, **13**, 59 (1992)
54. Natta G., *J. Polym. Sci.*, **34**, 21 (1959)
55. Rodriguez L.A.M., VanLooy H.M., *J. Polym. Sci.*, Part A1, **4**, 1971 (1966)
56. Busico V., Corradini P., DeMartino L., Proto A., Albizzati E., *Macromol. Chem.*, **186**, 1279 (1985)
57. Xie T., McAuley K.B., Hsu J.C.C., Bacon D.W., *Ind. Eng. Chem. Res.*, **33**, 449 (1994)
58. Karol F.J., Karapinka G.L., Wu C., Dow A.W., Johnson R.N., Carrick W.L., *J. Polym. Sci.*, Part A-1, **10**, 2621 (1972)
59. *British Pat. 1,140,649*, Solvay & Cie, Mar. 30, (1966)
60. Delbouille A., Toussaint H., *U.S. Pat. 3,594,330*, Solvay & Cie., Jul. 20, (1971)
61. Boor J., *Ziegler-Natta Catalysts and Polymerization*, Academic Press, New York, 154 (1979)
62. Orzechowski A., MacKensie J.C., *U.S. Pat. 3,166,542*, Cabot Corp., Jan. 19, (1965)
63. Orzechowski A., *U.S. Pat. 3,220,959*, Cabot Corp., Nov. 30, (1965)
64. Sinn H., Kaminsky W., *Adv. Organometallic Chem.*, **18**, 99 (1980)
65. Diedrich B., *Second Generation Ziegler Polyethylene Processes in Polymer Preprints*, ACS, Washington, Vol. 16, **1**, 316 (1975)
66. Böhm L.L., *Polymer*, **19**, 553 (1978)

67. Böhm L.L., *J. Appl. Polym. Sci.*, **29**, 279 (1984)
68. Barbé P.C., Cecchin G., Noristi L., *Adv. Pol. Sci.*, **81**, 1 (1987)
69. Soga K., Chen S., Doi Y., Shiono T., *Advances in Polyolefins*, Seymour R.B., Cheng T., Eds., Plenum Press, New York, 143 (1987)
70. Hewett W.A., Shokal E.C., *Brit. Pat.*, 904,510, Shell, (1960)
71. *Ger. Pat.*, 904,510, Mitsui Petrochemicals, (1960)
72. *Brit. Pat. 1,271,411*, Mitsui Petrochemicals, (1968)
73. *Brit. Pat.*, 1,286,867, Montecatini-Edison, (1968)
74. Lochner F.W., v.Seebach H.M., *Ind. Eng. Chem., Process Res. Div.*, **11**, 190 (1972)
75. Gianinni U., *Macromol. Chem., Suppl.*, **5**, 216 (1981)
76. Longi P., Giannini U., Cassata A., *British Pat. 1,335,887*, Montecatini Edison, (1973)
77. *Ger. Pat. Appl.*, 2,643,143, Montedison and Mitsui Petrochemicals, (1975)
78. Spitz R., Lacombe J.L., Guyot, A., *J. Polym. Sci., Pol. Chem.*, Ed. **16**, 1683 (1983)
79. Spitz R., Lacombe J.L., Guyot, A., *J. Polym. Sci., Pol. Chem.*, Ed. **22**, 2625 (1984)
80. Keii T., *Macromol. Chem.*, **183**, 2285 (1982)
81. Doi Y., Murata M., Yano Y., Keii T., *Ind. Eng. Chem., Prod. Res. Div.*, **21**, 580 (1982)
82. Soga K., Shiono T., *Effect of Diesters and Organosilicon Compounds on the Stability and Stereospecificity of Ziegler-Natta Catalysts in Ziegler-Natta and Metathesis Polymerizations*, Quirk R.P., Ed., Cambridge University Press, Cambridge (1988)
83. Arzoumanidis G.G., Karayannis N.M., Khelghatian H.M., Lee S.S., Johnson B.V., *U.S. Pat. 4,866,022*, Amoco Chemical Co., (1989)
84. Arzoumanidis G.G., Karayannis N.M., Khelghatian H.M., Lee S.S., Johnson B.V., *U.S. Pat. 4,988,656*, Amoco Chemical Co., (1991)
85. *Eur. Pat. 0,086,288*, Mitsui Petrochem. Co., (1983)
86. *Ger. Pat. 3,342,039*, BASF, (1985)
87. *Ger. Pat. 3,411,197*, BASF, (1985)
88. Galli P., Haylock J.C., *Prog. Polym. Sci.*, **16**, 443 (1991)

89. Ulrich H., *Introduction to Industrial Polymers*, Carl Hanser Verlag, München, 69 (1982)
90. Tait P.J.T., Berry I.G., *Monoalkene Polymerization: Copolymerization in Comprehensive Polymer Science*, Sir Geoffrey Allen, Chairman Ed. Board, Pergamon Press, **4(4)**, 575 (1989)
91. Ziegler K., Gellert H., Holzkamp E., Wilke G., Duck E., Kroll W., *Ann.*, **629**, 172 (1960)
92. Natta G., *Macromol. Chem.*, **16**, 213 (1955)
93. Nenitzescu C.D., Huch C., Huch A., *Angew. Chem.*, **68**, 438 (1956)
94. Friedlander H.N., Oita K., *Ind. Eng. Chem.*, **49**, 1885 (1957)
95. Gilchrist A., *J. Polym. Sci.*, **34**, 49 (1959)
96. Tait P.J.T., Watkins N.D., *Monoalkene Polymerization: Mechanisms in Comprehensive Polymer Science*, Sir Geoffrey Allen, Chairman - Ed. Board, Pergamon Press, **4(2)** 533 (1989)
97. Uelzmann H., *J. Polym. Sci.*, **32**, 457 (1958)
98. Uelzmann H., *J. Org. Chem.*, **25**, 671 (1960)
99. Natta G., Mazzanti G., *Tetrahedron*, **8**, 86 (1960)
100. Patat P., Sinn H., *Angew. Chem.*, **79** 496 (1958)
101. Carrick W.L., *J. Am. Chem. Soc.*, **80**, 6455 (1958)
102. Breslow D.S., Newburg N.R., *J. Am. Chem. Soc.*, **81**, 81 (1959)
103. Cossee P., *Tetrahedron Lett.*, **17**, 12 (1960)
104. Cossee P., *Proc. 6th Int. Congr. Coord. Chem.*, 241 (1961)
105. Cossee P., *J. Catal.*, **3**, 80 (1961)
106. Arlman J., *Proc. 3<sup>rd</sup> Int. Congr. Catal.*, **2**, 957 (1964)
107. Huang J., Rempel G.L., *Progress Pol. Sci.*, **20(3)** 459 (1995)
108. Ystenes W., *Makromol. Chem., Macromol. Symp.*, **66**, 71 (1993)
109. Kissin Y.V., *Stereospecificity of Heterogeneous Ziegler-Natta Catalysts in Isospecific Polymerization of Olefins with Heterogeneous Ziegler-Natta Catalysts*, Springer-Verlag, New York, Chapt. **3-3**, 249 (1985)
110. Chadwick J.C., Morini G., Albizzati E., Balbontin G., Mingozzi I., Cristofori A., Sudmeijer O., Kessel G.M.M., *Macromol. Chem. Phys.*, **197** (8), 2501 (1996)
111. Tsuruta T., *J. Polym. Sci., Part D*, **7**, 179 (1972)
112. Stehling F.C., Knox J.P., *Macromolecules*, **8**, 595 (1975)

113. Mauzak M., Varion J.P., Sigwalt P., *Polymer*, **18**, 1193 (1977)
114. Doi Y., *Macromol Chem.*, **180**, 2447 (1979)
115. Corradini P., Busico V., Guerra G. *Monoalkene Polymerization: Stereospecificity in Comprehensive Polymer Science*, Sir Geoffrey Allen, Chairman - Ed. Board, Pergamon Press, **4(3)** 29 (1989)
116. Natta G., Pino P., Mazzanti G., Longi P., *Gazz. Chim. Ital.*, **87**, 549 (1957)
117. Natta G., Pino P., Mazzanti G., *Ital. Pat. 526 101*, Montecatini, (1954)
118. Kissin Y.V., Tsvetskova V.I., Chirkov N.M., *Eur. Polym. J.*, **8**, 529 (1972)
119. Pino P., Mulhaupt R., *Angew. Chem.*, **19**, 857 (1980)
120. Caunt A.D., *J. Polym. Sci., Part C*, **4**, 49 (1963)
121. Coutinho F.M.B., Maria L.C., *Polym. Bull.*, **26**, 535 (1991)
122. Burfield D.R., Tait P.J.T., *Polymer*, **15**, 87 (1974)
123. Corradini P., Busico V., Guerra G., *Possible models for the Steric Control in the Heterogeneous High-Yield and Homogeneous Ziegler-Natta Polymerizations of 1-alkenes* in Kaminsky W., Sinn H., Eds., *Transition Metals and Organometallics as Catalysts for Olefin Polymerization*, Springer Verlag, Berlin, 379 (1988)
124. Luciani L., Kashiwa N., Barbe P.C., Toyota A., *U.S. Pat. 4 226 741*, Montedison S.p.A., Mitsui Petrochemical Ind., (1975)
125. Kissin Y.V., *Heterogeneous Ziegler-Natta Catalysis: Chemistry and Kinetics of the Formation and Functioning of Active Centers in Isospecific Polymerization of Olefins with Heterogeneous Ziegler-Natta Catalysts*, Springer-Verlag, New York, Chapt. **2-1**, 96 (1985)
126. Sacchi M.C., Shan C., Forlini F., Tritto I., Locatelli P., *Makromol. Chem. Rapid Commun.*, **14**, 231 (1993)
127. Xu J., Feng L., Yang S., Yang Y., Kong X., *Macromolecules*, **30**, 7655 (1997)
128. Tait P.J.T., in Kaminsky W., Sinn H., Eds., *Transition Metals and Organometallics as Catalysts for Olefin Polymerization*, Springer Verlag, Berlin, 309 (1988) and refs. therein
129. Kaminsky W., in *Transition Metal Catalyzed Polymerizations: Alkenes and Dienes*, Quirk R.P. Ed., Harwood, New York, **4**, 225 (1983)
130. Shteinbak V.S., Amerik V.V., Yakobson F.I., Kissin Y.V., Ivanyukov D.V., Krentsel B.A., *Eur. Polym. J.*, **11**, 457 (1975)
131. Joubert D.J., *3-Methyl-1-Butene Copolymers, MSc Thesis*, 23 (1995)



132. Natta G., Pasquon I., *Adv. Catal.*, **11**, 1 (1959)
133. Kissin Y.V., *Stereospecificity of Heterogeneous Ziegler-Natta Catalysts in Isospecific Polymerization of Olefins with Heterogeneous Ziegler-Natta Catalysts*, Springer-Verlag, New York, **I-2**, 14 (1985)
134. Kissin Y.V., *Stereospecificity of Heterogeneous Ziegler-Natta Catalysts in Isospecific Polymerization of Olefins with Heterogeneous Ziegler-Natta Catalysts*, Springer-Verlag, New York, **I-1**, 5 (1985)
135. Böhm L.L., *Polymer*, **19**, 545 (1978)
136. Cossee P., *Stereochemistry of Macromolecules*, Ketley A.D., Ed., Marcel Dekker, 155 (1967)
137. Kissin Y.V., *Kinetics of Olefin Polymerization with Heterogeneous Ziegler-Natta Catalysts in Isospecific Polymerization of Olefins with Heterogeneous Ziegler-Natta Catalysts*, Springer-Verlag, New York, **I-5**, 67 (1985)
138. Kissin Y.V., in *Transition Metal Catalyzed Polymerizations: Alkenes and Dienes*, Quirk R.P. Ed., Harwood, New York, **4**, 597 (1983)
139. Chiang R., *J. Phys. Chem.*, **69**, 1945 (1965)
140. Chiang R., *J. Pol. Sci.*, **36**, 31 (1959)]
141. Natta G., Pino P., Mazzanti G., Giannini U., *J. Am. Chem. Soc.*, **79**, 2976 (1957)
142. Breslow D.S., Newburg N.R., *J. Am. Chem. Soc.*, **79**, 5073 (1957)
143. Doak K.W., Schrage A., *Polymerization and Copolymerization Process in Crystalline Olefin Polymers Part I*, Ed. Raff R.A.V., Doak K.W., John Wiley & Sons, New York, 1 (1965)
144. Grogorjan E.A., Dyachkovskii F.S., Shilov A.E., *Vysokomol. Soedin*, **7**, 145 (1965)
145. Ewen J., *Stud. Surf. Sci. Catal.* In *Catalytic Polymerization of Olefins*, Keii T., Soga K. Eds., **25**, 271 (1986)
146. Chien J.C.W., Wang B., *J. Polym. Sci., Part A, Polym. Chem.*, **28**, 15 (1990)
147. Ewen J.A., *J. Am. Chem. Soc.*, **106**, 6355 (1984)
148. Wild F.R.W.P., Wasincione M., Hutter G., Brintzinger H.H., *J. Organomet. Chem.*, **288**, 63 (1985)
149. Wild F.R.W.P., Zsolnai L., Hutter G., Brintzinger H.H., *J. Organomet. Chem.*, **232**, 233 (1982)

150. Burger P., Hortmann K., Brintzinger H.H., *Makromol. Chem. Macromol. Symp.*, **66**, 127 (1993)
151. Röhl W., Brintzinger H.H., Rieger B., Zolk R., *Angew. Chem. Int. Ed. Eng.*, **29**, 279 (1990)
152. Kaminsky W., Engehausen R., Zournis K., Spaleck W., Rohrmann J., *Ibid.*, **193**, 1643 (1992)
153. Ewen J., Elder M.J., Jones R.L., Haspelagh L., Atwood J.L., Bott S.G., Robinson K., *Makromol. Chem., Macromol. Symp.*, **48/49**, 253 (1991)
154. Coates G.W., Waymouth R.M., *Science*, **267**, 217 (1995)
155. Herfert N., Fink G., *Makromol. Chem.*, **193**, 1359 (1992)
156. Horton A.D., *Trends Pol. Sci.*, **2**, 5, 158 (1994) and references therein
157. Tait P.J.T., Monteiro M.G.K., Yang M., Richardson J.L., *MetCon '96*, Houston, Proceedings, Session 1 (1996)
158. Soares J.B.P., Kim J.D., Rempel G.L., *Ind. Eng. Chem. Res.*, **36**, 1144 (1997)
159. Ribeiro M.R., Deffieux A., Portela M.F., *Ind. Eng. Chem. Res.*, **36**, 1224 (1997)
160. Soga K., Shiono T., *Prog. Polym. Sci.*, **22**, (7), 1503 (1997)
161. Kaminaka M., Soga K., *Makromol. Chem., Rapid Comm.*, **12**, 367 (1991)
162. Chien J.C.W., He D., *J. Polym. Sci., Part A., Polym. Chem.*, **29**, 1603 (1991)
163. Jordan R.F., Bajger C.S., Willet R., Scott B., *J. Am. Chem. Soc.*, **108**, 7410 (1986)
164. Chien J.C.W., Tsai W.-M., Rausch M.D., *J. Am. Chem. Soc.*, **113**, 8570 (1991)
165. Giannetti E., Nicoletti G.M., Mazzocchi R., *J. Polym. Sci. Polym. Chem. Ed.*, **23**, 2117 (1985)
166. Pellechia C., Grassi A., Zambelli A., *J. Mol. Catal.*, **82**, 57 (1993)
167. Miyatake T., Mizunuma K., Kakugo M., *Makromol. Chem., Macromol. Symp.*, **66**, 203 (1993)
168. Ewen, J.A., Jones, R.L., Elder, M.S., Rheingold, A.L., Liable-Sands, L.M., *J. Am. Chem. Soc.*, **120**, 10786 (1998)
169. Xu G., Ruckenstein, E., *Macromolecules*, **31**, 4724, (1998)
170. Schaffer, T.D., Canich, J.M., Squire, K.R., *Macromolecules*, **31**, 5145 (1998)
171. Miyake, S. Henling, M., Bercaw, J.E., *Organometallics*, **17**, 5520 (1998)
172. Shapiro P.J., Bercaw J.E., *3<sup>rd</sup> Chem. Congress of North America*, Toronto, Abs. INOR 584 (1988)

173. Stevens J.C., Timmers F.J., Wilson D.R., Schmidt G.F., Nickias P.N. Rosen R.K., Knight G.W., Lai S., *Eur. Pat. Appl. EP 416 815-A2*, (1991)
174. Stevens J.C., *INSITE<sup>TM</sup> Catalyst Structure / Activity Relationships for Olefin Polymerization in Catalyst Design for Tailor-Made Polyolefins*, Soga K., Terano M., Eds., Kodansha, Tokyo, 277 (1994)
175. Stevens J.C., *11<sup>th</sup> Int. Congr. Catal. Stud. Surf. Sci. Catal.*, **101**, 11 (1996)
176. Barnhart, R.W., Bazan, G.G., *J. Am. Chem. Soc.*, **120**, 1082 (1998)
177. Britovsec G.J.P., Gibson V.C., Wass D.F., *Angew. Chem. Int. Ed.*, **38**, 428 (1999)
178. Killian C.M., Brookhart M., Johnson L.K., Tempel D., Ittel S.D., McLain S.J., McCord E.F., *SPO '96, Proc. Int. Bus. Forum Spec. Polyolefins*, 6th, 117-120, Schotland Business Research: Skillman, N. J. (1996)
179. *New Catalysts to Polymerize Olefins*, C&EN, April 13, 11 (1998)
180. Small, B.L, Brookhart, M., Bennett, A.M, *J. Am. Chem. Soc.*, **120**, 4049 (1998)
181. McLain, S.J, Feldman, J., McCord, E.F., Gardner, K.H., Teasley, M.F., Coughlin, E.B., Sweetman, K.J., Johnson, L.K, Brookhart, M., *Macromolecules*, **31**, 6705 (1998)
182. Kim, J.S., Paulow, J.H., Wojcinski, L.M. II, Murtiza, S., Kader, S., Sen, A., *J. Am. Chem. Soc.*, **120**, 1932 (1998)
183. Killian C.M., Tempel D.J., Johnson L.K., Brookhart M., *J. Am. Chem. Soc.*, **118**, 11664 (1996)
184. Doi Y., Ueki S., Keii T., *Macromolecules*, **12**, 814 (1979)
185. Doi Y., Tokuhiro N., Nunomura M., Miyake H., Suzuki S., Soga K., *Living Polymerization of Olefins with Highly Active Vanadium Catalysts* in Kaminsky W., Sinn H., Eds., *Transition Metals and Organometallics as Catalysts for Olefin Polymerization*, Springer Verlag, Berlin, 379 (1988)
186. Brookhart M., DeSimone J.M., Grant B.E., Tanner M.J., *Macromolecules*, **28**, 5378 (1995)
187. Brintzinger H.H., Fischer D., Mülhaupt R., Rieger B., Waymouth R.M., *Angew. Chem., Int. Ed. Engl.*, **34**, 1143 (1995)
188. *Mitsui Chemicals Debuts New Post-metallocene Catalyst* Japan Chemical Week, p1, 15 July (1999)
189. Sinclair K.B., Wilson R.B., *Chem. Ind.*, p. 857 (1994)

190. Aaltonen P., Fink G., Löfgren B., Seppälä J., *Macromolecules*, **29**, 5255 (1996)
191. Aaltonen P., *Ph.D Thesis, Metallocene Catalyzed Copolymerization of Olefins with Functional Monomers*, Sept. 26 (1996)
192. Stehling, U.M., Stein, K.M, Kesti, M.R., Waymouth, R.M., *Macromolecules*, **31**, 2019 (1998)
193. Kaminski W., Steiger R., *Polyhedron*, **7**(22/23), 2375 (1988)
194. Corradini P., Guerra G., *Prog. Polym Sci.*, **16**, 239, (1991)
195. Pino P., Rotzinger B., von Achenbach E., *Catalytic Polymerization of Olefins*, Keii T., Soga K., Eds., Elsevier, Tokyo, 461 (1986)
196. Cavallo L., Guerra G., Vacatello M., Corradini P., *Macromolecules*, **24**, 1784 (1991)
197. Van der Leek Y., Angermund, K., Reffke M., Kleinschmidt R., Goretzki R., Fink G., *Chem. Eur. J.* **3**(4), 585 (1997)
198. Guerra G., Cavallo L., Corradini P., Longo P., Resconi L., *Polym. Prer. (Am. Chem. Soc., Div. Polym. Chem.)*, **37**(2), 469 (1996)
199. Guerra G., Cavallo L., Moscardi G., Vacatello M., Corradini P., *J. Am. Chem. Soc.*, **116**, 2988 (1994)
200. Bochmann M., *J. Chem. Soc., Dalton Trans.*, 255 (1996)
201. Hortmann K., Brintzinger H.H., *New J. Chem.*, **16**, 51 (1992)
202. Chien J.C.W., Sugimoto R., *J. Polym. Sci., Polym. Chem. Ed.*, **29**, 459 (1991)

## CHAPTER 3

### POLYOLEFINS

#### 3.1 GLOBAL PRODUCTION CAPACITIES

##### 3.1.1 POLYETHYLENE

The very first commercially produced polyolefin was highly branched LDPE, made in a free-radical, high-pressure process by ICI in 1933. Later, Du Pont and Union Carbide also obtained licenses for LDPE production from ICI. According to Müller [1] the LDPE capacities are currently increasing at rates of 5.7 % in Asia, 1.3 % in Europe and approximately 1.5 % in the Americas. Worldwide capacities reached about 19.5 million tons in the year 2000. Global capacities for 1999 are shown in Figure 3.1.

Global LDPE Capacities (1999)

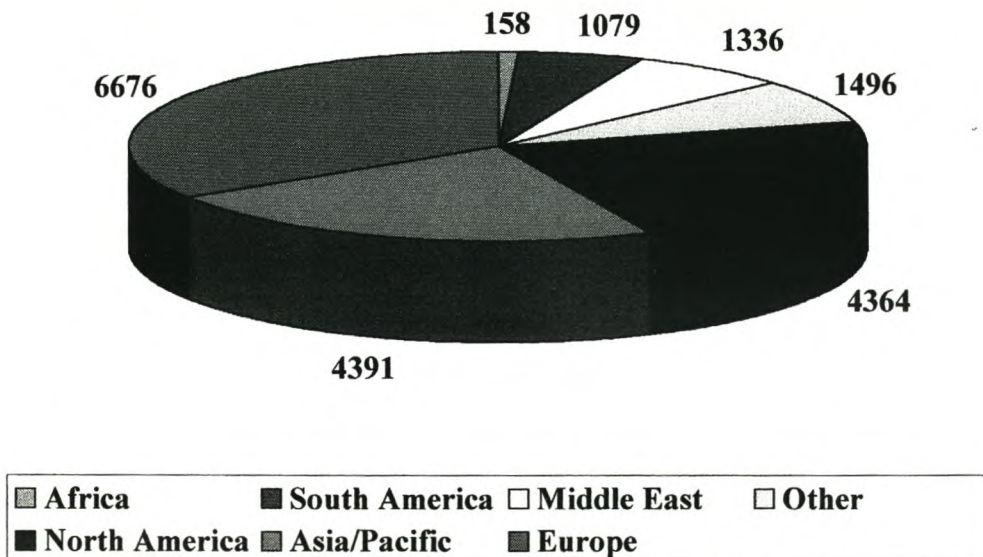
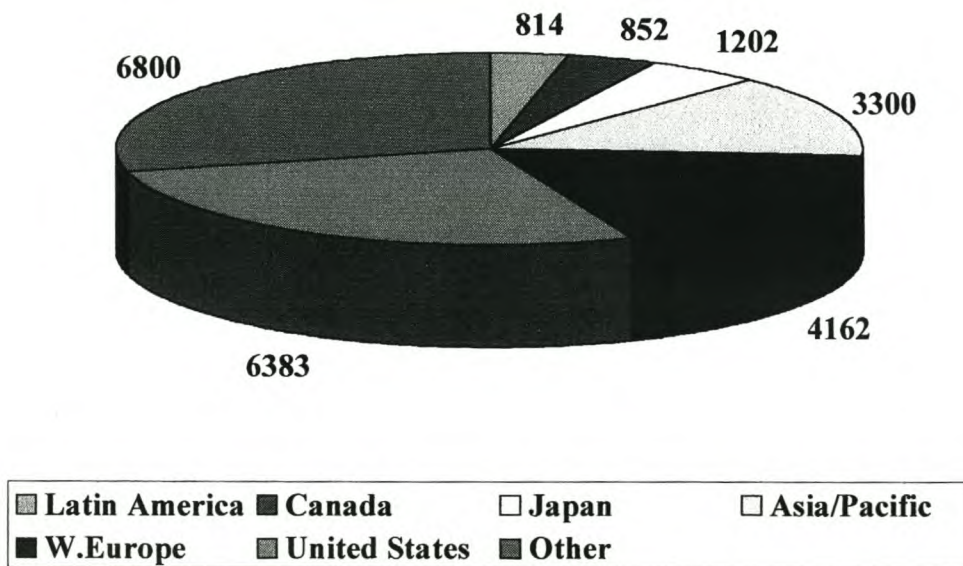


Figure 3.1. Global LDPE Capacities by Country

Because of the non-uniformity of the chains comprising this highly branched polymer, close packing of the chains during crystallization is not possible, hence its low density. As mechanical properties are directly linked to crystallinity, increased tensile strength and stiffness would only be obtained if the polymer chains could be made more linear. DuPont succeeded in producing a fairly linear PE with less than 0.8 branches per 1000 carbons and a density of  $0.955 \text{ g/cm}^3$ , also by a free-radical process but at pressures of 7000 bar, certainly not feasible for commercial production [2].

Ziegler patented his  $\text{TiCl}_4$  – triethyl aluminum catalyst system [3] capable of producing PE with densities between  $0.945$  and  $0.960 \text{ g/cm}^3$  at atmospheric pressure. About the same time a chromium catalyst, producing PE with even higher densities of  $0.960$  to  $0.970 \text{ g/cm}^3$  was discovered by Hogan and Banks [4]. Ziegler’s catalyst was licensed to Petrochemicals, Montecatini, Hoechst and Hercules and the chromium catalyst to Phillips. Production started in 1956 and 1957 - in the US by Phillips and in Europe by Hoechst [5]. Current world capacity is 23.5 million tons per year [6] with an average annual growth rate of 6.1% predicted. Global capacities for 1999 are shown in Figure 3.2.

**Global HDPE Capacities (1999)**



**Figure 3.2. Global HDPE Capacities by Country**

Additional capacity planned for the immediate future include 320 kt in Europe, 60 kt in the Americas and 535 kt for Asia-Pacific. A single closure is planned for the last quarter of 2000 of a 170 kt plant in Elenac, France [7].

The two main types of PE available, having either low or high density containing an unexplored density range, could not possibly satisfy all application needs. Union Carbide announced their *Unipol* process in 1977 [8,9] for producing linear PE having (controllable) low density in a fluidized-bed, gas-phase process. Properties of this LLDPE, superior to those of LDPE, are tailored by controlling the amount of branching introduced resulting from the amount of comonomer introduced into the polymer. Initially the comonomer 1-butene was used by Union Carbide and DuPont for gas-phase processes because of its availability, low cost and low boiling point. The latter property prevents its condensation in the gas-phase process, but higher  $\alpha$ -olefins including 1-hexene, and 4-methyl-1-pentene for producing high strength LLDPE was introduced later. The use of 1-octene, not suitable for gas phase processes, was developed and is currently used by Dow in their solution process. The composition of copolymers produced with heterogeneous Ziegler-Natta catalysts are not uniform because of the differences in copolymerization characteristics of the different active sites [10]. Metallocene catalysts are capable of producing resins having very narrow composition distributions [11]. Exxon was the first to introduce metallocene-catalyzed ethylene /  $\alpha$ -olefin resins (Exceed resins) in 1990 [12]. LLDPE gradually replaced LDPE in many applications and since 1983 has taken about 5% of the global LDPE market [13]. Total LLDPE capacity is estimated at 12 million tons per year and demand is expected to catch up with LDPE's market share of the global PE market by 2003. An annual growth rate of 8.5 % is anticipated through to 2005. In addition, combined LLDPE and HDPE capacity planned for the immediate future include 470 kt in Europe, 370 kt in the Americas, 360 kt in Africa/Middle East and 2305 kt for Asia-Pacific. Closure of the 135 kt Equistar plant in the USA was planned for 1999 [7]. Global capacities for 1999 are shown in Figure 3.3 and the top 10 global producers of polyethylenes for 1999 are shown in Figure 3.4.

**Global LLDPE Capacities (1999)**

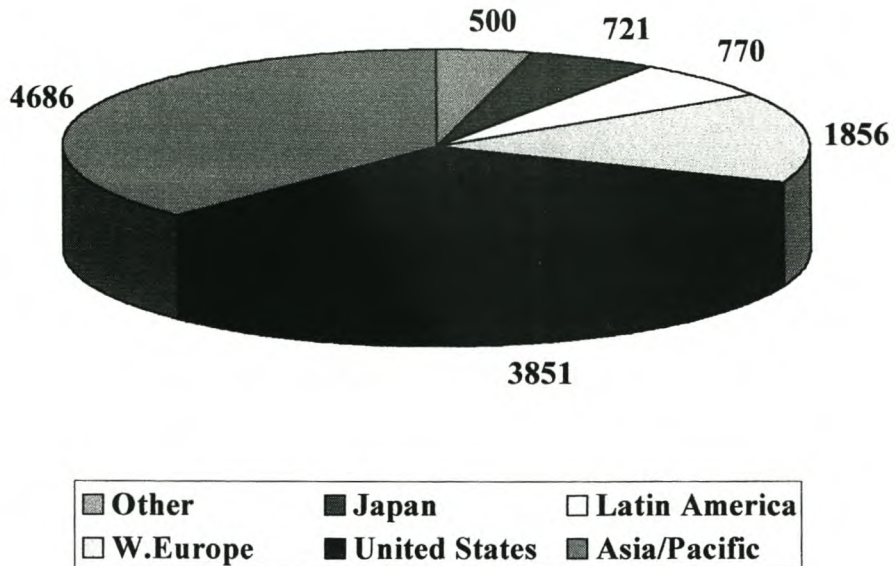


**Figure 3.3. Global LLDPE Capacities by Country**

**Top 10 Global PE Producers [ECN 21-27 June (1999)]**

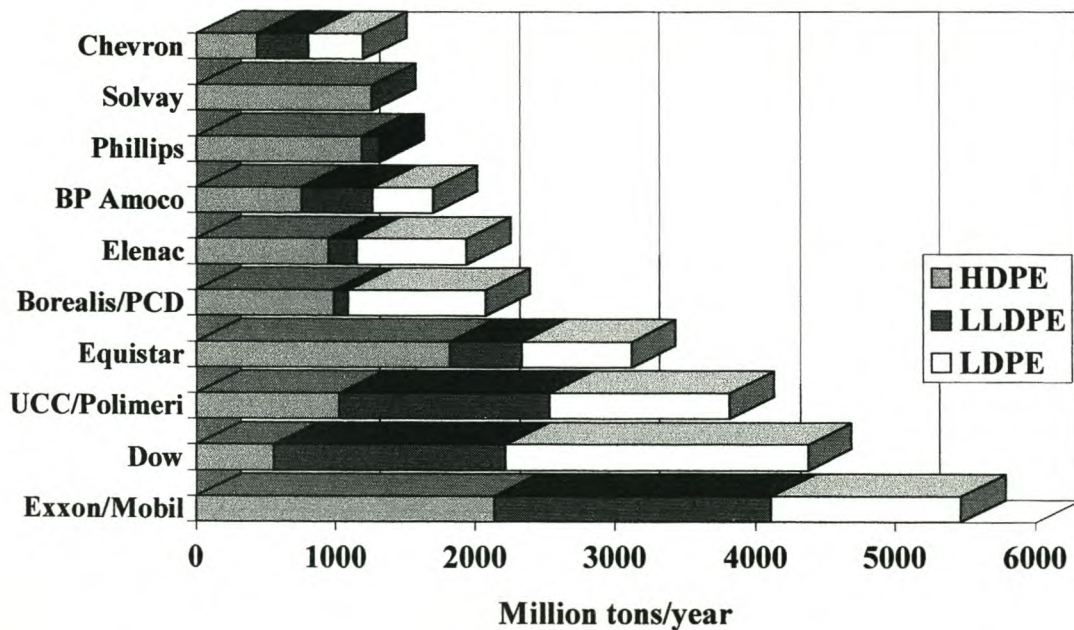


**Figure 3.4. Top 10 Global Polyethylene Producers**



### 3.1.2 POLYPROPYLENE

Natta was a consultant to Montecatini and, being involved in studying the kinetics of ethylene polymerization reaction, undertook the investigation of Ziegler's new catalyst [14]. Reacting propylene with the Ziegler catalyst, it was discovered that it produced a mixture of amorphous and crystalline polypropylene [15]. Two years later, Natta's group successfully synthesized regular, linear, head-to-tail polymers of  $\alpha$ -olefins [16].

The first company producing PP was Montecatini in Italy who went into production in 1957 and soon after, Hercules commenced production of PP in the U.S. [17]. Today global PP capacities total about 29 million tons per year [7]. Additional capacity planned for the immediate future include 160 kt in Europe, 950 kt in the Americas and 190 kt for Asia-Pacific. Closures include the 170 kt Montell plant in France, the 90 kt Targor plant in Germany and the 64 kt Japan Polyolefins plant.

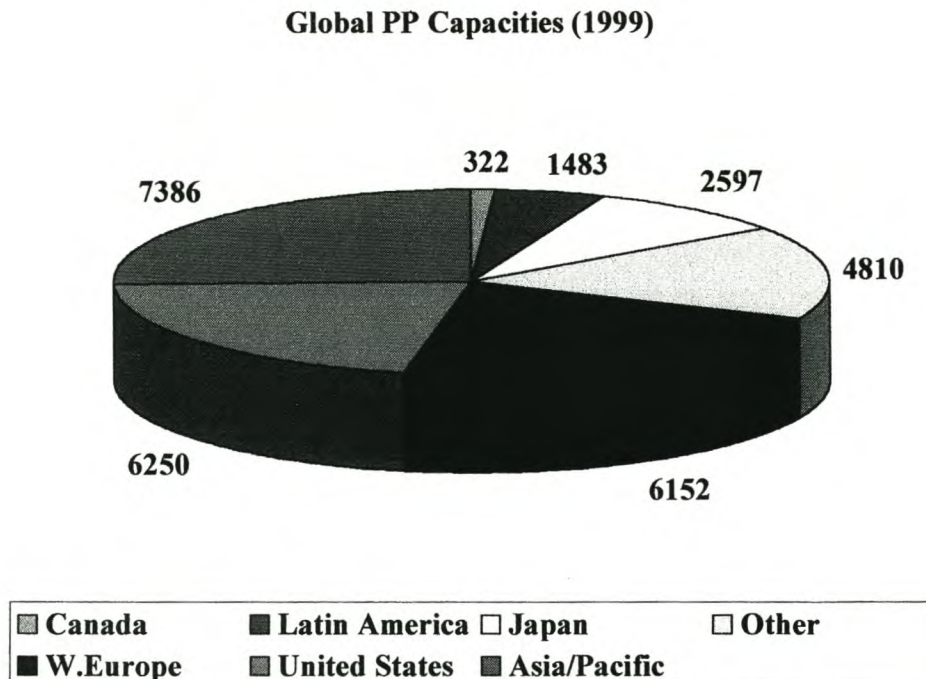


**Figure 3.5. Global Polypropylene Capacities per Country**

The global capacities per country and the top 10 producers for polypropylene are shown in Figures 3.5 and 3.6 respectively. Metallocene resins became available recently following successful industrial trials by companies including Exxon at its Baytown, Texas site, and Hoechst using the Spheripol process, both in 1995 [18]. Companies producing or planning to produce metallocene polypropylene resins include Asahi Chemical Industry [19], Chisso [20], Exxon [21] and Fina Oil & Chemical [22]. Global consumption of metallocene PP is about 40 kt/y in 1999 and is expected to increase by over 65%/y to 500 kt/y in 2003 [23].

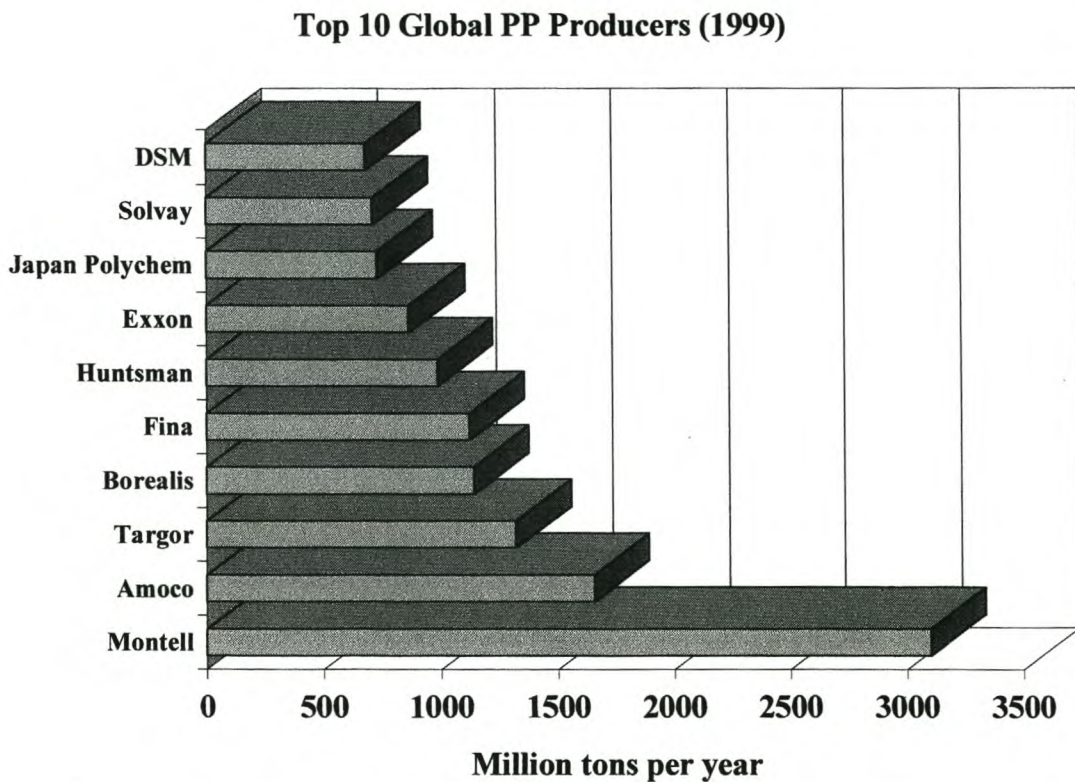


**Figure 3.6. Top 10 Global Polypropylene Producers**

## 3.2 POLYMERIZATION PROCESSES

Two very different processes are employed for the production of polyolefins. LDPE utilizes a free-radical catalyst in a high pressure process whereas the transition-metal catalyzed production of HDPE, LLDPE and PP is carried out at very much reduced pressures. Some overlap between the two processes does exist in the solution process for PE. The transition-metal catalyzed methods use three main types of processes which are: (a) The *slurry process* where the formed polymer particles are suspended in an inert hydrocarbon diluent, (b) the *solution process* in which the polymer formed in the reaction is dissolved in the polymerization medium and (c) the *gas-phase process* where the polymer particles are suspended in or fluidized by the monomer or monomer mixture, the gas of which is the polymerization medium; no liquid carrier medium is present.

### 3.2.1 POLYETHYLENE

#### 3.2.1.1 LDPE [24,25]

Low density polyethylene is produced in tubular reactors and stirred autoclaves at high pressures, typically 2000 bar, achieved by multistage compressing, using free-radical initiators. High pressures are necessary to provide a homogeneous reaction mixture. Reaction temperatures are typically between 220 and 350°C. Molecular weight and density increase with decreased temperature or increased pressure whereas long-chain branching increases with temperature and conversion and decreases with increasing pressure. Transfer agents which include  $\alpha$ -olefins, such as propylene and 1-butene, and also aliphatic hydrocarbons such as propane and butane decrease molecular weight. This allows the reactors to be run at increased pressures without an increase in molecular weight. The thick walls of the high-pressure vessels make heat transfer difficult with the result that the conversion per pass is usually low as the unreacted monomer is used to remove the heat of reaction. Molten polymer leaving the reactor is fed first to a high-pressure separator where most of the monomer is separated from the polymer. The low-boiling components and monomer recycle (overheads) from this unit contains some low molecular weight product which is

separated in a series of high pressure separation and cooling units for removal of the reaction heat. The cold monomer is then fed, together with fresh monomer, from the primary compression section to the secondary compression section, which feeds the reactor. The polymer from the high-pressure separator is fed into a low-pressure separation unit where the rest of the monomer is separated from the molten polymer. The bottoms of this unit feeds the extruder for pelletization. The overheads from this separator is fed to the first stage of compression (primary compression), a small amount of which is purged to prevent build-up of ethane and methane. Fresh monomer is combined with the low-pressure separator overheads at the primary compressor unit where the pressure is increased stepwise to feed pressure.

*Stirred Autoclave.* These processes are either single or multi stage and are stirred by different arrangements of paddles. Single stage reactors have length/diameter ratios of 2 – 4 for effective back mixing. Polymerization is achieved by adding one or more peroxide initiators having slightly different half-lives at the reaction temperature of 220 to 300°C. Reaction temperature is controlled by the introduction of cold ethylene. Multistage reactors have higher length / diameter ratios which can be as high as 15 to 18. Ethylene, comonomer (if used) and initiator are introduced in different stages, which are separated by baffles to create a series of reactors in one vessel. Residence times vary from 10 to over 60 seconds. A general scheme for the high pressure polymerization of ethylene is presented in Figure 3.7.

*Tubular Reactors.* Tubular reactors are essentially thick-walled jacketed pipes arranged in the shape of an elongated coil. The reactor can be single- or multi-staged. In the multi-stage reactor, initiator or ethylene can be injected at different stages along the length of the reactor. To prevent polymer build-up and consequent degradation and cross-linking on the reactor walls, velocity must be at least 10 m/s. Pressure is controlled by periodic opening of a dump valve to decrease the pressure by 200 to 500 bar. This speeds up the flow of molten polymer through the reactor and prevents polymer build-up. In a single-stage reactor, monomer at high pressure enters the reactor through a pre-heater that increases the temperature to the initiation temperature. Initiator may be added to the compressed ethylene at or lower than the initiation temperature.

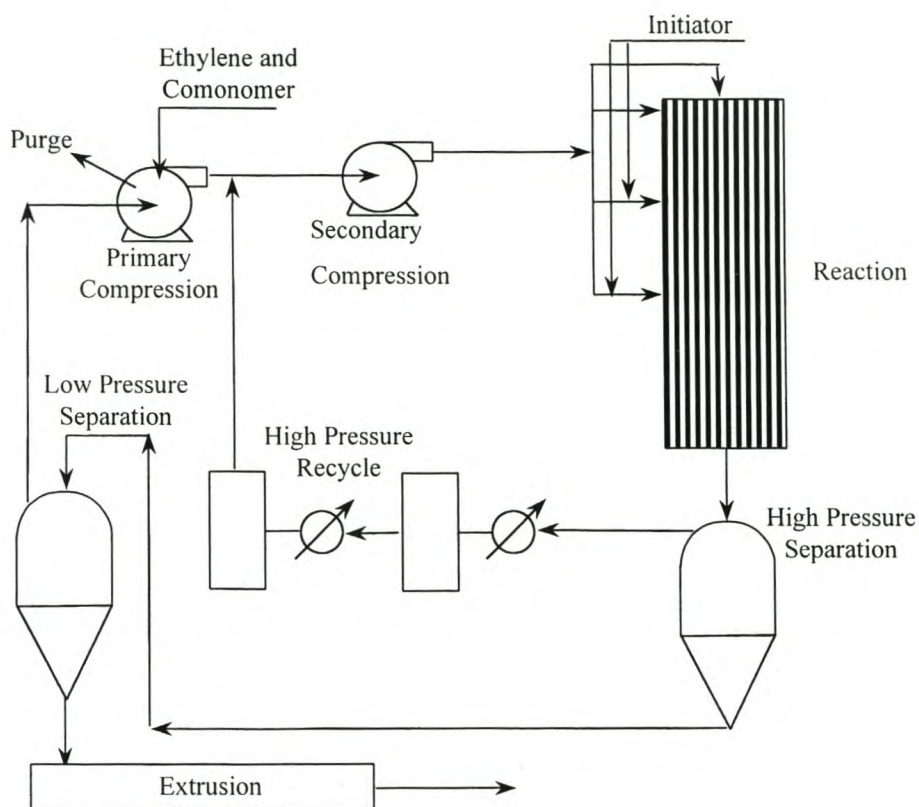


**Figure 3.7. High Pressure Polymerization of Ethylene**

As the reaction mixture passes along the reactor, the temperature increases as a result of the exothermic reaction and peaks at more than 300 °C. Some of this heat is removed by the jacket around the reactor. After the reaction temperature peak has been reached, the molten reaction mixture is passed into a high-pressure separator. The conversion per pass is between 15 and 20%. In multi-stage reactors, the partially cooled reaction mixture from the first zone is reinitiated by introducing another peroxide which creates a second (and further) reaction zone in series with its own temperature peak. In the ethylene side injection process, cold ethylene containing initiator is injected to provide cooling and to reinitiate polymerization in the second zone. The conversion per pass is between 22 and 30%.

### 3.2.1.2 HDPE [26,27]

*Solution Process.* Two processes are practiced: polymerization in heavy, saturated hydrocarbons and polymerization in molten polyethylene [28]. Catalysts are usually

either completely soluble or pseudo soluble. The latter occurs when the catalyst components are added separately as liquids, both soluble in the reaction medium, but form an insoluble solid catalyst by reacting with each other in the reactor. These processes were also the first to be used for metallocene catalysts.

Polymerization in hydrocarbon solvent, as used by Du Pont [29] and Dow [30], is carried out in a hydrocarbon solvent such as cyclohexane (in Du Pont's case) at temperatures between 120 to 200°C where the formed polymer is soluble. The catalyst system, hydrogen and ethylene (and a comonomer if used) are fed continuously to a stirred reactor at between 50 and 100 bar where the polymerization proceeds for about 5 to 10 minutes. The hot polymer solution is dumped into a flash tank where most of the solvent evaporates and is recycled. The polymer is fed to a devolatilization extruder for pelletization where the rest of the solvent together with low molecular weight products is removed. The Du Pont process is shown in Figure 3.8.

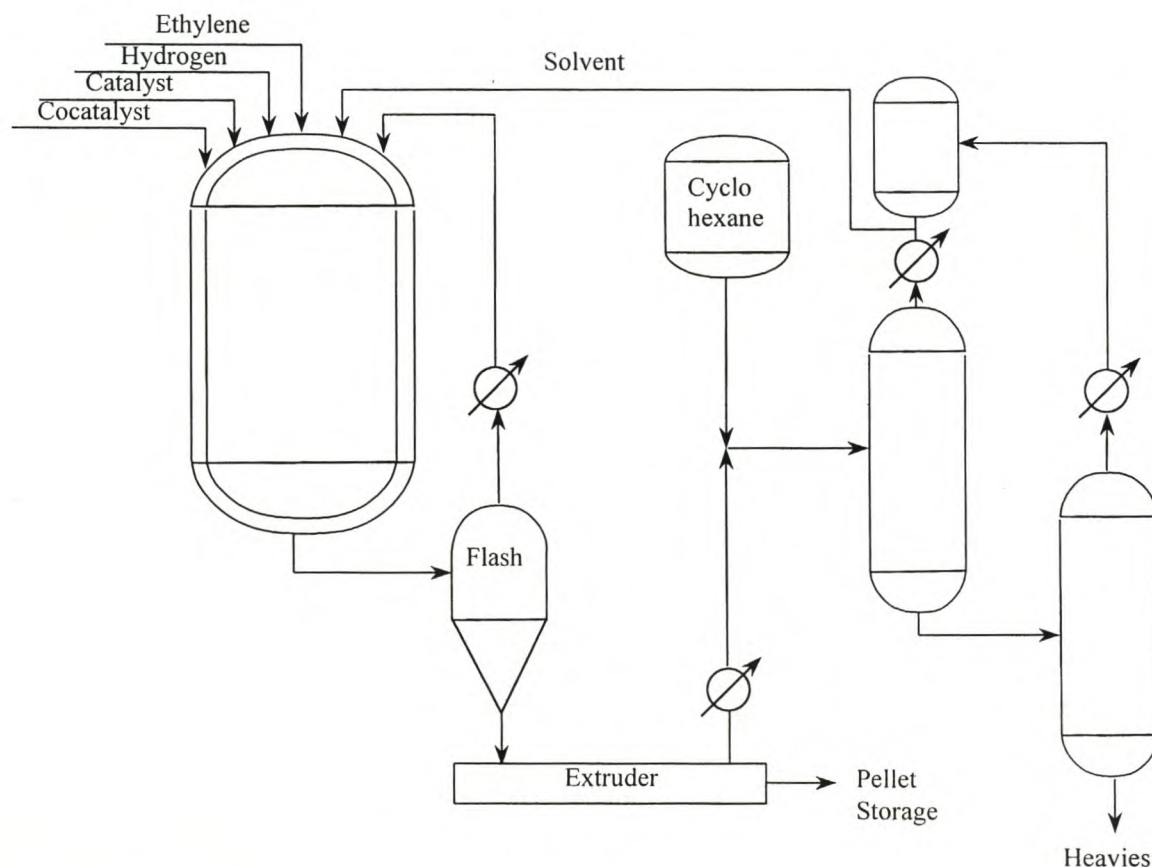


**Figure 3.8. Du Pont Solution Process**

In the process using molten PE [28], stirred autoclaves or tubular reactors previously used for LDPE production are modified for use in this process. Operating temperatures are between 170 to 350°C, pressures between 300 to 2000 bar and residence times typically below 1 minute.

Because solution viscosity increases with molecular weight, this process is primarily used for the production of low molecular weight polymer since high viscosity solutions increase the risk of reactor fouling as well as stirring and homogeneity problems. For low molecular weight polymer, solids content can reach 30 to 35% but to produce higher molecular weight polymer, solids content must be decreased.

*Slurry Process.* This is the oldest and most mature polymerization process. Due to its flexibility and ability to produce the full range of HDPE resins, from low molecular weight waxes to ultra high molecular weight polymers, this process accounts for over 60% of all PE produced worldwide. Two basic processes *viz.* a loop reactor and a stirred reactor, which in turn can be further sub-divided into four processes, are used. [31]. The stirred reactor process can be divided into the following four processes: (a) loop reactor with low-boiling diluent, (b) loop reactor with high-boiling diluent, (c) stirred tank with high-boiling diluent and (d) liquid pool process with low-boiling diluent.

In the loop reactor process, which was developed by Phillips and is shown in Figure 3.9, catalyst and monomer(s) are fed to the jacketed reactor in the form of a folded loop. This folded loop has four vertical legs of about 50 m in length and 0.5 to 1 m in diameter, arranged in a square and connected at their ends by four short semi-circular pipes of the same diameter. The reactor is filled with the diluent (light or heavy) which, together with the polymer in suspension at concentrations up to 25%, is circulated by a pump at speeds between 5 and 12 m/s. This high speed of the slurry continuously scrubs the inside of the reactor walls to prevent fouling and assist with the removal of reaction heat. Polymer is concentrated in settling legs from where it is continuously removed into a flash tank for solvent recovery. The polymer reactor powder is dried and pelletized. The reactor operates at temperatures between 70 and

110°C and pressures between 30 and 45 bar, depending on the diluent used. Residence time is between 30 minutes and 2.5 hours.

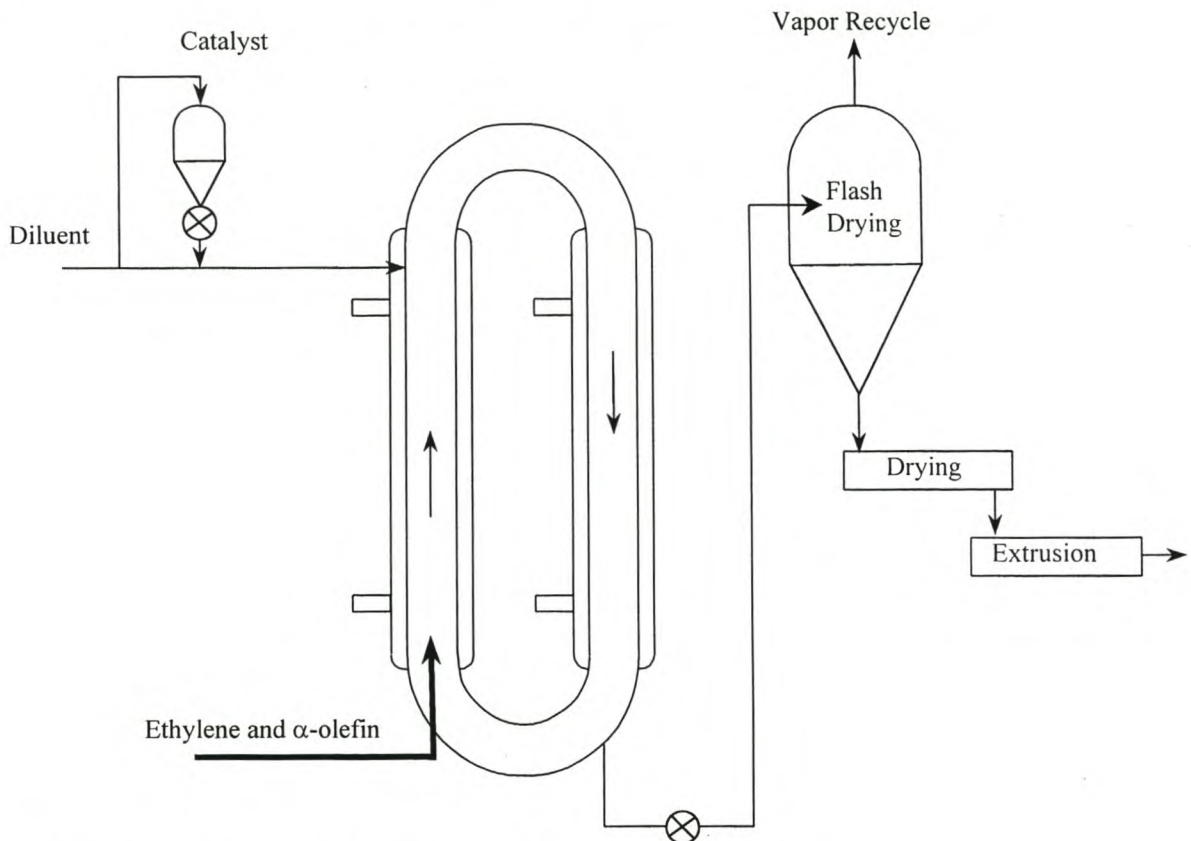


**Figure 3.9. Phillips Loop Reactor Process**

In the stirred reactor process, as used by Montedison, Hoechst, Solvay and Mitsui, diluent, the catalyst system, ethylene, hydrogen (and comonomer if used) are continuously fed to a stirred reactor at temperatures between 80 and 90°C and pressures between 10 and 30 bar. The polymer slurry (which can be transferred to a second reactor for post polymerization) is separated from the diluent in a centrifuge. The solvent is recycled to the reactor and the polymer reactor powder is steam-stripped, dried and pelletized.

*Gas-Phase Process.* This is the most recent polymerization process and was introduced by Union Carbide in 1968. In this process the polymer powder is fluidized by a stream of monomer (and comonomer if used) entering the reactor at a high flow rate through a perforated plate at the bottom of the reactor and leaving the reactor at the top. The gas is then cooled, compressed and reintroduced into the reactor.



Catalyst is fed to reactor above the distribution plate and liquid cocatalyst and comonomer, if used, is fed from the bottom together with the ethylene. The high circulation velocity necessary for heat removal and fluidization result in a conversion per pass of about 2%. The heavy polymer particles concentrated at the bottom of the reactor is periodically removed through a system of valves and transferred into a series of bins for removal of unreacted monomer and then pelletized. In order to prevent carry-over of the fluidized polymer particles with the recycle gas, the gas velocity is decreased in the top part of the reactor (called the disengagement zone) because of its larger diameter. The Union Carbide gas-phase process is shown in Figure 3.10.

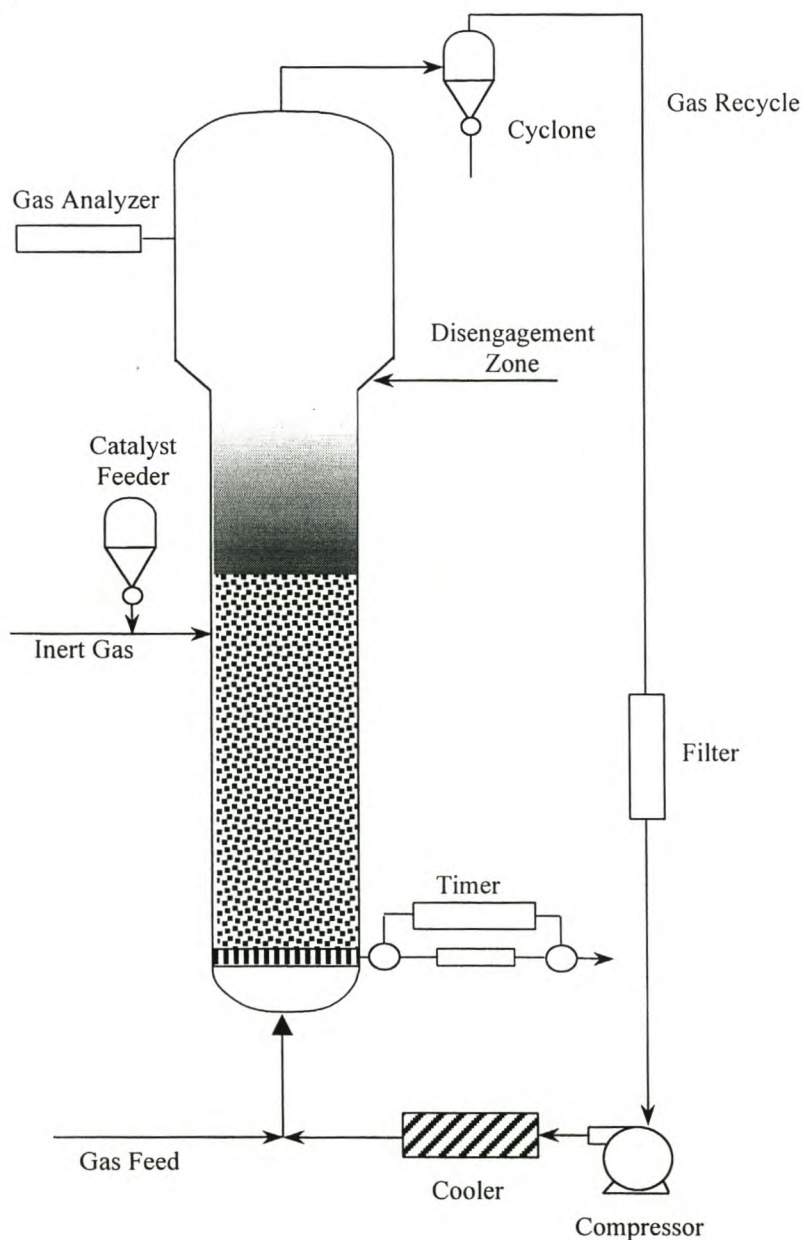


**Figure 3.10. Union Carbide Gas-Phase Process**

Other companies, including BP, Amoco and BASF also developed gas-phase technology. In the Amoco process, the reactor is a horizontal, segmented stirred-bed reactor. The polymer is agitated within each compartment by slowly turning blades and is kept in a sub-fluidized state by the introduction of ethylene (and comonomer if used) through inlets at the bottom whilst catalyst components together with light hydrocarbons are sprayed onto the bed from the top. Evaporation of the hydrocarbon sprayed onto the bed removes the heat of reaction. As the polymer bed grows, it spills over from the one compartment to the other until it is finally discharged from the reactor through a series of locks. Vaporized components including the hydrocarbon solvent, hydrogen, ethylene (and comonomer if used) are separated and rerouted back to the reactor. The reactor runs at temperatures between 70 and 80°C and a pressure of about 20 bar. BASF uses a vertical stirred bed reactor in which monomer(s) and catalyst components are introduced into the vigorously stirred bed of polymer powder. A stream of polymer particles is then continuously removed from the reactor, separated from the gas in a cyclone and pelletized. The gas stream is circulated through a cooling loop and rerouted to the monomer feed stream.

### **3.2.1.3 LLDPE**

Since the solution processes limit the range of molecular weights possible, processes making LLDPE earned importance early in the 1990s because these were the first processes to produce metallocene resins. Dow uses the solution process for their Dowlex range of ethylene / 1-octene resins produced with a Ziegler-Natta catalyst at temperatures up to 250°C and pressures from 30 to 200 bar. Single-site constrained geometry catalysts are used to produce the uniformly branched Insite resin [32,33] and the Engage and Affinity very low density resins.

Slurry processes are not widely applied, mainly because the copolymer resins swell to various degrees depending on the diluents and operating temperature used. These severely limit the achievable density to the medium density range of about 0.930g/cm<sup>3</sup> (in heavy solvents such as hexane) and 0.923 g/cm<sup>3</sup> (in very light diluents) [33]. The Phillips loop reactors utilize 1-butene, 1-hexene, 1-octene and 4-methyl-1-pentene as

comonomers, usually with iso-butane as solvent, and operate at temperatures in the 60 to 75°C range to prevent swelling.

The first gas phase, fluidized bed process for the production of LLDPE was introduced by Union Carbide in 1977. This so-called Unipol process was used with 1-butene as comonomer because it was available, inexpensive, allowed the production of polyethylenes with properties superior to LDPE and did not condense in the gas-phase reactor. Resins containing higher  $\alpha$ -olefins have superior properties to the 1-butene grades. This was the driving force for changing the gas-phase technology to utilize the higher  $\alpha$ -olefins as comonomers. By operating the process in condensed mode with 1-hexene, for example, the recycle gas is cooled below the dew-point. Fine 1-hexene droplets are formed and are carried by the gas stream into the reactor where the droplets evaporate. This increases the capability of the circulating gas stream to remove the heat of the reaction, thereby also increasing reactor productivity [34]. Operating temperature is a very important parameter in gas-phase production of LLDPE as these resins have lower softening points than HDPE and will therefore tend to become sticky at lower temperatures than HDPE. These sticky particles can cause fouling of the reactor walls and can easily form agglomerates, the insides of which are effectively isolated, resulting in poor heat exchange and the consequent formation of lumps of polymer charred on the inside. High comonomer content has exactly this same effect of producing sticky resins that cannot be handled in gas-phase reactors. The minimum resin density which can be obtained in gas-phase processes is therefore limited.

## **3.2.2 POLYPROPYLENE**

### **3.2.2.1 Early Processes**

The early catalysts used for propylene polymerization had low activities and polymers containing high amounts of the atactic fraction were produced. The  $\alpha$ -form of the early  $\text{TiCl}_3$  catalysts [35] yields polypropylene with isotacticities between 80 and 90% which made the development by Montecatini of the first industrial process for the production of polypropylene possible [36]. The low polymerization activity of the

Montecatini catalyst, typically 5 kg polyethylene per gram of transition metal, resulted in titanium residues in the polymer as high as 100 ppm. Correspondingly, chlorine levels are also high resulting in excessive corrosion and thermo-oxidative stability problems which necessitated the removal of catalyst residues [37]. The first commercial processes for the production of polypropylene utilized slurry technology in which the isotactic fraction was kept in suspension while the atactic fraction was in solution. The slurry was then filtered to separate the two fractions. Products obtained from this technology were limited to high molecular weight homopolymers, random copolymers containing small amounts of ethylene and impact polymers with low rubber content.

Polymerization was also carried out in liquid monomer and was pioneered by Rexall [38] and Phillips [39]. In the Rexall process a stirred vessel is used and in the Phillips process, the polymerization vessel is a loop reactor containing the rapidly circulating polymer / monomer suspension. Polymer separation from the gaseous monomer takes place in a cyclone at ambient pressure resulting in the atactic fraction remaining in the polymer. Although reactor fouling through atactic polymer build-up with the consequent decrease in heat transfer ability was addressed in these processes, the atactic polymer adversely affected polymer properties and necessitated its removal in a further step. Solvay introduced a high activity, highly stereoregulating catalyst which was used in liquid monomer processes without the necessity for atactic removal [40]. Montedison and Mitsui introduced a  $MgCl_2$ -supported catalyst which decreased the amount of corrosive catalyst residues to such an extent that the post production removal of catalyst became unnecessary [41].

Eastman Chemical was the first to utilize a high temperature solution process [42]. Polymerization temperature was kept above  $150^\circ C$  to prevent precipitation of the isotactic fraction, which increased both polymerization rate and chain transfer reactions and adversely affected stereoregularity.

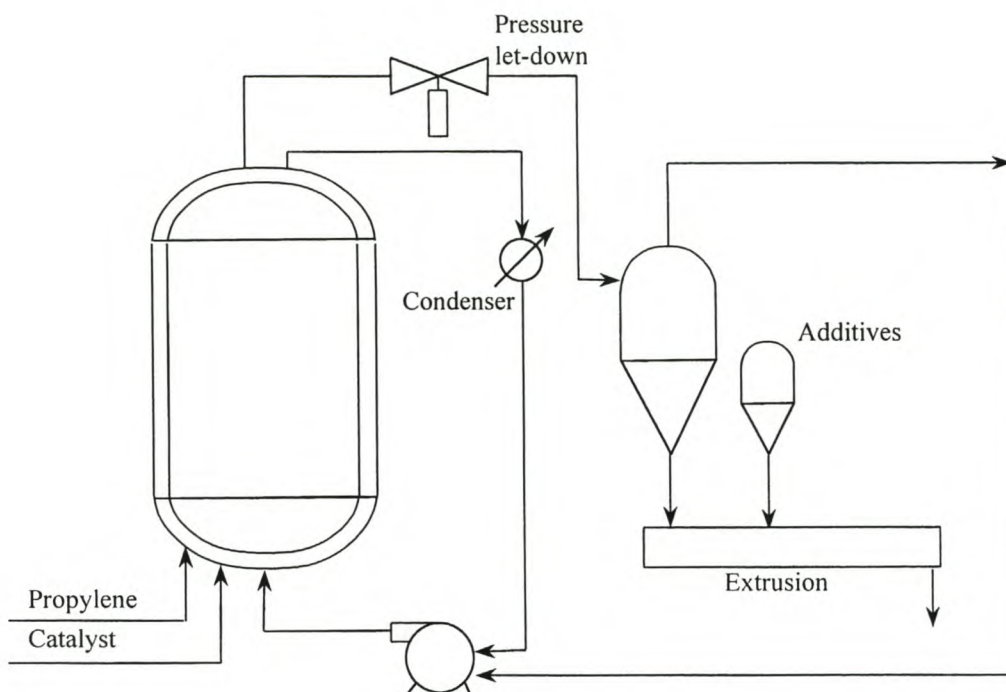


**Figure 3.11. Novolen Gas-Phase Process**

BASF pioneered gas-phase propylene polymerization processes by introducing the Novolen stirred-bed process [43] shown in Figure 3.11. The process runs at temperatures between 70 and 90 °C and pressures of about 30 bar. Unreacted monomer is condensed and recycled to provide additional heat transfer capability. Atactic removal was required, as it is not extracted as in the slurry processes.

### 3.2.2.2 Current Processes

Savings in post reaction work-up of polypropylene which was achieved by the introduction of superactive third-generation catalysts resulted in many companies upgrading older plants or building new ones to utilize this technology.

Himont's Spheripol process [36,44] consists of two sections. The first section contains one (or more) loop reactor(s) in which homo- or random copolymerization takes place in liquid monomer. Concentrated slurry is removed from the settling legs and fed to a cyclone where the polymer and gaseous monomer is separated. The monomer is condensed and fed back into the loop reactors while the polymer is fed

into (one or more) fluidized-bed gas-phase reactor(s) where ethylene and propylene is introduced for the formation of the desired rubber composition for impact polymers. The dense spherical polymer particles are steam-stripped from residual monomer while the catalyst is also deactivated by this procedure and then dried without the necessity of pelletization.

Mitsui's Hypol process [46] uses the Spheripol catalyst technology. The Novolen process of BASF has been rejuvenated through the use of superactive supported catalysts. Union Carbide has extended polyethylene technology to polypropylene and uses the Shell high activity catalyst (SHAC) in a cascade reactor set-up where homopolymer and random copolymer is produced in a large fluidized-bed, gas-phase reactor. The product can then be relayed either to the product discharge tank or to a second smaller reactor for the production of the rubber phase for impact polymers.

### 3.3 POLYMER PROPERTIES

#### 3.3.1 POLYETHYLENE

The properties of PE's are controlled through changes in density, molecular weight, molecular weight distribution and cross-linking [47]. For processes involving transition metal catalysts, density is controlled by changing the amount and type of  $\alpha$ -olefin comonomer in order to controllably destroy polymer crystallinity. In the high pressure, free-radical process for LDPE production, density is controlled to a certain extent by temperature. Molecular weight is controlled by the amount of chain transfer agent (usually hydrogen) added to Ziegler-Natta and metallocene catalysts although temperature also affects the rate of chain transfer. With the Phillips catalyst, hydrogen is not effective and molecular weight is primarily controlled with temperature. Primarily, the type of catalyst employed determines the molecular weight distribution. For LDPE, MWDs between 12 and 20, depending on the process, is obtained [24]. The density range of the different types of polyethylenes obtained with different catalysts are shown in Table 3.1 [47].

**Table 3.1. Density Range for Different Polyethylenes [47]**

Polymer Types	Catalysts*	Density (g/cm <sup>3</sup> )
High Density Polyethylene (HDPE)	Z-N, Cr, Met.	$\geq 0.941$
Ultra High Molecular Weight PE (UHMWPE)	Z-N, Met.	0.935 – 0.930
Medium Density Polyethylene (MDPE)	Z-N, Cr, Met.	0.926 – 0.940
Linear Low Density Polyethylene (LLDPE)	Z-N, Cr, Met.	0.915 – 0.925
Low Density Polyethylene (LDPE)	Free Radical	0.910 – 0.940
Very Low Density Polyethylene (VLDPE)	Metallocene	0.880 – 0.915

\*Z-N : Ziegler-Natta, Cr : Chromium, Met. : Metallocene

Ethylene/ $\alpha$ -olefin copolymers produced with chromium oxide catalysts have very broad MWD with  $M_w/M_n$  ratios from 12 to 35. HDPE produced with these Phillips catalysts have MWDs between 6 and 12. Molecular weight of typical commercial HDPE is between 80 000 and 1.2 million g.mol<sup>-1</sup>. For commercial LLDPEs produced with Ziegler-Natta catalysts MWD is between 2.5 and 4.5. Metallocene catalysts,

having only one type of active site present have a very narrow MWD, normally around 2.

### 3.3.1.1 LDPE

Increased molecular weight increases some polymer properties. These include melt flow index, resistance to abrasion and creep, tensile strength, stiffness, shrinkage, warping and film impact strength. Properties adversely affected by increased molecular weight include transparency, haze and gloss. Haze is present in all polyethylenes and is caused mainly through the difference in refractive index between the crystalline and amorphous phases. Impact strength and film tear resistance increase with a decrease in density. For use as packaging bags, film impact strength and tear resistance should be high, making LDPE very suitable for film application. It is therefore not surprising that film is the single biggest market for PE [48]. In Europe, 73% of the total LDPE production is used in film and sheet applications [49]. Properties of LDPE blown film are shown in Table 3.2 [48].

**Table 3.2. Blown Film Properties of LDPE [48]**

Property	Value
Density (g/cm <sup>3</sup> )	0.924
Melt Flow Index (dg/min.)	2.0
Haze (%)	5.0
Gloss (%)	70
Falling Dart Impact (g)	90
Puncture Energy (J/mm)	20
Tensile Strength (MPa)	
MD / TD	24 / 19
Elongation (%)	
MD / TD	310 / 580
Modulus (MPa)	
MD / TD	145 / 175

Because of the low density and crystallinity of LDPE, the polymer chains can undergo viscous flow quite easily under a wide range of temperatures, which is responsible for the ductile failure observed for LDPE under tensile or impact conditions [50]. Only at very low temperatures, (< -70°C) can LDPE fail in brittle fashion. Long-term failure is of the brittle type. Stress cracking, caused by low stresses which could be moulded-



in or stresses acting on the article during use and promoted by solvents, oxygen, detergents etc., is reduced by decreased density and molecular weight distribution and increased molecular weight and temperature. Cross-linking by radiation renders the polymer completely free from stress cracking. LDPE is highly resistant to many chemicals, mostly polar solvents, water penetration and many aqueous acidic or alkaline solutions and is therefore extremely suitable and extensively used for chemicals storage and packaging and food wrapping, bags and containers.

**Table 3.3. Properties of Typical Commercial LDPE Grades [25,52,50]**

Property	Range
Tensile Strength at Yield (MPa)	8 – 18
Elongation at Yield (%)	10 – 40
Break Strength (MPa)	10 – 17
Elongation at Break (5)	100 – 700
Young's Modulus (MPa)	90 – 500
Shore Hardness	40 – 60
Dielectric Constant at 60 Hz	2.25 – 2.35
Density (g/cm <sup>3</sup> )	0.912 – 0.94
Crystallinity (%)	20 – 60
Methyl Groups / 1 000 Carbons	10 – 60
Molecular Weight (g/mole)	500 – 60 000
Refractive Index ( $n_D^{25}$ )	1.51 – 1.53
Thermal Expansion 10 <sup>-5</sup> cm/cm per °C	10 – 20
Haze (%)	40 – 50
Gloss (%)	0 – 80
Water Absorption 24 hr (%)	< 0.02
Melting Temperature (°C)	102 – 120
Brittleness Temperature (°C)	< -70
Heat Distortion Temperature 0.455 MPa (°C)	40 – 65
Abrasion Resistance (mg/1 000 cycles)	10 – 15

When LDPE was first produced on a commercial scale, the biggest proportion of production went for the manufacturing of coaxial cable used in radar applications. [51] This was because of its extremely effective electrical insulating properties at domestic voltages and low to ultra-high frequencies. Properties of typical commercial LDPE grades are shown in Table 3.3 [25,52,50].

### 3.3.1.2 HDPE

Ethylene homopolymerized with Ziegler-Natta, Phillips or metallocene catalysts yields mainly linear polyethylene chains containing 0.5 to 3 branches per 1 000 carbon atoms. Because of its highly regular structure, these linear chains can crystallize much more easily than the highly branched LDPE. Indeed, crystallinity of linear polyethylene usually varies between 40 and 80% [27] but can be as high as 90% [50]. Its principal crystalline form is orthorhombic with a density of 1.00 g/cm<sup>3</sup> and amorphous density of 0.855 g/cm<sup>3</sup> [53]. Therefore, because of the higher proportion of the denser crystalline phase, the linear polyethylene homopolymers generally have higher densities than the branched ones and densities of 0.97 g/cm<sup>3</sup> are common. Ultra high molecular weight polyethylene also falls into this category, but because of the extremely long chains, entanglements hinders chain movement, resulting in decreased crystallinity to 40 % and a density of about 0.93 g/cm<sup>3</sup>. Typical properties of commercial HDPE are shown in Table 3.4 [27,52].

**Table 3.4. Typical Properties of Commercial HDPE [27,52]**

Property	Range
Tensile Strength at Yield (MPa)	25 – 40
Elongation at Yield (%)	5 – 12
Break Strength (MPa)	20 – 45
Elongation at Break (5)	50 – 1 200
Young's Modulus (MPa)	800 – 1 200
Shore D Hardness	50 – 70
Impact Strength (J/m)	40 – 750
Dielectric Constant at 1 MHz	2.2 – 2.4
Density (g/cm <sup>3</sup> )	0.95 – 0.97
Crystallinity (%)	40 – 90
Molecular Weight (g/mole)	80 000 – 1.2 million
Refractive Index ( $n_D^{25}$ )	1.53 – 1.54
Linear Thermal Expansion 10 <sup>-4</sup> cm/cm per °K	1 – 1.5
Volume Thermal Expansion 10 <sup>-4</sup> cm/cm per °K	2 – 3
Thermal Conductivity (W/(m.K))	0.42 – 0.52
Melting Temperature (°C)	125 – 135
Fusion Enthalpy ( <i>Orthorhombic Crystal</i> ) (kJ/mol)	4.01
Brittleness Temperature (°C)	-70 – -140
Heat Distortion Temperature 0.455 MPa (°C)	120 – 122
Coefficient of Thermal Expansion x 10 <sup>-5</sup> (K <sup>-1</sup> )	13

During fabrication, most articles will acquire some degree of molecular orientation. For film, fiber and strapping, orientation is introduced deliberately, but can also develop unintentionally e.g. through viscous flow of the melt into a mould and subsequent shrinking on crystallization resulting in moulded in stresses. By stretching below the melting point, as for fiber production, levels approaching 100% orientation can be achieved. Optical clarity is poor and articles moulded in HDPE are usually opaque because of the high degree of crystallinity. Electrical insulating properties are excellent and the polymers are widely used in this field [27]. Permeability by water, gases and organic compounds are low and combined with its high stiffness, the polymer is very suitable for use in making fuel and water tanks. This combination of properties also makes HDPE extremely suitable for blow moulding into many types of bottles and containers. This is the largest market for HDPE.

### 3.3.1.3 LLDPE

Polymer properties are directly related to crystallinity, which can be translated into density. The orthorhombic crystal density of polyethylene is  $1.0 \text{ g/cm}^3$  and amorphous density is  $0.855 \text{ g/cm}^3$  [53]. By changing the crystalline / amorphous ratio, the densities of LLDPE could theoretically be varied within these limits. Introduction of higher  $\alpha$ -olefins has the effect of breaking up the crystal structure, resulting in a decreased density [24]. Ziegler-Natta catalysts produce polymer with a non-uniform distribution of comonomer units [12], which makes it difficult to completely destroy crystallinity to obtain very low densities. In 1990, Exxon introduced a new type of LLDPE on the market, produced with metallocene catalysts. These polymers have a very uniform distribution of comonomer units along the polyethylene chain. Densities, and consequently crystallinity also, are generally lower at the same comonomer content when the comonomer distribution is narrow, i.e., uniformly branched. Table 3.5 presents the difference in copolymer properties between uniformly and non-uniformly branched copolymers [12].

**Table 3.5. Difference in LLDPE Properties Resulting From Uniform and Non-uniform Comonomer Distribution [12]**

Property	1-Butene			1-Octene
	Mitsui Uniform	Exxon Uniform	U. Carbide Non-Unif.	Dow Non-Unif.
Producer	Mitsui	Exxon	U. Carbide	Dow
Comonomer Distribution	Uniform	Uniform	Non-Unif.	Non-Unif.
Density (g/cm <sup>3</sup> )	0.88	0.88	0.89	0.912
Crystallinity (%)	20.4	21.2	25.6	42.9
Melt Index (dg/min.)	3.6	3.8	1.0	3.3
Melting Temperature (°C)	69.5	71.8	118.4	123.8
Young's Modulus (MPa)	30	25	57	150
Strain Recovery (%)	95	98	74	63
Haze(%)	4	4	46	51

As a result of the decreased crystallinity, melting temperatures and mechanical properties are lower. The uniform metallocene polymers are more rubbery than those having a non-uniform comonomer distribution as was noted from the nearly complete strain recovery observed. Optical clarity of the polymers is also far better than obtained for the non-uniform copolymers. It is believed that as the lengths of the side chains introduced into the polyethylene chains by higher  $\alpha$ -olefins increase, crystallization is progressively inhibited [48], increasing the number of tie-molecules and resulting in a stronger product. In the patent literature [54-58], inventors usually present a generic list of different comonomers which can be used to modify properties. These include, besides the even-numbered comonomers, also 1-pentene, 1-heptene, 1-nonene and higher  $\alpha$ -olefins. However, in very few cases is the actual use of these comonomers exemplified. In some cases, terpolymerization is also included in the generic description but again the reactions are rarely described [59]. The use of different  $\alpha$ -olefins as comonomer has a powerful effect on polymer properties as can be seen from Table 3.6 [12].

**Table 3.6. Properties of Commercial LLDPE Film with Non-uniform Comonomer Distribution [12]**

Property	Comonomer		
	1-Butene	1-Hexene	1-Octene
Density (g/cm <sup>3</sup> )	0.918	0.918	0.919
Melt Flow Index (dg/min.)	1.0	1.0	1.0
Falling Dart Impact (g)	150	250	350
Puncture Energy (J/mm)	70	85	61
Tensile Strength (MPa)			
MD / TD	38 / 31	38 / 32	43 / 34
Elongation (%)			
MD / TD	620 / 760	570 / 790	550 / 660
Modulus (MPa)			
MD / TD	230 / 260		

The range of copolymer properties of commercial LLDPE of both homogeneous and heterogeneous comonomer distributions is presented in Table 3.7.

**Table 3.7. Typical Properties of Commercial LLDPE Including Uniform and Non-uniform Composition Distributions [12]**

Property	Value
Density (g/cm <sup>3</sup> )	< 0.915 – 0.94
Melt Index (dg/min.)	0.5 – 30
Molecular Weight (g/mol)	50 000 – 200 000
Molecular Weight Distribution ( $M_w/M_n$ )	2.5 – 35
Crystallinity (%)	< 25 – 55
Melting Temperature (°C)	100 – 130
Brittle Temperature (°C)	-100 – -140

Stress crack resistance of LLDPE is generally better than LDPE because of its narrower molecular weight distribution and higher molecular weight [48]. LLDPE is relatively unreactive but contains more reactive tertiary hydrogens at each branch point and double bonds at some chain ends. It can be attacked by concentrated H<sub>2</sub>SO<sub>4</sub> and HNO<sub>3</sub> but is stable in their aqueous solutions, other inorganic and organic acids, bases and salt solutions and does not dissolve in any solvent at room temperature. At elevated temperatures, it is soluble in solvents such as xylenes, decalin, tetralin and chlorinated benzenes [12].

### 3.3.2 POLYPROPYLENE

Natta studied propylene polymerization with the Ziegler catalyst and defined three different stereoisomers of polypropylene [60]. In isotactic polypropylene the methyl groups are situated on the same side of the plane defined by the polymer backbone. This orderly placement of the methyl groups results in crystalline polypropylene. A 100% isotactic polymer has a crystallinity of 68% with a melting temperature of 174°C and density up to 0.943g/cm<sup>3</sup> [53,61]. Heat of fusion of the 100% crystalline monoclinic  $\alpha$  form is between  $165 \pm 18$  J/g [62] and 209 J/g [61]. The atactic polymer has the methyl groups placed randomly in the polymer chain, resulting in an irregular non-crystalline structure. The syndiotactic form has methyl groups alternating on both sides of the polymer backbone, again resulting in a crystallizable polymer of which the orthorhombic crystal density is 0.91 g/cm<sup>3</sup> [63]. Commercially, the isotactic isomer is the most important and typical properties of the homopolymer is shown in Table 3.8 [61,62].

**Table 3.8. Typical Property Range of Commercial, Mainly Isotactic Polypropylene Grades [61,62]**

Property	Value
Melt Flow Index (dg/min.)	0.4 – 35
Tensile Strength at Yield (MPa)	29 – 39
Elongation at Yield (%)	11 – 15
Elongation at Break (5)	500 - 900
Young's Modulus (MPa)	1 000 – 1 700
Shore D Hardness	70 – 80
Izod Impact Strength (J/m)	20 – 120
Rubber Modified High Impact (J/m)	70 – 640
Dielectric Constant at 1 KHz	2.2 – 2.3
Density (g/cm <sup>3</sup> )	0.90 – 0.91
Crystallinity (%)	40 – 68
Molecular Weight (g/mole)	220 000 – 700 000
Molecular Weight Distribution ( $M_w/M_n$ )	5 – 12
Thermal Conductivity (W/(m.K))	11.7
Melting Temperature (°C)	160 – 165
Fusion Enthalpy (J/g)	65 – 110
Brittleness Temperature (°C)	25
Glass Transition Temperature (°C)	-13 – 0
Heat Distortion Temperature 0.464 MPa (°C)	96 – 110

As with polyethylene, polymer properties are modified by copolymerization with other olefins. Commercially, ethylene and to a lesser extent 1-butene in terpolymers, are used as comonomers. Polymers with decreased melting temperature, heat distortion temperature, tensile strength and stiffness and improved optical clarity and impact strength are obtained [17]. Low temperature impact strength of the homopolymers is low and is usually improved by introducing ethylene – propylene rubber as a discrete phase. Although impact strength of random copolymers is better than that of the homopolymer, it is vastly inferior to the heterophasic block copolymers. Optimum balance of properties is obtained when the rubber phase particles have a diameter of approximately 1  $\mu\text{m}$  [62].

**Table 3.9. Properties of Polypropylene Films [62]**

Property	Non-oriented	Oriented
Tensile Strength (MPa)	20.7 – 62	172.3 – 206.8
Elongation (%)	400 – 800	60 – 100
Tear Strength (g/ $\mu\text{m}$ )	40 – 330	3 – 6
Elastic Modulus (MPa)	758 – 965	2 206 – 2 620
Impact Strength (N.cm)	9.8 – 29.4	49 – 147
Permeability 22°C, 0% rh		
O <sub>2</sub> (mol.m <sup>-1</sup> .s <sup>-1</sup> .PPa <sup>-1</sup> )	0.17 – 0.83	0.22
CO <sub>2</sub> (mol.m <sup>-1</sup> .s <sup>-1</sup> .PPa <sup>-1</sup> )	1 – 2.7	0.47 – 0.57

Polypropylene films have high gloss, clarity, stiffness, tensile strength and have higher temperature resistance than polyethylene films. Apart from LDPE, polypropylene is extensively used as packaging material. Typical properties of polypropylene films are shown in Table 3.9.

## 3.4 APPLICATIONS

### 3.4.1 POLYETHYLENE

#### 3.4.1.1 LDPE [24,25,64]

Because of the enormous amount of variation in molecular weight, branching and copolymerization possibilities, a large number of different polyethylenes having different application properties are available. By decreasing the amount of long chain branching, optical properties are generally improved. Most film grades are therefore made in tubular reactors where better control over the balance between short and long chain branching can be achieved. By far the largest segment of LDPE application is in the production of all types of film, from thick down to very thin gauge, stretch-wrap film. Copolymerization with polar comonomers (vinyl acetate and ethyl- and methyl acrylate) imparts greater low temperature flexibility, toughness, impact strength, heat sealability and good adhesion to the polymer. Acrylic or methacrylic acid copolymers introduce increased abrasion resistance and low temperature toughness. Copolymers containing carbon monoxide are photodegradable. Copolymers containing high vinyl acetate, acrylic and methacrylic acid and ethyl- and methyl acrylate components are useful and commonly used as hot-melt adhesives. Blends of LDPE with LLDPE are used to improve processing during the manufacturing of blown film [65]

Table 3.10 presents current volumes of LDPE per application for Western Europe, Japan and the United States [66].



**Table 3.10. Major Fields of Application for LDPE [66]**

<b>Application</b>	<b>W. Europe</b>	<b>Japan</b>	<b>USA</b>
Blow Molding	56	43	28
Extrusion			90
<i>Coating</i>	441		436
<i>Film, Sheet</i>	3329	759	1524
<i>Pipe, Conduit</i>	134	32	
<i>Wire, Cable</i>	205	82	69
Inj. Molding	199	82	131
Paper Treating	-	237	
Rotomoulding	-	-	52
Other	287	437	1195
<b>Total</b>	<b>4650</b>	<b>1674</b>	<b>3525</b>

*Film.* Cast film, produced by forcing the melt through a T or coathanger-type die, and cooled by passing over chilled rollers, has low haze, improved gloss and other enhanced optical properties. Blown film has the advantage of having molecular orientation which can be varied through variations in blow-up ratio and draw-down ratio and can be balanced to give film with very similar properties in both machine and transverse directions for maximum toughness. Film applications include household film for stretch and shrink wrap applications, packaging for food and clothing, agricultural film and garbage bags. Copolymers containing 2 – 5% vinyl acetate (EVA copolymers) have lower crystallinity and hence better clarity, impact strength and low temperature flex than the homopolymers. Those copolymers containing up to 12 % vinyl acetate have exceptional impact resistance and are highly puncture resistant. Because of their puncture resistance, EVA grades are very suitable for liquid packaging, shrink- and stretch wrap, frozen foods, produce bags, ice bags and heavy duty shipping sacks. Some are used as extrusion coatings on aluminum foil, polyester or polypropylene or as adhesive layers in composite structures. Copolymers with ethyl and methyl acrylate exhibit rubberlike properties and are used in disposable gloves and are often included in home hair-coloring packs and hospital sheeting. They have good adhesion properties and are commonly used in extrusion coating, co-extrusions and laminates. Copolymers with carbon-dioxide are used for sheeting for beverage can carriers due to their photodegradability through chain scission following absorption of light by the ketone groups.

*Injection moulding.* LDPE is flexible, tough and has good clarity and is therefore used in see-through household containers, soft, sealable lids which remain flexible even after removal from a freezer, milk bottle caps and toys. Articles manufactured from the more rubbery EVA copolymers include flexible toys, bumper pads and gasketing.

*Extrusion.* The first use of LDPE during the Second World War was as wire insulation [51] for radar application because of its insulating properties and low temperature flexibility. Although stress crack resistance of the thermoplastic resin is not exceptional it can be cross-linked to render it completely resistant to stress cracking. EVA copolymers have improved cross-linkability for wire and cable applications and these materials are also used as hose and soft tubing. Hose containing conductive carbon black are used where static electricity may present a fire hazard.

*Blow moulding.* LDPE with density on the low end of the scale has good flexibility and is used in e.g. squeeze bottles for sauces and copolymers with ethyl- and methyl acrylate are used in soft blow moulded squeeze toys.

### **3.4.1.2 HDPE [26,64,65]**

HDPE has higher crystallinity, density, environmental stress crack resistance, tensile strength and stiffness than LDPE, but has poor optical properties. Ultra high molecular weight polyethylene has many desirable properties but because of its high melt viscosity, can not be processed on the same equipment as the lower molecular weight material. UHMWPE is formed into sheets, bars, extruded profiles and machined into the desired shape such as human implants and gears. Since it has high chemical and abrasion resistance and a high coefficient of friction, it is a natural choice for protection of metal surfaces in high wear areas such as chutes and channels in e.g. the mining and lumber industry. It is also used for the manufacture of high strength fibers. Low molecular weight HDPE waxes are used in paper coatings, emulsions, printing inks, crayons and wax polishes and can be blended with higher molecular weight grades to improve rheology, hardness and abrasion resistance.

Table 3.11 shows the major application fields of HDPE in western Europe, Japan and the United States [66].

**Table 3.11. Volumes of Major Fields of Application for HDPE [66]**

<b>Application</b>	<b>W. Europe</b>	<b>Japan</b>	<b>USA</b>
Blow Molding	1602	149	1907
Extrusion			
<i>Coating</i>			27
<i>Film, Sheet</i>	710	413	1140
<i>Pipe, Conduit</i>	617	67	564
<i>Wire, Cable</i>	55		59
<i>Yarn, Fiber</i>		82	55
<i>Filaments</i>	139		
Inj. Molding	838	122	1037
Rotomoulding			60
Other	202	369	1534
<b>Total</b>	<b>4162</b>	<b>1202</b>	<b>6383</b>

*Blow moulding.* This is the single largest market for HDPE and articles manufactured by this process include bottles for household detergents, juices and milk. Blow moulding resins have high molecular weight and consequently, high melt viscosities to prevent the extruded parison from collapsing.

*Rotomoulding.* Large drums, water- and fuel tanks can not easily be blow moulded because the extruded parison becomes heavy and unstable above a specific size/weight depending on the resin's melt viscosity and may collapse. Some designs can not be blow moulded easily and are therefore moulded by the rotational moulding technique using the same high molecular weight resins used for blow moulding.

*Injection moulding.* Articles made by injection moulding is the second largest outlet for HDPE application where stiffness is more important than clarity. Uses include toys, food containers, crates for bottles and buckets.

*Film.* HDPE film is replacing paper and is commonly used for supermarket carry bags and garbage bags where good optical properties of the film are unnecessary.

*Extrusion.* Pipes of various diameters used for gas, oil, chemicals, water and sewerage transport as well as wire and cable coatings are extruded from HDPE. These products show chemical, corrosion, and stress crack resistance. Due to its high tensile strength, oriented tapes used for strapping, have largely replaced metal straps.

*Thermoforming.* HDPE is readily thermoformed and is used to produce large items such as canoes and truck-bed liners.

### **3.4.1.3 LLDPE [12,48,64]**

The inclusion into the PE backbone of different  $\alpha$ -olefins, using different catalysts, produce LLDPE with a range of properties which is virtually unlimited. The properties of PE's can thus be tailored to suit very specific needs and fields of application. Due to the linear chains and narrower molecular weight distribution, the rheological behavior of LLDPE is different from LDPE. Some modification of conventional LDPE equipment is necessary to process LLDPE. Its shear thinning is less than that of LDPE and it is therefore more viscous in the extruder. It also exhibits less strain hardening in the melt and extensional viscosity is lower. This allows extrusion at very high draw-down rates without the risk of bubble breaks during blown film extrusion.

Table 3.12 shows the major application fields of LLDPE in western Europe, Japan and the United States [66].

**Table 3.12. Volumes of Major Fields of Application for LLDPE [66]**

<b>Application</b>	<b>W. Europe</b>	<b>Japan</b>	<b>USA</b>
Blow Molding	8	11	9
Extrusion			
<i>Coating</i>	5		9
<i>Film, Sheet</i>	1518	479	1953
<i>Pipe, Conduit</i>	32	29	
<i>Wire, Cable</i>	38	7	92
<i>Other Extrusion</i>	-		159
Inj. Molding	100	35	278
Paper Treating	-	22	
Rotomolding			207
Other	155	138	1144
<b>Total</b>	<b>1856</b>	<b>721</b>	<b>3851</b>

*Film.* As with LDPE, the largest market for LLDPE is in film and sheet production (over 60% global LLDPE consumption [66]). LLDPE has better tensile strength, puncture resistance, toughness and low temperature properties than LDPE and it performs well at thicknesses as low as 25 $\mu$ m. The 1-butene copolymers have inferior properties compared to those utilizing higher  $\alpha$ -olefins such as 1-hexene and 1-octene grades. Film uses include garbage bags and stretch film, shopping bags, laundry bags and produce and freezer bags on rolls. Compositionally uniform very low density resins are used for the manufacture of clear film and laminated, heavy duty bags and sealing layers because their melting temperatures are lower than those of the other polyethylenes. Metallocene resins have high oxygen barrier properties which make them attractive as packaging of perishable foodstuffs. These resins and their blends with HDPE are for the same reason also used for blood bags and surgical disposable bags.

*Injection moulding.* This is the second largest market for LLDPE and more than half of these injection moulding grades are used in housewares. Products are stiffer which allows down-gauging of container wall thickness. The excellent gloss, clarity and low warpage properties make the polymers especially suitable for lids jars and other containers. Garbage cans and industrial containers can withstand rough treatment due to the increased impact properties of LLDPE. Compositionally uniform resins have

very high clarity and the polymers are used in making clear lids and disposable oxygen masks.

*Blow moulding and Rotational moulding.* The higher impact strength, gas permeability and clarity of LLDPE resins as opposed to HDPE resins opened up new markets in e.g. blown bottle applications. LLDPE is also competing with more expensive cross-linked and rubber filled HDPE grades. Articles produced range from small toys to very large agricultural water tanks and even square-edged containers can be successfully roto-moulded from LLDPE.

*Extrusion.* Because of its higher burst strength and environmental stress crack resistance compared with LDPE, LLDPE has replaced LDPE in drip-irrigation tubing. It is also used in swimming pool tubing and garden hoses. The very low density metallocene resins are replacing plasticized PVC in medical tubing on account of their high purity, flexibility and transparency. LLDPE is commonly used for low voltage power distribution including telecommunications wiring, automotive and appliance wires and underground power cable insulation since it has excellent dielectric properties. It is also abrasion resistant, is flexible, and has good low temperature properties. The metallocene resins impart flexibility and low temperature properties to LLDPE for use where these properties are necessary.

### **3.4.2 POLYPROPYLENE [17,62,64]**

The properties of polypropylene that distinguish it from the polyethylenes are high melting temperature which allows higher usage temperatures and high stiffness to allow manufacture of thin-walled articles. Stiffness can be increased even more by including mineral fillers or fibers. The ability to vary melt flow index and physical properties over a wide range for use in intricate moulds is excellent and the products produced have good surface finishes. PP also has the ability to be moulded into an integral hinge which can be flexed repeatedly without failure. In addition, PP can be radiation- and steam sterilized, is fiber-forming, water resistant, has good moisture-barrier properties and has low density. PP films offer high clarity, gloss and tensile strength and PP is resistant towards water-borne stains. Because of this combination of properties, polypropylene is applied in the fields described below. Table 3.13

shows current volumes of polypropylene usage in western Europe, Japan and the United States [66].

**Table 3.13. Volumes of Major Fields of Application for Polypropylene [66]**

<b>Application</b>	<b>W. Europe</b>	<b>Japan</b>	<b>USA</b>
Blow Moulding	90	36	86
Extrusion			
<i>Coating</i>			18
<i>Film, Sheet</i>	1318	486	673
<i>Wire, Cable</i>			6
<i>Fibers, Filaments</i>	1202	147	1643
<i>Other Extrusion</i>	356	203	69
Injection Moulding	2790	1284	1792
Other		441	1963
<b>Total</b>	<b>6152</b>	<b>2597</b>	<b>6250</b>

*Injection moulding.* Polypropylene is extensively used in the automotive industry. High impact block copolymers are used for battery cases, interior and exterior trim, bumpers and child safety seats. Glass reinforced and mineral filled polymers are used where stiffness and high temperature resistance are needed and include air-filter housings, and other engine parts. Homopolymers are used in ventilation systems. Another area of use is in container closures such as soft drink caps and child proof medicine caps. Because of its ability to form integral hinges, it also has application in eg. pill-vials and calculator bodies with the bottle and cap and the calculator body and cover moulded as a unit. Polypropylene is readily sterilized and is compatible with human tissue and therefore has many medical applications. These include use in disposable syringes and other hospital utensils, contact lens cases, and human implants. The random copolymers have good clarity and because of its stain resistance it is used in kitchenwares such as dishes, cups, cereal- and freezer containers and drying racks. Other applications are in video cassette covers, toys and garden furniture.

*Fibers.* Due to its fiber-forming capabilities it is used for fiber applications. Thick continuous monofilaments are used in carpeting and rope and thin melt-spun fibers are used for non-wovens. Due to its ability to float and its water resistance it has found marine applications. Thermal conductivity is low and it is therefore also

applied in insulating fabrics. Its stain resistance, low moisture absorbance and abrasion resistance makes it very attractive for low-maintenance, high-traffic carpeting. Non-woven materials find application in disposable nappy cover stock and nappy liners, surgical gowns, sponges and dressings and because it is resistant to biological degradation it makes excellent geotextiles for ground stabilization in erosion control and soil retention and drainage below paving and roads.

*Film.* Biaxially oriented polypropylene replaced cellophane as high clarity package wrappers with low tear resistance such as that used for cigarette packets and chewing gum packets. Its largest use is in form-fill applications such as potato chip, candy bar and other sweet wrappers.

*Blow-moulded bottles.* Its high clarity and barrier properties makes it very suitable for bottles for containing household detergents and cleaners, shampoo, syrup and juice and it also offers hot filling capability and low taste transfer problems.



### 3.5 REFERENCES

1. Müller W.F., *MBS Conf. Proc., Polyethylene '99*, II/1 (1999)
2. Luft G, Bitsch H., Seidl H., *J. Macromol. Sci., Chem.*, **11**(6), 1089 (1977)
3. Ziegler K., Holzkamp E., Breil H., Martin H., *Ger. Pat.*, 973,626, (1960)
4. Hogan, J.P., Banks R.L., *U.S. Pat. 2,825,721*, (1958)
5. Sailors H.R., Hogan J.P., *J. Macromol. Sci. Chem.*, **A15**, 1377 (1981)
6. Böhm L.L., Enderle H.F., Kaps R., Racky W., *MBS Conf. Proc., Polyethylene '99*, III/3 (1999)
7. *Modern Plastics International*, 149, May (1999)
8. Miller A.R., *U.S. Pat. 4,003,712*, Union Carbide, Jan. 18 (1977)
9. Levine I.J., Karol F.J., *U.S. Pat. 4,011,382*, Union Carbide, Mar. 8 (1977)
10. Sacchi M.C., Shan C., Forlini F., Tritto I., Locatelli P., *Makromol. Chem. Rapid Commun.*, **14**, 231 (1993)
11. Soares J.B.P., Kim J.D., Rempel G.L., *Ind. Eng. Chem. Res.*, **36**, 1144 (1997)
12. Kissin Y.V., *Olefin Polymers (Polyethylene)* in *Encyclopedia of Chemical Technology*, Kroschwitz J.I., Exec. Ed., John Wiley & Sons, New York, **17**, 756 (1995)
13. *Chemical Week*, May 26 (1999)
14. Boor J., *Ziegler-Natta Catalysts and Polymerization*, Academic Press, New York, 19 (1979)
15. Natta G., Pino P., Farina M, *Ricerca Sci.*, **25A**, 120 (1955)
16. Natta G., *J. Polym. Sci.*, **16**, 143 (1955)
17. Lieberman R.B., Barbe P.C., *Propylene Polymers* in *Encyclopedia of Polymer Science and Engineering*, Kroschwitz J.I., Exec. Ed., John Wiley & Sons, New York, **13**, 464 (1988)
18. Arzoumanidis G.G., *Commercial Applications of Metallocene Catalysts in Polyolefins: The Process and Product* in Blum H.R., Jordan R.F., Arzoumanidis G.G.. *Metallocenes: The Intensive Short Course*, The Catalyst Group, Session III, III-1 (1996)
19. *Modern Plastics International*, **29**, 1, 19 Jan. (1999)
20. *Asian Plastics News*, 6 Oct. (1998)
21. *Kunststof en Rubber*, **51**, 10, 56 Oct. (1998)

22. *Modern Plastics International*, **28**, 3, 33 Mar. (1998)
23. *Chemical Week*, **161**(24), 40, Jun. 23 (1999)
24. Doak K.W., *Ethylene Polymers in Encyclopedia of Polymer Science and Engineering*, Kroschwitz J., Exec. Ed., John Wiley & Sons, New York, **6**, 383 (1988)
25. Pebsworth L.W., *Olefin Polymers (Polyethylene) in Encyclopedia of Chemical Engineering*, Kroschwitz J.I., Exec. Ed., John Wiley & Sons, New York, **17**, 707 (1995)]
26. Beach D.L., Kissin Y.V., *Ethylene Polymers in Encyclopedia of Polymer Science and Engineering*, Kroschwitz J.I., Exec. Ed., John Wiley & Sons, New York, **13**, 454 (1988)
27. Kissin Y.V., *Olefin Polymers (Polyethylene) in Encyclopedia of Chemical Technology*, Kroschwitz J.I., Exec. Ed., John Wiley & Sons, New York, **17**, 724 (1995)
28. Choi K.Y., Ray W.H., *J. Macromol. Sci. Rev. Macromol. Chem., Phys.*, **C25**, 57 (1985)
29. Forsman J.P., *Hydrocarbon Process.*, 51. 132 (1972)] and Dow [*Plast. Technol.*, 26(2), 39 (1980)
30. *Plast. Technol.*, **26**(2), 39 (1980)
31. *Polyolefins through the 80s: A Time of Change*, SRI International, Menlo Park, Calif. (1983)].
32. Swogger K., Babb D., Dow Chemical Company, *Personal Communication*, Jul. (1999)
33. Lai S.-Y., *et al.*, *U.S. Pat. 5,272,236*, Dow Chemical Co., Dec. 21 (1993)
34. Burdett I.D., *Chemtech*, 616, Oct. (1992)
35. Natta G., Corradini, P., Allegra G., *J. Polym. Sci.*, **51**, 399 (1961)
36. Galli P., Haylock J.C., *Macromol. Chem., Macromol. Symp.*, **63**, 19 (1992)
37. Welch M.B., Hsieh H.L., *Olefin Polymerization Catalyst Technology in Handbook of Polyolefins*, Vasile C., Seymour R.B., Eds., Marcel Dekker, New York, 21 (1993)
38. *Brit. Pat. 1,044,811*, Rexall Drug and Chemical Co., Apr. 9 (1962)
39. Smith D.E., Keeler, R.M., Guenther E., *U.S. Pat. 3,476,729*, Phillips Petroleum Co., Nov. 4 (1969)
40. Hermans J.P., Henriouille P., *U.S. Patent 3,769,233*, Solvay & Cie, (1973)

41. *Ger. Pat. Appl.*, 2,643,143, Montedison and Mitsui Petrochemicals, (1975)
42. Hagemeyer H.G., Park V.K., *U.S. Pat.* 3,423,384, Eastman Kodak, Jan. 21 (1969)
43. Ross J.F., Bowles W.A., *Ind. Eng. Chem. Prod. Res. Dev.*, **24**, 149 (1985)
44. Galli P., Haylock J.C., *Prog. Polym. Sci.*, **16**, 443 (1991)
45. DiDrusco G., Rinaldi R., *Hydrocarbon Process.*, **63**(11), 116 Nov. (1984)
46. *Hydrocarbon Process.*, **72**(3), 204 (1993)
47. Kissin Y.V., *Olefin Polymers (Polyethylene)* in *Encyclopedia of Chemical Technology*, Kroschwitz J.I., Exec. Ed., John Wiley & Sons, New York, **17**, 702 (1995)
48. James D.E., *Ethylene Polymers* in *Encyclopedia of Polymer Science and Engineering*, Kroschwitz J., Exec. Ed., John Wiley & Sons, New York, **6**, 429 (1988)
49. *European Plastics News*, 41, Feb. (1999)
50. Doak K.W., *Ethylene Polymers* in *Encyclopedia of Polymer Science and Engineering*, Kroschwitz J.I., Exec. Ed., John Wiley & Sons, New York, **6**, 386 (1988)
51. Raff R., Lyle E., *Historical Developments in Crystalline Olefin Polymers* Part I, Ed. Raff R.A.V., Doak K.W., John Wiley & Sons, New York, 1 (1965)
52. Quirk R.P., Alsamraie M.A.A., *Physical Properties of Poly(ethylene)* in *Polymer Handbook*, Third Edition, Brandrup J., Immergut E.H., John Wiley & Sons, New York, V/15 (1989)
53. Fatou J.G., *Morphology and Crystallization in Polyolefins* in *Handbook of Polyolefins - Synthesis and Properties*, Vasile C., Seymour R.B., Eds., Marcel Dekker Inc., New York, 155 (1993)
54. Morita Y., Inoue H., Fujiyoshi K., *U.S. Pat.* 4,205,021, Mitsui Petrochemical Ind., May 27 (1980)
55. Anderson A.W., Stamanoff G.S., *U.S. Pat* 4,076,698, E.I. Du Pont de Nemours, Feb. 28 (1978)
56. Matsuura M., Kageyama Y., Hagiwara A., Shimada T., *U.S. Pat.* 4,530,983, Mitsubishi Petrochemical Co., Jul. 23 (1985)
57. Kluiber R.W., Carrick W.L., *U.S. Pat.* 3,073,809, Union Carbide Corp., Jan. 15 (1963)

58. Miwa Y., Shimada T., Hayashi S., Ukita M., Nakagawa H., Matsuura M., *U.S. Pat. 4,405,774*, Mitsubishi Petrochemical Co., Sep. 20 (1983)
59. Durand D.C., Morterol F.R.M.M., *EP 016 4215 A1*, BP Chemicals, London (1985)
60. Natta G., Pino P., Corradini P., Danusso F., Mantica E., Mazzanti G., Moraglio G., *J. Polym. Sci.*, **77**, 1708 (1955)
61. Quirk R.P., Alsamarraie M.A.A., *Physical Properties of Poly(propylene)* in *Polymer Handbook*, Third Edition, Brandrup J., Immergut E.H., John Wiley & Sons, New York, V/27 (1989)
62. Kissin Y.V., *Olefin Polymers (Polypropylene)* in *Encyclopedia of Chemical Technology*, Kroschwitz JI., Exec. Ed., John Wiley & Sons, New York, **17**, 784 (1995)
63. Natta G., Porri L., Corradini P., Morero D., *Atti Accad. Naz. Lincei Rend. Classe Sci. Fis. Mat. Nat.*, **20**, 560 (1956)
64. Seymour R.B., Vasile C., Rusu M., *Applications of Polyolefins*, in *Handbook of Polyolefins – Synthesis and Properties*, Vasile C., Seymour R.B., Eds., Marcel Dekker Inc., New York, **(31)**, 1007, (1993)
65. LeBlanc, J., Deex O., Duston F., Digest of polymer Developments – Polyolefins, Englehart S., Ed., Springborn Mat. Sci., Connecticut, **I(64)**, 11 (1992)]
66. *Modern Plastics International*, 64-71, Jan. (1999)

## CHAPTER 4

### EXPERIMENTAL

#### 4.1 POLYMERIZATION

##### 4.1.1 MATERIALS AND EQUIPMENT

Aluminum alkyls were obtained from Ethyl Corp., Akzo and Witco and diluted as required. MAO was received from Witco as a 30% solution in toluene and used as received

Di-*iso*-propyldimethoxysilane was obtained from Polifin's polypropylene plant and, after degassing, used as received.

Titanium tetrachloride was obtained from Aldrich and used as received. The metallocene catalysts  $(1\text{-EtCp})_2\text{ZrCl}_2$ ,  $(n\text{-BuCp})_2\text{ZrCl}_2$  and  $\text{Me}_2\text{Si}(\text{Ind})_2\text{ZrCl}_2$  were obtained from Witco and used as received.

All catalyst manipulations were carried out in a MBraun model MB 150 glovebox containing a nitrogen atmosphere with water levels below 0.2 ppm and oxygen levels below 1 ppm.

Solvents were obtained from Schümann-Sasol and purified by passing over 13X molecular sieves followed by Alcoa Selexsorb CD to remove moisture and polar compounds to levels below 5 ppm.

Ethylene 2.7 was obtained from Fedgas and propylene from Polifin's polypropylene plant. Both were used after passing through a 1.8 m column, 20 mm inside diameter, containing a 50:50 ratio of 13X molecular sieves and Alcoa Selexsorb CD.

$\alpha$ -Olefins were obtained from Sasol's Fischer-Tropsch process and purified by passing over 13X molecular sieves followed by Alcoa Selexsorb CD to remove moisture and polar compounds to levels below 5 ppm.

High purity nitrogen 5.0 and hydrogen were obtained from Fedgas and used after passing through Messer Griesheim Oxisorb columns.

All reactions were carried out on a Büchi BEP 280 reactor fitted with a computer assisted reactor control system developed in-house using Turbolink software which allows the independently controlled introduction of ethylene, propylene, comonomer, hydrogen, nitrogen and solvent. For propylene and solvent, Micro Motion flowmeters together with Badger control valves are used. Ethylene and hydrogen flows were measured and controlled by Brooks flow controllers and the monomers by Bronkhorst Liqui Flow flow controllers. The reactor was further provided with an inlet for catalyst introduction, a vacuum line, stirring facilities and both a bursting disc and preset temperature and pressure limit control which would automatically vent the reactor in the case of a thermal runaway or overpressure occurring. Reactor temperature was controlled by a Julabo ATS3 temperature control system by circulating the heating/cooling fluid through the reactor mantle. The reactor was fitted with two independent temperature sensors, one giving feedback to the temperature control unit and the other to the reactor control system. Pressure was measured in the vent line, also by two independent gauges, the one a normal mechanical dial gauge and the other an electronic pressure gauge feeding back to the reactor control unit. Pressure, temperature, feed rates and amounts were displayed in real time and were plotted against time.

For polymerizations in solution or slurry-phase, 1-liter, 5-liter and 10-liter reactors obtained from Büchi were used. One of the 1-liter reactors was equipped with double sight-glasses. For gas-phase polymerizations, 1-liter, 20-liter and 35-liter reactors with special stirrer configurations were designed and built in-house to meet the tight clearance specifications necessary for these reactions.

### 4.1.2 POLYETHYLENE

Ethylene was polymerized in the presence of one or two  $\alpha$ -olefins including 1-butene, 1-pentene, 1-hexene, 1-heptene, 1-octene and 1-nonene in order to assess the effects of these comonomers on polymer properties. The experimental procedures used for determining catalyst activities as well as those used for the preparation of ethylene co- and terpolymers using supported Ziegler-Natta and metallocene catalysts are described in the relevant chapters.

### 4.1.3 POLYPROPYLENE

Propylene was polymerized in the presence of different  $\alpha$ -olefins in order to improve impact, low temperature properties and optical properties typical of propylene homopolymers. In random copolymers, optical and low temperature properties are improved and in the block copolymers, mainly low temperature impact properties are improved. Specific linear  $\alpha$ -olefins used for the preparation of random copolymers included 1-pentene, 1-heptene and 1-nonene. For the block copolymers, only 1-pentene was used. The experimental procedures used for the preparation of these copolymers are described in the relevant chapters.

## **4.2 POLYMER CHARACTERIZATION**

### **4.2.1 MECHANICAL PROPERTIES**

#### **4.2.1.1 Tensile Properties**

Samples for tensile and impact properties were moulded on a manual plunger-type injection moulding machine. The melt temperature for polyethylene was 190°C and 220°C for polypropylene. Injection force depended on melt flow index and the mould was typically filled in about 2 seconds. After injection, the mould was opened and the sample rapidly cooled to ambient temperature by immersion in a water bath.

Tensile properties of injection-moulded test pieces were determined according to ASTM D 638 M on type M-III samples. These samples are 4 mm thick, have a 10 mm gauge length and are 2.5 mm wide in the narrow section. Samples were conditioned for 24 hours at 23°C before tensile properties were determined on a Hounsfield 10K C tensile testing apparatus. Modulus was measured at a rate of 1 mm/min. starting from an extension where the applied force reached 0.5 N. At a force of 1 N, the extension rate increase to 50 mm/min. for measurement of the other tensile properties.

#### **4.2.1.2 Impact Strength**

Izod impact strength was determined according to ASTM 256 on injection-moulded samples with dimensions 4 x 10 x 80 mm. Samples were notched 2.0 mm deep on a Ceast Notchvis and impact measurements were done on a Ceast Resil 25 impact tester fitted with a DAS 4000 Win data acquisition system.

#### **4.2.1.3 Hardness**

Hardness was determined according to ASTM D 2240 on a Pacific Transducer Corp. model 307L Type D durometer on injection-moulded samples with dimensions 4 x 10



x 80 mm. Hardness was taken as the value obtained after 3 seconds and the average of 5 measurements were calculated.

## 4.2.2 PHYSICAL PROPERTIES

### 4.2.2.1 Melt Flow Index

Melt flow index was determined on a Rosand Advanced Melt Flow Indexer according to ASTM D 1238 on dried polymer powder or pellets. The melt flow index of polyethylene was determined at 190°C and that of polypropylene at 230°C, both using a 2.16 kg force and a die of 8 mm length having a 2.01 mm inside diameter.

### 4.2.2.2 Density

Densities between 0.915 and 0.945 g/cc were measured on a density gradient method according to ASTM 1505. Densities higher or lower than this was determined by using a buoyancy method together with the Sartorius Specific Gravity Determination kit YDK 01:

The buoyancy method used entailed submerging a sample in distilled water in the submersion beaker for 24 hours. It was then removed from the water, dried and weighed in air ( $W_a$ ) after which the balance was zeroed, the sample submerged again and the weight noted ( $W_w$ ). Density ( $\rho$ ) was determined by using the following formula:

$$\rho = (W_a \cdot \rho_w) / (0.99983 \cdot W_w) + 0.0012 \text{ g/cm}^3 \quad (1)$$

where  $\rho_w$  is the density of distilled water at the measurement temperature.

### 4.2.2.3 Crystallinity

Weight percent crystallinity ( $w^c$ ) was determined by differential scanning calorimetry (DSC) by comparing the heat of fusion of the sample with the heat of fusion of the

ideal 100% crystalline material. With this method, crystallinity can be calculated according to the formula:

$$w^c = 100 \cdot \Delta H_f / \Delta H_{fC} \quad (2)$$

where  $\Delta H_{fC}$  is the heat of fusion of the crystalline phase, having a value between 290 J/g [1] and 300 J/g obtained from extrapolation data [2]. A value of 290 was used for ethylene co- and terpolymers. For polypropylene the extrapolated heat of fusion of a 100% crystalline sample is 209 J/g [3] and this value was used for determination of crystallinities of propylene copolymers. The DSC scans were recorded between 200 and 50°C.

Crystallinity was also calculated from the measured density using the equation:

$$w^c = \rho_c (\rho - \rho_a) / \rho (\rho_c - \rho_a) \quad (3)$$

where  $\rho_c$  is the density of the crystalline phase,  $\rho_a$  the density of the amorphous phase and  $\rho$  the measured density of the copolymer at ambient temperature [4].

#### 4.2.2.4 Composition and Microstructure

##### A. Polyethylene

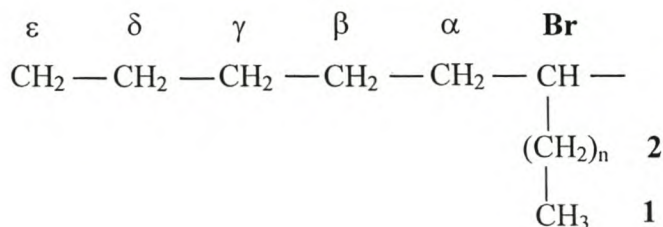
<sup>13</sup>C NMR analyses were done at 120°C on samples dissolved in *o*-dichlorobenzene on a Varian 400 MHz machine using a 90° pulse angle, a pulse width of 10 using 25 000 scans and a 30 sec. delay between scans. Composition was determined by ratioing the characteristic peaks of the different monomers making up the NMR spectrum of the copolymer. Basically this entailed comparing the peak area of the branching CH with that of the backbone carbons. Assignments were done making use of the literature where possible, combined with DEPT analyses and checked against the chemical shift assignments predicted by the additivity rules described by Grant and Paul [5]. Chemical shift predictions of a specific carbon according to the additive rules of Grant & Paul are made by determining the combined effects of the neighbouring ( $\alpha$

up to  $\epsilon$ ) carbons. Thus, the amount of carbon in the  $\alpha$ ,  $\beta$ ,  $\gamma$ ,  $\delta$  and  $\epsilon$  positions relative to carbon for which the chemical shift is being determined, is counted and each multiplied by its respective correction factor and added together. Apart from the standard influences of the neighbouring carbons, different types of carbons also affect each other differently. In this regard, for example, the chemical shift of a tertiary carbon atom having a secondary neighbour, 3(2), a secondary carbon atom having a tertiary neighbour, 2(3), and a primary carbon atom having a tertiary neighbour 1(3) have specific influences on the chemical shifts. To complete the calculation for a certain carbon, its direct neighbour types (in the  $\alpha$  position) is determined and each multiplied by their respective correction factors. This value is added to the value obtained from the first calculation and the constant of  $-1.87$  ppm added to give the predicted chemical shift in ppm.

**Table 4.1. Comparison of Observed and Calculated Chemical Shifts of Ethylene /  $\alpha$ -Olefin Copolymers**

<b>Ethylene / 1-Butene</b>	<b>1</b>	<b>2</b>	<b>Br</b>	$\alpha$	$\beta$	$\gamma$	$\delta$	$\epsilon$			
Grant&Paul	11.6	27.6	40.5	34.5	27.5	30.4	30.1	30.0			
Observed	11.1	27.2	39.6	34.0	26.7	30.4	30.0	30.0			
<b>Ethylene / 1-Pentene</b>	<b>1</b>	<b>2</b>	<b>3</b>	<b>Br</b>	$\alpha$	$\beta$	$\gamma$	$\delta$	$\epsilon$		
Grant&Paul	14.5	20.2	37.3	37.6	34.8	27.6	30.4	30.1	30.0		
Observed	14.5	20.2	36.9	37.9	34.5	27.2	30.4	30.0	30.0		
<b>Ethylene / 1-Hexene</b>	<b>1</b>	<b>2</b>	<b>3</b>	<b>4</b>	<b>Br</b>	$\alpha$	$\beta$	$\gamma$	$\delta$	$\epsilon$	
Grant&Paul	14.1	23.1	30.0	34.5	37.9	34.9	27.6	30.4	30.1	30.0	
Observed	14.0	23.3	30.0	34.1	38.1	34.5	27.2	30.4	30.0	30.0	
<b>Ethylene / 1-Heptene</b>	<b>1</b>	<b>2</b>	<b>3</b>	<b>4</b>	<b>5</b>	<b>Br</b>	$\alpha$	$\beta$	$\gamma$	$\delta$	$\epsilon$
Grant&Paul	14.1	22.7	32.9	27.1	34.8	38.0	34.9	27.6	30.4	30.1	30.0
Observed	13.9	22.7	32.6	26.8	34.4	38.1	34.4	27.2	30.4	30.0	30.0
<b>Ethylene / 1-Octene</b>	<b>1</b>	<b>2</b>	<b>3</b>	<b>4</b>	<b>5</b>	<b>6</b>	<b>Br</b>	$\alpha$	$\beta$	$\gamma$	$\delta$
Grant&Paul	14.1	22.7	32.5	30.0	27.5	34.9	38.0	34.9	27.6	30.4	30.1
Observed	13.9	22.8	32.1	30.0	27.2	34.5	38.2	34.5	27.2	40.4	30.1

For chemical shift assignments of copolymers containing little or no clustering of the comonomer units, the paper by Randall was used [6]. The assignments shown in Table 4.1 were used to label the carbon atoms shown in the structure below:



In Figures 4.1 to 4.4 the  $^{13}\text{C}$  NMR DEPT analyses of ethylene copolymers with 1-butene, 1-pentene, 1-hexene and 1-heptene are presented. Branches longer than five carbon atoms give rise to the same NMR spectra and those of ethylene copolymers with 1-octene and 1-nonene are therefore not shown. In Figures 4.1.to 4.4 the spectra at the bottom show all chemical shifts of the copolymer, those labeled CH show the CH chemical shifts, those labeled  $\text{CH}_2$  show the  $\text{CH}_2$  chemical shifts and those labeled  $\text{CH}_3$  show the  $\text{CH}_3$  chemical shifts.

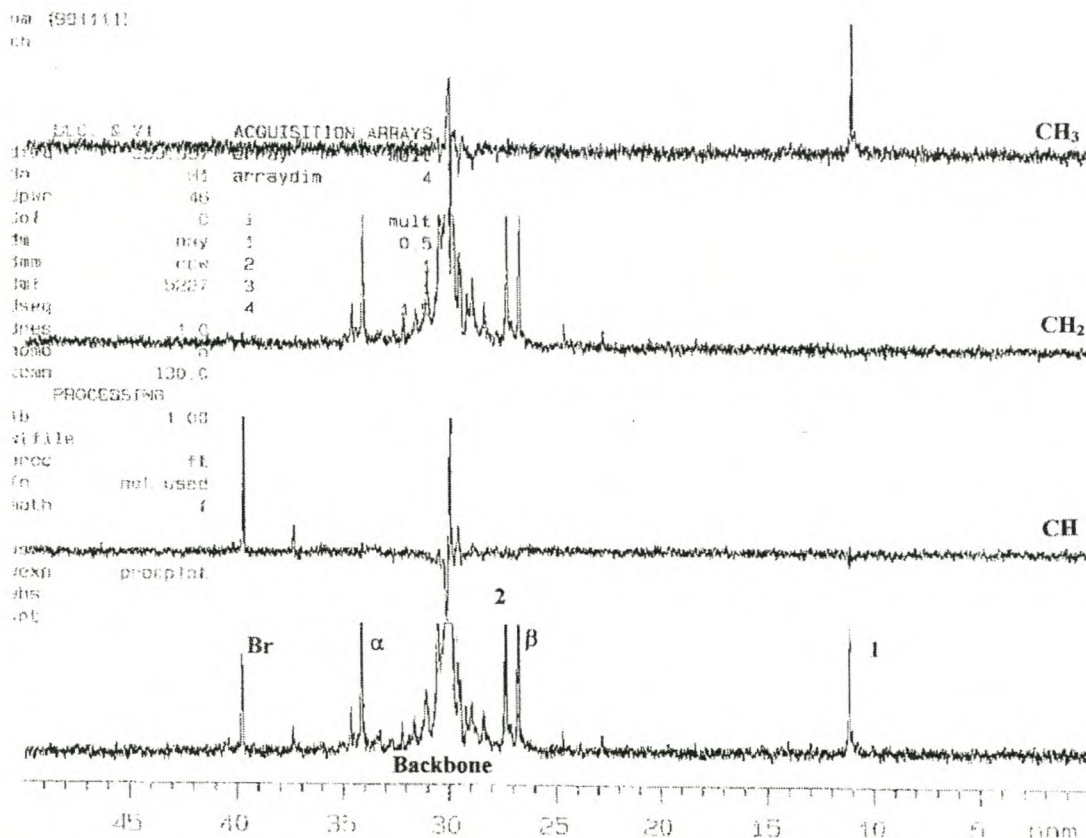


**Figure 4.1.**  $^{13}\text{C}$  NMR DEPT Spectrum of Ethylene / 1-Butene Copolymer.

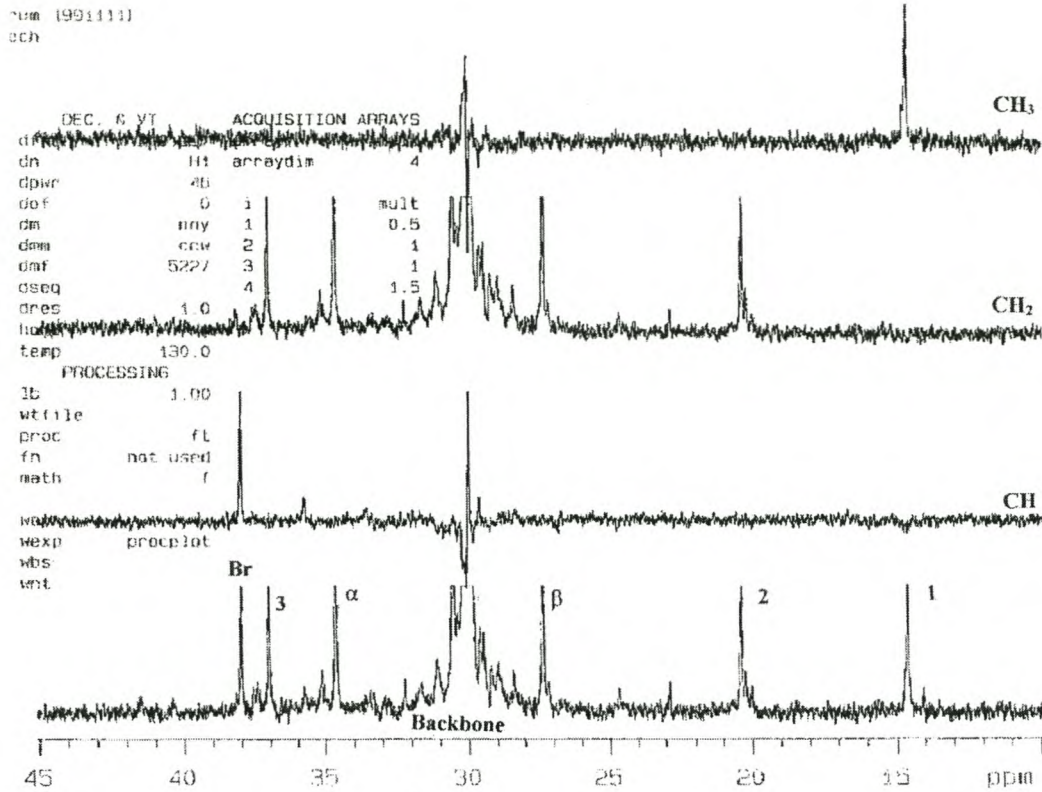


Figure 4.2. <sup>13</sup>C NMR DEPT Spectrum of Ethylene / 1-Pentene Copolymer

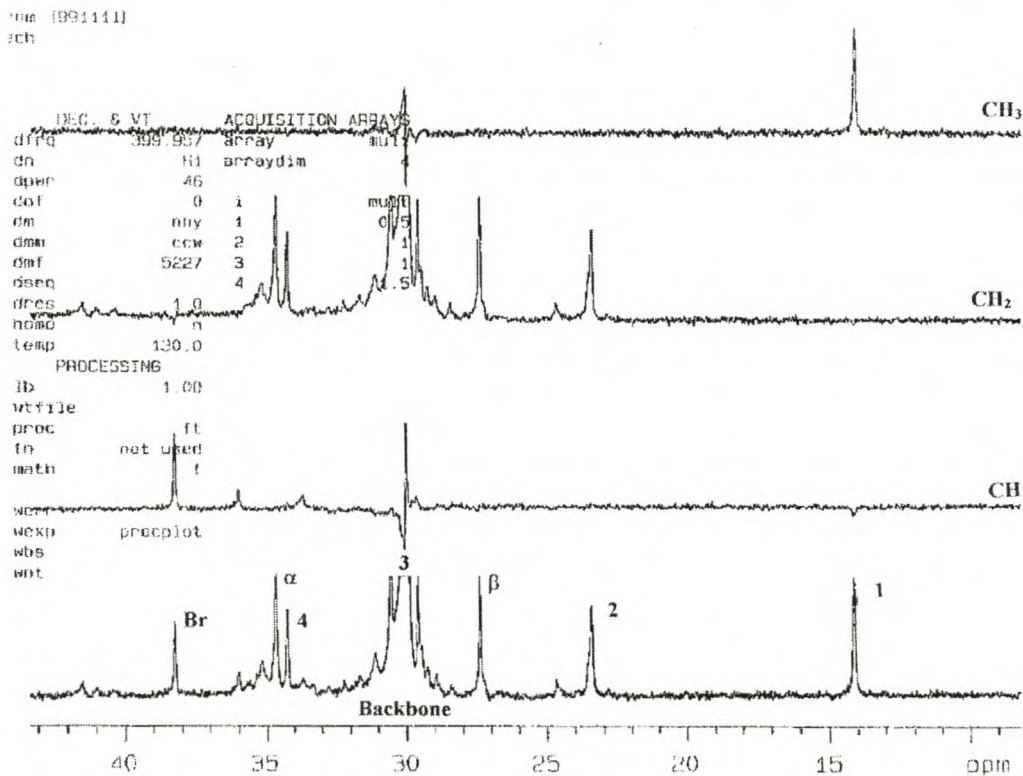
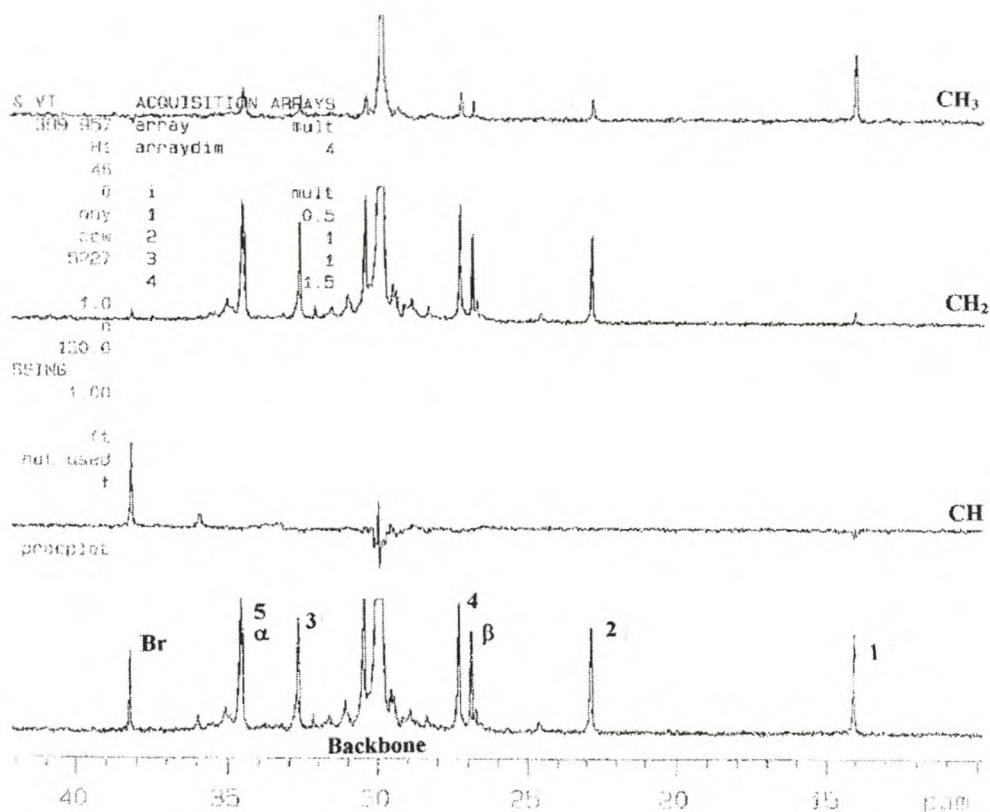


Figure 4.3. <sup>13</sup>C NMR DEPT Spectrum of Ethylene / 1-Hexene Copolymer



**Figure 4.4.**  $^{13}\text{C}$  NMR DEPT Spectrum of Ethylene / 1-Heptene Copolymer

For all ethylene /  $\alpha$ -olefin copolymers, the comonomer content in mole percent [C] was calculated according to the following formula:

$$[\text{C}] = 200 \text{ Br} / (\text{Total Backbone Carbons}) \quad (2)$$

where Br is the intensity of the branching CH peak as indicated on the spectra in Figures 4.1 to 4.4. The total intensity of the backbone carbon atoms are obtained from the sum of the branching CH carbons and the  $\alpha$ -CH<sub>2</sub>,  $\beta$ -CH<sub>2</sub>,  $\gamma$ -CH<sub>2</sub>,  $\delta$ -CH<sub>2</sub>,  $\epsilon$ -CH<sub>2</sub>, units etc. For backbone carbons further removed than the  $\gamma$  position from the branching carbon, all chemical shifts converge towards the same value which, for the ethylene polymer spectra, were positioned at 30 ppm. For  $\alpha$ -olefins larger than 1-hexene, it can be seen from 4. 1 that the  $\alpha$ -CH<sub>2</sub> in the side chain appears at the same chemical shift as the backbone  $\alpha$ -carbons. For  $\alpha$ -olefins larger than 1-heptene, the  $\beta$ -CH<sub>2</sub> in the side chain also appears at the same chemical shift as the backbone  $\beta$ -

carbons. In these cases, the intensity of the branching CH was subtracted from those of the  $\alpha$  and  $\beta$  carbon intensities.

In Table 4.2 the correction factors for the  $\alpha$  to  $\epsilon$  neighbours as well as those for the specific carbon types together with the neighbouring carbon counts and the predicted chemical shifts for ethylene /  $\alpha$ -olefin copolymers containing an isolated branch are shown.

**Table 4.2. Chemical Shift Prediction for Ethylene / ( $\alpha$ -Olefin) Copolymers Utilizing the Grant and Paul Additivity Rules**

Position	$\alpha$	$\beta$	$\gamma$	$\delta$	$\epsilon$	3(2)	2(3)	Constant
Factor	8.61	9.78	-2.88	0.37	0.06	-2.65	-2.45	-1.87
<b>Carbon</b>	<b>Ethylene / 1-Butene</b>							
<b>1</b>	1	1	2	2	2	0	0	11.62
<b>2</b>	2	2	2	2	2	0	1	27.56
<b>Br</b>	3	3	2	2	2	3	0	40.45
$\alpha$	2	3	3	2	2	0	1	34.46
$\beta$	2	2	3	3	2	0	0	27.5
$\gamma$	2	2	2	3	3	0	0	30.44
$\delta$	2	2	2	2	3	0	0	30.07
$\epsilon$	2	2	2	2	2	0	0	30.01
	<b>Ethylene / 1-Pentene</b>							
<b>1</b>	1	1	1	2	2	0	0	14.5
<b>2</b>	2	1	2	2	2	0	0	20.23
<b>3</b>	2	3	2	2	2	0	1	37.34
<b>Br</b>	3	3	3	2	2	3	0	37.57
$\alpha$	2	3	3	3	2	0	1	34.83
$\beta$	2	2	3	3	3	0	0	27.56
$\gamma$	2	2	2	3	3	0	0	30.44
$\delta$	2	2	2	2	3	0	0	30.07
$\epsilon$	2	2	2	2	2	0	0	30.01
	<b>Ethylene / 1-Hexene</b>							
<b>1</b>	1	1	1	1	2	0	0	14.13
<b>2</b>	2	1	1	2	2	0	0	23.11
<b>3</b>	2	2	2	2	2	0	0	30.01
<b>4</b>	2	3	3	2	2	0	1	34.46
<b>Br</b>	3	3	3	3	2	3	0	37.94
$\alpha$	2	3	3	3	3	0	1	34.89
$\beta$	2	2	3	3	3	0	0	27.56
$\gamma$	2	2	2	3	3	0	0	30.44
$\delta$	2	2	2	2	3	0	0	30.07
$\epsilon$	2	2	2	2	2	0	0	30.01

**Table 4.2 (cont.). Chemical Shift Prediction for Ethylene / ( $\alpha$ -Olefin) Copolymers Utilizing the Grant and Paul Additivity Rules**

Position	$\alpha$	$\beta$	$\gamma$	$\delta$	$\epsilon$	3(2)	2(3)	Constant
Factor	8.61	9.78	-2.88	0.37	0.06	-2.65	-2.45	-1.87
<b>Ethylene / 1-Heptene</b>								
<b>1</b>	1	1	1	1	1	0	0	14.07
<b>2</b>	2	1	1	1	2	0	0	22.74
<b>3</b>	2	2	1	2	2	0	0	32.89
<b>4</b>	2	2	3	2	2	0	0	27.13
<b>5</b>	2	3	3	3	2	0	1	34.83
<b>Br</b>	3	3	3	3	3	3	0	38
$\alpha$	2	3	3	3	3	0	1	34.89
$\beta$	2	2	3	3	3	0	0	27.56
$\gamma$	2	2	2	3	3	0	0	30.44
$\delta$	2	2	2	2	3	0	0	30.07
$\epsilon$	2	2	2	2	2	0	0	30.01
<b>Ethylene / 1-Octene</b>								
<b>1</b>	1	1	1	1	1	0	0	14.07
<b>2</b>	2	1	1	1	1	0	0	22.68
<b>3</b>	2	2	1	1	2	0	0	32.52
<b>4</b>	2	2	2	2	2	0	0	30.01
<b>5</b>	2	2	3	3	2	0	0	27.5
<b>6</b>	2	3	3	3	3	0	1	34.89
<b>Br</b>	3	3	3	3	3	3	0	38
$\alpha$	2	3	3	3	3	0	1	34.89
$\beta$	2	2	3	3	3	0	0	27.56
$\gamma$	2	2	2	3	3	0	0	30.44
$\delta$	2	2	2	2	3	0	0	30.07
$\epsilon$	2	2	2	2	2	0	0	30.01

When sufficiently large amounts of comonomer are present, branching occurs more frequently until long sequences of comonomer, uninterrupted by ethylene units, may appear. The chemical shifts of these sequences are well represented by those for the poly( $\alpha$ -olefins). The correction factors for the  $\alpha$  to  $\epsilon$  neighbours as well as those for the specific carbon types, together with the neighbouring carbon counts and the predicted chemical shifts of the homopolymers from polyethylene to poly(1-nonene), are shown in Table 4.3.



**Table 4.3. Grant and Paul Chemical Shift Prediction for Poly( $\alpha$ -Olefins)**

Position Factor	$\alpha$ 8.61	$\beta$ 9.78	$\gamma$ -2.88	$\delta$ 0.37	$\epsilon$ 0.06	3(2) -2.65	2(3) -2.45	1(3) -1.4	Constant -1.87
<b>Carbon</b>	<b>Polyethylene</b>								<b>Chemical Shift (ppm)</b>
<b>1</b>	2	2	2	2	2	0	0	0	30.01
	<b>Polypropylene</b>								
<b>1</b>	1	2	2	4	2	0	0	1	20.74
<b>Br</b>	3	2	4	2	4	2	0	0	27.68
$\alpha$	2	4	2	4	2	0	2	0	45.41
	<b>Poly(1-Butene)</b>								
<b>1</b>	1	1	2	2	4	0	0	0	11.74
<b>2</b>	2	2	2	4	4	0	1	0	28.42
<b>Br</b>	3	3	4	4	4	3	0	0	35.55
$\alpha$	2	4	4	4	4	0	2	0	39.77
	<b>Poly(1-Pentene)</b>								
<b>1</b>	1	1	1	2	2	0	0	0	14.5
<b>2</b>	2	1	2	2	4	0	0	0	20.35
<b>3</b>	2	3	2	4	4	0	1	0	38.2
<b>Br</b>	3	3	5	4	6	3	0	0	32.79
$\alpha$	2	4	4	6	4	0	2	0	40.51
	<b>Poly(1-Hexene)</b>								
<b>1</b>	1	1	1	1	2	0	0	0	14.13
<b>2</b>	2	1	1	2	2	0	0	0	23.11
<b>3</b>	2	2	2	2	4	0	0	0	30.13
<b>4</b>	2	3	3	4	4	0	1	0	35.32
<b>Br</b>	3	3	5	5	6	3	0	0	33.16
$\alpha$	2	4	4	6	6	0	2	0	40.63
	<b>Poly(1-Heptene)</b>								
<b>1</b>	1	1	1	1	1	0	0	0	14.07
<b>2</b>	2	1	1	1	2	0	0	0	22.74
<b>3</b>	2	2	1	2	2	0	0	0	32.89
<b>4</b>	2	2	3	2	4	0	0	0	27.25
<b>5</b>	2	3	3	5	4	0	1	0	35.69
<b>Br</b>	3	3	5	5	7	3	0	0	33.22
$\alpha$	2	4	4	6	6	0	2	0	40.63
	<b>Poly(1-Octene)</b>								
<b>1</b>	1	1	1	1	1	0	0	0	14.07
<b>2</b>	2	1	1	1	1	0	0	0	22.68
<b>3</b>	2	2	1	1	2	0	0	0	32.52
<b>4</b>	2	2	2	2	2	0	0	0	30.01
<b>5</b>	2	2	3	3	4	0	0	0	27.62
<b>6</b>	2	3	3	5	5	0	1	0	35.75
<b>Br</b>	3	3	5	5	7	3	0	0	33.22
$\alpha$	2	4	4	6	6	0	2	0	40.63
	<b>Poly(1-Nonene)</b>								
<b>1</b>	1	1	1	1	1	0	0	0	14.07
<b>2</b>	2	1	1	1	1	0	0	0	22.68
<b>3</b>	2	2	1	1	1	0	0	0	32.46
<b>4</b>	2	2	2	1	2	0	0	0	29.64
<b>5</b>	2	2	2	3	2	0	0	0	30.38
<b>6</b>	2	2	3	3	5	0	0	0	27.68
<b>7</b>	2	3	3	5	5	0	1	0	35.75
<b>Br</b>	3	3	5	5	7	3	0	0	33.22
$\alpha$	2	4	4	6	6	0	2	0	40.63

Between these two extremes of isolated branching and very long ( $\alpha$ -olefin) homopolymer sequences, different combinations of the ethylene / comonomer sequences exist. The calculated and observed values for the CH<sub>2</sub> and the branching CH of the ethylene dyad-centered sequences EEEE, EEEC and CEEC, the comonomer dyad-centered sequences CCCC, CCCE and ECCE and the ethylene / comonomer-centered dyads in the sequences EECC, CECC, EECE and CECE are shown in Table 4.4. E represents ethylene and C the comonomer.

**Table 4.4. <sup>13</sup>NMR  $\alpha$ -Carbon Peak Assignments of the Indicated Dyad Sequences for Copolymers of Ethylene with Higher  $\alpha$ -Olefins**

<b>Ethylene / 1-Butene</b>	<u>CCCC</u>	<u>CCCE</u>	<u>ECCE</u>	<u>EECC</u>	<u>CECC</u>	<u>EECE</u>	<u>CECE</u>
Predicted $\alpha$	39.7	39.3	38.9	34.5	35.3	34.5	34.9
Predicted - Branch	35.6	38/35.4	37.9	37.9	38	40.4	40.5
Observed $\alpha$	40.3	39.6	39.1	34.1	34.9	34.1	34.6
Observed Branch	34.7	39.0/34.6	37.3	37.3	37.3	39.7	40.3
<b>Ethylene / 1-Pentene</b>							
Predicted $\alpha$	40.5	40.1	39.7	35.3	35.7	34.8	35.2
Predicted Branch	32.8	35.2/32.7	35.1	35.1	35.2	37.6	37.6
Observed $\alpha$	41.4	40.8	40.1	35.0	35.6	34.5	35.0
Observed Branch	33.0	35.8/33.0	35.8	35.8	35.8	38.0	35.8
<b>Ethylene / 1-Hexene</b>							
Predicted $\alpha$	40.5	40.1	39.7	35.3	35.7	34.8	35.3
Predicted Branch	33.2	35.6/33	35.5	35.5	35.6	37.9	38
Observed $\alpha$	41.4	40.9	40.1	35.1	35.8	34.6	35.1
Observed Branch	33.6	35.8/33.6	35.8	35.8	35.8	38.1	38.1
<b>Ethylene / 1-Heptene</b>							
Predicted $\alpha$	40.6	40.2	39.8	35.3	35.8	34.9	35.3
Predicted Branch	33.2	35.6/33.1	35.6	35.6	35.6	38	38.1
Observed $\alpha$	40.1	-	-	34.9	35.8	34.4	34.9
Observed Branch	33.2	36/33.2	36	36	36	38.2	38.2
<b>Ethylene / 1-Octene</b>							
Predicted $\alpha$	40.6	40.2	39.8	35.3	35.8	34.9	35.3
Predicted Branch	33.2	35.6/33.1	35.6	35.6	35.6	38	38.1
Observed $\alpha$	41.4	40.9	40.3	35.4	35.9	34.6	35.4
Observed Branch	33.9	35.9/33.9	35.9	35.9	35.9	38.2	38.2
<b>Ethylene / 1-Nonene</b>							
Predicted $\alpha$	40.6	40.2	39.8	35.3	35.8	34.9	35.3
Predicted Branch	33.2	35.6/33.1	35.6	35.6	35.6	38	38.1
Observed $\alpha$	-	-	-	35.1	35.6	34.4	35.1
Observed Branch	-	36/-	36	36	36	38.1	38.1

The number-average sequence lengths  $\bar{n}_E$  and  $\bar{n}_C$  for ethylene and comonomer were calculated from the dyad sequence concentrations from equations 3 and 4 [7]:

$$\bar{n}_E = \{(EE) + 0.5(EC)\}/0.5(EC) \quad (3)$$

$$\bar{n}_C = \{(CC) + 0.5(EC)\}/0.5(EC) \quad (4)$$

where (EE) and (CC) are the dyad concentrations of the CH<sub>2</sub> of ethylene and comonomer in sequences EEEE, EEEC and CEEC for ethylene and CCCC, CCCE and ECCE for the comonomer. (EC) is the dyad concentration of the CH<sub>2</sub> of ethylene and comonomer in sequences EECC, CECC, EECE and CECE.

## B. Polypropylene

In Figures 4.5 and 4.6 the  $^{13}\text{C}$  NMR DEPT analyses of propylene copolymers with 1-pentene and 1-heptene are presented. Branches longer than five give rise to the same NMR spectra and that of the propylene / 1-nonene copolymers are therefore not shown. In Figures 4.5 and 4.6 the spectra at the bottom show all chemical shifts of the copolymer, those labeled CH show the CH chemical shifts, those labeled  $\text{CH}_2$  show the  $\text{CH}_2$  chemical shifts and those labeled  $\text{CH}_3$  show the  $\text{CH}_3$  chemical shifts.

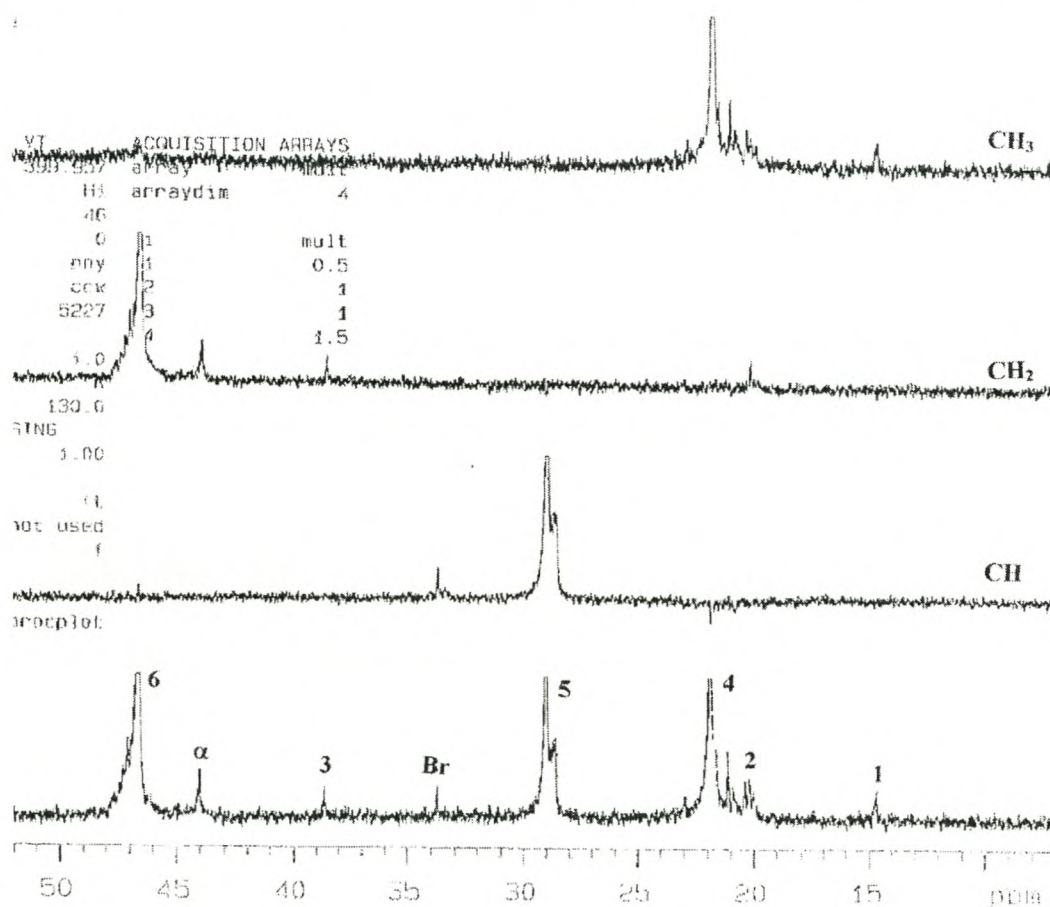
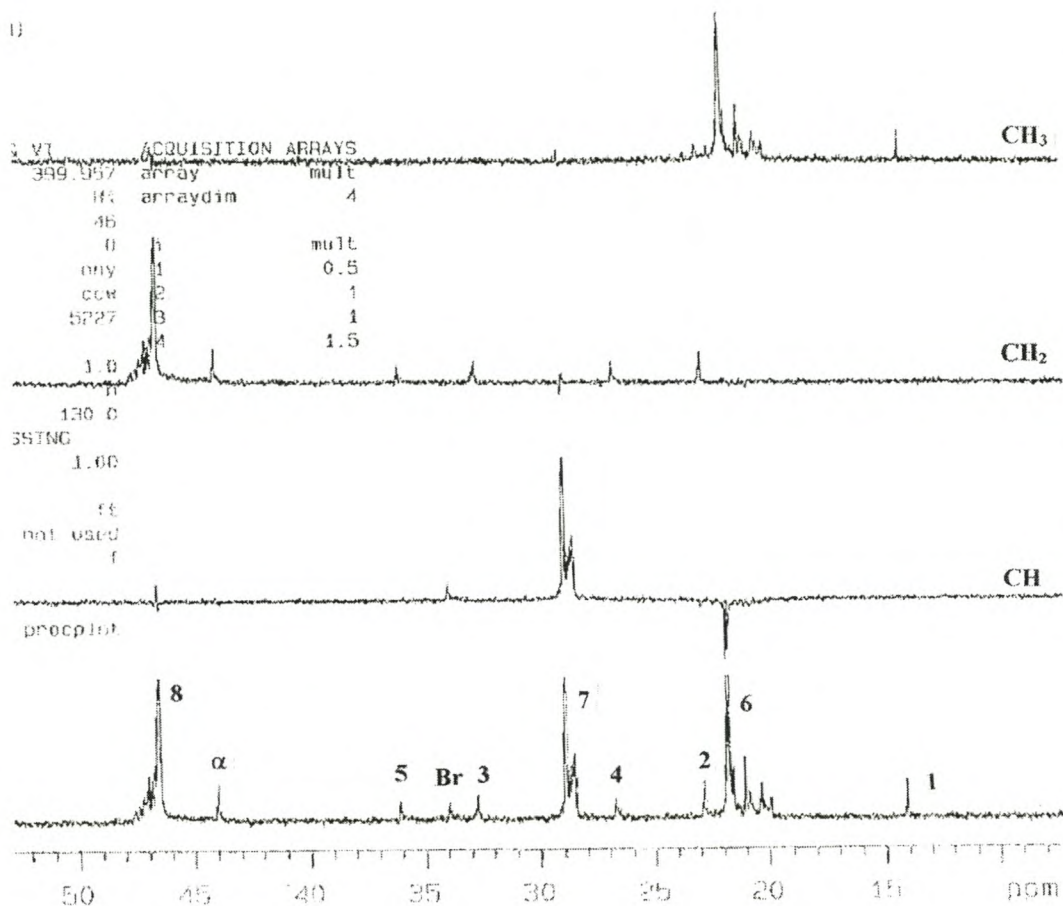
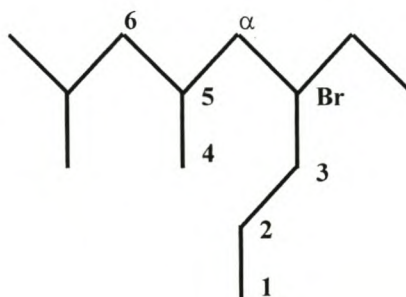


Figure 4.5.  $^{13}\text{C}$  NMR DEPT Spectrum of a Propylene / 1-Pentene Copolymer



**Figure 4.6.**  $^{13}\text{C}$  NMR DEPT Spectrum of a Propylene / 1-Heptene Copolymer

In Table 4.5 the chemical shifts of propylene copolymers with 1-pentene, 1-heptene and 1-nonene as comonomer, predicted by the Grant and Paul additivity rules, are presented. It will be noted that an additional correction factor for the effect of a tertiary carbon on a primary carbon was added. Carbon atoms are numbered according to the structure below, counting from the methyl group of the side chain towards the branching - and  $\alpha$ -carbon of the comonomer, followed by the methyl, branch and  $\alpha$ -carbons of the propylene unit.



**Table 4.5. Chemical Shift Prediction for Propylene / ( $\alpha$ -Olefin) Copolymers Utilizing the Grant and Paul Additivity Rules**

Position	$\alpha$	$\beta$	$\gamma$	$\delta$	$\epsilon$	3(2)	2(3)	1(3)	Constant
Factor	8.61	9.78	-2.88	0.37	0.06	-2.65	-2.45	-1.4	-1.87
<b>Carbon</b>	<b>Propylene / 1-Pentene</b>								<b>Chemical Shift (ppm)</b>
1	1	1	1	2	2				14.5
2	2	1	2	2	4				20.35
3	2	3	2	4	2	0	1		38.08
Br	3	3	5	2	4	3			31.93
$\alpha$	2	4	3	5	2	0	2		42.9
4	1	2	2	4	3	0	0	1	20.8
5	3	2	4	3	5	2			28.11
6	2	4	2	4	3	0	2		45.47
	<b>Propylene / 1-Heptene</b>								
1	1	1	1	1	1				14.07
2	2	1	1	1	2				22.74
3	2	2	1	2	2				32.89
4	2	2	3	2	4				27.25
5	2	3	3	5	2		1		35.57
Br	3	3	5	3	5	3			32.36
$\alpha$	2	4	3	5	3		2		42.96
6	1	2	2	4	3			1	20.8
7	3	2	4	3	5	3			25.46
8	2	4	2	4	3		2		45.47
	<b>Propylene / 1-Nonene</b>								
1	1	1	1	1	1				14.07
2	2	1	1	1	1				22.68
3	2	2	1	1	1				32.46
4	2	2	2	1	2				29.64
5	2	2	2	3	2				30.38
6	2	2	3	3	5				27.68
7	2	3	3	5	3		1		35.63
Br	3	3	5	3	5	3			32.36
$\alpha$	2	4	3	5	3		2		42.96
8	1	2	2	4	3			1	20.8
9	3	2	4	3	5	3			25.46
10	2	4	2	4	3		2		45.47

For all propylene /  $\alpha$ -olefin copolymers, the comonomer content in mole percent [C] was calculated according to the following formula:

$$[C] = 200 \text{ Br} / (\text{Total Backbone Carbons}) \quad (5)$$

where Br is the intensity of the branching CH peak as indicated on the spectra in Figures 4.5 and 4.6. The total, backbone carbons are obtained from the sum of the peak intensities at 29 ppm, 47 ppm and the  $\alpha$  and Br carbons as indicated on the spectra in Figures 4.5 and 4.6. At higher comonomer concentrations, sequences other

than PPCP (representing the isolated branch) appear and should be included in the calculations of comonomer content. In Table 4.6 the predicted and observed chemical shifts of the CH<sub>2</sub> and branching CH for the PPPP, PPPC and CPPC, CCCC, CCCP and PCCP and PPCC, CPCC, PPCP and CPCP sequences for the propylene /  $\alpha$ -olefin copolymers are presented.

**Table 4.6. <sup>13</sup>NMR  $\alpha$ -Carbon and Branching Carbon Peak Assignments of the Indicated Dyad Sequences for Copolymers of Propylene with Higher  $\alpha$ -Olefins**

<b>Propylene / 1-Pentene</b>	<b>CCCC</b>	<b>CCCP</b>	<b>PCCP</b>	<b>PPCC</b>	<b>CPCC</b>	<b>PPCP</b>	<b>CPCP</b>
Predicted $\alpha$	40.5	40.5	40.39	43	43	43	43
Predicted - Branch	32.8	32.7/32.4	32.4	32.4	32.4	32	32
Observed $\alpha$	40.9	40.9	40.9	43.5	43.4	43.4	43.5
Observed Branch	33	33	33	33	33	33	33
<b>Propylene / 1-Heptene</b>							
Predicted $\alpha$	40.6	40.6	40.5	43	43.1	43	43
Predicted Branch	33.2	32.9/32.8	32.8	32.8	32.8	32.4	32.4
Observed $\alpha$	-	-	-	44.1	44.1	44.1	44.1
Observed Branch	33.9	33.9	33.9	33.9	33.9	33.9	33.9
<b>Propylene / 1-Nonene</b>							
Predicted $\alpha$	40.6	40.6	40.5	43	43.1	43	43
Predicted Branch	33.2	32.9/32.8	32.8	32.8	32.8	32.4	32.4
Observed $\alpha$	-	-	-	44.1	44.1	44.1	44.1
Observed Branch	33.9	33.9	33.9	33.9	33.9	33.9	33.9

Similar to the calculations of sequence lengths for the ethylene copolymers, those for the propylene copolymers were calculated from Equations 6 and 7 [7] where the intensities of the CH<sub>2</sub> dyads in the sequences PPPP, PPPC and CPPC, CCCC, CCCP and PCCP and PPCC, CPCC, PPCP and CPCP were used.

$$\tilde{n}_P = \{(PP) + 0.5(PC)\}/0.5(PC) \quad (6)$$

$$\tilde{n}_C = \{(CC) + 0.5(PC)\}/0.5(PC) \quad (7)$$

where (PP) (CC) and (PC) are the dyad concentrations of the CH<sub>2</sub> carbons of the corresponding sequences.

The composition of the propylene / 1-pentene copolymers were also determined on a Perkin Elmer FT-IR 1720X instrument on compression moulded film samples of 0.3 mm thickness moulded on a Graseby Specac press at 180°C by making use of a calibration curve obtained by plotting absorbance over film thickness against concentration of poly (1-pentene) melt-blended with polypropylene. The moderately strong peak at 969  $\text{cm}^{-1}$  in the spectrum of PP arises from coupling vibrations, while the rocking of the  $\text{CH}_3$  group at 734  $\text{cm}^{-1}$  was used to determine the branch derived from 1-pentene. In Figure 5.7 an IR spectrum indicating the peaks used for the determination, is presented.

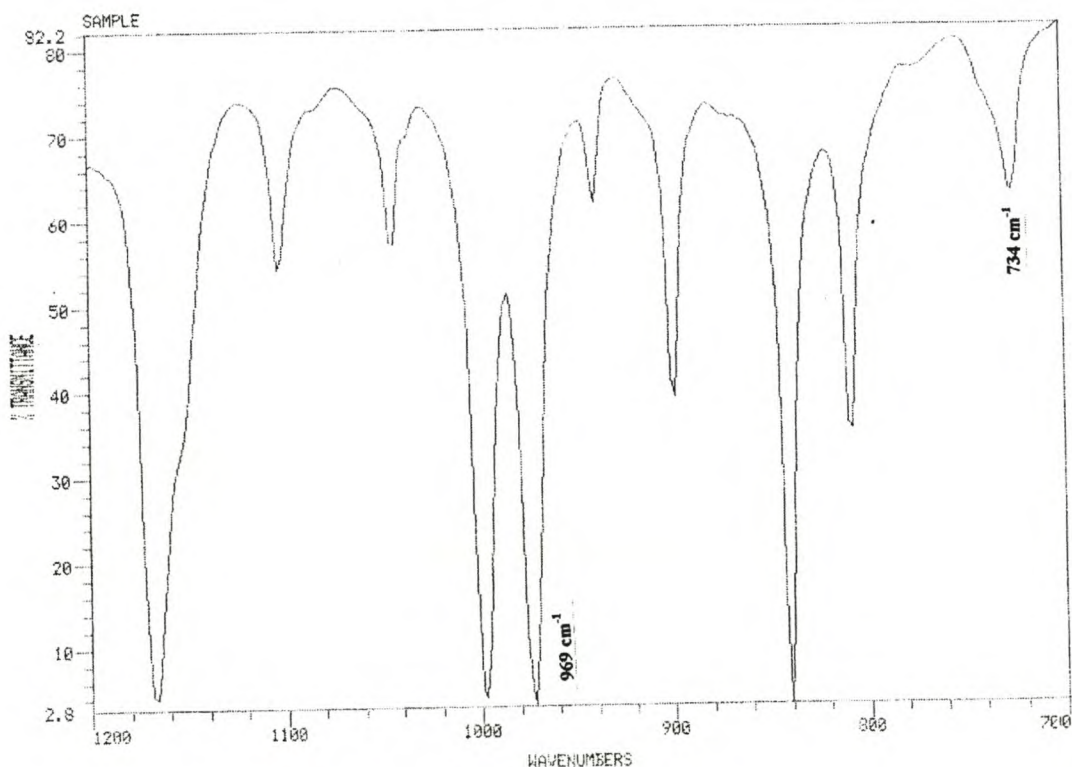


**Figure 4.7. IR Spectrum of Propylene / 1-Pentene Copolymer**

#### **4.2.2.5 Molecular Weight**

Molecular weights of the polypropylenes were determined on a Waters 150 CV GP chromatograph equipped with data module and computer acquisition system. Determinations have been done on the copolymer samples dissolved at 150°C in 1,2,4-trichlorobenzene. Each set of samples included a polystyrene standard and the



NBS 1475a standard in order to check the validity of data against the calibration curve data. Polystyrene standards, spanning the MW range 3 100 000 – 1 000 g/mol were used for calibration. Differential Refractive Index was used for detection.

#### **4.2.2.6 Scanning Electron Microscopy (SEM)**

SEM photos of the fracture surfaces of propylene / 1-pentene block copolymers were taken from images obtained from a Cambridge S350 electron microscope with a Tungsten filament at a high voltage of 3 kV under a vacuum of  $5 \times 10^{-6}$  Torr. Samples were mounted on aluminum stubs and coated on a Bio-Rad E5200 Auto Sputter Coater with three layers of gold deposited at 30 seconds per layer. No etching or staining was necessary.

#### **4.2.3 THERMAL PROPERTIES**

Melting and crystallization behaviour was determined on a Perkin Elmer DSC-7 fitted with a TAC 7/PC instrument controller. A typical sequence is as follows: the samples were heated from 50 to 200°C at 20°C/min, held at 200°C for 1 minute, cooled to 50°C at a rate of 20°C/min during which time the crystallization curve was recorded. At 50°C, the temperature was kept constant for 1 min after which the melting curve was recorded between 50 and 200°C at a heating rate of 10°C/min.

For a different set of experiments, where the effect of slow cooling on thermal properties was investigated, a cooling rate of 0.3°/min. instead of 20°C/min. was used.

### 4.3 REFERENCES

1. Burfield D.R., Kashiva N., *Makromol. Chem.*, **186**, 2657 (1985)
2. Bogdanov B.G., Michailov M., *Properties of Polyolefins* in *Handbook of Polyolefins – Synthesis and Properties*, Vasile C., Seymour R.B., Eds., Marcel Dekker Inc., New York, 295 (1993)
3. Quirk R.P., Alsamarraie M.A.A., *Physical Properties of Poly(propylene)* in *Polymer Handbook*, Third Edition, Brandrup J., Immergut E.H., John Wiley & Sons, New York, V/27 (1989)
4. Faucher J.A., Reding F.P., *Relationship Between Structure and Fundamental Properties in Crystalline Olefin Polymers Part I*, Ed. Raff R.A.V., Doak K.W., John Wiley & Sons, New York, 677 (1965)
5. Grant D.M., Paul E.G., *J. Am. Chem. Soc.*, **86**, 2984 (1964)
6. Randall J.C., *Long-Chain Branching in Polyethylenes* in *Polymer Characterization by ESR and NMR*, **6**, 93 (1980)
7. Herbert I., *Statistical Analysis of Copolymer Sequence Distribution* in *NMR Spectroscopy of Polymers*, Ibbett R.N., Ed., Blackie Acad. & Proff., London, (2), 50 (1993)

## CHAPTER 5

### ZIEGLER-NATTA CATALYSTS

#### 5.1 INTRODUCTION

One of the most prominent features of Ziegler-Natta catalysts is the presence of a wide variety of different active sites having different accessibilities and activities which is responsible for the wide molecular weight distribution and comonomer distributions usually observed [1]. Catalysts with very protected active sites will thus incorporate large comonomers such as 1-octene or 1-nonene with more difficulty than the smaller 1-butene and 1-pentene molecules. When attempting to copolymerize ethylene with one of the higher  $\alpha$ -olefins, such catalysts will produce mainly high density polyethylene because the larger comonomer unit can not be incorporated into the growing polymer chain. By opening up the active sites of the catalyst, larger comonomer units have better access to the active sites and will therefore be incorporated into the polymer chains, thus producing a polyethylene copolymer having decreased density. Apart from the steric demands of the higher  $\alpha$ -olefins on the catalyst, their reactivities also influence the requirements for a catalyst capable of producing a polyethylene containing sufficient comonomer units at reasonable productivity. As the size of the comonomer molecule increases, its reactivity generally decreases [2]. Therefore, the ideal polyethylene catalyst should have accessible active sites that can produce linear low density material from the higher  $\alpha$ -olefins at high catalytic activity.

However, catalysts for producing crystalline polypropylene should not only have accessible active sites capable of incorporating the higher  $\alpha$ -olefins in the polypropylene backbone, but monomer placement in the chain should be regular, *i.e.* the monomer should only enter the coordination complex with a specific orientation of its methyl group.

As the range of olefins produced by the Sasol Fischer-Tropsch process include both linear and bulky branched compounds, some of which have low reactivities, it was necessary to investigate  $\text{MgCl}_2$ -supported catalysts capable of producing ethylene copolymers containing higher linear  $\alpha$ -olefins up to 1-nonene and  $\text{C}_5$  and  $\text{C}_6$  branched  $\alpha$ -olefins at high catalyst activities. Further, catalysts should be capable of producing isotactic copolymers of propylene with these comonomers.

Because the active sites were anchored to the support, the preparation of the support has a direct influence on the nature of the active sites and consequently on the overall catalyst performance. Therefore, the investigation regarding these catalysts was initially focussed on support preparation.

## 5.2 EXPERIMENTAL

### 5.2.1 MATERIALS AND EQUIPMENT

All chemicals used for the preparation of catalysts were obtained from Aldrich at the highest purity available and were used as received except di-*n*-butyl ether which was received from Merck and ethyl benzoate, obtained from Riedel de Haën.

Heptane was obtained from Schümann-Sasol and purified by passing over 13X molsieve followed by Alcoa Selexsorb CD to remove moisture and polar compounds to levels below 5 ppm.

$\delta$ -Type  $\text{TiCl}_3$  was obtained from Akzo Nobel and was used as received. Metallocene catalysts and methyl aluminoxane were obtained from Witco and used as received.

Initial reaction of  $\text{MgCl}_2$  with polar compounds were done under inert conditions in a fume-hood and solvent evaporation was conducted on a Büchi rotavapor. All other manipulations were carried out in an MBraun MB 150 GI glovebox with moisture levels below 0.2 ppm and oxygen levels below 1 ppm.

### 5.2.2 ANALYSES

#### 5.2.2.1 X-Ray Diffraction

X-ray diffractograms were obtained from measurements on a Siemens D500 powder diffractometer fitted with a scintillation detector. In a glovebox under inert conditions, the catalyst or support material was placed in a stainless steel sample holder. A 50  $\mu\text{m}$  thick polyethylene film was clamped down on top of the sample to protect the sample from the atmosphere. The sample was immediately radiated with cobalt  $\text{K}\alpha^1$  radiation (wavelength 1.78897Å) at  $2\theta$  angles from  $5^\circ$  to  $80^\circ$  in steps of  $0.05^\circ$  with a two second counting time between steps.

### 5.2.2.2 Surface Area and Pore Size

BET surface area and pore size were determined on a Micrometrics Gemini II, model 2375 Surface Area Analyzer using the version 4.02 software. The dry, powdered sample of the catalyst or support was treated with pure nitrogen on a Micrometrics Flow Prep apparatus at 100°C overnight before the measurements were made.

### 5.2.2.3 Titanium Oxidation States

Contact between dried catalyst and methanol produced protons.  $\text{Ti}^{2+}$  reacts with protons with the formation of hydrogen and  $\text{Ti}^{3+}$ . The hydrogen content was determined by means of GC and used in the calculation of the  $\text{Ti}^{2+}$  content.

$\text{Ti}^{3+}$  reacts with  $\text{Fe}^{3+}$  to form  $\text{Ti}^{4+}$  and  $\text{Fe}^{2+}$ . The concentration of the latter is determined by means of a characteristic orange phenanthroline complex. This allows the determination of  $\text{Ti}^{3+}$ .

The total titanium content was analyzed by ICP (Inductively Coupled Plasma). Knowledge of the  $[\text{Ti}^{2+}]$  and  $[\text{Ti}^{3+}]$  then yields the original  $\text{Ti}^{4+}$  concentration of a particular catalyst.

### 5.2.2.4 Catalyst Composition

*Elemental Analyses.* An accurately weighed sample of the catalyst was treated with a 10% aqueous sulphuric acid solution in an ultrasonic bath to digest the catalyst sample. The solution was analysed for Al, Mg and Ti by means of ICP. Standard solutions of the elements were also prepared to determine the accuracy and the precision of each element concentration. The results were calculated as mass % of the dried catalyst samples.

ICP cannot, however, be used to determine the chloride content. Therefore, a second aqueous solution of each sample was prepared with distilled water and submitted for an ionic chromatographic analysis to determine the chloride content. Standard solutions of NaCl were used for calibration of the chloride content.

*Organic Ligands.* An accurately weighed catalyst sample was treated with a known amount of methanol to liberate the ligand. This treatment of the catalyst with methanol releases protons which may damage the GC column. Therefore, a solution of sodium bicarbonate in methanol containing methyl orange as indicator was prepared and added to the catalyst solution to neutralize the medium. The total amount of methanol was then used to determine the catalyst concentration. For each of the organic components (e.g, alcohols) standard solutions were evaluated by GC from which the concentration of each ligand was calculated.

#### 5.2.2.5 Copolymer Composition

The amount of comonomer present in the co- and terpolymers was determined from  $^{13}\text{C}$  NMR analyses according to the procedures fully described in Chapter 4.

### 5.2.3 POLYETHYLENE CATALYST PREPARATION

Catalysts were prepared according to the procedures previously described [3-8]. The first basic procedure involved the following:

Under a nitrogen atmosphere in a glovebox, an amount of  $\text{MgCl}_2$  containing between 1.5 and 5% water is stirred in the presence of an ether in purified heptane at temperatures between ambient and reflux for up to 3 hours. To this pre-activated support, an excess of tri-ethyl aluminum (preferably a 10% solution in heptane) was added dropwise under continuous stirring for periods up to 8 hours followed by repeated washing with heptane to remove unreacted tri-ethyl aluminum. To this material, an alcohol or alcohol mixture of two to three linear or branched alcohols having 2 to 9 carbon atoms was added and reacted in a heptane slurry at temperatures between ambient and reflux for 2 to 3 hours. This treatment was followed by the addition of an excess of  $\text{TiCl}_4$  followed by refluxing the slurry for 2 to 3 hours. Extensive washing with heptane to remove all titanium compounds not fixed onto the  $\text{MgCl}_2$  support was then performed.

In a second procedure,  $\text{MgCl}_2$  was dissolved in a combination of ethanol and di-butyl ether during a pre-activation step and the organic components were then slowly removed under reduced pressure on a rotary evaporator while care was taken to prevent

crystallization taking place. To this syrupy complex, an excess of tri-ethyl aluminum solution in heptane was added dropwise to prevent heat build-up. The paste was continuously ground. The resulting smooth slurry was then stirred for 15 hours at ambient temperature and then thoroughly washed with heptane. To this pre-activated  $\text{MgCl}_2$  was added a mixture of alcohols. The mixture was then ground in the presence of 50 ml heptane to yield a smooth paste of the activated support which was then stirred for another 24 hours. To this slurry was added an excess of  $\text{TiCl}_4$ . The mixture was refluxed for 1 hour after which it was cooled and thoroughly washed with heptane to remove all soluble species to yield the supported catalyst.

Specific methods of preparation used during the investigation are described in the text below.

#### 5.2.4 POLYETHYLENE CATALYST ACTIVITY

For catalyst activity determinations, a standard method of polymerization was used and described in reference [3]. The description for such a polymerization is as follows:

To a thoroughly cleaned 1-liter stainless steel autoclave flushed with high purity nitrogen was added 300 g of heptane and the temperature was set at 85°C. When the correct temperature was reached, 10 ml of a 10% solution tri-ethyl aluminum in heptane was added and the solution was stirred for 5 minutes. An amount of catalyst slurry, typically 0.1 ml containing about 0.01g catalyst was introduced and left to react for 5 minutes to form the active catalyst. At this point, ethylene was introduced at a rate of 15 g/min. until a pressure of 20 bar was reached. The reaction was continued at this pressure for 60 minutes after which the reactor was vented and the catalyst deactivated by the introduction of *iso*-propanol. The polymer was washed with acetone, dried and weighed to determine catalyst activity as gram polyethylene per gram catalyst per hour.



### 5.2.5 POLYPROPYLENE CATALYST PREPARATION

In References [5] and [9] the methods of preparation of various stereoregulating catalysts suitable for slurry and gas-phase polymerization of propylene are described. A general outline of the preparation methods used is as follows:

MgCl<sub>2</sub> was dissolved in a combination of ethanol and di-butyl ether during a pre-activation step and the organic components slowly removed under reduced pressure on a rotary evaporator while care was taken to prevent crystallization taking place. This complex (X) was treated in the following ways to yield the final catalyst:

- A. Complex X was reacted with an excess of TiCl<sub>4</sub> at 50°C to yield an aspecific catalyst A containing 11.3% titanium.
- B. Complex X was reacted with an excess of tri-ethyl aluminum, washed with heptane and react with ethyl benzoate (EB) in a 0.2 EB:Mg molar ratio at 60°C for 120 minutes. This compound was then reacted with an excess of TiCl<sub>4</sub> at 50°C for different times to yield catalysts B1 to B6.
- C. Complex X was reacted with di-iso butyl phthalate (DIBP) in a 0.2 DIBP:Mg molar ratio at 60°C for 1 hour. This compound was washed and then reacted with an excess of TiCl<sub>4</sub> at 80°C for up to 1 hour to yield catalyst C containing 6.4% titanium.

The detailed descriptions of the different preparation methods are presented in Section 5.4.

### 5.2.6 PROPYLENE / 1-PENTENE COPOLYMERIZATION

To a 10-liter automated autoclave at 70°C and containing 3 000g of purified *n*-heptane was added tri-ethyl aluminium as cocatalyst, diphenyl dimethoxy silane as external electron donor and a magnesium chloride-supported titanium trichloride catalyst. 30 mg Hydrogen was then introduced as molecular weight regulator. After 15 minutes ageing of the catalyst, a continuous flow of propylene together with 1-pentene was started and the reaction was continued for 2 hours at 15 bar. The slurry

was deactivated with *iso*-propanol, filtered and the copolymer washed with acetone and dried in a vacuum oven at 80°C.

When the  $\delta$ -TiCl<sub>3</sub> catalyst from Akzo was used, the silane addition step was omitted.

### **5.2.7 CATALYST KINETICS**

The procedure used for the copolymerization reaction was used for the determination of kinetic rate / time profiles for homo- and copolymerization with different catalysts in a slurry phase. The total amount of the monomer(s) at the correct ratio were introduced into a 5-liter reactor and the polymerization terminated at different times in order to measure polymer yield and comonomer content.

## 5.3 POLYETHYLENE CATALYSTS

### 5.3.1 CRYSTALLOGRAPHIC CHANGES

Because the activation of  $\text{MgCl}_2$  using physical or chemical means are known and well-documented in the literature [10-15], the influence of only slightly modifying the crystal structure was thought worth investigating. Different methods of support activation were investigated to determine the preparation method yielding catalysts with highest activity and being capable of incorporating the  $\alpha$ -olefins produced in the Sasol process. In order to understand how different treatments of the  $\text{MgCl}_2$  used as support material affects its crystal structure, X-ray diffractograms of the  $\text{MgCl}_2$  were recorded after different steps used in the catalyst preparation. The amorphous support material and the catalysts prepared are moisture and air sensitive and it was thus necessary to record the diffractograms using a specially designed sample holder. The powder sample was therefore packed in a drybox and sealed by clamping down a  $50\mu\text{m}$  polyethylene film on top of the sample which was then scanned immediately. It can be seen from the diffractograms shown in Figures 5.1 to 5.3 that the only large change was observed when the  $\text{MgCl}_2 \cdot 6\text{H}_2\text{O}$  was treated with tri-ethyl aluminum while similar treatment of the  $\text{MgCl}_2$  containing 1.5% water did not change its crystal structure. From this observation it seems that treatment of the with tri-ethyl aluminum (which reacts with the crystal water) results in a crystal structure similar to that of  $\text{MgCl}_2$  containing only small amounts of water. The peak at  $25^\circ$  on the  $2\theta$  scale and the halo around it is that of the sample holder and its PE cover. The aim of the diffractograms was only to illustrate *differences* between different preparative methods and not to determine the different crystal structures. The empty sample holder was thus not subtracted from the measurements. In Figure 5.4, where the diffractogram of the nearly amorphous final catalyst is shown in blue, the peak at  $25^\circ$  and the halo between  $20$  and  $29^\circ$  associated with the sample holder and the polyethylene cover can be seen.

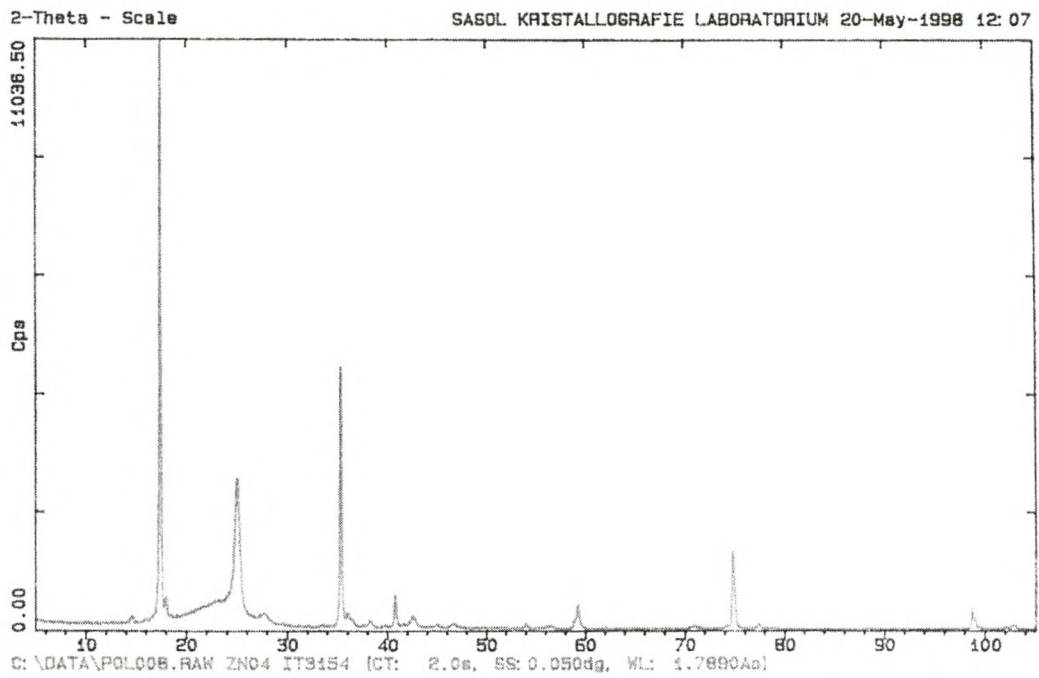


**Figure 5.1. X-Ray Diffractogram of  $MgCl_2$  Containing 1.5% Water**

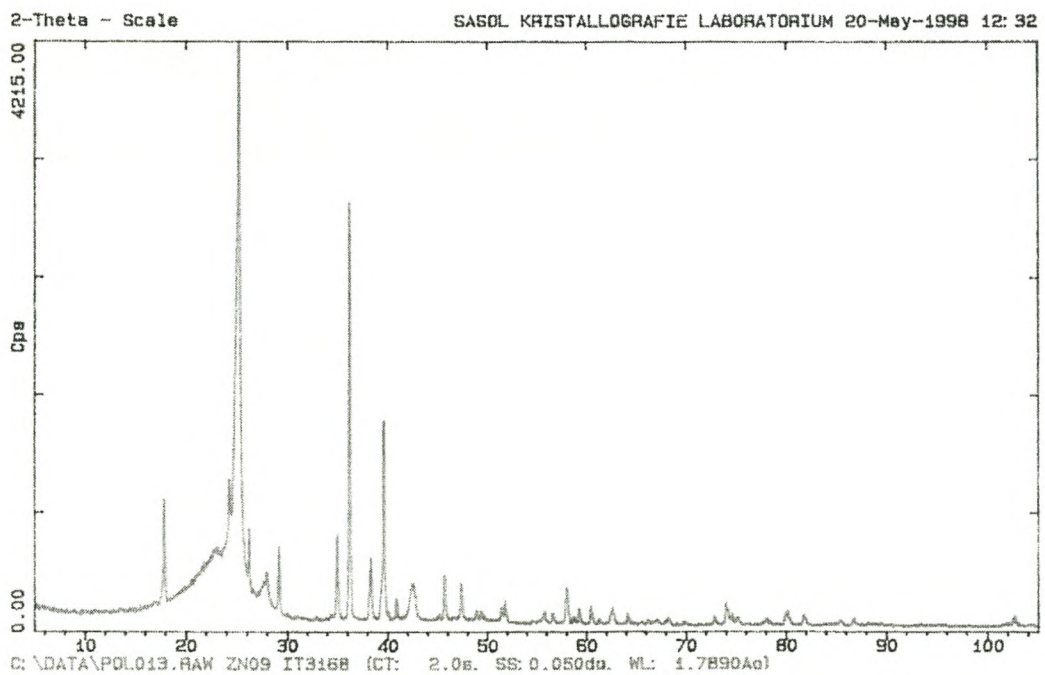


**Figure 5.2. X-Ray Diffractogram of  $MgCl_2 \cdot H_2O$**

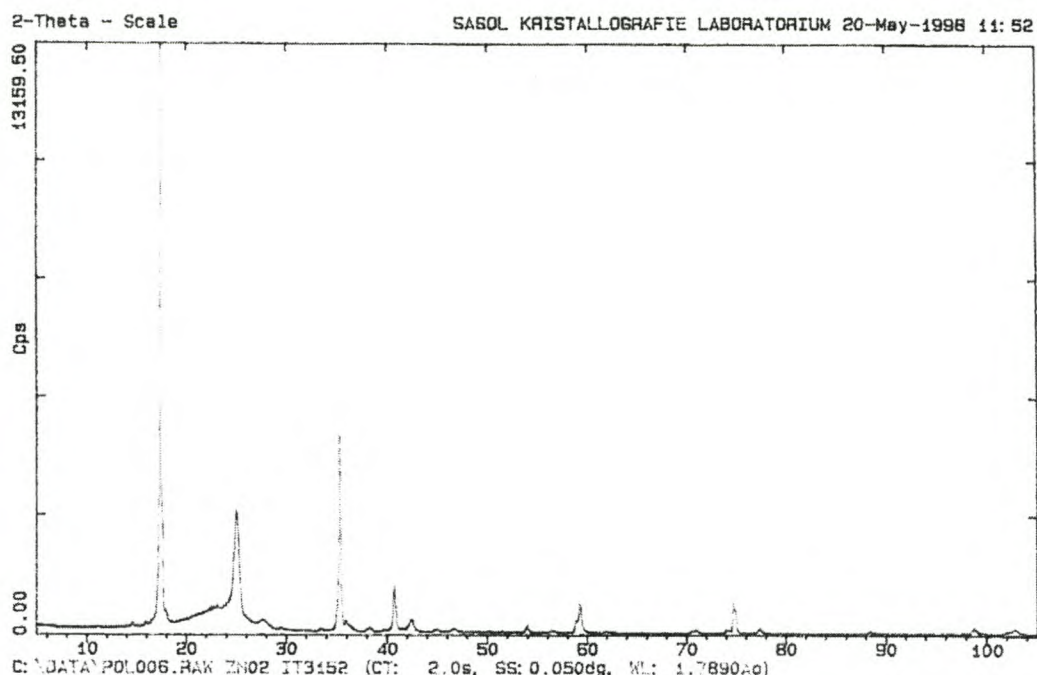


**Figure 5.3. X-Ray Diffractogram of  $\text{MgCl}_2 \cdot \text{H}_2\text{O}$  Treated with Tri-Ethyl Aluminum**

It can be seen by comparison of Figures 5.2 and 5.3 that tri-ethyl aluminum treatment of the  $\text{MgCl}_2 \cdot 6\text{H}_2\text{O}$  resulted in a diffractogram very similar to that of the  $\text{MgCl}_2$  containing 1.5% water shown in Figure 5.1. Tri-ethyl aluminum treatment therefore only *changes* the crystal structure of  $\text{MgCl}_2 \cdot 6\text{H}_2\text{O}$ . By dissolving a 1.5% water containing  $\text{MgCl}_2$  in an ethanol / di-butyl ether mixture followed by reaction with tri-ethyl aluminum, a diffractogram showing very little residual crystallinity was obtained.

Figure 5.4 shows the XRD patterns of the reaction products after each step of a complete catalyst preparation procedure. The XRD pattern at the bottom is that of the starting material ( $\text{MgCl}_2$  containing 1.5% water). The green XRD pattern was obtained after treatment with di-pentyl ether and the red one when this product was treated with tri-ethyl aluminum. The blue XRD pattern at the top is that of the final catalyst. Some crystallinity was preserved during each consecutive step in the preparation. This procedure entailed refluxing 20g of a  $\text{MgCl}_2$  containing 1.5% water in 40 ml di-pentyl ether for 3 hours followed by a heptane wash. This pre-activated support was then reacted with an excess of tri-ethyl aluminum, again followed by a heptane-washing step. To this solid was then added 20 ml of a 1:1 molar mixture of ethanol and heptanol. The

sticky paste was covered to prevent evaporation and left for 3 days after which it was washed with heptane and reacted with an excess of  $\text{TiCl}_4$  to form the active catalyst after washing with heptane to remove all heptane-soluble material.

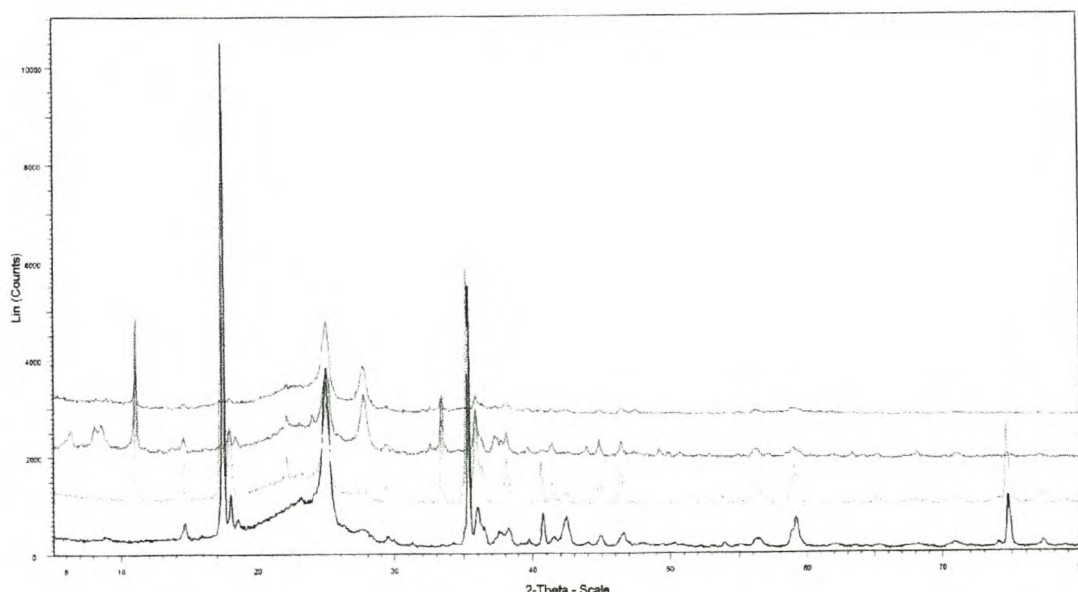


**Figure 5.4. X-Ray Diffractogram of Reaction Products Obtained from Different Steps During Catalyst Preparation**

It can be seen from the stepwise changes in crystallinity shown in Figure 5.4 that in this preparation method, the crystallinity of the support, different to the complete destruction of crystallinity in one treatment as found when the  $\text{MgCl}_2$  was dissolved and reprecipitated by the addition of tri-ethyl aluminum or  $\text{TiCl}_4$ , the crystallinity was only slightly changed in each consecutive step. Only during the last step, where the transition metal is anchored to the support, the final crystallinity of is the catalyst rendered virtually amorphous.

### 5.3.2 CATALYST ACTIVITY

The basic steps followed for preparation of the different catalysts are similar to that described in Section 5.2.3, but with differences relating to the pre-activation and activation steps in that different ethers and alcohol mixtures were used. The different preparation methods used are summarized in Table 5.1.

**Table 5.1. Preparation Methods of Different MgCl<sub>2</sub>-Supported Catalysts.**

Catalyst	Water Content (%)	Pre-treatment – Amount (ml)	Alkyl Aluminum	Activation Step – Alcohol(s)	Amount (ml)	Activity (kg/g/hr)
1	1.5	THF - 1.4	DEAC	C <sub>8</sub> -OH	2.0	13.4
2	1.5	THF - 1.4	DEAC	C <sub>7</sub> -OH	2.0	14.6
3	1.5	THF - 1.4	DEAC	C <sub>5</sub> -OH	2.0	29.4
4	1.5	THF - 1.4	DEAC	C <sub>4</sub> -OH	2.0	37.7
5	5.0	THF - 1.4	TEA	C <sub>4</sub> -OH / C <sub>5</sub> -OH	1.0/1.0	32.3
6	1.5	DBE – 2.0	TEA	C <sub>2</sub> -OH / C <sub>4</sub> -OH / C <sub>5</sub> -OH	0.4/0.8/0.8	51.9
7	1.5	DBE – 2.0	TEA	C <sub>2</sub> -OH / C <sub>4</sub> -OH / C <sub>6</sub> -OH	0.8/0.7/0.5	83.0

THF = Tetra hydro furan, DBE = Di-butyl ether

By comparing catalysts 1 to 4 prepared using different alcohols during the support activation step, it seems from Table 5.1 that their activities decrease as the carbon number of the alcohol increase. However, in each case 2 ml of the alcohol was used and therefore, by relating this volume to the total moles of –OH present, this increase is probably the direct result of the higher amount of –OH capable of forming magnesium / alcohol complexes.

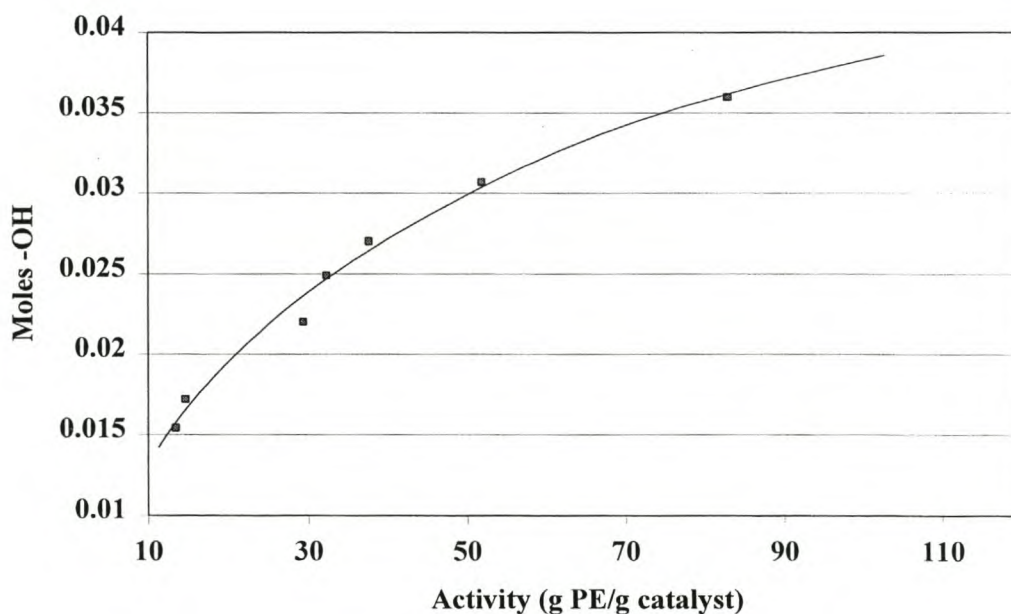


**Figure 5.5. Effect of Different Amounts of Alcohols and Alcohol Mixtures on Catalyst Activity**

When TiCl<sub>4</sub> was linked to a support having a large surface area isolation of the titanium centres, which increase the population of accessible active sites, was the main reason the activities attained being higher for supported catalysts than those of the unsupported

catalysts [16]. Increasing the amount of alcohol assists in the breakdown of the crystalline structure, which results in an increased surface area with an associated increase in activity. This effect is illustrated in Figure 5.5. Even use of a combination of alcohols, together with other changes such as the use of a different ether in the pre-activation step, still gives a catalyst activity that is related to the total amount of complexing alcohol present during the support activation step.

To be able to compare results all of the polymerization experiments were determined under the same conditions. However, an arbitrary time of 15 minutes to allow for alkylation of the catalyst to form the active centres was used. It was found by optimization of this alkylation reaction that this also had an effect on overall catalyst activity. The optimum ageing time of one of the catalysts was determined by varying the ethylene introduction time. In this series of experiments, the catalyst was left in contact with tri-ethyl aluminum at the polymerization temperature of 85°C for different times before the reaction was started by the introduction of ethylene. This allowed reaction between the potential active sites and the cocatalyst to occur prior to polymerization. The dependence of activity on catalyst ageing time is shown in Figure 5.6.

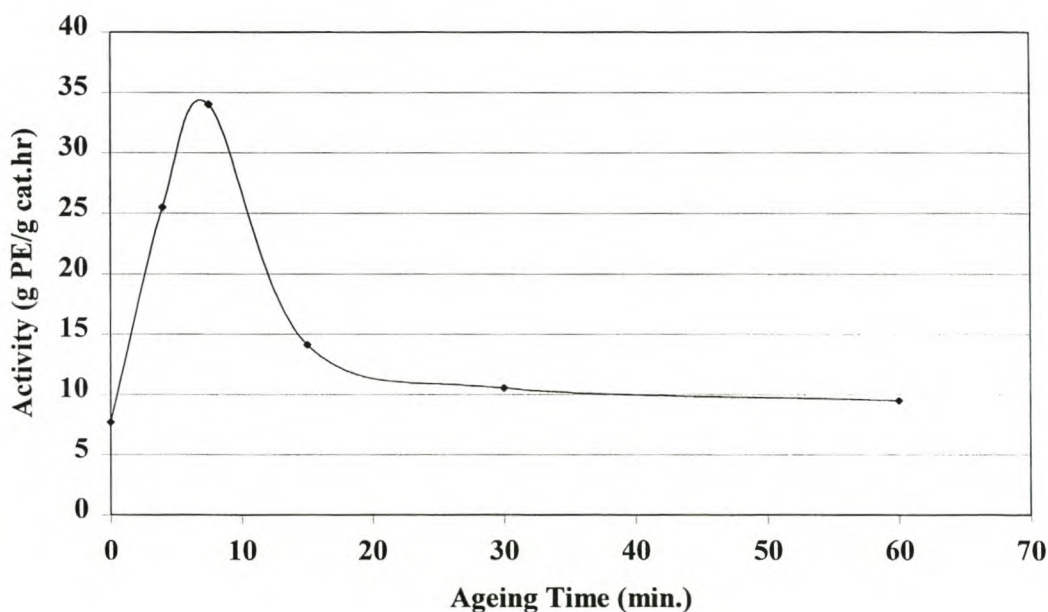


**Figure 5.6. Activity vs. Ageing Time for Catalyst 2**



From Figure 5.6 it can be seen that the ageing time has a profound effect on the overall catalyst activity. If the ageing time is too short, all potential active sites do not get alkylated and this results in a decreased concentration of active centres and therefore a decreased activity. However, by stirring the activated catalyst at the reaction temperature without monomer present, catalyst activity was found to be lower than when ageing time was shorter. The true reason for this was not investigated. However, it is thought to arise from spontaneous catalyst deactivation common in high activity supported catalysts [17] as a result of reactions such as that proposed by Kei and Doi [18,19]. This entails a bimolecular disproportionation between active species with a consequent reduction of  $Ti^{3+}$  by the cocatalyst to an inactive  $Ti^{2+}$  species. The effect of different alcohols on ageing time was not investigated, but it is believed that only the amount of alcohol, and not the length of its alkyl chain, will affect the ageing behaviour.

Table 5.2 presents the properties of similarly prepared catalysts having different titanium contents. The total organic content of the catalysts can be obtained by difference and consists of the ether, alcohol or alcohol mixture used during the support preparation.

**Table 5.2. Properties of  $MgCl_2$ -Supported Ziegler-Natta Catalysts**

Catalyst	Al Content (%)	Mg Content (%)	Cl Content (%)	Ti Content (%)	Activity (Kg PE/g Ti)
3	1.06	6.10	42.4	9.28	317
5	2.94	8.08	71.6	4.41	730
6	1.89	10.8	68.8	7.6	683
7	0.95	6.53	67.5	12.2	680
8	3.08	7.46	38.9	5.02	293
9	2.63	5.06	59.3	8.8	769
10	3.66	8.72	58.5	16.9	462
11	0.66	11.12	64.0	11.1	523

It can be seen from the activities (kg PE / g Ti / hr.) calculated (see Table 2) that no clear correlation exists between titanium content and activity. All activity values are situated between about 300 to 800 kg PE per gram of transition metal. From this observation it can thus be said that the catalytic abilities of the titanium species present on the support, which includes their oxidation states ( $Ti^{2+}$  species are undesirable) as well as the degree to which they are protected, influence the overall catalyst activity, rather than the amount of titanium species present.

Two catalysts prepared according to the second procedure outlined in Section 5.2.3 were analyzed for their titanium oxidation states, and their activities were compared. Catalyst 10 was prepared using 20 g of  $\text{MgCl}_2$  dissolved in 200 ml ethanol and 140 ml di-butyl ether. To the syrupy complex was added 180 g of a 50% tri-ethyl aluminum solution in heptane. To the pre-activated  $\text{MgCl}_2$  was added 10 ml of a 1:1:1 molar mixture of ethanol, butanol and pentanol and the procedure in Section 5.2.3 followed to obtain the final catalyst. For the preparation of catalyst 12, 20 ml of the alcohol mixture was used.

**Table 5.3. Properties of Differently Prepared Catalysts Comparing Activities with Titanium Composition**

Catalyst	Ti Content (%)	Mmole Ti/g catalyst			Activity (Kg PE/g cat)	Activity (Kg PE/g Ti)
		Ti <sup>2+</sup>	Ti <sup>3+</sup>	Ti <sup>4+</sup>		
10	16.9	0.0034	0.291	3.23	78	462
12	6.91	0.0099	0.059	1.37	290	4197

The composition and properties of these catalysts are presented in Table 5.3. Once again, even with these very different catalysts, it can be seen that no 1:1 correlation seems to exist between titanium content and catalytic activity. Catalyst 10 has more than double the titanium content of catalyst 12 and the amount of the desirable titanium species (Ti<sup>3+</sup> including the active species) are also more, but its activity is much lower. This strongly suggests that the active sites of catalyst 10 are more protected than those of catalyst 12 and that only a fraction of them are active during polymerization. Other possibilities also exist, eg. non-exposed Ti that may vary with concentration. As an observation it should be mentioned that the activity of catalyst 12 decreased to only about 10% (30 kg/g cat) that of the freshly prepared catalyst over a period of 3 months. Activity dropped another 50% to 15 kg/g cat over a further 2 month period whereas no substantial loss in activity of the less active catalyst 10 was noticed over a 3 month period.

It can thus be seen from the above that two very important factors affecting catalyst activity of these particularly prepared catalysts are the amount of alcohol present during support activation as well as the time allowed for alkylation.

However, the primary aim of this investigation was not only to prepare a catalyst capable of producing polyethylene at high productivities. The catalysts should also be able to incorporate higher  $\alpha$ -olefins in the polyethylene backbone in order to produce linear low density polyethylene.

### 5.3.3 COMONOMER INCORPORATION

To evaluate the incorporation of different comonomers by these catalysts, the comonomer incorporation ratio for monomer x ( $CIR_x$ ), can be estimated from the equation:

$$CIR_{x1} = [C_{x1}] (m_{x1}/M_{x1} + m_{x2}/M_{x2} + m_{Et}/M_{Et})(M_{x1} / m_{x2}) \quad (5.1)$$

where  $[C_{x1}]$  is the comonomer content in mole percent,  $m_{x1,2}$  and  $m_{Et}$  are the masses of comonomer x1, x2 and ethylene fed to the reactor and  $M_{x1}$  and  $M_{Et}$  are the molecular weights of the comonomer and ethylene respectively. A low value will indicate difficult comonomer incorporation whereas a value of 100 indicates that the catalyst does not distinguish between the different comonomers and reflects a perfect comonomer response. The monomer ratio fed to the reactor will be that found in the copolymer.

The more protected the active sites, the more difficult it will be for the larger, sterically disadvantaged comonomers to come close enough to the active site to be captured by the metal in order to be inserted into the growing chain. A low value may therefore also be an indication of the nature of protected active sites. The CIRs observed for different catalysts are shown in Table 5.4.

From Table 5.4 it can be seen by comparing CIR values that even for the same catalyst, the CIR values for a specific comonomer are slightly scattered. This is believed to result from the different monomer ratios which change the environment in which each monomer compete for placement into the growing polymer chain. In general, however, it can be seen that for a specific catalyst, 1-butene inserts easier than 1-pentene which

inserts easier than 1-hexene and so on which is in line with the different reactivities of these monomers as discussed by Kissin [2].

**Table 5.4. Comonomer Incorporation for Different Catalysts During Co- and Terpolymerization with Ethylene**

Catalyst	Comonomers	Monomer Ratio (C <sub>2</sub> /C <sub>5</sub> /C <sub>x</sub> )	Composition (%)	Density (g/cm <sup>3</sup> )	CIR C <sub>5</sub>	CIR C <sub>x2</sub>
<b>1</b>	C <sub>5</sub>	56/100	4.6	0.930	11	-
	C <sub>5</sub> /C <sub>8</sub>	100/100/10	3.0/0.2	0.928	11	12.0
<b>2</b>	C <sub>5</sub> /C <sub>4</sub>	90/80/40	2.6/2.0	0.919	11.5	14.2
	C <sub>5</sub> /C <sub>8</sub>	80/100/20	3.4/0.4	0.923	10.6	10.0
<b>3</b>	C <sub>5</sub> /C <sub>6</sub>	100/20/110	0.7/3.1	0.922	12.7	12.2
<b>4</b>	C <sub>5</sub> /C <sub>4</sub>	100/140/50	0.9/3.4	0.929	8.3	9.7
<b>5</b>	C <sub>5</sub> /C <sub>6</sub>	100/80/120	1.6/2.0	0.930	8.6	8.6
	C <sub>5</sub> /C <sub>6</sub>	100/20/180	-/2.1	0.941	-	5.9
<b>6</b>	C <sub>5</sub> /C <sub>6</sub>	100/60/20	0.8/0.2	0.949	4.4	3.9
	C <sub>5</sub> /C <sub>6</sub>	100/100/20	1.6/0.3	0.936	5.9	5.7
	C <sub>5</sub> /C <sub>6</sub>	100/30/90	0.4/1.1	0.940	4.7	5.2
	C <sub>6</sub>	100/120	1.2	0.947	-	4.2
<b>7</b>	C <sub>5</sub> /C <sub>6</sub>	100/20/100	0.7/3.1	0.927	12.4	13.2
<b>9</b>	C <sub>4</sub>	100/30	1.8	0.950	-	13.8
	C <sub>5</sub> /C <sub>6</sub>	90/100/20	2.1/-	0.945	7.2	-
	C <sub>5</sub> /C <sub>6</sub>	100/50/50	1/0.8	0.942	6.8	6.6
	C <sub>5</sub> /C <sub>6</sub>	90/80/20	2.0/0.4	0.939	8.0	7.7
<b>11</b>	C <sub>5</sub> /C <sub>6</sub>	80/100/20	2.6/0.4	0.929	8.2	7.6
	C <sub>5</sub> /C <sub>6</sub>	100/90/30	2.4/0.6	0.930	9.4	8.4
<b>12</b>	C <sub>5</sub> /C <sub>6</sub>	90/90/90	4.4/3.8	0.923	19.0	19.7
	C <sub>5</sub> /C <sub>8</sub>	100/100/100	5.7/2.9	<0.910	23.0	19.6
	C <sub>5</sub> /C <sub>8</sub>	100/60/140	4.4/3.6	<0.910	29.0	16.7
	C <sub>5</sub> /C <sub>8</sub>	100/25/175	1.0/5.0	<0.910	22.5	17.9
<b>13</b>	C <sub>9</sub>	100/25	0.6	0.945	-	11.4
	C <sub>9</sub>	100/50	1.8	0.930	-	15.0
	C <sub>7</sub>	100/60	3.2	0.925	-	22.0
	C <sub>7</sub>	100/40	2.6	0.931	-	25.4
	C <sub>8</sub>	100/100	3.1	0.923	-	15.3
<b>Commercial Ti/Mg Catalyst A</b>	C <sub>5</sub> /C <sub>8</sub>	100/100/100	1.4/0.6	0.938	5.7	4.0
	C <sub>5</sub> /C <sub>4</sub>	100/100/30	2.0/1.4	0.928	7.7	14.0
	C <sub>5</sub>	100/200	3.0	0.938	6.7	-
<b>Commercial Ti/Mg Catalyst B</b>	C <sub>4</sub>	100/20	2.6	0.940	-	29.0
	C <sub>5</sub>	100/20	2.0	0.942	27.0	-
	C <sub>8</sub>	100/20	0.3	0.950	-	6.4
<b>Commercial Cr Catalyst C</b>	C <sub>5</sub>	85/300	2.0	0.942	3.4	-
	C <sub>6</sub>	85/300	1.8	0.942	-	3.3
<b>(<i>n</i>BuCp)<sub>2</sub> ZrCl<sub>2</sub></b>	C <sub>5</sub>	95/50	8.2	0.918	47.2	-
<b>Cp<sub>2</sub>ZrCl<sub>2</sub></b>	C <sub>5</sub>	75/50	5.2	0.925	25.0	-

By comparing the CIRs obtained with catalysts 1 to 11 prepared by chemical activation of the support, it can be seen that some catalysts do not incorporate comonomer well. These catalysts, most notably 6, 9 as well as commercial catalyst A and the chromium catalyst C, have CIRs around 0.05 (i.e. 5% incorporation). Some of the other catalysts in

this group showed only slightly improved comonomer incorporation ratios of about 0.1 to 0.15, depending on the comonomer. However, when comparing these with catalysts 12 and 13, similarly prepared using both chemical and physical activation of the support, it can be seen that the comonomer incorporation of this catalyst is much improved. Incorporation of 1-pentene of up to about 30% and that for the less reactive and more bulky 1-octene and 1-nonene of up to almost 20% were achieved which compare well with the 1-pentene incorporation observed with commercial catalyst B and the  $\text{Cp}_2\text{ZrCl}_2$  metallocene.

Catalysts having low comonomer incorporation have densities mostly above  $0.930 \text{ g/cm}^3$ , whereas the terpolymers obtained with catalyst 12 achieved densities below  $0.90 \text{ g/cm}^3$ . Although the densities, taken on face value, seem in many instances not to be in agreement with the measured composition, it will be shown in later discussions in Chapters 6 and 7 that the properties of different co- and terpolymers are very much in line with what is expected from the ethylene / comonomer ratios used.

Catalyst 13 was also tested for homopolymerization of different  $\alpha$ -olefins. For these tests, 10 ml of the particular  $\alpha$ -olefin was placed in an insulated vial equipped with a magnetic stirrer and temperature probe. A mixture of 0.003 g of catalyst and 4 ml of a 1.0% solution of tri-ethyl aluminum, prereacted for 5 minutes, was added to this vial and the increase in temperature monitored against reaction time. The increase in reaction temperature against reaction time for 3 different olefins are shown in Figure 5.7.

As expected from its higher reactivity and the fact that its molar content is higher, it can be seen that the exotherm obtained from 1-hexene is the highest and for the same reason, that of 1-nonene is the lowest. The fact that homopolymerization of high  $\alpha$ -olefins could be accomplished with this catalyst indicates that it has a substantial amount of "open" active sites capable of incorporating these olefins into a polymer chain. As a rule, Ziegler-Natta catalysts have a range of different active sites which is responsible for the relatively wide molecular weight distribution of polymers produced.

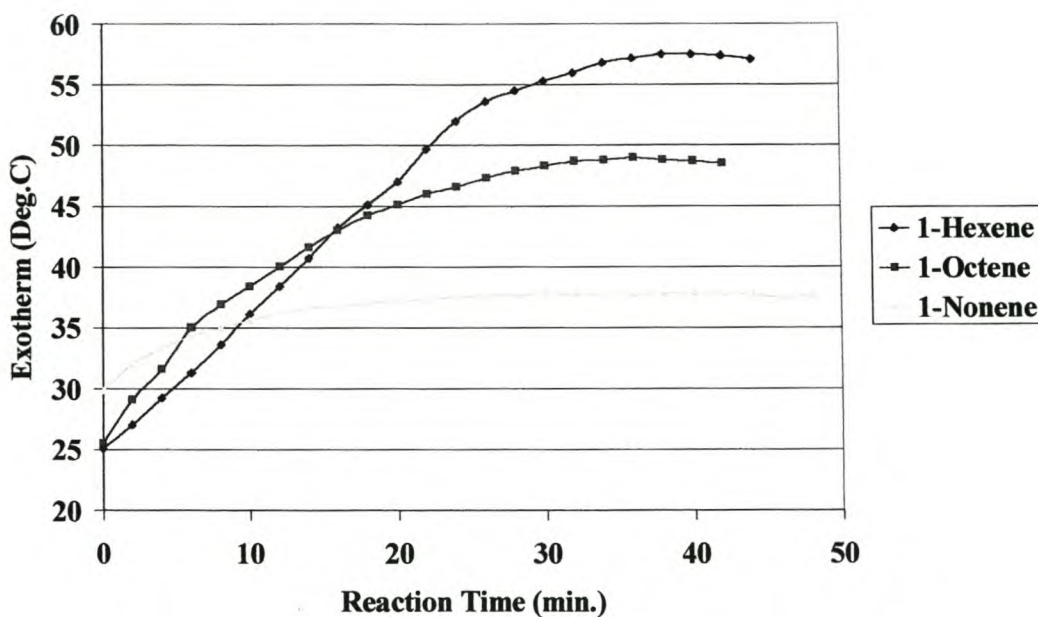


**Figure 5.7. Temperature Profiles for Different  $\alpha$ -Olefin Homopolymerizations**

During studies of the effects of different compounds present in the Sasol Fischer-Tropsch  $\alpha$ -olefins, alkynes and cyclic and linear 1,3 and 1,4 dienes were found to be highly deactivating towards the “open”, unprotected active sites. When a 1,3 diene for example is inserted, the second double bond of this molecule can easily coordinate with the metal center but insertion is impossible. This effectively deactivate the active site. For a 1,4 diene, the insertion of the second double bond will result in a three-membered ring to be built in the polymer chain. The concentration of these species, if formed, were too low to detect. This deactivation by the 1,3 and 1,4 dienes resulted in ethylene / octene copolymers containing low amounts of 1-octene when reactions were carried out using low amounts of catalyst. These compounds can therefore be used to selectively deactivate the “open” sites to obtain an estimate of the catalyst’s design. Using very pure 1-octene, ethylene / 1-octene copolymers were produced with an amount of catalyst sufficiently high to incorporate almost all of the 100 g 1-octene and 100 g ethylene present in the feed into the copolymer over a period of 1 hour to ensure a CIR of almost 100. With an amount of 0.3 mmole titanium, 96% of the 1-octene was incorporated. A series of experiments was then carried out where the 1-octene was spiked using different amounts of cyclopentadiene, including amounts in excess and amount less than the 0.3 mmole

titanium. The copolymer yields obtained in this series of experiments are shown in Figure 5.8.

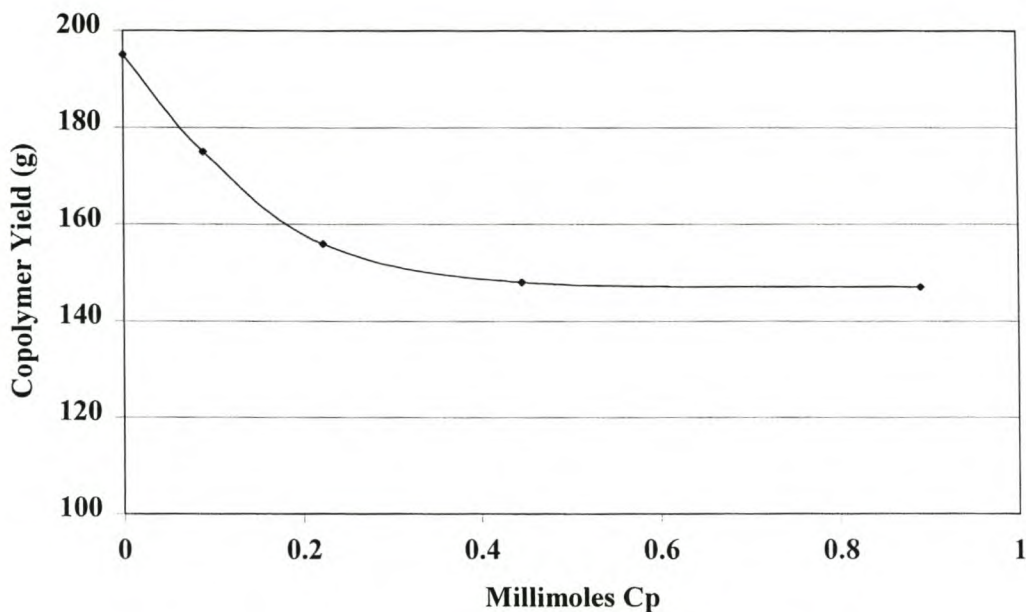


**Figure 5.8. Ethylene / 1-Octene Copolymer Yields Obtained Using Different Amounts of Cyclopentadiene (Cp) as Catalyst Deactivator**

It can be seen from Figure 5.8 that even with a large amount of Cp present catalyst activity was decreased to about 75%, but the reactor pressure at the end of the reaction was low, indicating almost complete consumption of ethylene. This activity therefore implies that only about 50% of the octene present in the reactor was converted to polymer. By decreasing the amount of Cp from 0.89 to about 0.3 mmoles, no substantial increase in activity was observed. At Cp levels below 250 ppm (0.222 mmole), enough active sites capable of polymerizing 1-octene become available to result in 98% conversion at zero Cp spiking. The straight lines obtained by extrapolating from zero and 0.89 respectively intersect at a Cp content of about 0.2 mmoles. This indicates that at levels higher than this, most of the active sites capable of reacting with Cp are deactivated although the sites remaining are not so protected as to prevent consumption of 50% of the 1-octene. From these observations it can thus be concluded that one third of the active sites of catalyst 13 are “open” and easily deactivated, while the rest are more protected, although not as much that low density polymers could not be obtained. These active sites are expected to consist of a

distribution of less protected and more protected Ti atoms. However, no further deactivating compounds were used to evaluate this effect in detail.

A further observation made during the investigation of the effects of small amounts of other olefins (branched olefins, dienes, cyclic olefins) typically found in Fischer-Tropsch derived olefins was that an increase in molecular weight accompanied the catalyst deactivation by these olefins. Copolymerization of ethylene with 1-octene containing different levels of these other olefins yielded polymers having different molecular weights. The higher the levels of these deactivating compounds, the higher the molecular weight became. Because the deactivating species target the unprotected active sites, which produce the lower molecular weight fraction, the molecular weight of the copolymer prepared using a comonomer which contains these deactivating olefins were expected to increase as the “open” sites do not fully participate in the copolymerization. This reasoning is also supported by the decreased capability of the catalyst to incorporate 1-octene in the copolymer when these deactivating olefins are present in the reaction mixture.

It can thus be stated that the effect of these deactivating compounds is twofold: (a) The deactivating compounds target the unprotected active sites which are responsible for producing the high comonomer content copolymer fraction and (b) restricts transfer reactions to produce the lower molecular weight fraction polymers. The presence of these deactivating olefins will necessitate a decreased ethylene / comonomer feed ratio and an increased hydrogen concentration if a copolymer having a certain density and molecular weight is required.

However, even with these species present in the comonomers used to obtain CIRs for catalysts 12 and 13 as presented in Table 5.4, it can be seen that comonomer incorporation was still high. Therefore, from the discussions above it should be appreciated that catalysts with both high activity as well as high comonomer incorporation could be prepared which are capable of producing linear low density polyethylene using  $\alpha$ -olefins containing a wide variety of deactivating olefins typically produced in Sasol’s Fischer-Tropsch process.



### 5.3.4 PREPOLYMERIZATION

For slurry and solution polymerization reactions, heat transfer using catalysts with high activities does not pose any problems. For gas phase processes, however, hot spots can easily develop if active sites are not distributed properly. If the temperature resulting from such a localized thermal runaway reaction occurs around a catalyst particle and the temperature increases above the melting temperature of the formed polymer, other particles will stick to it, and in so doing, thermally isolate the particle. The temperature of such a particle will therefore increase even further while it continues growing by picking up other growing polymer particles with its sticky, molten surface. The end result of such a reaction is the presence of large “eggs” of charred polymer. When a lower density copolymer is prepared, its melting temperature is correspondingly decreased and even greater care has to be taken to prevent the formation of hot-spots.

To be able to use the same catalyst for slurry, solution and gas-phase copolymerization reactions, the active centers of high activity catalysts should thus be “diluted”. This was managed by means of two methods. In the first, the amount of catalyst 12 needed for a specific reaction was mixed with a thoroughly washed and dried polyethylene copolymer powder prepared in a slurry reaction prior to its use as catalyst diluent. This mixture was then ground together with tri-ethyl aluminum and the resulting moist powder was introduced into the reactor followed by the immediate introduction of the monomers. It is desirable that the copolymer used as diluent should be similar to the one being prepared in the gas phase, but in all the cases described in Table 5.5 below, an ethylene / 1-pentene copolymer having a 0.92 density was used. The second method entails a 30 minute slurry copolymerization of ethylene and 1-pentene to low conversions, typically 1:5 to 1:20 catalyst:copolymer ratio. The prepolymer prepared for this investigation was prepared according to the usual heptane slurry copolymerization techniques at 80°C wherein 1 g of catalyst 12 was contacted for 5 minutes with 10 ml of a 10% solution of tri-ethyl aluminum in heptane before 15 g ethylene together with 3 g 1-pentene was introduced into the reactor and the mixture reacted for 30 minutes. The resulting slurry was then drained into, washed and filtered by means of a device connected to the bottom of the reactor

after which it was sealed and transferred to the glovebox where the prepolymerized catalyst was dried. This catalyst, similar to the polymer diluted catalyst, was also reacted with 1 ml tri-ethyl aluminum prior to being introduced into the gas-phase reactor. Results of terpolymerization reactions conducted with these two types of catalysts are presented in Table 5.5.

**Table 5.5. Gas-Phase Terpolymerization of Ethylene and Two Higher  $\alpha$ -Olefins Using Modified Catalysts**

PE Copo / Catalyst 12	Amount C <sub>2</sub> (g)	Amount C <sub>5</sub> (g)	C <sub>x</sub>		Yield (g)	Density (g/cm <sup>3</sup> )	Activity (kg/g Ti)
			Type	Amount (g)			
1 / 0.07	120	9	C <sub>6</sub>	9	134	0.922	27.3
1 / 0.07	113	16	C <sub>6</sub>	6	135	0.930	27.5
1 / 0.07	113	12	C <sub>6</sub>	10	105	0.917	21.4
1 / 0.07	120	12	C <sub>8</sub>	12	118	0.919	24.1
<b>Prepolymer (g)</b>							
1	120	8	C <sub>8</sub>	16	75	0.925	15.3
1	100	14	C <sub>4</sub>	6	80	0.920	16.3
1	100	10	C <sub>4</sub>	10	90	0.927	18.4

From Table 5.5 it can be seen that catalyst activity based on the amount of titanium was substantially decreased by dilution and prepolymerization. In none of the cases were hot spots observed, which indicates that active centers were successfully "diluted" so that localized heat build-up and the consequent thermal runaway reactions were prevented. It can also be seen from the comonomer incorporation ratios and densities that these modifications were not detrimental to the availability of the active sites of these catalysts to accept bulky comonomers.

## 5.4 POLYPROPYLENE CATALYSTS

Control over the monomer placement to yield stereospecific polymers was shown to result from control by the active site itself (enantiomorphic control) [20]. Corradini *et al* [21] confirmed this based on  $^{13}\text{C}$  NMR analysis of isotactic polypropylene with low amounts of copolymerized ethylene. If steric control was due to the chirality of the last inserted monomer, insertion of a propylene unit following insertion of an achiral ethylene molecule would be non-stereospecific. By using a catalyst not specifically prepared to have chiral active sites, low isotacticity will result.

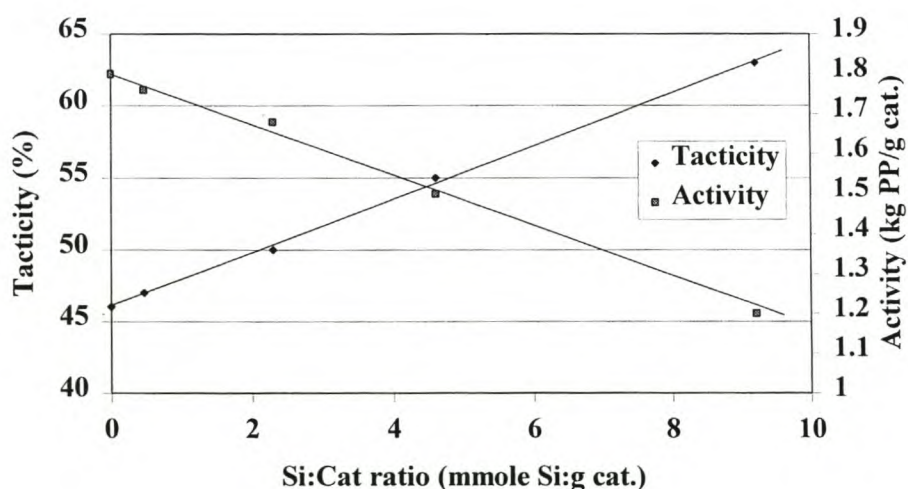


**Figure 5.9. Tacticity and Activity of the Non-Stereospecific Catalyst A as Function of External Modifier Content**

It is known that  $\text{MgCl}_2$ -supported catalysts require the use of both internal and external electron donors [22] to obtain high isotacticity without decreasing catalyst activity too much [23]. The external donor, usually a silane compound, is added to the catalyst together with the alkyl aluminum compound while the internal donor is introduced during catalyst preparation. Aspecific catalyst A was evaluated in terms of activity and tacticity of polypropylene produced, as a function of the amount of diisopropyl dimethoxy silane external modifier used. The results of the

homopolymerization reactions conducted in heptane slurry at 85°C are presented in Figure 5.9.

From Figure 5.9 it can be seen that tacticity of the polymer increases at the expense of catalyst activity when the amount of external modifier is increased. However, even at a very high external modifier content of 1.6 g silane per gram catalyst (9.2 mmole Si:g cat), polymer tacticity remains low. The fact that a partially isotactic polymer was prepared with the non-stereospecific catalyst A is an indication that chiral active sites are present on this catalyst. By selective poisoning or modification of the non-stereospecific sites, it should in principle be possible to increase the stereospecificity of this catalyst. By reacting this catalyst with di-iso butyl phthalate followed by a further  $\text{TiCl}_4$  treatment, catalyst stereospecificity was indeed increased to about 90% when only 1.4 mmole silane per gram catalyst was used as external modifier. Thus, the introduction of the phthalate resulted in the modification of the active sites in such a manner as to force mainly isotactic placement of the propylene units during polymerization.

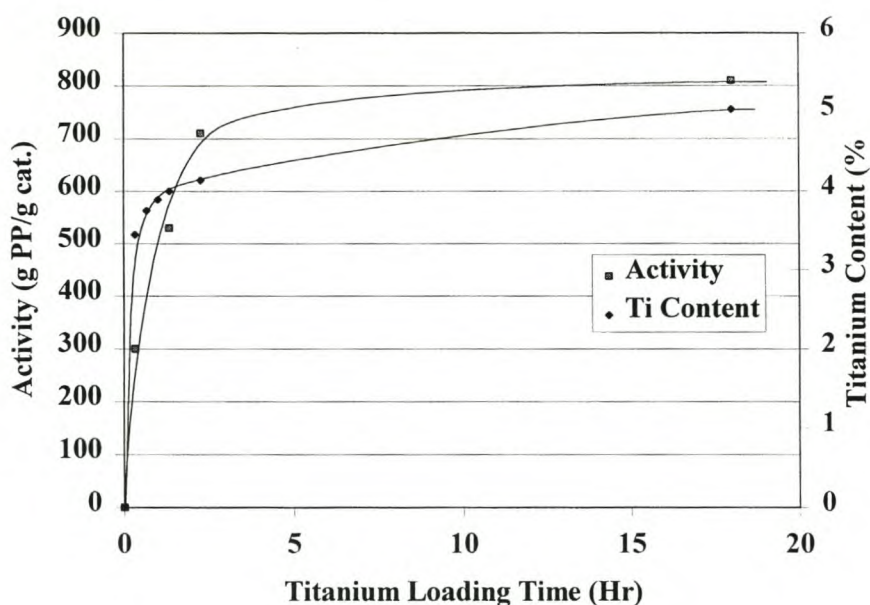


**Figure 5.10. Effect of Titanium Loading Time on Catalyst Activity and Titanium Content**

This confirms that the preparation of a catalyst suitable for stereoregular polymers should include the introduction of an electron donor during support preparation, before the final  $\text{TiCl}_4$  treatment, to yield a catalyst containing mainly chiral active sites.

The catalysts obtained by reacting the ethyl benzoate treated complex with  $\text{TiCl}_4$  at  $50^\circ\text{C}$  for different periods were used to polymerize propylene in order to determine activities. These catalysts were analyzed and their titanium content was found to increase to a limiting value of about 5%.

As expected, increased titanium loading (same support) gave increased activities. It can further be seen from Figure 5.10 that neither activity nor titanium content increase substantially after about 2 hours reaction time.

Following these initial practice runs, catalysts suitable for use as slurry and gas-phase copolymerization of propylene with higher  $\alpha$ -olefins were prepared. The different methods, and polymers prepared therefrom, were previously described [5,9,24].

Three different methods were used. The first involved dissolution of anhydrous  $\text{MgCl}_2$  in a mixture of dibutyl ether (DBE) and ethanol. The complex was then dried and treated in three separate steps with  $\text{TiCl}_4$ , di-iso butyl phthalate (DIBP) and again with  $\text{TiCl}_4$  to yield the final catalyst. In the second method the dried complex was first reacted with tri-ethyl aluminum, then treated with a phthalate, followed by  $\text{TiCl}_4$  after which the phthalate and  $\text{TiCl}_4$  treatments were repeated. (In one preparation the tri-ethyl aluminum treatment was omitted.) In the third method, the anhydrous  $\text{MgCl}_2$  was dissolved in a mixture of an ether and a single or two different alcohols, the latter carefully removed to prevent crystallization, and then treated with tri-ethyl aluminum. To this compound was added ethyl benzoate and this was followed by a  $\text{TiCl}_4$  treatment to yield the catalyst. In all the preparation methods, the solid compounds were washed thoroughly after the tri-ethyl aluminum and  $\text{TiCl}_4$  treatments. A summary of the conditions used to prepare the different catalysts is presented in Table 5.6.

**Table 5.6. Summary of Different Preparation Methods for Catalysts Suitable for Isospecific Copolymerization of Propylene and Higher  $\alpha$ -Olefins**

Catalyst	Pre-activation	TEA	Internal Donor and Titanium Loading Steps				Tacticity (%)	Activity (kg PP/g cat)
	Compounds		Donor	TiCl <sub>4</sub>	Donor	TiCl <sub>4</sub>		
14	DBE/EtOH	No	-	Yes	DIBP	Yes	89	1.5
15	DPE/EtOH	Yes	DNBP	Yes	EB	Yes	93	0.9
16	DBE/EtOH	Yes	EB	Yes	-	-	90	1.6
17	DPE/EtOH/PrOH	Yes	EB	Yes	-	-	91	1.8

BPE : Di-pentyl ether, EtOH : Ethanol, DNBP : Di-*n*-butyl phthalate, PrOH : *l*-Propanol

From Table 5.6 it can be seen that all of the catalysts produced propylene homopolymers with isotacticities of about 90%. All homopolymerizations were carried out using 1.4 mmole of di-isopropyl dimethoxy silane as external modifier. An optimization of the type and amount of external modifier used in order to obtain the maximum tacticity was not investigated. It can be seen that catalyst 15 prepared by introducing two donors gave the highest tacticity but catalyst activity per gram of catalyst was lower. If one considers the action of the donor compound used [15], this is not unexpected because the donors selectively poison aspecific sites, resulting in a decreased amount of active titanium and thus a decreased activity. The active sites remaining have higher stereospecificities. It therefore seems that the double treatment of the catalyst with a donor compound poisoned or inactivated more of the aspecific sites than obtained from a single treatment.

#### 5.4.1 KINETICS

A comparative study on the kinetics of different catalysts has been presented [25]. The yield / time profiles for propylene / 1-pentene copolymers obtained for reactions conducted in heptane slurry at 85°C comparing catalyst 14 with a commercial  $\delta$ -TiCl<sub>3</sub> obtained from Akzo are presented in Figure 5.11 below. Determining the derivative of the yield vs. time curves gave the rate / time profiles for the different catalysts. For these reactions, a fixed amount of propylene and 1-pentene was introduced into the reactor at the start of the reaction and the pressure was allowed to decrease during the course of the reaction. It can be seen that under these conditions, the total productivity of the Akzo catalyst is about half that of the supported catalyst.

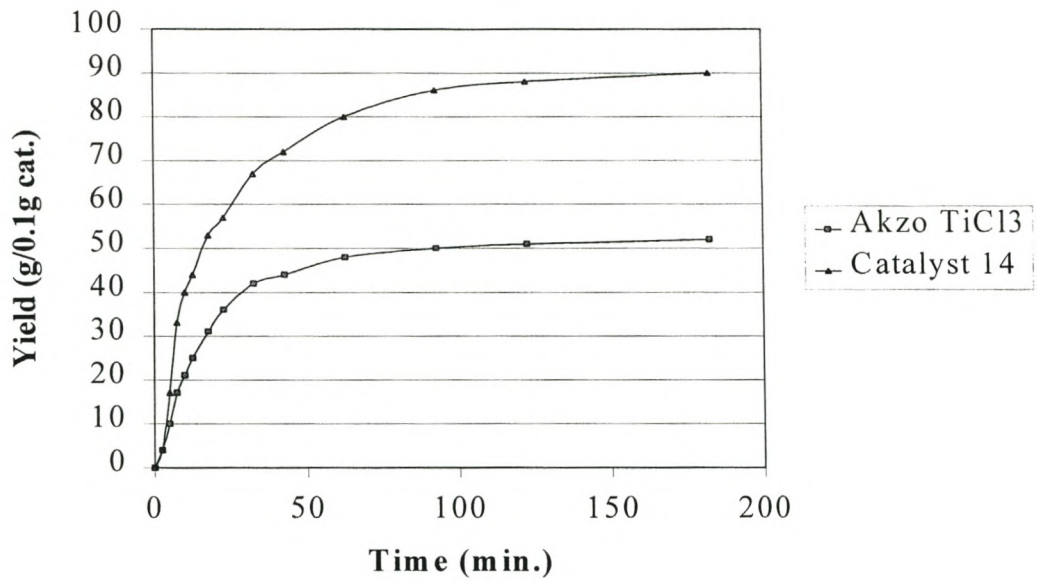


**Figure 5.11. Increase in Copolymer Yield with Reaction Time Using Different Catalysts**

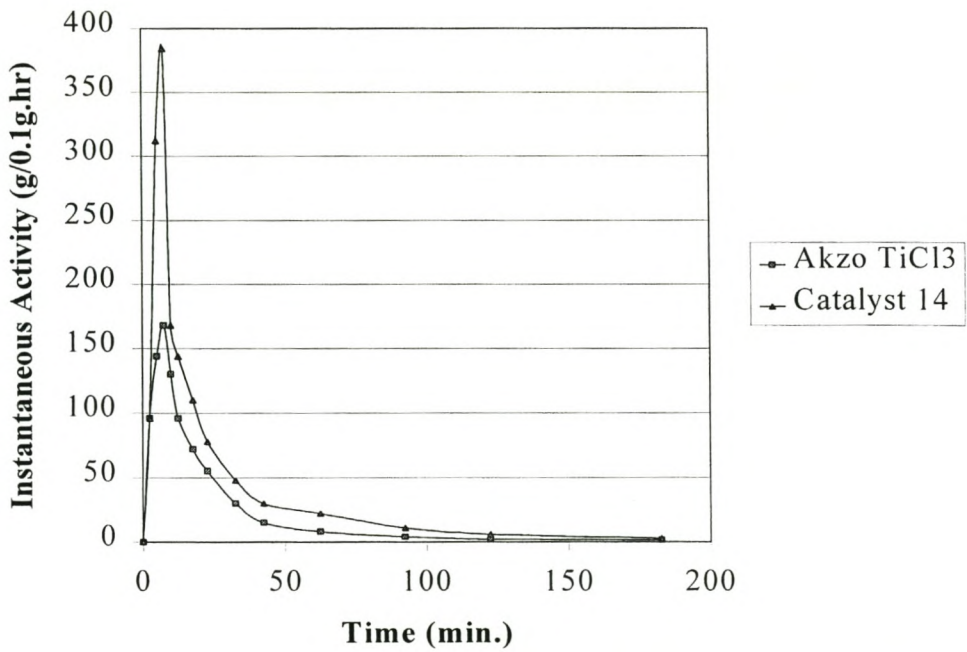


**Figure 5.12. Rate / Time Profiles for Copolymerizations Using Different Catalysts**

The instantaneous activities of the different catalysts (Figure 5.12) reveals that the activities of these catalysts are very different. During the first 10 to 15 minutes the activity of catalyst 14 is almost 3 times higher than that of the Akzo catalyst and after this initial high activity reached during the acceleration period, it rapidly drops to closely follow the decay of the Akzo catalyst. This very high activity of catalyst 14 suggests that it is not suitable for gas phase reactions and should preferably be diluted, eg. by methods of polymer dilution and prepolymerization as described for the polyethylene catalysts.

#### 5.4.2 COMONOMER INCORPORATION

Samples taken at different times during a propylene / 1-pentene copolymerization reaction revealed a change in the 1-pentene concentration as the reaction progresses. This can be ascribed to the fact that the total amounts of propylene and 1-pentene were introduced at the beginning of the reaction and both monomers' concentrations were allowed to decrease throughout the polymerization reaction. As the propylene concentration decreases, 1-pentene has a statistically better chance of being incorporated, resulting in an increased 1-pentene content at increased reaction times.

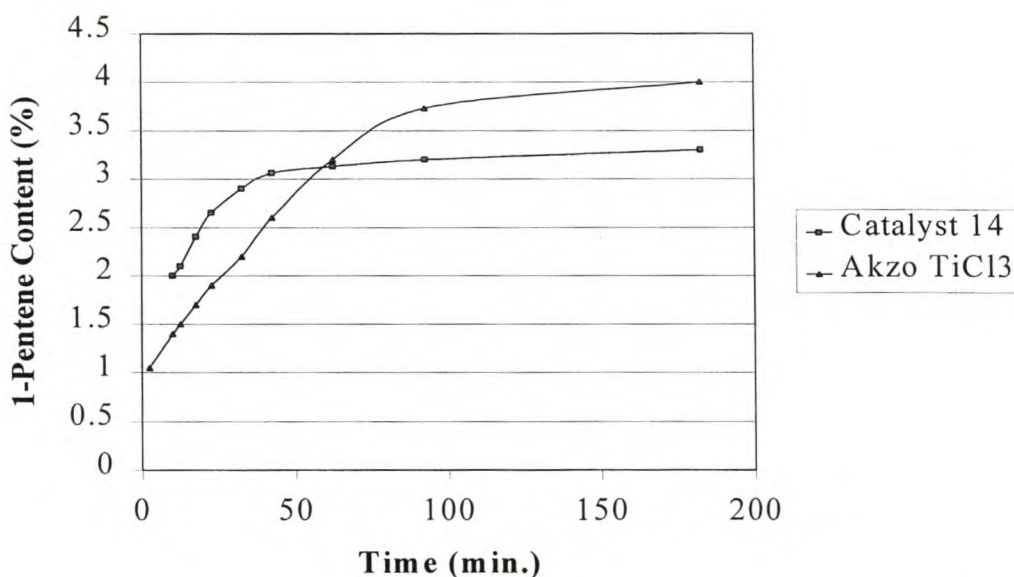


**Figure 5.13. Change in 1-Pentene Concentration with Time Using Different Catalysts**



It was noticed by comparing the 1-pentene concentrations shown in Figure 5.13 with the polymer yields presented in Figure 5.11 that catalyst 14 incorporates up to 60% of the available 1-pentene whilst propylene conversion was over 90 %. It can further be seen that about 70% of the available 1-pentene is incorporated into the copolymer using the Akzo catalyst even though 50% of the propylene remains unreacted after 3 hours. Although the comonomer incorporation of these two catalysts are very similar, the overall activity of the Akzo is much lower.

The ease with which the different catalysts accept bulky monomers (CIR) can be calculated from Equation 5.1 by comparing the amount of comonomer observed in the propylene copolymer to the amounts of monomers fed to the reactor. Results of slurry copolymerization reactions with different catalysts are presented in Table 5.7.

**Table 5.7. Comonomer Incorporation Ratios of Different Catalysts Used for Co- and Terpolymerization of Propylene with Higher  $\alpha$ -Olefins**

Catalyst	Comonomers	Monomer Ratio (C <sub>3</sub> /C <sub>5</sub> /C <sub>x</sub> )	Composition (%)	CIR C <sub>5</sub>	CIR C <sub>x2</sub>
14	C <sub>5</sub> /C <sub>10</sub>	100/15/30	2.0/0.9	24.6	11.8
	C <sub>9</sub>	100/50	2.0	-	12.6
	C <sub>9</sub>	100/75	3.0	-	15.0
	C <sub>7</sub>	100/25	2.0	-	20.7
	C <sub>7</sub>	100/60	4.0	-	19.5
15	C <sub>5</sub>	100/50	3.1	13.4	-
17	C <sub>5</sub> /C <sub>2</sub>	100/30/4	4.0/2.0	26.9	80.6
	C <sub>5</sub> /C <sub>2</sub>	100/20/1	2.5/1.0	23.6	75.6
	C <sub>5</sub> /C <sub>2</sub>	100/20/3	2.5/3.0	24.2	77.6

By comparing the 1-pentene incorporations in Table 5.7, calculated for catalysts 14 and 17, with that of catalyst 15 it can be seen that the latter catalyst has a response towards 1-pentene almost half that of the other two catalysts. In Table 5.6 it was shown that catalyst 15 produced a propylene homopolymer having the highest isotactic content, but with the lowest activity. As discussed previously, the double treatment of the catalyst with the donor compounds probably deactivated more of the aspecific sites than with a single treatment. These compounds will preferentially poison or block the open, unprotected sites, which incidentally are also those not capable of rejecting a comonomer with the wrong orientation for isotactic polymerization. The more protected sites, capable of exerting control over the orientation of the approaching are only

poisoned [26] or blocked [27] by high levels of these donor compounds, leading to a decrease in activity. It may thus be realised that by poisoning the unprotected active sites, the relative ratio between these and the protected, highly isotactic sites decrease. The less stereospecific sites are however, more capable of accepting bulky comonomers in the coordination complex and thus by decreasing the amount of less-stereospecific active sites, the overall capability of the catalyst to incorporate comonomer will thus be decreased.

## 5.5 CONCLUSIONS

Sasol produces a wide variety of different  $\alpha$ -olefins and recently started to present these to polymer producers. In order to demonstrate the use of these  $\alpha$ -olefins as comonomers for ethylene and propylene copolymers, it was thus necessary to first investigate the preparation of catalysts having a combination of high activity, high comonomer incorporation and in the case of propylene copolymers, also sufficient stereospecificity.

It is known that by attaching  $\text{TiCl}_4$  to a support having large surface area, the population of accessible active sites are increased and hence the activity of the catalyst will be increased. In addition, protected active sites will incorporate the more bulky comonomers with difficulty.

Different methods to produce catalysts conforming to these requirements were investigated. The preparation of the support was deemed important and both chemical and chemical / mechanical activation of the support was investigated.

The amount of alcohol used during the support activation step was found to be directly related to the activity of the final catalyst. It was also observed that the time allowed for alkylation of the active centers affected overall catalyst activity and that an optimum alkylation time existed. No clear correlation between total titanium content and activity was observed. From this observation it is believed that accessibility rather than the amount of the titanium species present on the support, influences overall catalyst activity.

The degree to which active sites are protected was evaluated from the amount of comonomer present in the final copolymer based on the amount added to the reaction. A combination of chemical and mechanical activation of the support was found to produce catalysts capable of incorporating the highest amounts of comonomer.

Cyclic and linear 1,3 and 1,4 dienes present in the Fischer-Tropsch  $\alpha$ -olefins were found to be detrimental to both catalyst activity and 1-octene incorporation during

copolymerization reactions. It was shown that catalysts capable of producing low density copolymers from the Fischer-Tropsch olefins containing these deactivating species, could be prepared. Cyclopentadiene was consequently used to selectively deactivate unprotected active catalyst sites in order to determine the ratio between protected and "open" active sites on catalysts having high activity and comonomer incorporation.

The high activity catalysts are not suitable for gas-phase copolymerization because of the formation of hot-spots in the reactor. These catalysts were consequently "diluted" by dispersion in a pre-formed polymer powder or by prepolymerization. It was observed that catalyst activity based on titanium content was substantially decreased, but comonomer incorporation was not.

Catalysts for producing crystalline polypropylene should not only have accessible active sites capable of incorporating the higher  $\alpha$ -olefins in the polypropylene backbone, but should also be capable of exerting control over the orientation of the monomers being inserted. It is known that such stereospecific catalysts require the presence of both an internal and external electron donor to produce highly isotactic polymers. The external donor compound can be easily changed as it is introduced together with the catalyst before polymerization. It was shown that isotacticity increased linearly with an increase in external modifier at the expense of catalyst activity. The external donor was thus kept constant and the effect of changes to the internal donor investigated. The internal donor was introduced during catalyst preparation. It was shown that a double treatment of the support or catalyst before the final  $\text{TiCl}_4$  fixation was effective at increasing stereospecificity. The less stereospecific sites are however, more capable of accepting bulky comonomers in the coordination complex. Thus, by decreasing the amount of less-stereospecific active sites, the overall capability of the catalyst to incorporate comonomer was decreased.

## 5.6 REFERENCES

1. Tait P.J.T., Berry I.G., *Monoalkene Polymerization: Copolymerization in Comprehensive Polymer Science*, Sir Geoffrey Allen, Chairman Ed. Board, Pergamon Press, **4**(4) 575 (1989)
2. Kissin Y.V., *Stereospecificity of Heterogeneous Ziegler-Natta Catalysts in Isospecific Polymerization of Olefins with Heterogeneous Ziegler-Natta Catalysts*, Springer-Verlag, New York, **I-5**, 67 (1985)
3. Tincul I., Joubert D.J., Potgieter I.H., *PCT Int. Appl. W.O. 97/45460*, Sasol Technology R&D, (1997)
4. Tincul I., Joubert D.J., Potgieter I.H., *PCT Int. Appl. WO 97/45454*, Sasol Technology R&D, Jun. 2 (1997)
5. Joubert D.J., Potgieter I.H., Tincul I. Young D.A., *PCT/GB99/00241*, Sasol Technology R&D, Jan 25 (1999)
6. Joubert D.J., Tincul I. Young D.A., *RSA Appl. 98/6441*, Sasol Technology R&D, Jul. 20 (1999)
7. Joubert D.J., Tincul I., Moss J.R., *Inorganic '99 Conf. Proc.*, 49 (1999)
8. Joubert D.J., Tincul I., van Reenen A.J., *Unesco Conf. Proc.*, Mar. (1999)
9. Joubert D.J., Potgieter A.H., Potgieter I.H., Tincul I., *PCT Int. Appl. WO99/01485*, Sasol Technology R&D, (1998)
10. Tornqvist E.G.M., Seelback C.W., Langer A.W., *U.S. Patent 3,128,252*, Esso Research and Engineering, Apr. 7, (1964)
11. Tornqvist E.G.M., Langer A.W., *U.S. Patent 3,032,510*, Esso Research and Engineering, (1962)
12. Welch M.B., Hsieh H.L., *Olefin Polymerization Catalyst Technology in Handbook of Polyolefins*, Vasile C., Seymour R.B., Eds., Marcel Dekker, New York, 21 (1993)
13. Sinn H., Kaminsky W., *Adv. Organometallic Chem.*, **18**, 99 (1980)
14. Diedrich B., *Second Generation Ziegler Polyethylene Processes in Polymer Preprints*, ACS, Washington, Vol. 16, **1**, 316 (1975)
15. Tait P.J.T., *Monoalkene Polymerization: Ziegler-Natta and Transition Metal Catalysts in Comprehensive Polymer Science*, Sir Geoffrey Allen, Chairman - Ed. Board, Pergamon Press, **4**(1) 1(1989)

## CHAPTER 6

### ETHYLENE COPOLYMERS

#### 6.1 INTRODUCTION

Each discovery in the development of polyethylene introduced a new member to the polyethylene family with some unique properties, which made it suitable for certain applications. However, the continued demands placed on the polymer as it was introduced into new, and sometimes uncompromising environments kept polyethylene research areas bustling with activity.

LDPE produced by the free-radical process [1,2] was too soft for some applications and the high pressures used for its production were undesirable. HDPE produced at lower pressures using a silica-supported chromium oxide catalyst in the Phillips process [3] or at even lower pressures using the Ziegler catalyst [4,5] generates a more crystalline material with improved properties such as tensile strength and stiffness. This opened up new markets, but the low temperature flex, impact and optical properties were adversely affected by the new processes. LLDPE, first produced in the gas-phase in the Unipol process [6,7], bridged the gap between LDPE and HDPE through the controlled decrease in density as a result of comonomer units incorporated into the polyethylene backbone. This controlled, short-chain branching gave this new member of the family its unique combination of high tear and impact strength, environmental stress crack resistance and barrier properties. The properties of LLDPE depend mainly on the amount, but also on the type of comonomer applied. Initially this comonomer was 1-butene but later also 1-hexene and 1-octene were used. However, the inter- and intramolecular comonomer distribution, inherent properties resulting from the multi-active center Ziegler-Natta catalysts used, were not homogeneous, resulting in fractions of differing solubilities and melting temperatures. Single-site catalysts gave copolymers with very homogeneous comonomer

distributions resulting in highly regular chains, the properties of which can be tightly controlled. Polymers ranging from very low densities up through the low, medium and high density range can be prepared by these catalysts.

All of the above-mentioned polymers are produced by different companies. These companies rely on their own catalysts and processes to produce polymers with unique properties which may give them a competitive advantage over other companies. It is clear that the role of the comonomer on polymer properties has been very much neglected in the past. Sasol's Fischer-Tropsch oil-from-coal process (Figure 6.1), produces many linear and branched  $\alpha$ -olefins which could be useful as comonomers. These can be isolated from the Fischer-Tropsch stream by a relatively cheap refinery operation. Unique monomers include the odd-numbered olefins such as 1-pentene, 1-heptene and 1-nonene as well as the branched olefins 3-methyl-1-butene, 3-methyl-1-pentene and 4-methyl-1-pentene to name but a few.

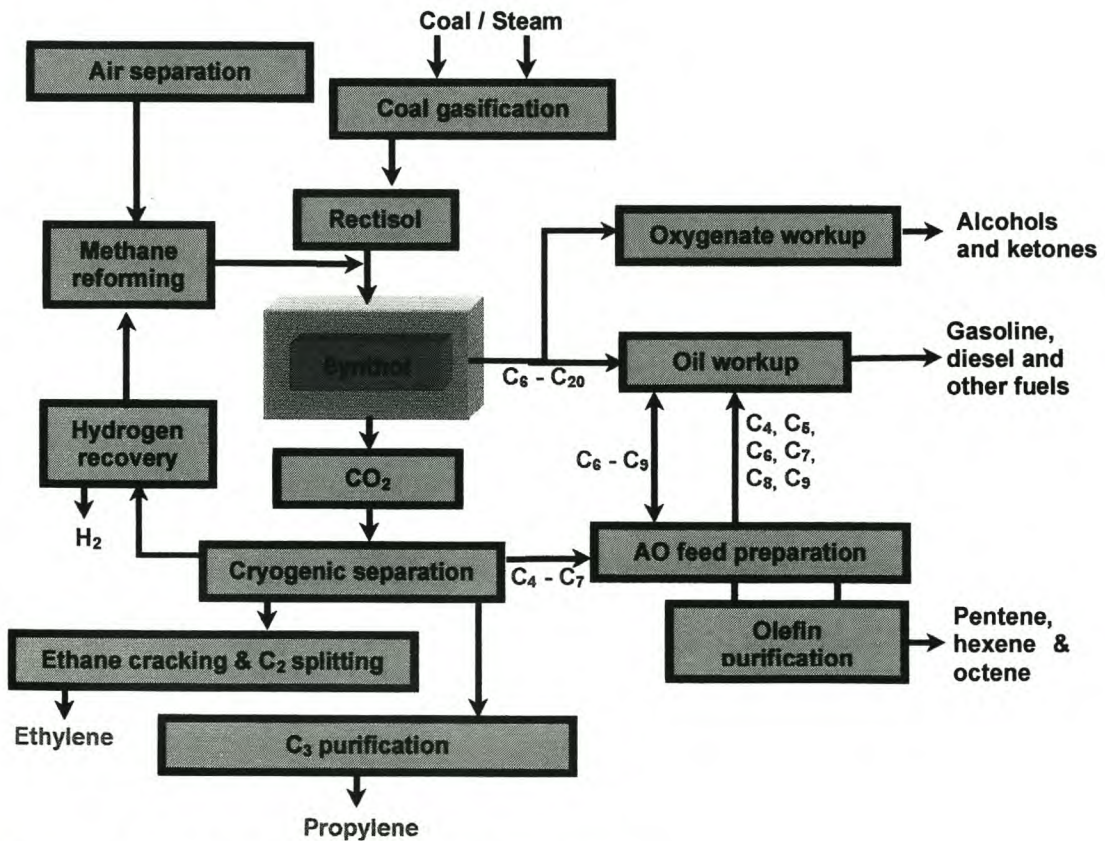


Figure 6.1. Sasol Fischer-Tropsch Process

The different types of olefins obtained from the Fischer-Tropsch process are shown in Figure 6.2. Currently, Sasol has existing capacity for producing ethylene (400 kt/a), propylene (250 kt/a), 1-pentene (70 kt/a), 1-hexene (100 kt/a) and 1-octene (50 kt/a), but additional capacity (normal alpha in Figure 6.2) still exist. In addition, other branched and internal olefins are also present.

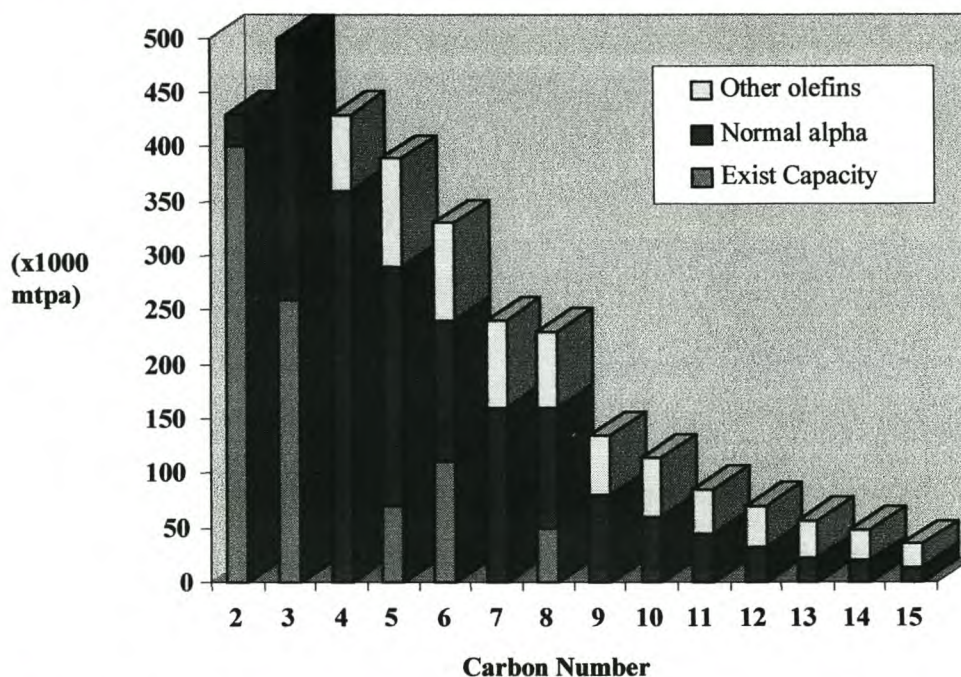


Figure 6.2. Olefins Obtained from the Fischer-Tropsch Process

Table 6.1. Comparison Between LLDPE Grades of Similar Density Containing Different Comonomers

	1-Butene	1-Hexene	1-Octene
Density (g/cm <sup>3</sup> )	0.918	0.918	0.919
Melt Flow Index (dg/min.)	1.0	1.0	1.0
Dart Impact (g)	150	250	350
Puncture energy (J/mm)	70	85	61
Tensile Strength (MPa)			
MD	38	38	43
TD	31	32	34
Elongation at Break (%)			
MD	620	570	550
TD	760	790	660

The type of comonomer used has a substantial influence on copolymer properties, thereby introducing a further dimension by which polymer properties can be tailored.



In Table 6.1 film properties of different copolymers are compared [8]. It is believed that as the lengths of the side chains introduced into the polyethylene chains by higher  $\alpha$ -olefins increase, crystallization is progressively inhibited [8]. This increases the number of tie-molecules and hence produces a stronger product.

Light is scattered when passing between phases of different refractive indices; In polymers this can be detected as haze. Polyethylene, being semi-crystalline consists of crystalline and amorphous phases having room temperature densities of 1.00 and 0.855 g/cm<sup>3</sup> respectively [9]. Since the refractive index increases with increased density [10] it can be realized that large difference in densities between crystalline and amorphous phases will result in light scattering. By incorporating comonomer units in the polyethylene backbone, the density is decreased and the refractive indices become more equal. This results in less light-scattering and thus decreased haze of the copolymers. The larger  $\alpha$ -olefins are more effective at disrupting crystallinity and this effect will therefore be more pronounced with the higher  $\alpha$ -olefins. It should, however, be noted that with the heterogeneous copolymers, being in effect blends of polyethylene with ethylene /  $\alpha$ -olefin copolymers of varying composition, it was observed that at very high comonomer contents, phase separation was observed, resulting in a drastic *increase* in haziness.

When decisions are made by polymer producers to change to a different comonomer, the disruption to the production process should preferably be as small as possible to minimize investment costs. Changes related to the polymer itself should also not be too drastic as this will impact on the product portfolio and may make the production of some grades for well-established markets difficult to obtain. In this regard, the impact on both the production process and polymer properties when changing between 1-butene, 1-hexene and 1-octene copolymers may have been too large to justify the investment costs. Smaller changes may prove to be much more valuable. A plant running on 1-hexene for example may be able to run 1-pentene or 1-heptene or be adapted to do so without the need for extensive changes, thereby increasing its product portfolio by operating as a swing plant. This was not an earlier option as these monomers were not previously available at competitive prices. It is in this light

that the study of the effect of comonomer incorporation into ethylene/ $\alpha$ -olefin copolymers was undertaken.

To highlight the benefits of using higher  $\alpha$ -olefins, an explanation of the relationship between monomer reactivity and feed ratios on addition probabilities is deemed necessary. For the linear  $\alpha$ -olefins, activity generally decreases with increasing chain length as can be seen from Table 6.2 [11].

**Table 6.2. Reactivities of  $\alpha$ -Olefins Relative to Propylene**

Monomer	C <sub>2</sub>	C <sub>3</sub>	C <sub>4</sub>	C <sub>5</sub>	C <sub>6</sub>	C <sub>10</sub>	C <sub>18</sub>	4MP1	3MP1	3MB1
Reactivity	20-8	1	0.62-0.22	0.45-0.2	0.36-0.16	0.28-0.12	0.15-0.1	0.15	0.048	0.06-0.024

The first order Markov model for ethylene (E) and a comonomer (C) can be used to estimate the preferred addition probabilities for any mole ratio  $x$  ( $= E/C$ ) [12] from equations:

$$P_{EC} = (1 + r_E \cdot x)^{-1} \quad (6.1)$$

$$P_{CE} = (1 + r_C \cdot x^{-1})^{-1} \quad (6.2)$$

The probability that comonomer C will add before ethylene to the growing chain end during copolymerization can be derived from equations 6.1 and 6.2 and is given by the expression:

$$P_C = (x + r_C) / x(1 + x \cdot r_E) \quad (6.3)$$

By substitution of the relative olefin reactivities  $r_E$  and  $r_C$  in this equation [11], it is possible to see that 1-butene will add more aggressively to the growing chain end than for example 1-decene. It is evident from the above that clustering of comonomer units, which results in heterogeneous comonomer distributions, decreased with decreased activity of the comonomer.

From Equation 6.1 it is easy to see that increased comonomer concentration in the feed ( $x$  small) will result in an increased probability of comonomer addition to the growing chain, thereby increasing the possibility of clustering. Use of higher  $\alpha$ -olefins as comonomer instead of lower  $\alpha$ -olefins, can be recognized from Equation 6.3. Thus, less of the higher  $\alpha$ -olefin is necessary to obtain the same density, which directly decreases the probability of clustering. Secondly, it can be deduced from Equation 6.3 that the decreased activity of the higher  $\alpha$ -olefins decreases the chance of addition to a growing chain during copolymerization with ethylene. This decreased clustering therefore results in better distribution of comonomer units along the chain, making them more effective at reducing polymer density. It is thus conceivable that it should, at least in principle, be possible to obtain lower densities with the higher  $\alpha$ -olefins than what is possible with the lower  $\alpha$ -olefins. It should be realized that this effect will only become significant at high comonomer concentrations. The probability of only a few branches clustering is small. This is however, only a theoretical assessment of the probability of different comonomers to cluster and obviously, not all effects have been accounted for in this discussion.

In this part of the study, the effects that different comonomers have on copolymer properties were investigated.

## 6.2 EXPERIMENTAL

*Slurry Polymerization.* A typical procedure for the slurry copolymerization of ethylene and an  $\alpha$ -olefin in the presence of a supported Ziegler-Natta catalyst is given below:

To a thoroughly cleaned 1 liter autoclave, fitted with stirring and heating/cooling facilities, and flushed with nitrogen was added 350 g heptane and the temperature set at 85°C. The catalyst system, comprising 0.03 g of supported catalyst 13, as described in Chapter 5, and 10 ml of a 10% solution of tri-ethyl aluminum in heptane, was added and reacted under stirring in the presence of 200 mg hydrogen for 5 minutes to activate the catalyst. Simultaneous flows of ethylene at a rate of 10 g/min. and the  $\alpha$ -olefin at the required ratio were started. After 10 minutes the ethylene and comonomer feeds were stopped and the reaction continued for another 50 minutes. The reactor was depressurized and the catalyst deactivated by the addition of 100 ml *iso*-propanol. The slurry was filtered and the polymer washed with acetone and dried under vacuum at 80°C.

*Polymerization using a metallocene catalyst.* A typical procedure for the solution copolymerization of ethylene and an  $\alpha$ -olefin in the presence of a metallocene catalyst, is given below:

Highly purified toluene (350 ml) was added to a 1-liter stainless steel reaction vessel provided with agitation and heated to 60°C. Under inert conditions,  $2 \times 10^{-3}$  mmole of the metallocene catalyst was reacted with 10 ml of a 30% solution of MAO in toluene and the reaction mixture transferred to the reactor in a gas tight syringe. Ethylene (100 g) was fed to the reactor at a rate of 2 g/min and at the same time the desired ratio of the comonomer were introduced over a period of 50 minutes. After a further period of 10 minutes the polymerization vessel was depressurized and the catalyst deactivated with *iso*-propanol. The resultant copolymer was filtered, washed with acetone and dried in a vacuum oven at 70°C for 24 hours.

$^{13}\text{C}$  NMR analyses were done at  $120^\circ\text{C}$  on samples dissolved in *o*-dichlorobenzene on a Varian 400 MHz machine using a  $90^\circ$  pulse angle, a pulse width of 10, and 25 000 scans with a 30 sec. delay. Composition was determined through the ratio between characteristic peaks of the different monomers making up the NMR spectrum of the copolymer. Basically the ratio between the peak areas of the branching -CH and that of the backbone carbons was determined and expressed as a percentage. Assignments were done making use of the literature where possible, combined with DEPT analyses and checked against the chemical shift assignments predicted by the additivity rules described by Grant and Paul [13].

Melt flow index (MFI) was determined according to ASTM D 1238, mechanical properties according to ASTM D 638 M hardness according to ASTM D 2240 and notched Izod impact strength according to ASTM 256.

Densities between 0.915 and 0.945 g/cc were measured using a density gradient method according to ASTM 1505. Densities higher or lower than this was determined by using the buoyancy method.

Melting behavior was determined on a Perkin Elmer DSC-7 fitted with a TAC 7/PC instrument controller. The samples were heated from  $50$  to  $200^\circ\text{C}$  at  $20^\circ\text{C}/\text{min}$ , held at  $200^\circ\text{C}$  for 1 minute, cooled to  $50^\circ\text{C}$  at a rate of  $20^\circ\text{C}/\text{min}$  during which time the crystallization curve was recorded. At  $50^\circ\text{C}$ , the temperature was kept constant for 1 min after which the melting curve was recorded between  $50$  and  $200^\circ\text{C}$  at a heating rate of  $10^\circ\text{C}/\text{min}$ . In some experiments, a cooling rate of  $0.3^\circ\text{C}/\text{min}$ . was used.

Detailed descriptions of the experimental methods are presented in Chapter 4.

### 6.3 RESULTS AND DISCUSSION

A summary of significant results are shown in Table 6.3. These results will be discussed in more detail in following Sections.

**Table 6.3. Properties of Ethylene /  $\alpha$ -Olefin Copolymers**

1-Butene (%)	Density (g/cm <sup>3</sup> )	MFI (dg/min.)	Yield Strength (MPa)	Modulus (MPa)	Hardness	Impact Strength (kJ/m <sup>2</sup> )
2.5	0.942	1.2	18.1	650	56	14.5
3.7	0.937	2.4	14.9	499	51	16.8
4.64	0.935	2.7	14.4	450	49	21.1
11.4	0.915	1.3	8.9	243	40	35.1
17.1	0.90	11	5.2	116	23	15.2
<b>1-Pentene (%)</b>						
2.0	0.954	1.9	18.5	700	56	17.1
3.4	0.936	1.8	14.3	487	51	28.3
4.1	0.933	2.0	13.1	426	49	35.4
5.94	0.927	4.5	11.4	360	45	34.7
12.6	0.885	5.0	7.7	235	37	No Break
14.1	0.876	10	7.2	280	35	No Break
20.4	0.860	5.3	5.1	117	24	No Break
<b>1-Hexene (%)</b>						
1.15	0.946	1.1	20	760	58	12.9
2.63	0.936	4.8	15.5	514	51	27.2
3	0.933	2.2	14.1	485	50	31.5
3.42	0.930	0.9	13.2	438	48	34.2
5.1	0.918	3.6	9.2	342	42	35.7
7.01	0.902	0.7	8.4	336	37	33.3
7.86	0.897	16	5.7	340	27	No Break
<b>1-Heptene (%)</b>						
0.9	0.946	2.86				11.3
1.4	0.940	1.77	18.64	690		19.3
2.5	0.931	1.86	13.8	490		30.8
3.2	0.925	1.58	11.73	395		35.8
<b>1-Octene (%)</b>						
0.4	0.949	0.2	28.0	913	62	15.1
1.2	0.939	0.97	18.1	700	56	30.1
1.4	0.937	0.84	17.4	663	55	34
2.0	0.930	1.2	13.9	530	51	32.1
2.5	0.926	3.0	12.1	398	48	45.1
<b>1-Nonene (%)</b>						
0.6	0.945	1.5	22.4	826	60	16.5
1.5	0.931	0.3	15.3	607	53	40.0
1.8	0.928	0.4	13.0	532	51	51.1

### 6.3.1 COMONOMER SEQUENCE DISTRIBUTIONS

By using  $^{13}\text{C}$  NMR, the true comonomer sequence distributions  $\tilde{n}_x$  of the different copolymers can be calculated according to the equations:

$$\tilde{n}_E = (N_{EE} + 0.5N_{EC})/0.5 N_{EC} \quad (6.4)$$

$$\tilde{n}_C = (N_{CC} + 0.5N_{EC})/0.5 N_{EC} \quad (6.5)$$

where  $N_{EE}$  and  $N_{CC}$  is the intensity of the  $\text{CH}_2$  carbons of ethylene or the comonomer centered dyads EEEE, EEEC, CEEC and CCCC, CCCE, ECCE respectively and  $N_{EC}$  is the intensity of the  $\text{CH}_2$  carbons of the EECE, EECC, CECE, CECC dyads [12]

Unit cell dimensions of the orthorhombic polyethylene crystal are  $a = 7.418$ ,  $b = 4.945$  and  $c = 2.545 \text{ \AA}$ , the latter being the chain repeat distance which is identical to the repeat distance of the fully extended chain [14,15]. These values for the unit cell changes slightly with temperature, but in copolymers unit cell expansion in the  $a$  and  $b$  axes were observed and attributed to the partial inclusion of comonomer units in the crystal structure [16] – 22% for methyl branches, 10% for ethyl and 6% for hexyl branches. Lamellar thickness is limited by the distance between branches and thus, from the repeat distance, the *average* maximum lamellar thickness was calculated from the observed *average* ethylene sequence length  $\tilde{n}_E$  as well as the comonomer sequence lengths were the equations discussed in Section 6.1. Results are shown in Table 6.4.

**Table 6.4. Comonomer Sequence Distribution of Ethylene /  $\alpha$ -Olefin Copolymers**

1-Butene (%)	$\bar{n}_E$	$\bar{n}_C$	Maximum Average Lamellar Thickness (Å)
2.5	98.2	1.48	250
3.7	65.7	1.48	168
4.64	59.4	1.96	151
11.4	29.5	1.76	75
17.1	14.56	1.46	37
<b>1-Pentene (%)</b>			
3.4	75.4	1.1	192
5.94	54.8	1.0	140
12.6	41.1	1.34	105
14.1	27.3	1.44	70
20.4	20.4	1.8	52
<b>1-Hexene (%)</b>			
1.15	237	1.0	604
2.63	95	1.0	242
3	69.9	1.26	178
3.42	56.5	1.13	144
5.1	51.1	1.36	130
7.01	27.8	1.28	71
7.86	21.44	1.26	55
<b>1-Heptene</b>			
1.4	103.2	1.0	263
2.5	64.9	1.0	165
3.2	34	1.0	87
<b>1-Octene (%)</b>			
0.4	530	1.0	1352
1.18	118	1.0	301
1.4	110.8	1.0	283
2.0	83.3	1.0	212
2.5	55.5	1.0	142
<b>1-Nonene (%)</b>			
0.6	221	1.0	564
1.5	137	1.0	349
1.8	54.7	1.0	140

Assignment of NMR peaks used for the calculations were done according to the literature [17] together with calculations based on the Grant and Paul parameters [13] and DEPT analyses (Table 6.5).



**Table 6.5.**  $^{13}\text{C}$ NMR  $\alpha$ -Carbon Peak Assignments of the Indicated Dyad Sequences for Copolymers of Ethylene with Higher  $\alpha$ -Olefins

<b>Ethylene / 1-Butene</b>	<u>EEEE</u> , <u>EEEC</u> , <u>CEEC</u>	<u>CCCC</u>	<u>CCCE</u>	<u>ECCE</u>	<u>EECC</u>	<u>CECC</u>	<u>EECE</u>	<u>CECE</u>
Grant&Paul	30	39.7	39.3	38.9	34.5	35.3	34.5	34.9
Observed	30	40.3	39.6	39.1	34.1	34.9	34.1	34.6
<b>Ethylene / 1-Pentene</b>								
Grant&Paul	30	40.5	40.1	39.7	35.3	35.7	34.8	35.2
Observed	30	41.4	40.8	40.1	35.0	35.6	34.5	35.0
<b>Ethylene / 1-Hexene</b>								
Grant&Paul	30	40.5	40.1	39.7	35.3	35.7	34.8	35.3
Observed	30	41.4	40.9	40.1	35.1	35.8	34.6	35.1
<b>Ethylene / 1-Heptene</b>								
Grant&Paul	30	40.6	40.2	39.8	35.3	35.8	34.9	35.3
Observed	30	40.1	-	-	34.9	35.8	34.4	34.9
<b>Ethylene / 1-Octene</b>								
Grant&Paul	30	40.6	40.2	39.8	35.3	35.8	34.9	35.3
Observed	30	41.4	40.9	40.3			34.6	
<b>Ethylene / 1-Nonene</b>								
Grant&Paul	30	40.6	40.2	39.8	35.3	35.8	34.9	35.3
Observed	30	-	-	-	35.1	35.6	34.4	35.1

Calculations of comonomer sequence lengths could, with one exception at 1-octene, not be done with the  $\text{C}_7$  to  $\text{C}_9$  copolymers as the intensities of the  $\text{CH}_2$  carbons in the ECCE, CCCE and CCCC dyads at the comonomer concentrations investigated were too small for the peaks to be distinguished from the baseline noise. However, it can be seen that at similar concentrations of comonomer in the chains, ethylene sequences are generally longer in the ethylene / 1-butene copolymers than in the rest of the copolymers. This indicates that, in line with what was expected from the decreasing reactivities, a less clustered comonomer distribution are obtained when the higher  $\alpha$ -olefins is used as comonomer.

### 6.3.2 DENSITY

A graphic representation of the results shown in Table 6.2 is given in Figure 6.3.

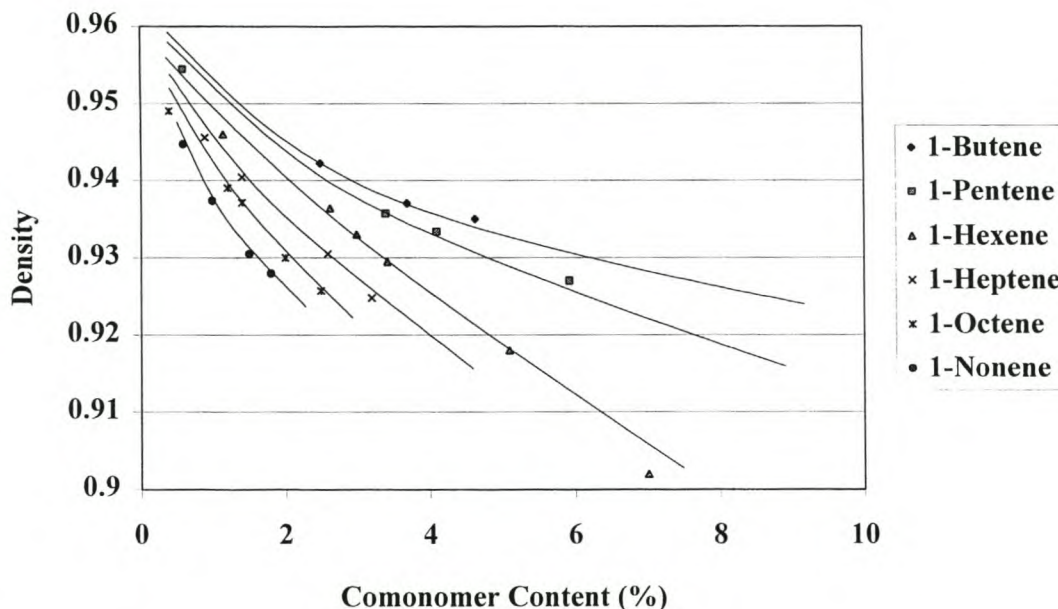


**Figure 6.3. Decrease in Density with Different  $\alpha$ -Olefins**

Polyethylene is semi-crystalline and consists of crystalline and amorphous phases of densities of respectively 1.00 and 0.855 g/cm<sup>3</sup> at room temperature [9]. An increase in the amount of branches reduces the capability of the copolymer to crystallize by shortening the crystallizable ethylene sequences which results in a decrease in density. At very high comonomer contents, the density of the different phases clearly approach those of the homopolymer of the  $\alpha$ -olefin used as comonomer. For the remainder of the discussion it is sufficient to consider only the crystalline and amorphous regions. The representation of a rudimentary semi-crystalline structure accepted in the literature [18] consisting of the crystalline, interfacial and amorphous regions will not be used. It is believed that the effect of the thickening transition layer with increased comonomer content is too small to have a noticeable effect on properties of the copolymers discussed here.

The ability of different comonomer units to disrupt crystallinity is displayed in Figure 6.3 and through casual inspection it can be observed that at similar comonomer contents, the longer the branch, the lower the density. It can also be seen that density

decrease is more gradual with the lower  $\alpha$ -olefins than with the higher ones. This may be explained by the more efficient rejection of the higher olefins by the crystal, thereby forcing the formation of thinner less perfect lamellae. Because of the small size of e.g. the ethyl branch from 1-butene, the defect it causes in the polyethylene crystal structure is small and therefore, necessitates the incorporation of large amounts of 1-butene to achieve low density. The amount of 1-butene cannot, however, be increased *ad infinitum* as this changes the backbone from that of mainly polyethylene to that of poly(1-butene). Because poly(1-butene) is a semi-crystalline solid with a density of about 0.93 to 0.94 g/cm<sup>3</sup> [19], long sequences of 1-butene in a chain may crystallize by itself and thereby fail to act as an “impurity” to disrupt polyethylene crystallization. 1-Butene tends to cluster [20] during copolymerization *i.e.* it tends to form sequences rich in 1-butene along the copolymer chains. This clustering (even if the comonomer can not crystallize) results in a decreased efficiency of the comonomer to disrupt crystallization and a higher amount of 1-butene is thus needed to obtain a certain density. The longer the side chain, the more effective it is at decreasing density [21]. It is assumed that starting with 1-pentene, crystallization is subject to two structural factors: (a) the branch length and (b) the crystallizable sequence length. It is evident that the longer branches will have a greater effect on crystallinity, but crystallization of these copolymers is also determined to a large extent by the branch distribution in the chain. The branch distribution in the chain defines a sequence length distribution of the crystallizable monomer units, which are the building blocks of crystals [22]. If the branches are not distributed evenly along the chain, very long and very short runs of ethylene will exist. The long sequences which can therefore crystallize freely, result in well-formed, dense lamellae which accentuates the heterogeneity of such a system. “Very long” crystallizable sequences favor conditions for chain folding to occur. When the sequences are short the system will yield initial lamellar thicknesses in the same order of magnitude as the sequence length. At an even shorter sequence length, fringed micelle-like nucleation becomes likely. A critical sequence length of 14 was calculated below which ethylene sequences could not be packed into a stable crystal lattice [23]. Crystallization of these copolymers is therefore dependent to a large extent by the branch distribution in the chain and in order to decrease crystallinity more effectively it is desirable to prevent clustering.

If the effect of the higher  $\alpha$ -olefins to decrease density is judged on the size of its branch relative to 1-butene, the concentration of the higher  $\alpha$ -olefin necessary to obtain a certain density can be calculated and compared with the observed values (Table 6.6).

**Table 6.6** Observed vs. Calculated Comonomer Content at a Fixed Density of  $\rho = 0.930 \text{ g/cm}^3$

Monomer	Branch Length	Relative Effect	Observed Content (%)	Calculated Content (%)	Difference
1-Butene	2	1	6.5	-	-
1-Pentene	3	1.5	4.8	4.3	0.50
1-Hexene	4	2	3.3	3.25	0.05
1-Heptene	5	2.5	2.6	2.6	0.00
1-Octene	6	3	2.1	2.17	-0.07
1-Nonene	7	3.5	1.6	1.86	-0.26

Calculations relative to a 1-butene content of 6.5% shows a very close correlation between density and branch length. The difference between observed and calculated content shows a small but definite decrease, which is in agreement with the reasoning regarding the increasingly effective depression of density resulting from decreased clustering. However, this should not be taken as experimental evidence for improved homogeneity. Such a conclusion can only be made if the trend persists at progressively lower densities.

### 6.3.3 MECHANICAL PROPERTIES

#### 6.3.3.1 Tensile Strength

The relationship between tensile strength and modulus is graphically demonstrated in Figure 6.4.

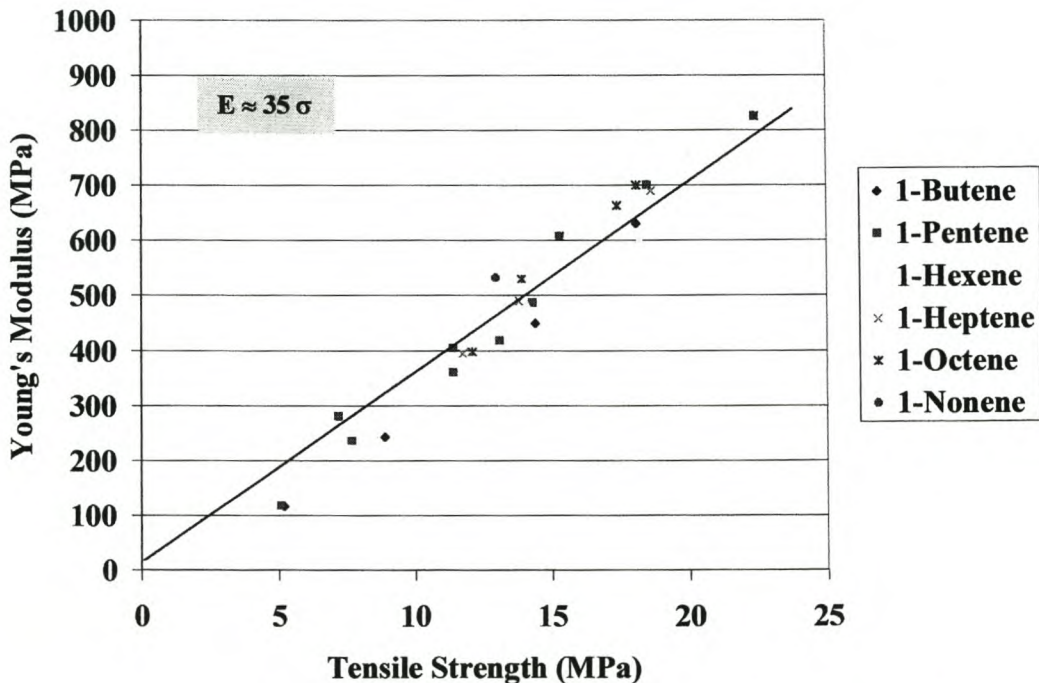


Figure 6.4. Relationship between Tensile Strength and Young's Modulus for Ethylene /  $\alpha$ -Olefin Copolymers

It is known from earlier studies that certain short range deformation properties of polyolefins such as tensile strength at yield, modulus, hardness and melting temperature are dependent on crystallinity [24]. However, a comparison of these properties for the series of C<sub>4</sub> to C<sub>9</sub> copolymers with ethylene is as far as we know, not available in the literature. In general there exists a direct relationship between tensile strength and modulus and it is expected that an increase in tensile strength at yield will be mirrored in an increase in modulus. This is in accordance with a previous representation of decreased yield strength with decreased modulus observed for LLDPE using 1-octene as comonomer [25].

Molecular weight has a significant effect on tensile properties [26,27] because spherulites are held together by tie-molecules which span the amorphous interspherulitic regions. Below a certain length, chains can not act as tie-molecules because they can not be trapped at both ends in the lamellae of two adjacent spherulites. Low molecular weight polymer is therefore brittle and has low tensile and impact strength. During crystallization, the longer molecules tend to crystallize first, resulting in separation based on molecular weight with the low molecular weight material concentrated in the amorphous interspherulitic region [21]. The presence of comonomer units in a chain results in this defect-containing part of the molecule being excluded from the crystal which must then form part of the amorphous or interfacial region. This increases the amount of high-molecular weight polymer in the amorphous region capable of acting as tie-molecules. The copolymers prepared in this study have different molecular weights as can be seen from the values of their melt flow indices and for this reason, values are somewhat dispersed. In general, high molecular weight polymers have values below the line and low molecular weight polymers have values above the line. By using this relationship, the validity of tensile results, independent of comonomer content, could easily be verified. Although different catalysts produce copolymers having different microstructures, it was observed that data points of terpolymers produced with a different supported catalyst, as well as those produced with metallocene catalysts, were still well represented by the same line.

### **6.3.3.2 Tensile Strength: The Effect of Comonomer Type**

The tensile deformation of polyethylene was extensively investigated in the past. However, the structural basis related to the deformation process is less publicized and even less understood. It is assumed that under a tensile load, slippage of chain folded layers and consequent unraveling and reorientation in the direction of the applied force occurs during neck formation and cold drawing [28]. Tensile strength at yield depends on the ability of the lamellae to resist this unraveling and reorientation. Changes in the crystalline/amorphous ratio, lamellar thickness and strength of the crystal will therefore have an effect on tensile strength at yield. The lamellar thickness is determined by the average separation between comonomer units [21,29] which is directly related to comonomer concentration and randomness of distribution.

Long runs of a regular chain will be trapped in the crystalline phase with the rest of the chain forming part of the interlamellar amorphous phase. This can also act as a tie-molecule when it forms part of different lamellae. To unravel these lamellae, a high tensile force will be needed. As the chain becomes less regular, more of it will be present in the amorphous phase and the lamellae may become thinner and less pure, thereby increasing the amount of tie-molecules. The more the crystalline/amorphous ratio changes and the thinner and less pure the lamellae become, as a result of branching, the easier their chain-folded structure can be destroyed, either thermally or mechanically.

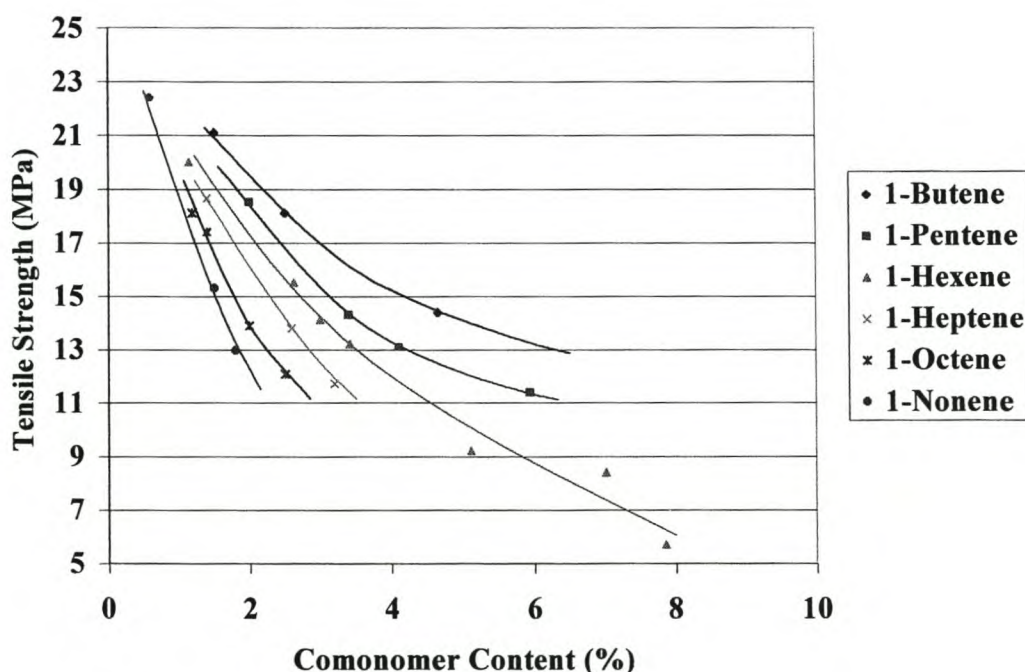


**Figure 6.5. Comparison of Tensile Strength of Different Ethylene /  $\alpha$ -Olefin Copolymers**

The comparison of tensile strengths of copolymers containing different  $\alpha$ -olefins is presented in Figure 6.5. As previously observed [24], tensile strength at yield can be related directly to density and it is therefore not surprising that the same trend related to comonomer content observed for density was also manifested in the tensile behavior of these copolymers. A horizontal line at 13 MPa intersects all tensile curves. By calculating the comonomer contents of the different copolymers based on the sizes of the side chains relative to that of 1-butene at this tensile strength, a close

relationship between branch length and tensile strength was observed as shown in Table 6.7.

**Table 6.7. Observed vs. Calculated Comonomer Content at a Fixed Tensile Strength of 13 MPa**

Monomer	Relative Effect	Observed Content (%)	Calculated Content (%)	Difference	Expected Tensile Strength (MPa)
1-Butene	1	6.3	-	-	13
1-Pentene	1.5	4.3	4.2	0.10	13.2
1-Hexene	2	3.6	3.15	0.45	14
1-Heptene	2.5	2.8	2.52	0.28	14
1-Octene	3	2.3	2.1	0.20	13.8
1-Nonene	3.5	1.9	1.8	0.10	13.6

It was mentioned that the use of higher  $\alpha$ -olefins results in an increased number of tie-molecules which make their copolymers with ethylene stronger than ethylene / 1-butene copolymers [8]. As can be seen from the small deviation of the expected tensile strength from 13 Mpa, this effect was, however, not observed.

### 6.3.3.3 Tensile Strength: The Effect of Density.

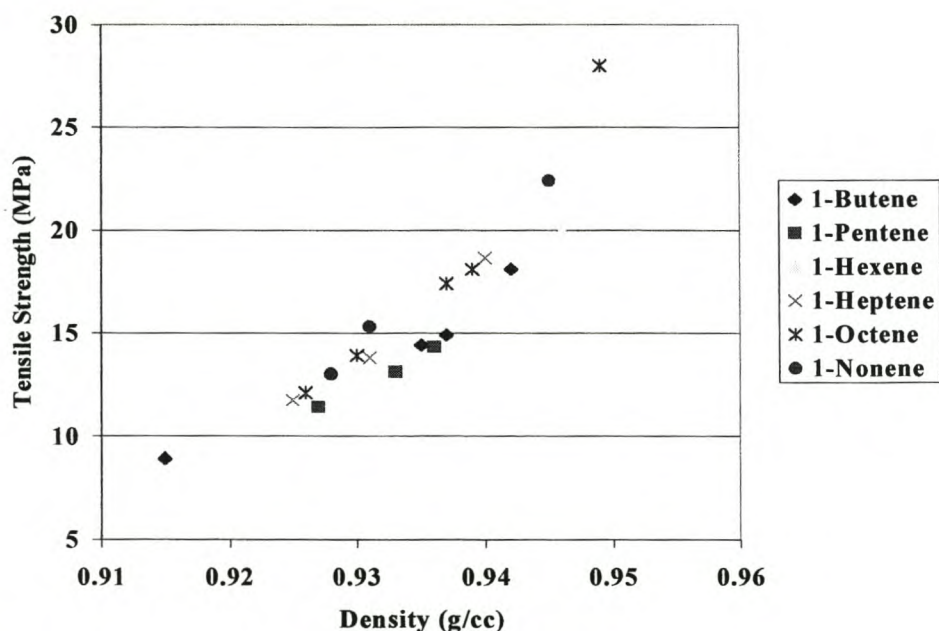


**Figure 6.6. Dependence of Tensile Strength at Yield on Density**



In Figure 6.6, yield strength is plotted against density in the range 0.91 to 0.95 g/cm<sup>3</sup>. The increase in tensile strength with density is unambiguous. However, no clear distinction can be made between copolymers prepared using different comonomers. This is in accordance with a recent discussion on a series of polyethylenes showing that crystallinity is related more to density than to molecular structure [30].

#### 6.3.3.4 Modulus

By definition, Young's modulus is determined by

$$E = L.F / (\Delta L.A) \quad (8)$$

where  $L$  is the original length of the sample,  $F$  the force needed to extend it by a length  $\Delta L$  and  $A$  is the cross sectional area [31]. It is therefore expected that an increased amount of tie-molecules will require a larger force to extend the sample, resulting in modulus values higher than those calculated based on comonomer size alone.

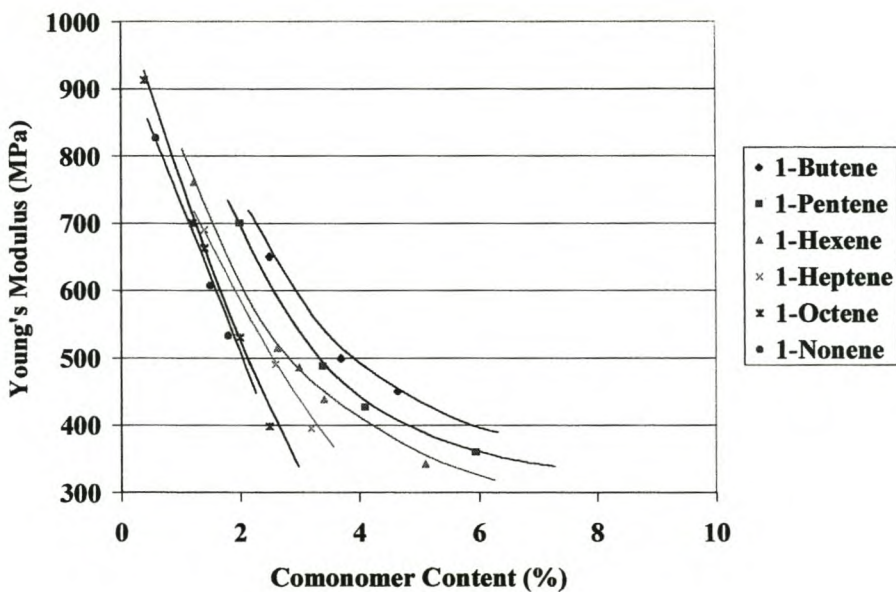


**Figure 6.7. Comparison of Young's Modulus of Different Ethylene /  $\alpha$ -Olefin Copolymers**

The comparison of Young's modulus of copolymers prepared with different  $\alpha$ -olefins is presented in Figure 6.7. Although the basic trend of decreasing modulus with increased size of the comonomer branch still prevails the curves are much more closely packed. During crystallization, polymer chains are "sucked in" by the chain-folding occurring on the crystal face. For this reason, tie-molecules are usually drawn tight between spherulites, keeping the structure together. By applying a tensile force to the structure, the chains roughly oriented in the direction of the applied stress, can immediately take up the load. They hence resist elongation, very similar to the known effect of increased modulus resulting from polymer chains bonded to the surface of reinforcing fillers for rubbers [32]. It is therefore expected that an increased amount of tie-molecules will require a larger force to extend the sample, resulting in modulus values higher than those calculated based on comonomer size alone. A horizontal line at 500 MPa intersects all of the curves and as before was used in the calculation of comonomer content based on 1-butene branch length. A very significant difference between calculated and observed values was noticed. For the 1-nonene copolymers, for example, a modulus of 500 MPa was only reached at a 1-nonene content of about 3.5%. However, based on the bulkiness of the heptyl side chain relative to the ethyl group from 1-butene, this value was expected to be reached at a 1-nonene content of 2%. A vertical line at this calculated content intersects the 1-nonene modulus curve at 710 MPa, which is substantially higher than 500 MPa. These modulus values of the different copolymers expected at the calculated content were approximated and are presented in Table 6.8.

**Table 6.8. Observed vs. Calculated Comonomer Content at a Fixed Young's Modulus of 500 MPa**

Monomer	Relative Effect	Observed Content (%)	Calculated Content (%)	Difference	Expected Modulus (MPa)
1-Butene	1	3.8	-	-	500
1-Pentene	1.5	3.3	2.5	0.8	600
1-Hexene	2	2.8	1.9	0.9	630
1-Heptene	2.5	2.5	1.56	0.94	660
1-Octene	3	2.1	1.27	0.83	690
1-Nonene	3.5	2.0	1.09	0.91	710

It is known that the modulus of uniformly branched copolymers are *lower* than that of heterogeneously branched ones [33]. From their relative reactivities, it is expected that the higher  $\alpha$ -olefins should have a more random comonomer distribution and therefore, their moduli are expected to decrease more rapidly than that predicted from their increased bulkiness relative to 1-butene. However, in Table 6.8 it can be seen that the expected moduli are higher. This observation supports the remark made by James [8] that the improved strength of the copolymers prepared with the higher  $\alpha$ -olefins are possibly the result of an increased number of tie-molecules. Improved randomness, expected from the use of these higher  $\alpha$ -olefins, could therefore not be demonstrated as a decrease in modulus was not observed. Hardness, similar to Young's modulus, also shows this reinforcing effect from the higher  $\alpha$ -olefins which can be ascribed to the increased number of tie-molecules.

### 6.3.3.5 Impact Strength

The effect of the type of comonomer used on the impact strength of the ethylene/ $\alpha$ -olefin copolymers is shown in Figure 6.8.

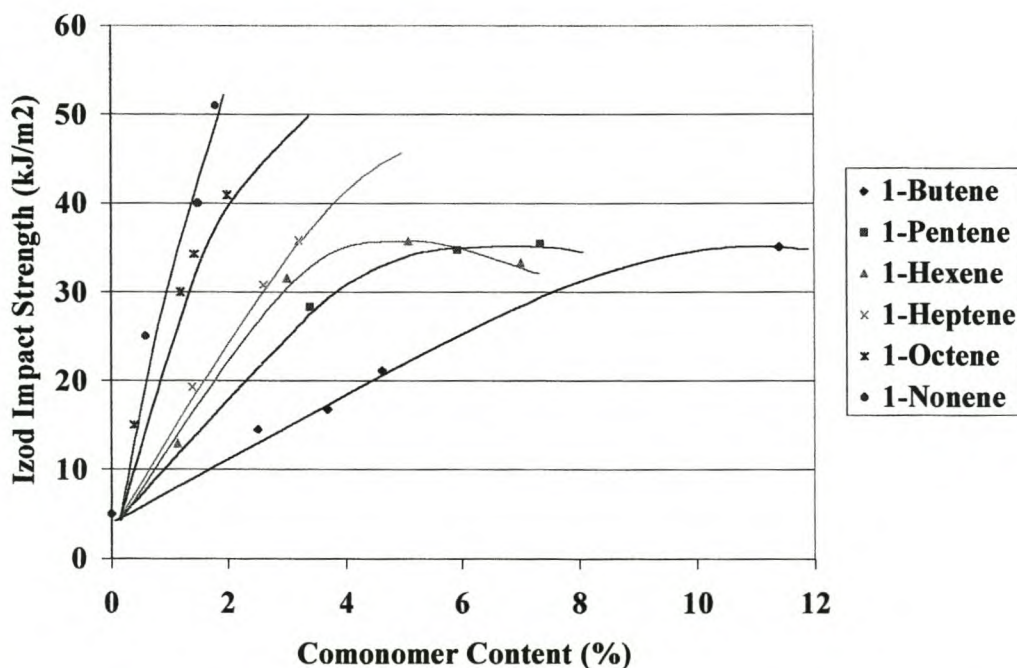


Figure 6.8. Notched Izod Impact Strength of Ethylene /  $\alpha$ -Olefin Copolymers

Impact strength depends on how effective the energy at a propagating crack tip can be dispersed. Large amounts of energy can be dissipated through viscous flow [34] such that the chains will orient in the direction of the applied stress, the oriented chains which are load bearing [35]. When only a relatively small amount of tie-molecules are present and the lamellae are thick and well formed it is easy to imagine that the amount of tie-molecules may not be sufficiently large to withstand breakage during the process of orientation in the crack tip. When the lamellae are connected by more tie-molecules, as is the case with increased branching where a higher ratio of the chains are excluded from the crystallites, viscous flow becomes easier. This dissipates large amounts of energy in addition to forming highly oriented polymer in the crack tip which blunts it and retards the growth of the crack. Depending on the degree of orientation achieved, the propagation of a crack can be terminated completely, probably because the modulus in the loading direction is substantially increased relative to the surrounding unoriented matrix [36].

The notched Izod impact strength shows a marked effect resulting from the type of  $\alpha$ -olefin used. It can be seen from Figure 6.8 that impact strength increases with increased comonomer content. With copolymers containing 1-butene to 1-hexene it can be seen that the impact strength reached a maximum and started decreasing as the polymer became more rubbery and ductile. As was expected from increased side chain length, impact strength increases and it can also be seen that the slopes of the curves gradually increase with increased comonomer size. However, the increase is not related to side chain length alone. By once again using 1-butene as a standard, the expected slopes were calculated.

**Table 6.9. Observed vs. Expected Slopes of Impact Curves of Different Ethylene /  $\alpha$ -Olefin Copolymers**

Monomer	Relative Effect	Expected Slope	Actual Slope
1-Butene	1.0	3.5	3.5
1-Pentene	1.5	5.3	6.7
1-Hexene	2.0	7.0	8.6
1-Heptene	2.5	8.8	10.2
1-Octene	3.0	10.5	20.0
1-Nonene	3.5	12.3	25.0

From Table 6.9 and Figure 6.9 it can be seen that the actual initial slopes of the impact vs. content curves progressively deviate from those calculated for the higher  $\alpha$ -olefins. Here, similar to the strengthening effect observed with modulus, the increased impact strength is also larger than that expected from calculations based on branch size.

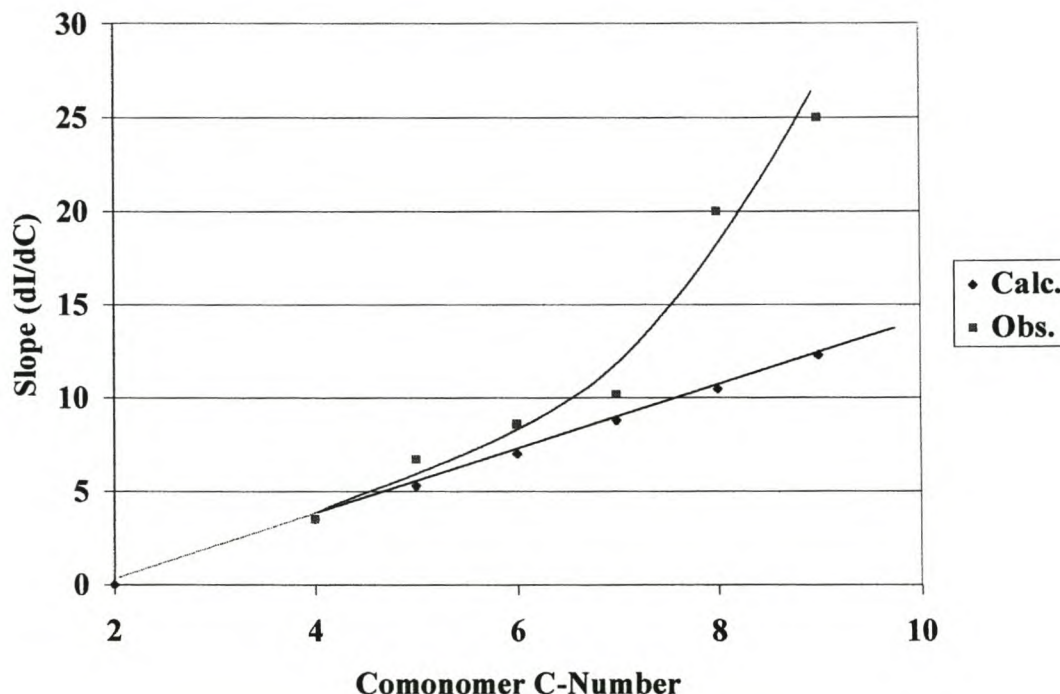


**Figure 6.9. Deviation of Slopes of the Actual Impact Curves From the Expected Values**

The ability of the higher  $\alpha$ -olefins to improve impact strength seems to be associated with the combined effect of increased amount of tie-molecules in the flexible amorphous material which can undergo viscous flow to absorb energy during impact and the subsequent increased modulus resulting from orientation of chains pulled out of the lamellae which retard crack growth. On the other hand it was previously mentioned that lower crystallinity promotes lower yield stress, making fracture initiation easier. Once initiated the fracture zone fibrillates and crack propagation becomes more difficult [37]. This was attributed to a second stage of crack growth. The first stage would be the initiation of the craze preceding the crack, the rate of which is governed by the yield point of the matrix. The second stage is crack

initiation and propagation, governed by the rate of fibril disentanglements at the base of the craze determined primarily by the tie-molecules.

The experimental results obtained from the mechanical properties thus seem to be in agreement with the belief that an increased number of tie-molecules is primarily responsible for the improved mechanical properties of copolymers containing higher the  $\alpha$ -olefins [8].

#### 6.3.4 THERMAL PROPERTIES

It can be recognized from the discussion of the mechanical properties of ethylene /  $\alpha$ -olefin copolymers that properties can be related directly to the balance between its crystalline and amorphous features. From a casual inspection of the melting temperatures of the different comonomers shown in Table 6.10 it is clear that the comonomer effect on thermal properties are not as prominent as with mechanical properties and are probably related to the heterogeneous distribution of active sites in the Ziegler-Natta catalyst used. These heterogeneous active centers will form heterogeneous copolymers because of differences in copolymerization characteristics of the different active sites [38] resulting in intermolecular and intramolecular heterogeneity, *i.e.* different chains having different compositions and a single chain having the comonomer units heterogeneously distributed therein. These chains either contain very small amounts of comonomer (such as chains formed by protected active sites) or contain a relatively high amount of clustered comonomer units (formed by “open” active sites). From the similar melting temperatures combined with the decreased fusion enthalpy with increased comonomer content it can be seen that long crystallizable sequences of ethylene remain present. During crystallization and driven by thermodynamic forces, these long crystallizable sequences are “sucked in” by the growing lamellae from the amorphous regions [39]. This excludes the non-crystallizable comonomer-rich sequences and therefore chain-folding is continued unhindered into well-formed crystallites having a thickness directly related to the crystallization temperature or degree of supercooling [17]. If branching occurs so often that the sequences are shorter than the fold-lengths, the lamellar thickness can

be limited by the length of the crystallizable sequences because the side chains are not easily incorporated in the crystalline lattice [21].

**Table 6.10. Thermal Properties of Ethylene /  $\alpha$ -Olefin Copolymers**

1-Butene (%)	Density (g/cm <sup>3</sup> )	Melt Peak (°C)	Cryst. Peak (°C)	Heat of Fusion (J/g)	Crystallinity (%)		
					By Density	$\Delta$	By $\Delta H_f$
2.50	0.942	124	111	140	64	16	48
3.70	0.937	124	111	123	60	18	42
4.64	0.935	124	111	126	59	16	43
11.40	0.915	123	108	89	45	14	31
17.10	0.900	115/121	108/101	44	35	20	15
<b>1-Pentene (%)</b>							
3.40	0.936	125	112	120	60	19	41
4.10	0.933	125	114	121	58	16	42
5.94	0.927	124	112	108	54	17	37
12.60	0.885	124	112	85	23	-6	29
14.10	0.876	124	112	73	17	-8	25
20.40	0.860	123	111	51	4	-14	18
<b>1-Hexene (%)</b>							
1.15	0.946	127	116	159	66	11	55
2.63	0.936	125	114	137	60	13	47
3.00	0.933	124	111	130	58	13	45
3.42	0.930	125	112	113	56	17	39
5.10	0.918	123	108	107	47	10	37
7.01	0.902	125	112	95	36	3	33
7.86	0.897	124	112	66	32	9	23
<b>1-Heptene (%)</b>							
0.90	0.946	125	111	156	66	12	54
1.40	0.940	125	111	144	62	12	50
2.50	0.931	124	111	114	56	17	39
3.20	0.925	125	111	99	52	18	34
<b>1-Octene (%)</b>							
0.40	0.949	129	115	163	68	12	56
1.20	0.939	126	111	142	62	13	49
1.40	0.937	126	111	138	60	12	48
2.00	0.930	125	111	122	56	14	42
2.50	0.926	124	111	100	53	19	34
<b>1-Nonene (%)</b>							
0.60	0.945	127	115	147	66	15	51
1.50	0.931	126	111	92	56	24	32
1.80	0.928	125	111	95	54	21	33

The heterogeneous distribution of comonomer units which result is very long and very short crystallizable sequences is therefore responsible for a range of lamellar thicknesses, the thick ones having higher melting temperatures than the thinner ones [39]. After chain-folding, heterogeneous copolymer chains containing different lengths of crystallizable sequences longer than the fold length of the initial crystal thickness necessary for crystallization at a specific temperature may be included in the same crystal of a certain thickness, all of which will melt at the same temperature [40]. It can be seen from Table 6.10 that the melting and crystallization temperature peaks for all of the heterogeneous comonomers, irrespective of the content in the copolymers, are very similar over a wide density range indicating that the average separation between branches are large. This suggests that the comonomer distributions are heterogeneous and that they contain crystallizable sequences long enough not to limit fold-lengths or lamellar thicknesses and consequently the melting temperature. Only at much higher comonomer contents, do the crystallizable sequences become so short that the melting peaks emerge at lower temperatures.

**Table 6.11. Thermal Properties of Copolymers Prepared with Metallocene Catalysts**

1-Butene (%)	Catalyst	Density (g/cm <sup>3</sup> )	Melt Peak (°C)	Equilib Melt Temp (°C)	Heat of Fusion (J/g)	Crystallinity	
						By Density	By $\Delta H_f$
2.4	(1-EtCp) <sub>2</sub> ZrCl <sub>2</sub>	0.942	122	132.5	146	64	50.3
<b>1-Pentene (%)</b>							
2.8	(1-EtCp) <sub>2</sub> ZrCl <sub>2</sub>	0.935	-	131.6		59	
4.0	( <i>n</i> -BuCp) <sub>2</sub> ZrCl <sub>2</sub>	0.930	104/114	129.1	94	56	32
<b>1-Hexene (%)</b>							
1.6	(1-EtCp) <sub>2</sub> ZrCl <sub>2</sub>	0.942	124	134.2	155	64	53.4
1.8	Me <sub>2</sub> Si(Ind) <sub>2</sub> ZrCl <sub>2</sub>	0.939	123	133.8	112	62	38.6
<b>1-Heptene (%)</b>							
4.3	Me <sub>2</sub> Si(Ind) <sub>2</sub> ZrCl <sub>2</sub>	0.905	123	128.4	59	38	20.3
<b>1-Octene (%)</b>							
1.0	(1-EtCp) <sub>2</sub> ZrCl <sub>2</sub>	0.942	121	135.5	148	64	51.0
9.6	Me <sub>2</sub> Si(Ind) <sub>2</sub> ZrCl <sub>2</sub>	0.880	110	117.1	10	20	3.4
13.4	Me <sub>2</sub> Si(Ind) <sub>2</sub> ZrCl <sub>2</sub>	-	80	109.0	13		4.5
<b>1-Nonene (%)</b>							
3.1	Me <sub>2</sub> Si(Ind) <sub>2</sub> ZrCl <sub>2</sub>	0.90	128	131.0	157	34	54.1



Homogeneous copolymers on the other hand, have their co-units homogeneously distributed along the chains, resulting in much shorter crystallizable sequences and a strong dependence on comonomer content because thick lamellae are not present. A small difference in the amount of (unclustered and randomly distributed) co-units in these copolymers results in a significant change in melting temperature and melting peaks are generally broad [40]. This can clearly be seen from the melting temperatures (Table 6.11) of ethylene /  $\alpha$ -olefin copolymers prepared with metallocene catalysts compared to the melting temperatures of copolymers prepared with the conventional Ziegler-Natta catalysts. These heterogeneous copolymers may contain much higher amounts of comonomer, but have melting temperatures higher than 123°C.

Flory's equation can be used to calculate the equilibrium melting temperature,  $T_m$ , valid only for truly random copolymers [41]:

$$1/T_m - 1/T_m^0 = -R \ln X_E / \Delta H_u \quad (6.9)$$

where  $T_m^0$  is the melting temperature of linear polyethylene taken as 137°C,  $R = 1.9872 \text{ cal.mol}^{-1}.\text{deg.}^{-1}$  is the gas constant,  $X_E$  is the mole fraction of the crystallizable unit (ethylene in this case) and  $\Delta H_u$  is the heat of fusion of the repeat unit, taken as 785 cal. per methylene unit [31]. However, it was shown that different comonomers having different branch lengths disrupt crystallinity to different extents and the equation may need to be modified to accommodate this effect. In Table 6.11 the melting temperatures for the homogeneous copolymers, calculated from Equation 6.9, are shown and it can be seen that only a very rough correlation exists. The melting peaks of these copolymers obtained experimentally are, however very broad and flat. Accurate positioning of the peak melting temperature is therefore difficult. For similar comonomer contents, increasing the branch length does not change the mol fraction crystallizable ethylene ( $X_E$ ) and the effect of the branch length is thus not accounted for in Equation 6.9.

Melting peak temperatures of the heterogeneous copolymers prepared with the Ziegler-Natta catalyst rapidly drop to about 123 – 125°C after which the melting

temperature is fairly insensitive towards large differences in comonomer content. Calculation of melting temperatures for these heterogeneously branched copolymers produced anomalous results and estimations of melting temperatures for these copolymers are of no value.

By using the experimental melting temperatures in the same equation (6.9), the ethylene /  $\alpha$ -olefin copolymerization statistics can be calculated. The effect of the propagation probability of the crystallizable ethylene units ( $P_{EE}$ ) on the chain microstructure can be summarized as follows:

$$P_{EE} = X_E \rightarrow \text{Random,}$$

$$1 > P_{EE} > X_E \rightarrow \text{Block}$$

$$0 < P_{EE} < X_E \rightarrow \text{Alternating}$$

**Table 6.12 Chain Propagation Probabilities**

<b>1-Butene (%)</b>	<b>T<sub>m</sub> (°C)</b>	<b>X<sub>E</sub></b>	<b>P<sub>EE</sub></b>	<b>Char.</b>	<b>1-Heptene (%)</b>	<b>T<sub>m</sub> (°C)</b>	<b>X<sub>E</sub></b>	<b>P<sub>EE</sub></b>	<b>Char.</b>
2.50	124	0.975	0.939	Alt	0.90	125	0.991	0.944	Alt
3.70	124	0.963	0.939	Alt	1.40	125	0.986	0.944	Alt
4.64	124	0.9536	0.939	Alt	2.50	124	0.975	0.939	Alt
11.40	123	0.886	0.934	Block	3.20	125	0.968	0.944	Alt
17.10	121	0.829	0.925	Block					
<b>1-Pentene (%)</b>					<b>1-Octene (%)</b>				
3.40	125	0.966	0.944	Alt	0.40	129	0.996	0.962	Alt
4.10	125	0.959	0.944	Alt	1.20	126	0.988	0.948	Alt
5.94	124	0.9406	0.939	Alt	1.40	126	0.986	0.948	Alt
12.60	124	0.874	0.939	Block	2.00	125	0.98	0.944	Alt
14.10	124	0.859	0.939	Block	2.50	124	0.975	0.939	Alt
20.40	123	0.796	0.934	Block					
<b>1-Hexene (%)</b>					<b>1-Nonene (%)</b>				
1.15	127	0.9885	0.953	Alt	0.60	127	0.994	0.953	Alt
2.63	125	0.9737	0.944	Alt	1.50	126	0.985	0.948	Alt
3.00	124	0.97	0.939	Alt	1.80	125	0.982	0.944	Alt
3.42	125	0.9658	0.944	Alt					
5.10	123	0.949	0.934	Alt					
7.01	125	0.9299	0.944	Block					
7.86	124	0.9214	0.939	Block					

In Table 6.12 the calculated  $P_{EE}$  values are shown from which it can be seen that at least two different types of active sites are present. The one has an alternating character and predominates at low comonomer contents, and the other has a blocky character that emerge at higher comonomer contents. From this observation it may be concluded that the more protected active sites, responsible for producing mainly unbranched polyethylene chains, have an alternating character while the unprotected sites, capable of incorporating comonomer, have a blocky character.

The melting curves of 1-butene, 1-heptene and 1-nonene copolymers having similar comonomer content but different densities are shown in the top part of Figure 6.10 and those of 1-pentene and 1-hexene having similar densities but different contents are shown in the bottom part. It was expected that the differences in comonomer distribution would be shown in the broadening of the melt peaks with increased randomness [33]. However, the three curves of the 1-butene, 1-heptene and 1-nonene copolymers in Figure 10, show no significant differences (comonomer content of about 2.5%). However, the two curves of the 1-pentene and 1-hexene copolymers containing substantially higher levels of comonomer at the same density shows that the 1-hexene copolymer melting peak is slightly broader and the low temperature shoulder is slightly higher than that of the 1-pentene peak, even though the latter contains more branches. This, therefore, suggests that at sufficiently high comonomer content, peak broadening occurs when the higher  $\alpha$ -olefins are used as comonomer. Copolymers with high contents of the higher  $\alpha$ -olefins are lacking in this study and the extent to which they are incorporated in a more random fashion could not be quantified.

Even though the position of the melting peaks of the heterogeneous copolymers do not change much with comonomer content, the heat of fusion is greatly affected by the amount of crystalline material present in the sample as can be seen from Table 6.9 and Figure 6.11. The comonomer units in the polyethylene chain are usually not incorporated in the crystallites, but are concentrated in the amorphous and interfacial regions, resulting in a smaller proportion of crystalline material in the sample. The amount of energy necessary to melt a copolymer is therefore lower, even if the crystallite thickness requires a high melting temperature.

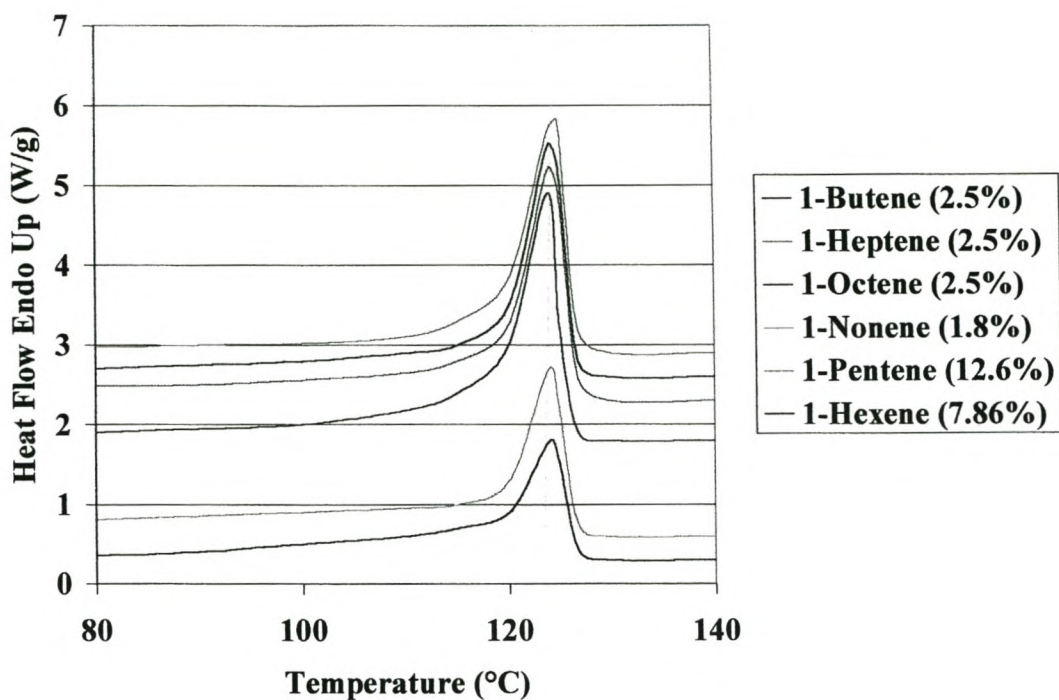


Figure 6.10. Melting Curves for Heterogeneous Ethylene /  $\alpha$ -Olefin Copolymers

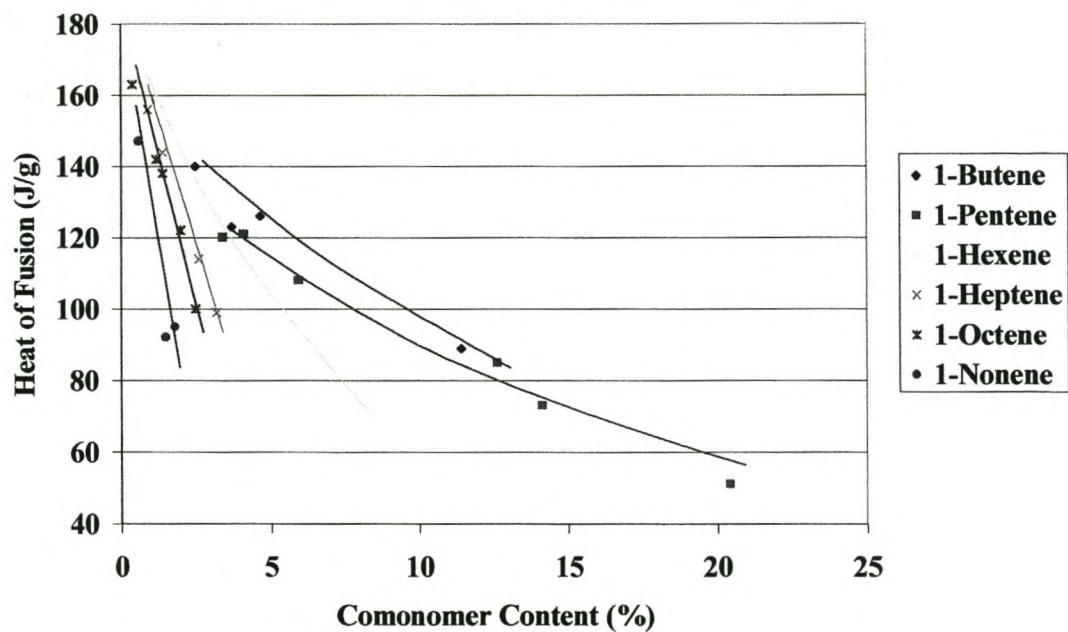


Figure 6.11. Heats of Fusion of Different Ethylene /  $\alpha$ -olefin Copolymers

The extent of crystallinity can be estimated from different properties of these copolymers. First, these copolymers comprise crystalline and amorphous regions, which known room temperature densities of  $1.00 \text{ g/cm}^3$  for the crystalline phase and  $0.855 \text{ g/cm}^3$  for the amorphous phase [9]. By measuring the overall density of a copolymer, room temperature mass fraction crystallinity can be calculated using the formula:

$$w^c = \rho_c (\rho - \rho_a) / \rho (\rho_c - \rho_a) \quad (6.10)$$

where  $\rho_c$  is the density of the crystalline phase,  $\rho_a$  the density of the amorphous phase and  $\rho$  the measured density of the copolymer [31]. Secondly, copolymers of different densities require different energies to melt the crystalline regions. By comparing the heat of fusion of a copolymer to that of a 100% crystalline phase, crystallinity can also be determined from:

$$w^c = \Delta H_f / \Delta H_{fC} \quad (6.11)$$

where  $\Delta H_{fC}$  is the heat of fusion of the crystalline phase, taken as  $290 \text{ J/g}$  [33]. This value for  $\Delta H_{fC}$  should actually be smaller as the DSC measurements in crystallization were stopped at  $50^\circ\text{C}$ , below which a substantial amount of crystallization are still continuing. An amount of polymer is therefore still in the molten state. Calculated crystallinities based on this value for  $\Delta H_{fC}$  are shown in Table 6.9. The calculated crystallinities based on density are generally higher than those obtained from thermal data and are in agreement with the observations reported by Mandelkern *et al.* [42]. This difference, amounting to between 20 and 30% of the bulk crystallized injection-moulded samples may in some cases, notably with 1-heptene, 1-octene and 1-nonene, be even higher, depending on the amount of high comonomer content fraction present in the sample which is still molten at  $50^\circ\text{C}$ .

## 6.4 CONCLUSIONS

Many linear and branched  $\alpha$ -olefins useful as comonomers are produced from Sasol's Fischer-Tropsch oil-from-coal process. These can be isolated by a relatively cheap refinery operation. Unique monomers include the odd-numbered olefins such as 1-pentene, 1-heptene and 1-nonene. The type of comonomer used has a substantial influence on copolymer properties, thereby introducing a further dimension by which polymer properties can be tailored. In earlier times, this was not an option as these monomers were not previously available at competitive prices. It is in this light that the study of the effect of comonomer incorporation into ethylene/ $\alpha$ -olefin copolymers was undertaken.

Comonomer sequence distributions and average lamellar thicknesses of different ethylene /  $\alpha$ -olefin copolymers were calculated from CH<sub>2</sub> dyad concentrations determined by <sup>13</sup>C NMR spectroscopy. It was observed that at similar comonomer concentrations, ethylene sequences are generally longer in the ethylene / 1-butene copolymers than in the rest of the copolymers synthesized. This indicates that a more random comonomer distribution is obtained when the higher  $\alpha$ -olefins are used as comonomer.

The progressive exclusion of larger comonomer units in the polyethylene backbone from the polyethylene crystal results in a decrease in lamellar thickness and crystal perfection and thus density. It was observed that, for similar comonomer contents, the longer the branch derived from the comonomer unit, the more density is decreased. Clustering of comonomer units result in long, crystallizable sequences of polyethylene, uninterrupted by branches. This clustering results in a decreased efficiency of the comonomer to disrupt crystallization and a higher amount of the comonomer is thus needed to obtain a certain density. It was shown that an inverse relationship exists between branch size and density. The effect of one heptyl branch derived from 1-nonene is thus 3.5 times as large as the effect of an ethyl branch derived from a 1-butene unit.

It is known that short range deformation properties of polyolefins such as tensile strength at yield, modulus, hardness and melting temperature are dependent on crystallinity and thus on density. Similar to what was found for density, a close relationship between branch length and tensile strength was observed. In line with this, it was found that for all the copolymers investigated, a linear relationship between tensile strength and density exists which is independent on  $\alpha$ -olefin type

Modulus, hardness and impact strength, on the other hand, did show an effect resulting from the comonomer type. Modulus and hardness were not depressed as much as was expected from calculations based on comonomer branch length. It is believed that the increased number of tie-molecules is responsible for this effect. The improved impact strength seems to be associated with the effect of an increased amount of tie-molecules in the flexible amorphous material, which undergoes viscous flow to absorb energy during impact.

Melting peak temperatures of the copolymers prepared with the Ziegler-Natta catalyst decreases to about 123 – 125°C after which it shows only limited sensitivity towards large differences in comonomer content which. This in general, indicates a heterogeneous comonomer distribution. Homogeneous copolymers have broad melting peaks and it was shown that at sufficiently high comonomer content, peak broadening occurs when the higher  $\alpha$ -olefins are used as comonomer. This also indicates that more random comonomer distributions are obtained with the higher  $\alpha$ -olefins.

From calculations of chain propagation probabilities it was shown that two distinctly different types of active sites exist. The protected sites responsible for producing mainly polyethylene have an alternating character while the unprotected sites responsible for incorporating comonomer have a blocky character.

## 6.5 REFERENCES

1. Fawcett E.W., Gibson R.O., *J. Chem. Soc.*, 386 (1934)
2. Fawcett E.W., Gibson R.O., Perrin M.W., Paton J.G., Williams E.G., *Brit. Pat. 471,590*, Imperial Chemical Industries, Sept. 6 (1937)
3. Hogan, J.P., Banks R.L., *U.S. Pat. 2,825,721*, Phillips Petroleum (1958)
4. Ziegler K., Holzkamp E., Breil H., Martin H., *Angew. Chem.*, **67**, 426 (1955)
5. Ziegler K., Holzkamp E., Breil H., Martin H., *Angew. Chem.*, **67**, 541 (1955)
6. Miller A.R., *U.S. Pat. 4,003,712*, Union Carbide, Jan. 18 (1977)
7. Levine I.J., Karol F.J., *U.S. Pat. 4,011,382*, Union Carbide, Mar. 8 (1977)
8. James D.E., *Ethylene Polymers* in *Encyclopedia of Polymer Science and Engineering*, Kroschwitz J., Exec. Ed., John Wiley & Sons, New York, **6**, 429 (1988)
9. Fatou J.G., *Morphology and Crystallization in Polyolefins* in *Handbook of Polyolefins - Synthesis and Properties*, Vasile C., Seymour R.B., Eds., Marcel Dekker Inc., New York, 155, (1993)
10. Mills N.J., Optical Properties in *Encyclopedia of Polymer Science and Engineering*, Kroschwitz J.I., Exec. Ed., John Wiley & Sons, New York, **10**, 493 (1988)
11. Kissin Y.V., *Stereospecificity of Heterogeneous Ziegler-Natta Catalysts* in *Isospecific Polymerization of Olefins with Heterogeneous Ziegler-Natta Catalysts*, Springer-Verlag, New York, **I-5**, 67 (1985)
12. Herbert I., *Statistical Analysis of Copolymer Sequence Distribution* in *NMR Spectroscopy of Polymers*, Ibbett R.N., Ed., Blackie Acad. & Proff., London, (2), 50 (1993)
13. Grant D.M., Paul E.G., *J. Am. Chem. Soc.*, **86**, 2984 (1964)
14. Vasile C., General Survey on the Properties of Polyolefins, in *Handbook of Polyolefins – Synthesis and Properties*, Vasile C., Seymour R.B., Eds., Marcel Dekker Inc., New York, 561 (1993)
15. Billmeyer F.W. Jr., *Textbook of Polymer Science*, John Wiley & Sons, New York, 141 (1962)
16. Hosoda S., Nomura H., Gotoh Y., Kihara H., *Polymer*, **31**, 1999 (1990)



17. De Pooter M., Smith P.B., Dohrer K.K., Bennett K.F., Meadows M.D., Smith C.G., Schouwenaars H.P., Geerards R.A., *J. Appl. Polym. Sci.*, **42**, 399 (1991)
18. Mandelkern L., *Crystallization and Melting in Comprehensive Polymer Science*, Sir Allen G, Chairman Ed. Board, Pergamon Press, Oxford, **2** (11), 363 (1989)
19. Krentsel B.A., Kissin Y.V., Kleiner V.J., Stotskaya L.L., *Polymers of Higher Linear  $\alpha$ -Olefins in Polymers and Copolymers of Higher  $\alpha$ -Olefins*, Carl Hanser Verlag, Munich, (4), 85 (1997)
20. Randall J.C., Hsieh E.T., <sup>13</sup>C NMR in Polymer Quantitative Analyses in NMR and Macromolecules, ACS Symp Ser., **247**, (9), 131 (1984)
21. Vaughan A.S., Bassett D.C., *Crystallization and Morphology in Comprehensive Polymer Science*, Sir Allen G, Chairman Ed. Board, Pergamon Press, Oxford, **2** (12), 415 (1989)
22. Seeger M., Cantow H.J., Marty S., *Anal. Chem.*, **276**, 267 (1975)
23. Burfield D.R., Kashiwa N., *Makromol. Chem.*, **186**, 2657 (1985)
24. Huff T., Bushman C.J., Cavender J.V., *J. Appl. Polym. Sci.*, **8**, 825 (1967)
25. El-Kindi M., Schreiber H.P., *Antec '91*, 1371 (1991)
26. Kissin Y.V., *Olefin Polymers (Polyethylene) in Encyclopedia of Chemical Technology*, Kroschwitz JI., Exec. Ed., John Wiley & Sons, New York, **17**, 724 (1995)
27. Bogdanov B.G., Michailov M., *Properties of Polyolefins in Handbook of Polyolefins – Synthesis and Properties*, Vasile C., Seymour R.B., Eds., Marcel Dekker Inc., New York, 295 (1993)
28. May A.N., *Appl. Mat. Res.*, **81**, Apr (1966)
29. Bodor G., Dalcolmo H.J., Schröter O., *Coll. Polym. Sci.*, **267**, 480 (1989)
30. Kennedy M.A., Peacock A.J., Mandelkern L., *Macromolecules*, **27**, 5297 (1994)
31. Faucher J.A., Reding F.P., *Relationship Between Structure and Fundamental Properties in Crystalline Olefin Polymers Part I*, Ed. Raff R.A.V., Doak K.W., John Wiley & Sons, New York, 677 (1965)
32. Beuche F., *Rubber Elasticity in Physical Properties of Polymers*, Interscience, New York, (2), 37 (1962)

33. Kissin Y.V., *Olefin Polymers (Polyethylene)* in *Encyclopedia of Chemical Technology*, Kroschwitz J.I., Exec. Ed., John Wiley & Sons, New York, **17**, 756 (1995)
34. Berry J.P., *J. Polym. Sci.*, **50**, 107, 318 (1961)
35. Young R.J., *Strength and Toughness in Comprehensive Polymer Science*, Sir Allen G, Chairman Ed. Board, Pergamon Press, Oxford, **2** (15), 511 (1989)
36. Kambour P.P., *Crazing in Encyclopedia of Polymer Science and Engineering*, Kroschwitz J.I., John Wiley & Sons, New York, **4**, 299 (1988)
37. Channel A.D., Clutton E.C., *Polymer*, **33**, (19), 4112 (1992)  
James D.E., *Ethylene Polymers in Encyclopedia of Polymer Science and Engineering*, Kroschwitz J.I., Exec. Ed., John Wiley & Sons, New York, **6**, 429 (1988)].
38. Sacchi M.C., Shan C., Forlini F., Tritto I., Locatelli P., *Makromol. Chem. Rapid Commun.*, **14**, 231 (1993)
39. Hingman R., Rieger J., Kersting M., *Macromolecules*, **28**, 3801 (1995)
40. Mathot V.B.F., *The Crystallization and Melting Region in Calorimetry and Thermal Analysis of Polymers*, Mathot V.B.F., Ed., Carl Hanser Verlag, Munich, **9**, 231 (1994)
41. Flory P.J., *Principles of Polymer Chemistry*, Cornell Univ. Press, New York, 568 (1953)
42. Mandelkern L., Allou A.L., Gopalan M., *J. Phys. Chem.*, **72**, (1), 309 (1968)

## CHAPTER 7

# ETHYLENE / 1-PENTENE / LINEAR $\alpha$ -OLEFIN TERPOLYMERS

### 7.1 INTRODUCTION

Copolymerization of ethylene with higher  $\alpha$ -olefins using supported Ziegler-Natta catalysts is hampered by increased steric hindrance. The higher  $\alpha$ -olefins are also less reactive and insertion into the polyethylene chain becomes increasingly more difficult as the side chain lengths increase. In order to amplify the statistical chances of these olefins being inserted relative to ethylene, the ethylene / olefin feed ratio should be decreased resulting in a decreased rate of polymerization. However, as shown in Chapter 6 a relationship between density and branch length exists and that less of the higher  $\alpha$ -olefins are necessary to achieve certain property responses. Therefore, a trade-off exists between reaction rate and comonomer content. It was also observed that properties change in relatively large steps between different comonomers. This may not be a desirable feature of the reactions. In order to erase these boundaries between different comonomers and to obtain a full range of properties, a third monomer can be introduced during polymerization to “dilute” the effect of the primary comonomer and thus only slightly modify some properties of the polymer without substantial changes to the polymerization process. Terpolymerization can therefore be employed for the production of different grades of polymers that differ only slightly from the copolymer grades. Alternatively a more linear transition towards totally different grades using increasingly higher amounts of the third monomer is also possible. It can thus be realized that instead of the large jumps in polymer properties observed between copolymers prepared using different comonomers, terpolymerization can lead to more subtle changes in properties than can be achieved by using different combinations and ratios of comonomers. A

comprehensive study of all possible combinations of the comonomers is extremely complex, but in order to illustrate the possibilities, the effect of the presence of a third monomer on the properties of ethylene / 1-pentene copolymers was investigated [1].

## 7.2 EXPERIMENTAL

*Slurry polymerization.* A typical procedure for the slurry terpolymerization of ethylene and 1-pentene using a third monomer is given below:

Highly purified heptane (300 g) was introduced into a 1-liter stainless steel polymerization vessel provided with agitation. After thorough purging of the vessel with nitrogen, 10 ml of a 10% solution of tri-ethyl aluminum in heptane and 0.03 g of supported catalyst 13 (Chapter 5) were introduced into the vessel. The temperature was set to 85°C and 100 mg of hydrogen was introduced. After 10 minutes, 100 g of ethylene at a flow rate of 2 g/min. and the desired ratio of 1-pentene and the third monomer were introduced over a period of 50 minutes. After a further period of 10 minutes the polymerization vessel was depressurized and the catalyst deactivated with *iso*-propanol. The resultant terpolymer was filtered, washed with acetone and dried in a vacuum oven at 70°C for 24 hours.

*Solution polymerization.* A typical procedure for the solution terpolymerization of ethylene and 1-pentene using a third monomer is given below:

Highly purified cyclohexane (300 g) was introduced into a 1-liter stainless steel polymerization vessel provided with agitation. After thorough purging of the vessel with nitrogen the temperature was raised to 95°C and 0.05 g of supported catalyst 13 (Chapter 5) was introduced into the vessel. The temperature was raised to 105°C and 150 mg of hydrogen introduced into the vessel. After 10 minutes, 100 g of ethylene at a flow rate of 2 g/min. and the desired ratio of 1-pentene and the third monomer were introduced over a period of 50 minutes. After a further period of 10 minutes the polymerization vessel was depressurized and the catalyst deactivated with *iso*-propanol. The resultant terpolymer was filtered, washed with acetone and dried in a vacuum oven at 70°C for 24 hours.

*Gas-phase polymerization.* A typical procedure for the gas-phase terpolymerization of ethylene and 1-pentene using a third monomer is given below:

Under inert conditions 1.0 g of prepolymerized catalyst 12 as described in Chapter 5 was added to 0.5 ml of a 10 wt % solution of tri-ethyl aluminium in heptane. This mixture was introduced into a 1-liter stainless steel gas phase reaction vessel which was preheated to 80°C. The reaction vessel was provided with a combination of helical and vertical stirring. Hydrogen (300 mg) was introduced and the reaction vessel pressurized to 5 bar with nitrogen. Ethylene (100 g) was fed to the reactor at a rate of 2 g/min and at the same time 1-pentene and the third monomer were introduced, in the desired ratio, over a period of 50 minutes. After a further period of 10 minutes the polymerization vessel was depressurized and the catalyst deactivated with *iso*-propanol. The resultant terpolymer was filtered, washed with acetone and dried in a vacuum oven at 70°C for 24 hours.

For the gas-phase reactions, only low-boiling comonomers with carbon numbers not higher than 6 were used.

*Polymerization using a metallocene catalyst.* A typical procedure for the solution terpolymerization of ethylene and 1-pentene using a third monomer in the presence of a metallocene catalyst, is given below:

Highly purified toluene (350 ml) was added to a 1-liter stainless steel reaction vessel provided with agitation and heated to 60°C. Under inert conditions,  $2 \times 10^{-3}$  mmole of the metallocene catalyst was reacted with 10 ml of a 30% solution of MAO in toluene and the reaction mixture transferred to the reactor in a gas tight syringe. Ethylene (100 g) was fed to the reactor at a rate of 2 g/min and at the same time the desired ratio of 1-pentene and the third monomer were introduced over a period of 50 minutes. After a further period of 10 minutes the polymerization vessel was depressurized and the catalyst deactivated with *iso*-propanol. The resultant terpolymer was filtered, washed with acetone and dried in a vacuum oven at 70°C for 24 hours.

$^{13}\text{C}$  NMR analyses were done at 120°C on samples dissolved in *o*-dichlorobenzene on a Varian 400 NMR spectrometer using a 90° pulse angle, a pulse width of 10, 25 000 scans with a 30 second delay. Composition was determined through the ratio between

characteristic peaks of the different monomers making up the NMR spectrum of the copolymer. Basically the ratio between the peak areas of the branching -CH and that of the backbone carbons was determined and expressed as a percentage. Assignments were done making use of the literature where possible, combined with DEPT analyses and checked against the chemical shift assignments predicted by the additivity rules described by Grant and Paul [2].

Melt flow index (MFI) was determined according to ASTM D 1238, mechanical properties according to ASTM D 638 M, hardness according to ASTM D 2240 and notched Izod impact strength according to ASTM 256.

Densities between 0.915 and 0.945 g/cc was measured on a density gradient method according to ASTM 1505. Densities higher or lower than this was determined by using the buoyancy method.

Melting behavior was determined on a Perkin Elmer DSC-7 fitted with a TAC 7/PC instrument controller. The samples were heated from 50 to 200°C at 20°C/min, held at 200°C for 1 minute, cooled to 50°C at a rate of 20°C/min during which time the crystallization curve was recorded. At 50°C, the temperature was kept constant for 1 min after which the melting curve was recorded between 50 and 200°C at a heating rate of 10°C/min. In some experiments, a cooling rate of 0.3°C/min. was used.

Detailed descriptions of the experimental methods were presented in Chapter 4.

## 7.3 RESULTS AND DISCUSSION

The terpolymer data points cannot be represented by a single line because the *total content*, the ratios between the two comonomers and the distribution of the comonomers in the terpolymers determine its placement in the plot area. This results in considerable scattering of data points. In the density, tensile strength, modulus and impact strength plots, which will be presented in the following sections, the different properties of the terpolymers are shown as data points. The same color will be used for the points and the solid lines which represent the respective copolymers. In Figure 7.1 for example, the blue data points represent the ethylene / 1-pentene / 1-butene terpolymer densities while the solid blue line represents the ethylene / 1-butene copolymer densities.

### 7.3.1 DENSITY

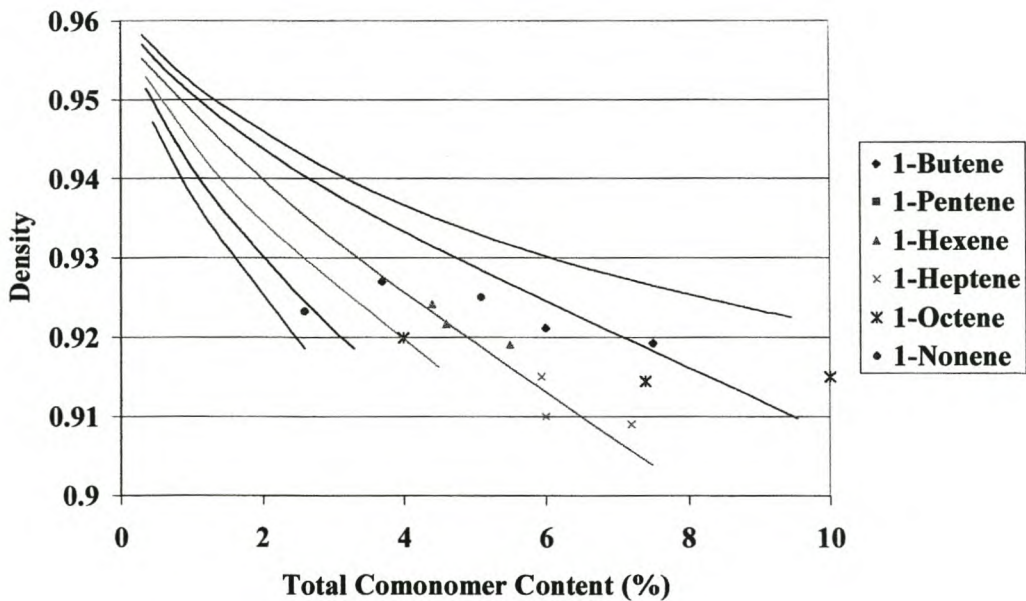


**Figure 7.1. Densities of Terpolymers of Ethylene, 1-Pentene and a Third  $\alpha$ -Olefin. The Solid Lines Represent Trends of the Relevant Copolymers**



The densities of terpolymers of ethylene and 1-pentene modified with different third  $\alpha$ -olefins are presented in Figure 7.1. In order to show the differences between the densities of co- and terpolymers, the lines representing the different copolymers are shown together with some of the representative terpolymer densities to first illustrate the behavior of the terpolymers. The data points are given in Table 7.1.

From the observation made in Chapter 6 that comonomer branch length is the primary factor determining density, it was expected that the introduction of a small amount of a higher  $\alpha$ -olefin in a predominantly ethylene / 1-pentene copolymer would tend to lower the density of the terpolymer towards the ethylene / 1-nonene copolymer density curve. Any specific terpolymer type would therefore have densities between those of the ethylene /  $\alpha$ -olefin copolymers with the corresponding comonomers. The position on the graph will be determined by the relative amounts of the comonomers. However, not all the terpolymers behave as expected. While terpolymers containing 1-nonene, 1-octene and 1-heptene behave as expected, the 1-hexene terpolymers have densities very similar to the ethylene / 1-hexene copolymers. Even more unusual is the data for the 1-butene terpolymers; the densities are in most cases even lower than those of the ethylene / 1-pentene copolymers. Because of this difference, a distinction will be made between 1-butene-, 1-hexene- and higher  $\alpha$ -olefin-containing terpolymers.

**Table 7.1. Properties of Solution Phase Metallocene-catalyzed Ethylene / 1-Pentene /  $\alpha$ -Olefin Terpolymers**

Sample Nr.	1-Pentene/1-Butene (%)		Density (g/cm <sup>3</sup> )	MFI (dg/min.)	Yield Strength (MPa)	Modulus (MPa)	Impact Strength (kJ/m <sup>2</sup> )
1	1.8	0.6	0.941	1.3	16.5	580	14.1
2	5.4	1.8	0.916	0.1	12.9	281	44.4
	1-Pentene/1-Hexene (%)						
3	4.0	0.4	0.924	33	11.4	340	42.6
4	0.7	1.1	0.936	2.9	17.3	496	49.2
5	0.6	0.8	0.939	1.2	19.4	640	43.7
	1-Pentene/1-Octene (%)						<b>52</b>
6	1.4	1.2	0.919	7.0	13.6	416	52.3
7	1.0	0.4	0.944	5.4	16.6	573	9.6

The properties of ethylene/ 1-pentene /  $\alpha$ -olefin terpolymers prepared with metallocene- and a conventional supported Ziegler-Natta catalyst are presented in Tables 7.1 and 7.2 respectively.

**Table 7.2. Properties of Ethylene / 1-Pentene /  $\alpha$ -Olefin Terpolymers Obtained with a Conventional Ziegler-Natta Catalyst**

Sample Nr.	1-Pentene/1-Butene (%)		Density (g/cm <sup>3</sup> )	Process	MFI (dg/min.)	Yield Strength (MPa)	Modulus (MPa)	Impact Strength (kJ/m <sup>2</sup> )
8	3.0	2.4	0.920	Gas	0.9	8.2	211	36.6
9	1.9	1.7	0.927	Gas	3.0	8.9	278	36.8
10	4.0	5.0	0.921	Soln	6.0	7.2	164	27.4
11	4.0	2.0	0.921	Soln	13.8	5.9	180	29.6
12	0.7	6.8	0.919	Soln	12.0	5.7	141	25.0
	1-Pentene/1-Hexene (%)							
13	0.7	0.5	0.949	Slurry	7.7	23.2	843	5.0
14	0.5	5.0	0.919	Gas	2.0	9.88	266	42
15	2.4	1.1	0.922	Gas	0.8	10.5	292	45.6
16	0.4	1.2	0.940	Slurry	10	18.6	610	5.1
17	0.6	1.0	0.939	Slurry	12	17.7	560	6.4
18	3.0	0.3	0.928	Slurry	14	12.7	375	15.4
19	1.0	5.2	0.918	Slurry	29	10.4	192	29
20	0.6	0.9	0.945	Slurry	3.8	17.5	592	3.9
21	3.0	0.3	0.930	Gas	0.5	10.7	308	44.2
22	2.4	2.0	0.922	Gas	4.0	9.3	286	39.3
	1-Pentene/1-Heptene (%)							
23	4.9	1.1	0.915	Slurry	6.0	8.5	302	50.8
24	3.8	3.4	0.909	Slurry	2.1	6.0	315	50.8
25	0.8	4.1	0.915	Slurry	4.5	8.9	320	46.2
	1-Pentene/1-Octene (%)							
26	1.6	2.6	0.917	Slurry	4.0	9.85	294	39.4
27	3.4	2.2	0.919	Slurry	5.6	9.1	292	39.8
28	8.8	12	-	Slurry	85	3.2	187	-
29	1.0	6.0	0.900	Slurry	9.5	9.1	270	-
30	0.6	0.6	0.941	Slurry	2.3	18.8	555	-
31	0.6	3.2	0.919	Soln	3.1	5.0	170	42.2
32	3.8	3.6	0.914	Soln	2.6	7.6	241	38.9
	1-Pentene/1-Nonene (%)							
33	1.4	1.2	0.923	Slurry	4.4	5.5	270	50.5
34	3.6	0.4	0.930	Slurry	5.1	12.5	499	30.0
35	0.3	1.0	0.934	Slurry	3.4	18.2	685	27.1

Apart from the low impact values obtained from 1-hexene containing terpolymers prepared in slurry reactions no substantial difference in properties between terpolymers prepared in slurry, solution and gas phase was observed.

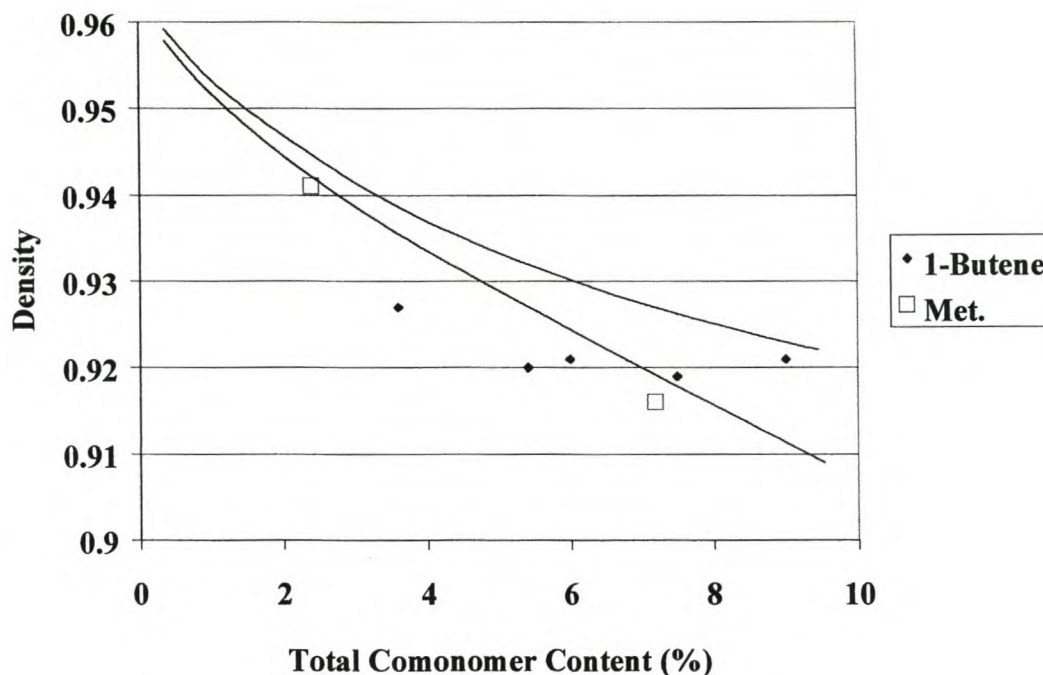


**Figure 7.2. Densities of Ethylene / 1-Pentene / 1-Butene Terpolymers Containing Different Ratios of the Comonomers. The Solid Lines Represent the Trend of the Relevant Copolymers**

In Figure 7.2 the data points for 1-butene containing terpolymers prepared with both the conventional (blue diamonds) and metallocene (open squares) catalysts are presented in comparison to the 1-butene and 1-pentene copolymer density curves. The combination of 1-pentene and 1-butene in the terpolymer seems to evoke some kind of synergistic effect which decreases the terpolymer density more than that obtained for the ethylene / 1-pentene copolymers. As the density is determined by the extent to which crystallinity is destroyed, it seems that the combination of 1-pentene and 1-butene is more effective at disrupting crystallinity. This improved disruption of crystallinity at similar total comonomer content can be realized when the comonomer units are distributed more randomly along the chains. It has been mentioned that 1-butene is inclined to cluster during copolymerization. When the different accessibility

of different active sites in Ziegler-Natta catalysts are considered it can be recognized that some sites are more protected than others, hence the intermolecular heterogeneity of the copolymers prepared with these catalysts. 1-Pentene is more bulky than 1-butene and will therefore be rejected by more sites than those rejecting 1-butene. From these different types of active centers, it was reasoned that three main types of polymer chains can be present in the terpolymers: (a) ethylene homopolymer or low 1-butene content copolymer, (b) ethylene / 1-butene copolymer and (c) ethylene / 1-butene / 1-pentene terpolymer. At similar *total* comonomer content as found in an ethylene / 1-butene copolymer the 1-butene concentration and consequently, also its statistical chance of clustering, is decreased. Those chains containing (mainly) 1-butene as comonomer will therefore have less 1-butene present and as a result be less clustered, *i.e.* the 1-butene units will be more randomly distributed. The same type of active sites, which also copolymerizes 1-butene, will however, still copolymerize all of the 1-pentene.

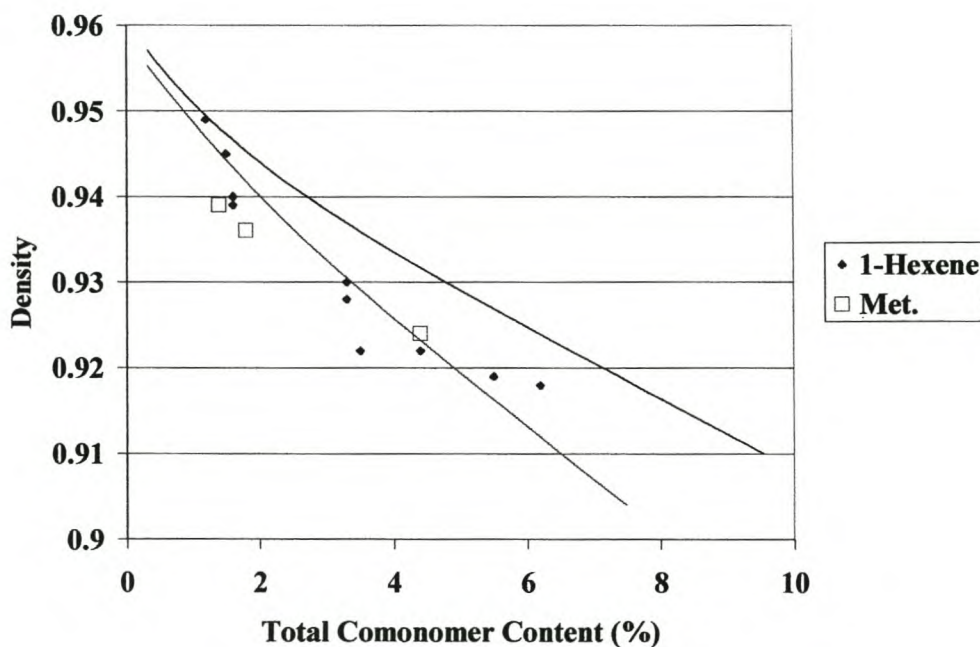


**Figure 7.3. Densities of Ethylene / 1-Pentene / 1-Hexene Terpolymers Containing Different Ratios of the Comonomers. The Solid Lines Represent the Trend of the Relevant Copolymers**

It is not expected that the clustering of comonomer in the chains containing both 1-butene and 1-pentene will be different from the distribution which can be anticipated mathematically (based on amounts of the different comonomers present). The terpolymer chains containing both 1-butene and 1-pentene will therefore, even if the degree of clustering is higher, have a higher comonomer content which contribute towards a lower density. This synergistic effect was also observed by other workers in this field, but no attempt has previously been made to explain this finding [3].

In Figure 7.3, the densities of ethylene / 1-pentene / 1-hexene terpolymers are compared to those of the 1-pentene and 1-hexene containing copolymers. It can be seen that a smaller effect of decreased density was obtained with the 1-hexene containing terpolymers and that the data points of the ethylene / 1-pentene / 1-hexene terpolymer are situated more or less on the ethylene / 1-hexene copolymer density curve. The relative reactivity of 1-pentene is lower than that of 1-butene and it therefore has a lower tendency to cluster. The effect was therefore expected to be smaller than that of the 1-butene containing terpolymers and this was observed.

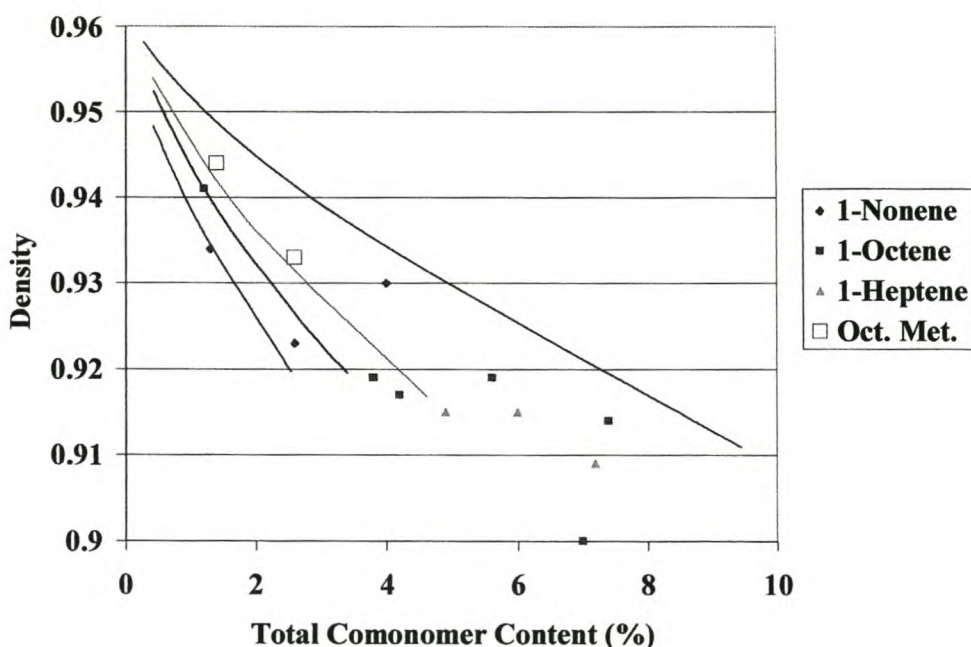


**Figure 7.4. Densities of Ethylene / 1-Pentene / Higher  $\alpha$ -Olefin Terpolymers Containing Different Ratios of the Comonomers. The Solid Lines Represent the Trends of the Relevant Copolymers**

In Figure 7.4 it can be seen that for the terpolymers containing 1-heptene, 1-octene and 1-nonene as third comonomer, no data points lie outside the limits set by the relevant copolymers. It can be appreciated that as the difference in size between the comonomers increases, the more active sites will reject the larger comonomer, resulting in an increase in the amount of the ethylene / 1-pentene copolymer, which has a higher density than the ethylene / higher  $\alpha$ -olefin. The amount of terpolymer containing both 1-pentene and the higher  $\alpha$ -olefin, which has a lower density than the ethylene / higher  $\alpha$ -olefin copolymer, is therefore decreased. The result is that the tendency of the terpolymer chains to decrease density below that of the ethylene / higher  $\alpha$ -olefin copolymer is overpowered by that of the higher density ethylene / 1-pentene copolymer.

### 7.3.2 MECHANICAL PROPERTIES

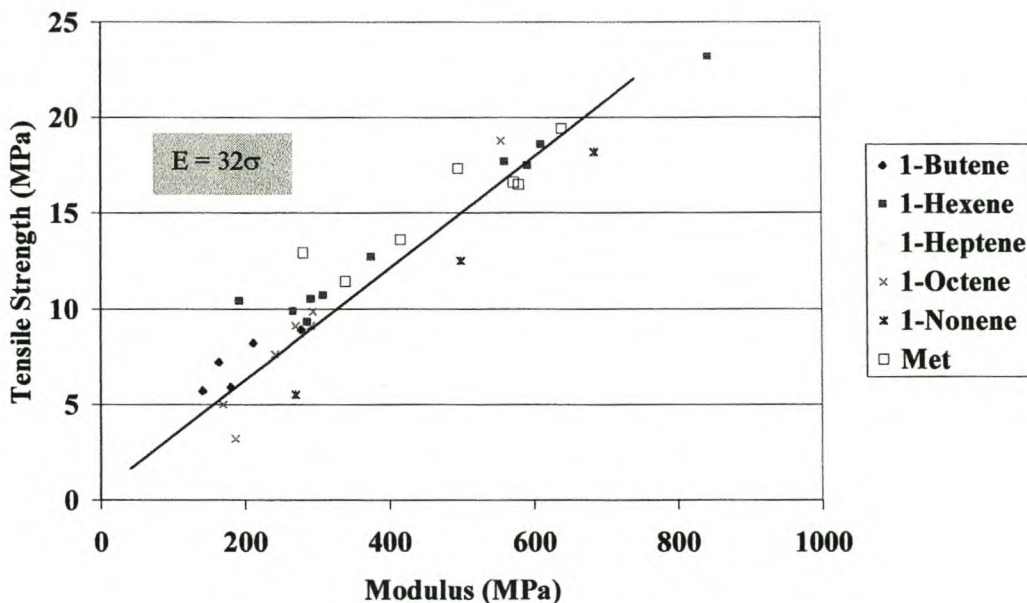


**Figure 7.5. Relationship Between Tensile Strength and Modulus**

The relationship between tensile strength at yield and modulus is presented in Figure 7.5. The correlation does not seem to be as good as that of the copolymers (Chapter 6), but the trend is unmistakable and the equation of the lines are very similar.

### 7.3.2.1 Tensile Strength

Terpolymer data points for tensile strength at yield (blue diamonds) is plotted together with the ethylene / 1-pentene and ethylene / 1-butene copolymer tensile curves, and regardless of the polymerization process employed, the tensile strength follow the same trend as that discussed for density. All data points lie below the ethylene / 1-pentene tensile curve.

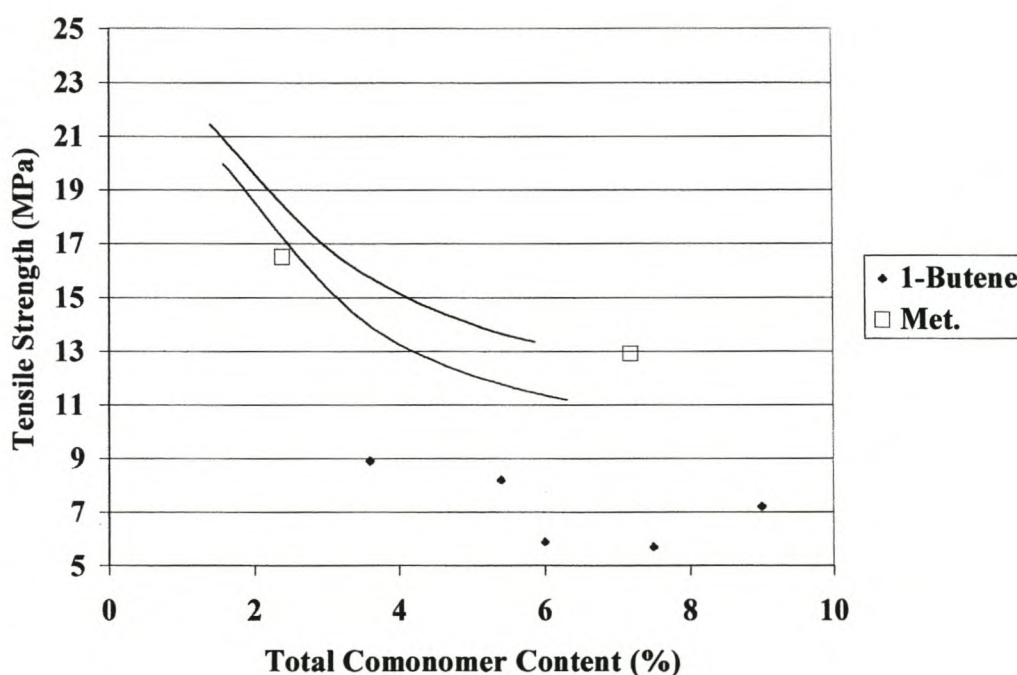


**Figure 7.6. Tensile Strength of Ethylene / 1-Pentene / 1-Butene Terpolymers Containing Different Ratios of the Comonomers. The Solid Lines Represent the Trends of the Relevant Copolymers**

Figure 7.7 presents the tensile strength of ethylene / 1-pentene / 1-hexene terpolymers in comparison with the 1-butene and 1-pentene containing copolymers. It can be seen that the terpolymers containing different amounts of 1-pentene and 1-hexene again follows the trend of density and the data points are scattered around the ethylene / 1-hexene tensile curve.

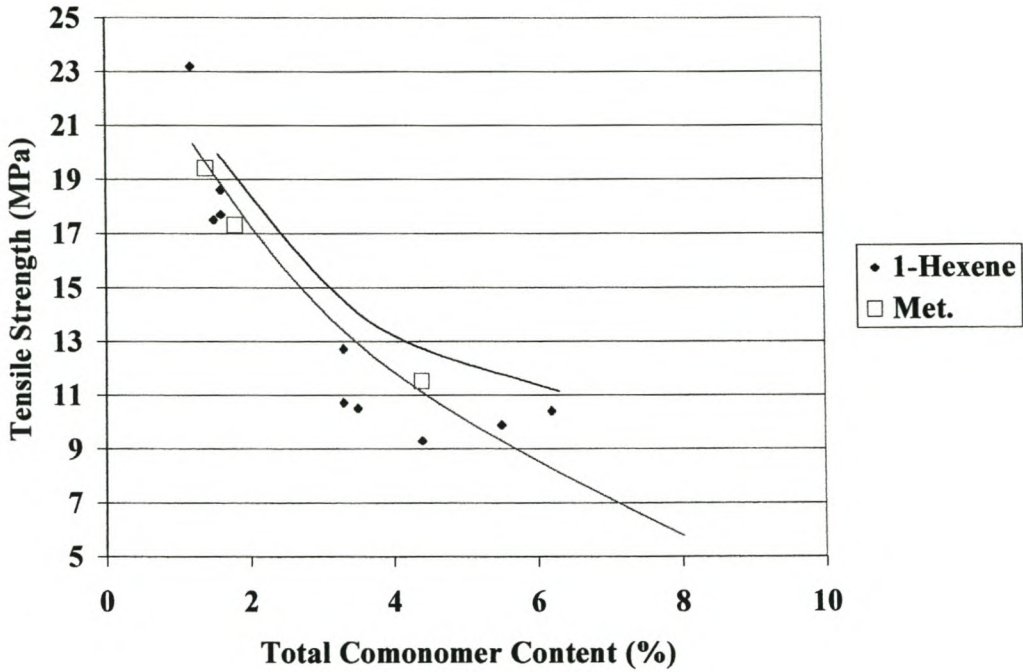


**Figure 7.7. Tensile Strength of Ethylene / 1-Pentene / 1-Hexene Terpolymers Containing Different Ratios of the Comonomers. The Solid Lines Represent the Trends of the Relevant Copolymers**

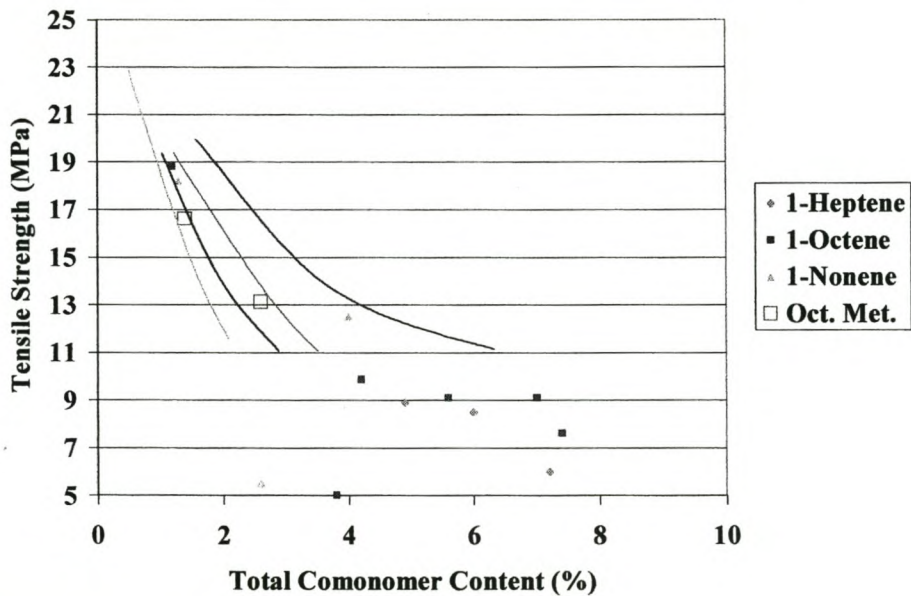


**Figure 7.8. Tensile Strength of Ethylene / 1-Pentene / Higher  $\alpha$ -Olefin Terpolymers Containing Different Ratios of the Comonomers. The Solid Lines Represent the Trends of the Relevant Copolymers**



From Figure 7.8 it is evident that the density / tensile strength relationship can also be observed for the higher  $\alpha$ -olefin terpolymers where all data points are situated between the ethylene / 1-pentene and ethylene /  $\alpha$ -olefin copolymer tensile strength curves.

As can be seen from the tensile plots in Figures 7.6, 7.7 and 7.8, the metallocene-catalyzed terpolymers (open squares) have tensile strengths in the same range as those of the terpolymers prepared with the conventional Ziegler-Natta catalyst. This agrees with the finding mentioned in Section 7.3.1 that similar densities were observed for the terpolymers prepared with the conventional and metallocene catalysts. The high tensile value of the metallocene-catalyzed ethylene / 1-pentene / 1-butene terpolymer having an MFI of 0.1dg/min. can be ascribed to its high molecular weight.

#### **7.3.2.2 Young's Modulus**

As expected, Young's modulus for the terpolymers containing 1-butene as third monomer also follows the trend observed for the density and all 1-butene containing terpolymer moduli are lower than both the ethylene / 1-pentene and ethylene / 1-butene copolymer modulus curves as is shown in Figure 7.9. The values for the metallocene-catalyzed terpolymers seem not to follow the trend for tensile strength and density. However, because the tensile strength of the terpolymer with MFI 0.1dg/min. is high, it is to be expected that the modulus will be higher. That of the terpolymer with modulus 580 MPa follows the tensile strength / modulus relationship and as a result also follows the trend observed for density.

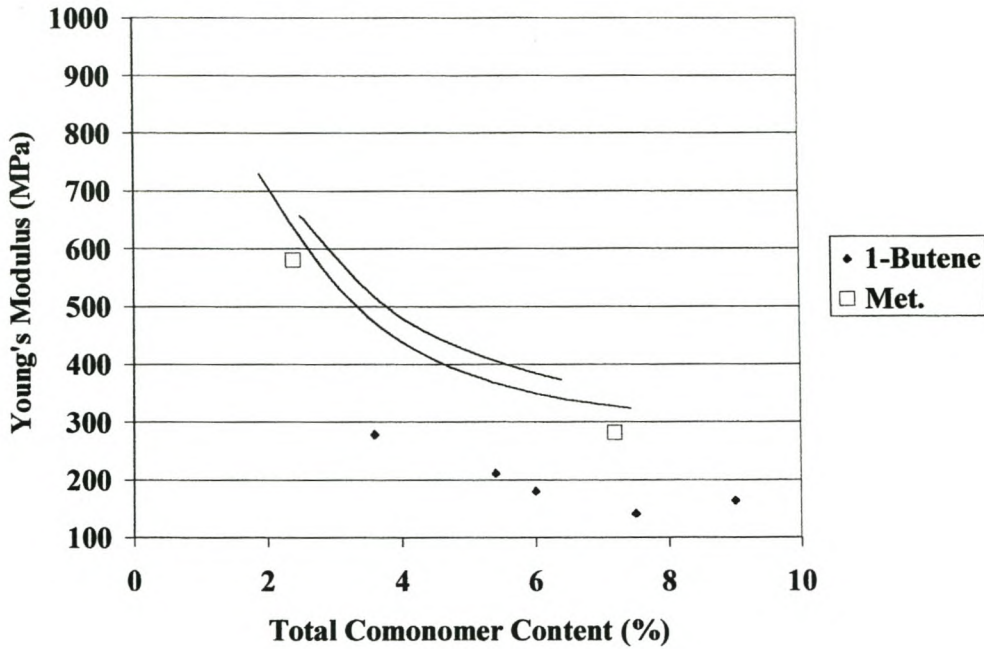


**Figure 7.9. Young's Modulus of Ethylene / 1-Pentene / 1-Butene Terpolymers Containing Different Ratios of the Comonomers. The Solid Lines Represent the Trends of the Relevant Copolymers**

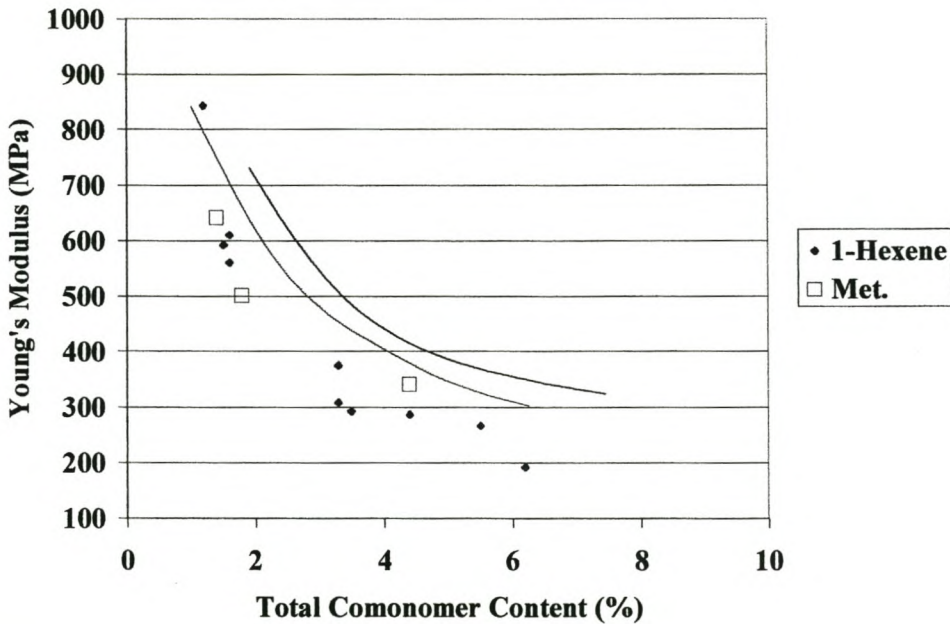


**Figure 7.10. Young's Modulus of Ethylene / 1-Pentene / 1-Hexene Terpolymers Containing Different Ratios of the Comonomers. The Solid Lines Represent the Trends of the Relevant Copolymers**

For the terpolymers containing 1-hexene as third monomer, it can be seen from Figure 7.10 that data points for the modulus are slightly lower than the ethylene / 1-hexene copolymer modulus curve, again emphasizing the synergistic effect observed for the densities of the 1-hexene containing terpolymers.

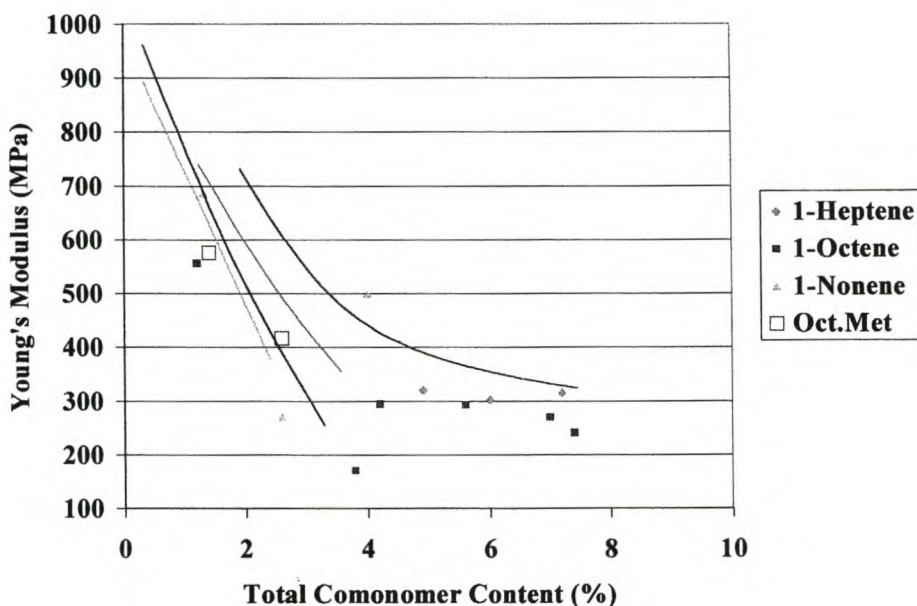


**Figure 7.11. Young's Modulus of Ethylene / 1-Pentene / Higher  $\alpha$ -Olefin Terpolymers Containing Different Ratios of the Comonomers. The Solid Lines Represent the Trends of the Relevant Copolymers**

As can be seen from Figure 7.11, the modulus of terpolymers containing higher  $\alpha$ -olefins as third monomer follow the same trend observed as discussed for density and tensile strength although exceptions do occur. Also, in line with observations made for densities of metallocene-catalyzed terpolymers, these polymers all showed modulus values in the same range as the terpolymers prepared with the conventional Ziegler-Natta catalyst.

It was observed that both tensile strength at yield and Young's modulus of the 1-butene and 1-hexene containing terpolymers were lower than those of the copolymers. A better distribution of comonomer can be deduced from the lower density, which implies that the crystallizable sequences are shorter. In Section 7.3.3 (see later) the results show that these shorter sequences result in decreased melting temperatures.

Understandably, the thinner lamellae are easier to “unravel” during deformation and consequently lead to a decrease in tensile properties. However, such morphology results in improved mobility of the polymer chains as a larger weight fraction is concentrated in the amorphous phase. It should therefore be expected that the terpolymers, depending on their composition, would exhibit more ductile behavior.

### 7.3.2.3 Impact Strength

In Figure 7.12 impact strength of terpolymers containing 1-butene as third monomer is indicated together with the impact curves of the ethylene / 1-pentene and ethylene / 1-butene copolymers.

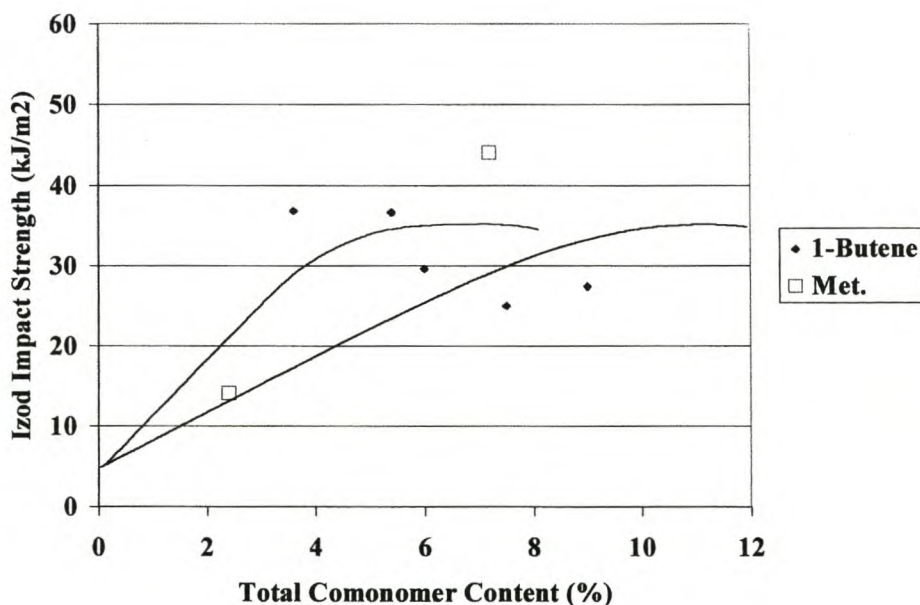


**Figure 7.12. Notched Izod Impact Strength of Ethylene / 1-Pentene / 1-Butene Terpolymers Containing Different Ratios of the Comonomers. The Solid Lines Represent the Trends of the Relevant Copolymers**

The impact values of the Ziegler-Natta catalyzed terpolymers seem to be scattered around the two copolymer curves, but on closer inspection it seems that the impact strength maximum was reached at a total comonomer content of about 4%. As the matrix is plasticized by the increased amount of comonomer, the impact values of the higher content terpolymers decrease. It is known that impact strength is dependent on

molecular weight [4,5] and it is therefore not surprising that the metallocene-catalyzed terpolymer having an MFI of 0.1dg/min. has a higher impact strength than the rest of the terpolymers.

In Figure 7.13 the impact values of the 1-hexene containing terpolymers are shown as compared to those of the 1-pentene and 1-hexene containing copolymers. Disregarding the values of terpolymers prepared in the slurry phase, it again seems that the maximum impact strength of the Ziegler-Natta catalyzed terpolymers was reached at a lower total comonomer content (about 3%) than that observed for the corresponding copolymers. Impact values decrease at total comonomer contents higher than 3%. No significant difference between the impact values of metallocene and Ziegler-Natta catalyzed terpolymers was observed, although the impact maximum was apparently reached at an even lower comonomer content.

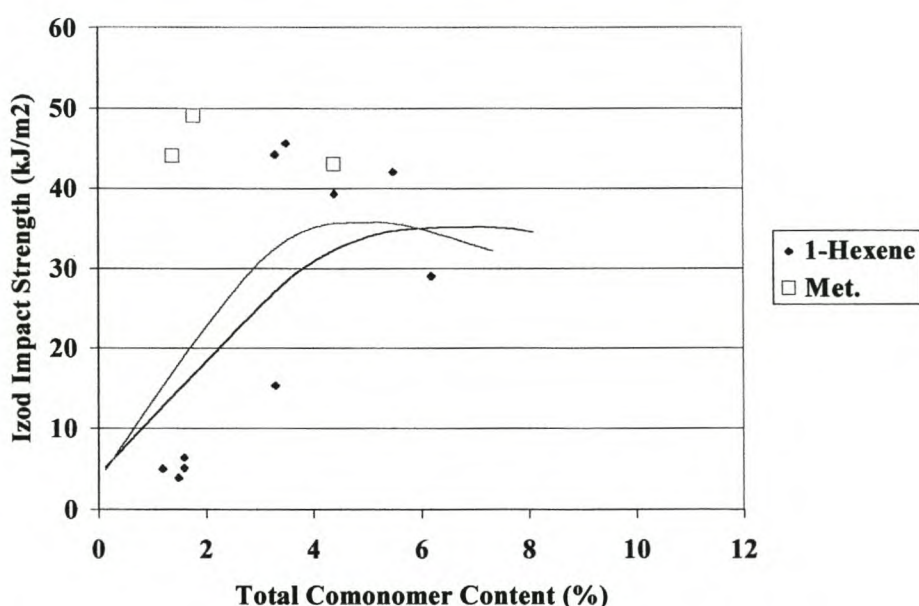


**Figure 7.13. Notched Izod Impact Strength of Ethylene / 1-Pentene / 1-Hexene Terpolymers Containing Different Ratios of the Comonomers. The Solid Lines Represent the Trends of the Relevant Copolymers**

The impact strength of terpolymers containing the higher  $\alpha$ -olefins as third comonomer are shown in Figure 7.14. The data show the same trend as was observed for the density and tensile strength data. Apart from the 1-octene containing

terpolymer prepared with a metallocene catalyst, all terpolymer impact values are situated between the boundaries set by the ethylene / 1-pentene and ethylene / higher  $\alpha$ -olefin copolymer impact curves.

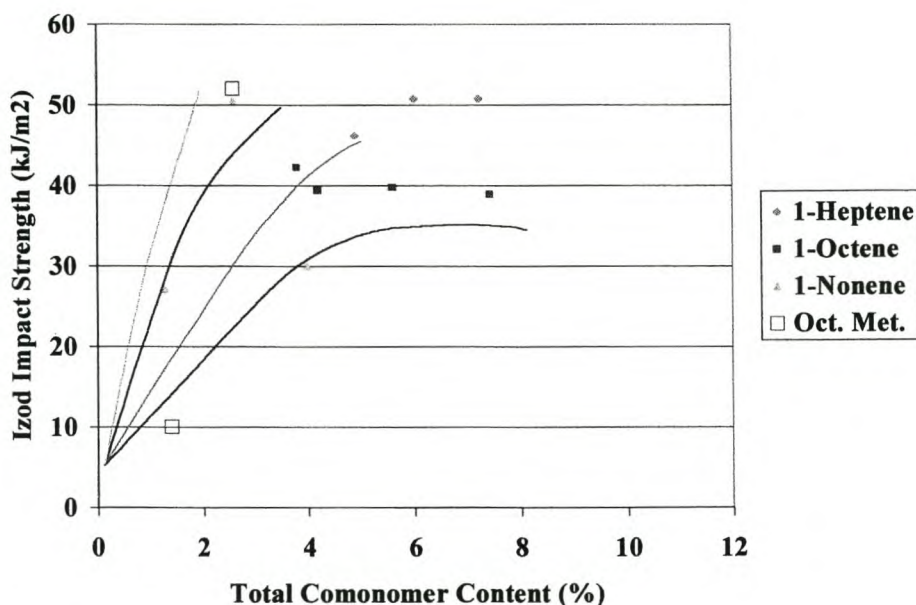


**Figure 7.14. Notched Izod Impact Strength of Ethylene / 1-Pentene / Higher  $\alpha$ -Olefin Terpolymers Containing Different Ratios of the Comonomers. The Solid Lines Represent the Trends of the Relevant Copolymers**

The decrease in crystallinity of the terpolymers is also regarded as being responsible for the higher impact strength observed for most of the terpolymers. The metallocene-catalyzed terpolymers seem in some cases to have higher impact strengths than those prepared with conventional Ziegler-Natta catalysts, but insufficient data is available to confirm this proposal.

### 7.3.3 THERMAL PROPERTIES

It can be seen in all the terpolymer density plots that no clear distinction could be made between the metallocene-catalyzed and conventional Ziegler-Natta catalyzed terpolymers. This is in agreement with what should be expected of terpolymers having similar (more random) comonomer distributions. Because density is directly related to crystallinity and crystallinity to thermal behavior, the influence of

crystallizable sequence lengths on the crystallization and melting behavior of the conventional and metallocene-catalyzed terpolymers is thus expected.

### 7.3.3.1 Ethylene / 1-Pentene / 1-Butene Terpolymers

The thermal properties of the ethylene / 1-pentene / 1-butene terpolymers together with their densities are shown in Table 7.3.

**Table 7.3. Thermal Properties of Metallocene- and Ziegler-Natta Catalyzed Ethylene / 1-Pentene / 1-Butene Terpolymers**

Sample	Composition (%)		Density (g/cm <sup>3</sup> )	Heat of Fusion (J/g)	Melting Peak (°C)	Crystallinity (%)	
	1-Pentene	1-Butene				By Density	By $\Delta H_f$
1	1.8	0.6	0.941	140	120	63.0	48.3
2	5.4	1.8	0.916	80	114	45.9	27.6
<b>Ziegler-Natta</b>							
8	3.0	2.4	0.920	70	120	48.7	24.1
9	1.9	1.7	0.927	84	125	53.6	29.0
10	4.0	5.0	0.921	51	121	49.4	17.6
11	4.0	2.0	0.921	60	122	49.4	20.7
12	0.7	6.8	0.919	50	121	48.0	17.2

As was expected from the densities of the terpolymers, which were lower than those of the ethylene / 1-butene and ethylene / 1-pentene copolymers, the fusion enthalpies of the terpolymers were also lower. The fusion enthalpies of the metallocene- and Ziegler-Natta catalyzed terpolymers are presented in Table 7.3. Contrary to what was expected of the metallocene terpolymers (where the comonomer distribution is more random), the fusion enthalpies of the metallocene terpolymers are *higher* than those with similar comonomer content prepared with a Ziegler-Natta catalyst. Fusion enthalpy is expressed as the total amount of heat necessary to completely melt a unit weight of polymer. The higher fusion enthalpies of the metallocene terpolymers may indicate that the crystallites (although they are thinner and have lower melting temperatures) are less flawed. This may be attributed to crystallizable sequences of similar lengths building up the crystallite. In homogeneous copolymers, the comonomer distribution, and consequently also the crystallizable sequence length distribution, is narrow. This is not the case for heterogeneous copolymers and chains

X

containing very long and very short crystallizable sequences may cocrystallize which leads to imperfections when short sequences are built into or trapped in the crystal.

Crystallinity was determined from density and fusion enthalpy as was done for the copolymers described in Chapter 6. The terpolymers also comprise crystalline and amorphous regions with room temperature densities of 1.00 g/cm<sup>3</sup> and 0.855 g/cm<sup>3</sup> for the crystalline and amorphous phases respectively [6]. By measuring the overall density of a copolymer, crystallinity can be calculated using the formula:

$$w^c = \rho_c (\rho - \rho_a) / \rho (\rho_c - \rho_a) \quad (7.1)$$

where  $\rho_c$  is the density of the crystalline phase,  $\rho_a$  the density of the amorphous phase and  $\rho$  the measured density of the copolymer [7]. The terpolymers of different densities require different energies to melt the crystalline regions. By comparing the heat of fusion of a terpolymer to that of a 100% crystalline phase, crystallinity can also be determined from:

$$w^c = 100 \cdot \Delta H_f / \Delta H_{fC} \quad (7.2)$$

where  $\Delta H_{fC}$  is the heat of fusion of the crystalline phase, taken as 290 J/g [8]. Calculated crystallinities are shown in Table 7.3. Similar to that found for the copolymers, crystallinities calculated from density were generally higher than those obtained from thermal data. This is in agreement with the observation reported by Mandelkern *et al.* [9]. The crystallinities calculated using fusion enthalpy was expected to be lower than those calculated from density because crystallization was stopped at 50°C.

The melting temperatures of the samples prepared with the Ziegler-Natta catalyst are only modestly sensitive towards the amount of comonomer introduced. Melting temperatures decreased rapidly from about 135°C (for the homopolymer) after introduction of comonomer; thereafter the melting temperature remained nearly constant. Comparison of the terpolymers prepared with the Ziegler-Natta catalyst and the copolymers show in general, that the melting temperatures of the terpolymers are



slightly lower and are spread over a wider range than those of the copolymers. During crystallization, very long and very short crystallizable sequences are responsible for a range of lamellar thicknesses, the thick ones having higher melting temperatures than the thinner ones [10]. This results in a range of melting temperatures. Thus, as discussed for copolymers, the decreased melting temperatures can only be ascribed to the thinner lamellae caused by a decreased length of crystallizable sequences. This can be realized if the comonomer units are less clustered, resulting in increased separation between comonomer units in the terpolymer chains. This consequently decreases the length of the crystallizable ethylene sequences. However, the decrease in melting temperature is less than for the metallocene-catalyzed terpolymers which indicates that, although a higher degree of randomness was apparently achieved by terpolymerization with the Ziegler-Natta catalyst, the latter polymers still contain a substantial amount of intramolecular heterogeneity.

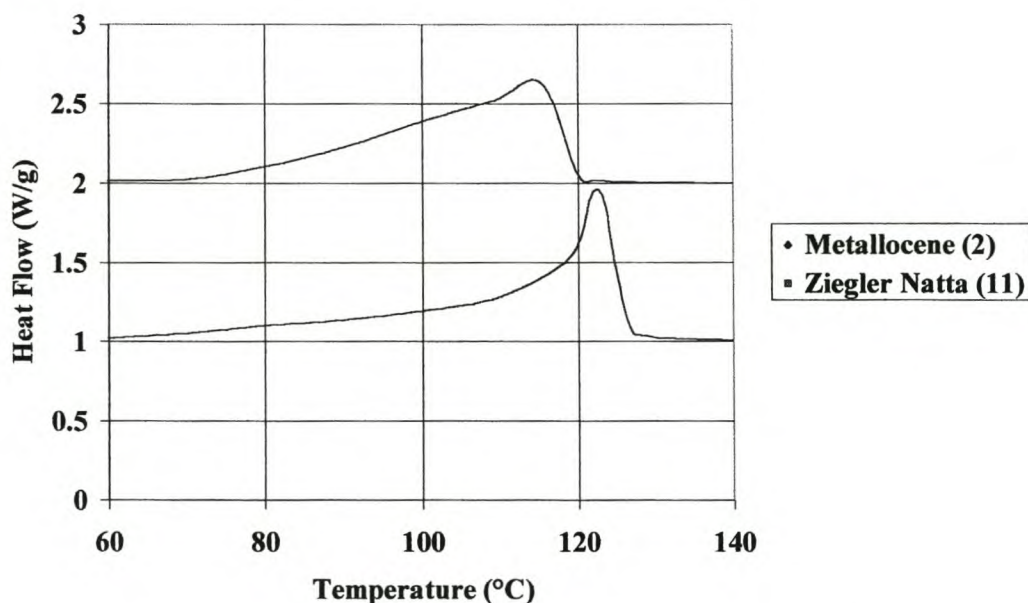


**Figure 7.15. Comparison of the Melting Curves of Metallocene- and Ziegler-Natta Catalyzed Ethylene / 1-Pentene / 1-Butene Terpolymers**

In Figure 7.15, the melting curves of samples 2 and 11 are shown. Both have similar total comonomer content, but melting peaks as well as peak widths are very different. The metallocene-catalyzed sample 2 has a lower melting temperature as well as a

broader melting peak which indicates that its comonomer distribution is more random. From the DSC curves of the terpolymers prepared with the Ziegler-Natta catalyst a narrow, high-temperature peak together with a very broad, low-temperature shoulder were observed. This shoulder, resulting primarily from shorter lengths of crystallizable sequences [10], and thus a higher concentration of comonomer, is not high enough to affect the width of the primary high-temperature peak. Randomness within the Ziegler-Natta catalyzed terpolymers could thus not be assessed through the differences in the widths of the high-temperature peaks.

At the cooling rate of 20°C/min. used, the low- and high-temperature peaks could in most cases not be resolved. Some of the terpolymers were therefore cooled from the melt at a rate of 0.3°C/min. in an attempt to separate these peaks in order to determine their separate melting temperatures. The results are presented in Table 7.4.

**Table 7.4. Thermal Properties of Metallocene- and Ziegler-Natta Catalyzed Ethylene / 1-Pentene / 1-Butene Terpolymers Cooled at a Rate of 0.3°C/min.**

Sample Nr.	Composition (%)		Heat of Fusion (J/g)	Melting Peaks (°C)	Low / High Ratio
	1- Pentene	1- Butene			
2	5.4	1.8	132	119/104	65/35
<b>Ziegler-Natta</b>					
8	3.0	2.4	101	123/110	56/44
9	1.9	1.7	111	124/112	48/52
11	4.0	2.0	71	124/114	58/42
12	0.7	6.8	63	124/115	60/40

In general, higher melting temperatures and heats of fusion were obtained at lower cooling rates. Crystallization is a nucleation-controlled process [11] and lamellar thickness is related to the critical size of the nucleus. At low cooling rates, *i.e.* low degrees of supercooling, the critical size of the nucleus is larger than that formed at a higher degree of supercooling. This results in an increased lamellar thickness and thus a higher melting temperature. In addition, by decreasing the cooling rate, sufficient time is allowed for crystallizable sequences to be sucked in by the growing crystal face through the viscous melt and not getting trapped prematurely in the amorphous phase. This slow crystallization also allows for the non-crystallizable

material to be excluded from the growing crystal face [12]. This is not possible during rapid crystallization when the increasing melt viscosity decreases chain mobility.

As can be seen from Table 7.4, it is possible to separate the low- and high temperature peaks by decreasing the cooling rate. In Figure 7.16 the DSC traces of samples 2 and 8 from Table 7.3, cooled from the melt at the normal 20°C/min. and those of the corresponding samples from Table 7.4, cooled at a rate of 0.3°C/min. The data show improved resolution between the melting temperatures of the two phases represented by the low and high temperature events.

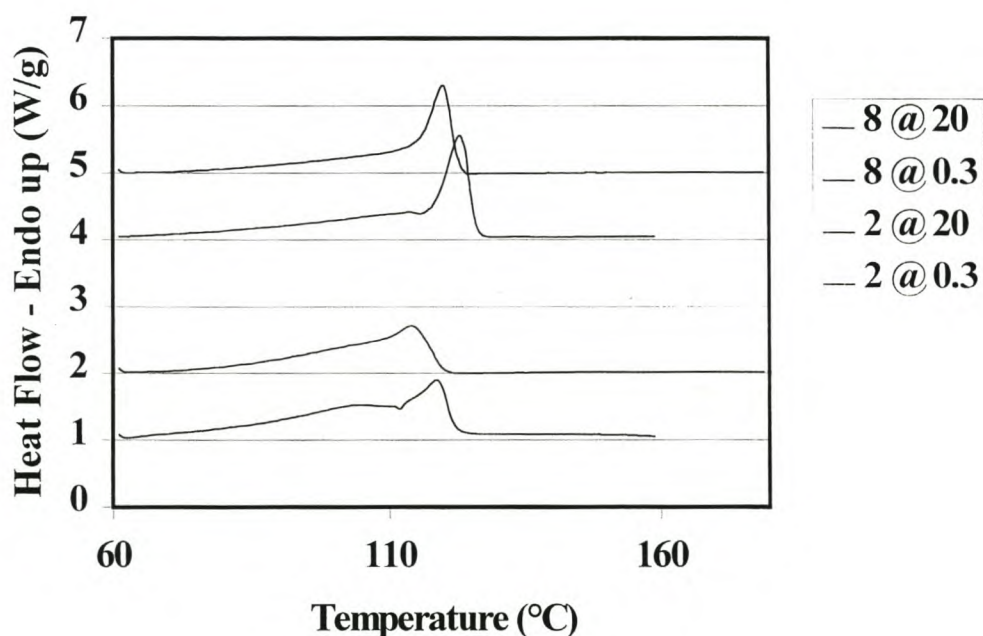


**Figure 7.16. Comparison of DSC Curves of Metallocene and Ziegler-Natta Catalyzed Terpolymers Cooled at Different Rates**

The widths of the melting curves of the metallocene-catalyzed terpolymer which suggest that this terpolymer has a homogeneous comonomer distribution are immediately apparent from Figure 7.16. The melting curves of the Ziegler-Natta catalyzed samples on the other hand (sample 8, Figure 7.6), are dominated by a

narrow, high-temperature peak. As mentioned in the discussion of the single-peaked melting curves obtained at fast cooling rates, randomness of these terpolymers could not be assessed through the differences in their high-temperature peak widths. However, the contribution of the low-temperature peak is often not realized. The total area under the curves of the slow-cooled samples shown in Figure 7.16 can be divided into a low-temperature peak and a high-temperature peak. Judged from the areas under the low and high temperature melting peaks of these slow-cooled samples, it was determined that on average, about 50% of the heat necessary to completely melt these terpolymers is consumed by the broad, low temperature peaks. In the metallocene-catalyzed polymer, the low-temperature peak constitutes about 65% of the total heat. It can thus be seen that even a small low-temperature peak has a substantial effect on the thermal behavior of a copolymer even though its contribution is often not reflected in the single melting temperature.

### 7.3.3.2 Ethylene / 1-Pentene / 1-Hexene Terpolymers

Thermal properties of ethylene / 1-pentene / 1-hexene terpolymers are presented in Table 7.5.

**Table 7.5. Thermal Properties of Metallocene- and Ziegler-Natta Catalyzed Ethylene / 1-Pentene / 1-Hexene Terpolymers**

Sample Nr.	Composition (%)		Density (g/cm <sup>3</sup> )	Heat of Fusion (J/g)	Melting Peak (°C)	Crystallinity (%)	
	1- Pentene	1- Hexene				By Density	By $\Delta H_f$
3	4.0	0.4	0.924	94	114/106	51.5	32.4
<b>Ziegler-Natta</b>							
13	0.7	0.5	0.949	144	124	68.3	49.7
14	0.5	5.0	0.919	86	122	48.0	29.7
15	2.4	1.1	0.922	105	122	50.1	36.2
21	3.0	0.3	0.930	114	123	55.6	39.3

Comparing these terpolymers, with the ethylene / 1-hexene copolymers it can be seen that fusion enthalpies are slightly lower. This finding is similar to that observed for the 1-butene containing terpolymers where a synergistic effect was also observed from the combination of 1-butene and 1-pentene.

Similar to the 1-butene containing terpolymers it can again be observed from Table 7.5 that the position of the melting peaks of the heterogeneously branched samples prepared with the Ziegler-Natta catalyst are only modestly sensitive towards degree of branching. Melting temperatures decreased rapidly from about 135°C (for the homopolymer) after introduction of comonomer; thereafter the melting temperature remained nearly constant. However, melting temperatures of the terpolymers are once again lower than those of the ethylene / 1-hexene copolymers discussed in Chapter 6, but not as low as that of the metallocene-catalyzed terpolymer. This is thus a further indication that a more random comonomer distribution is obtained by the combined introduction of 1-pentene and 1-hexene in the ethylene backbone. For the Ziegler-Natta catalyzed terpolymers, only single melting peaks were obtained when a cooling rate of 20°C/min. was used.

Similar to Figure 7.15, the melting curves of two samples prepared by a metallocene and a Ziegler-Natta catalyst respectively, both having similar total comonomer content, is shown in Figure 7.17. The metallocene-catalyzed sample 3 has a lower melting temperature as well as a broad, double melting peak which indicates that its comonomer distribution is more random than that of sample 21.

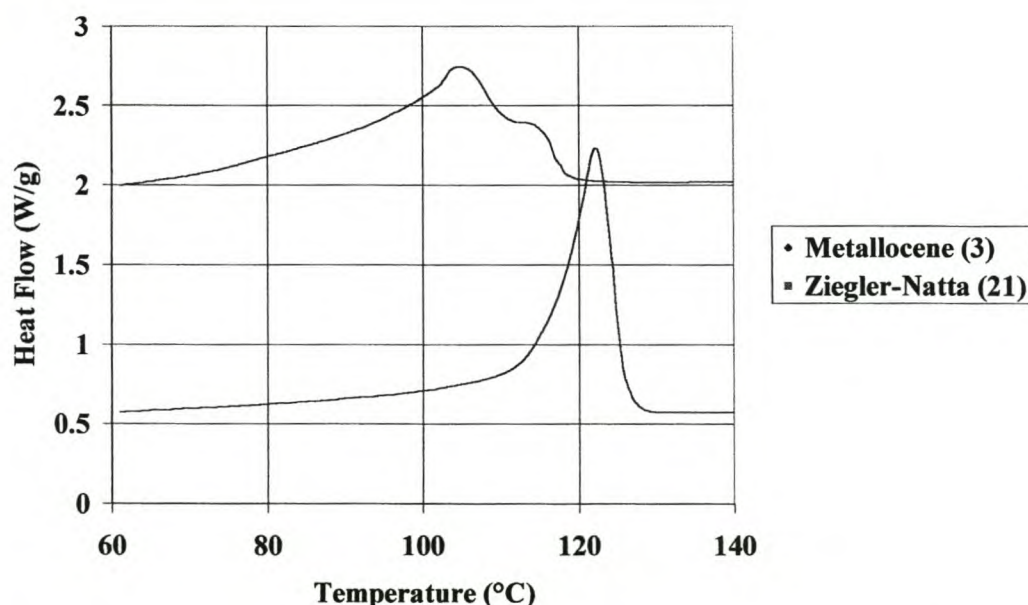


**Figure 7.17. Comparison of the Melting Curves of Metallocene- and Ziegler-Natta Catalyzed Ethylene / 1-Pentene / 1-Hexene Terpolymers**

In a separate experiment, similar to that performed on some of the ethylene / 1-pentene / 1-butene terpolymers, some of the ethylene / 1-pentene / 1-hexene terpolymers were crystallized at a rate of 0.3°C/min., the results of which are shown in Table 7.6.

**Table 7.6. Thermal Properties of Metallocene- and Ziegler-Natta Catalyzed Ethylene / 1-Pentene / 1-Hexene Terpolymers Crystallized at 0.3°C/min.**

Sample Nr.	Composition (%)		Heat of Fusion (J/g)	Melting Peaks (°C)	Low / High Ratio
	1- Pentene	1- Hexene			
3	4.0	0.4	94	115/104	90/10
<b>Ziegler-Natta</b>					
14	0.5	5.0	105	123/113	56/44
15	2.4	1.1	114	125/115	52/48
21	3.0	0.3	117	126/*	-

\* Not possible to separate from main peak

The terpolymers crystallized under these conditions, also revealed separate low and high temperature peaks. The exception was sample 21 which contained a high proportion of one of the comonomers. From the increase in fusion enthalpy it can be seen that the slower crystallization rate improved the extent of crystallization. The melting peaks are slightly higher as a result of the larger nuclei formed at the lower undercooling which resulted in thicker, higher-melting lamellae. The ratios between the low- and high temperature peaks of the Ziegler-Natta catalyzed terpolymers was about 1:1. This is very similar to that of the 1-butene containing terpolymers prepared with the same catalyst.

### 7.3.3.3 Ethylene / 1-Pentene / Higher $\alpha$ -Olefin Terpolymers

Thermal properties of ethylene / 1-pentene / higher  $\alpha$ -olefin terpolymers are presented in Table 7.7. Similar to that observed for the 1-butene- and 1-hexene containing terpolymers, the melting temperatures of the Ziegler-Natta catalyzed terpolymers presented in Table 7.7 rapidly decrease on introduction of a small amount of comonomer. Thereafter only a slow decrease in the melting peaks was observed. Melting temperatures are also lower than copolymers containing these C<sub>7</sub> to C<sub>9</sub> higher

$\alpha$ -olefins (Chapter 6). As expected, calculated crystallinities based on density are generally lower than those calculated from fusion enthalpy [9].

**Table 7.7. Thermal Properties of Metallocene- and Ziegler Natta Catalyzed Ethylene / 1-Pentene / Higher  $\alpha$ -Olefin Terpolymers**

Sample Nr.	Composition (%)		Density (g/cm <sup>3</sup> )	Heat of Fusion (J/g)	Melting Peak (°C)	Crystallinity (%)	
	1- Pentene	1- Heptene				By Density	By $\Delta H_f$
Ziegler-Natta							
23	4.9	1.1	0.915	63	124	45.2	21.7
24	3.8	3.4	0.909	50	123	40.9	17.2
Metallocene	1-Pentene	1-Octene					
7	1.0	0.4	0.944	137	123	65.0	47.2
Ziegler-Natta							
27	3.4	2.2	0.919	89	122	48.0	30.7
28	8.8	12	-	33	122	-	11.3
29	1.0	6.0	0.900	40	124	34.5	13.7
30	0.6	0.6	0.941	153	128	63.0	52.8
31	0.6	3.2	0.919	71	123	48.0	24.5
32	3.8	3.6	0.914	83	123	44.5	28.6
Ziegler-Natta	1-Pentene	1-Nonene					
33	1.4	1.2	0.923	43	123	50.8	23.8
34	3.6	0.4	0.930	39	122	55.6	37.2

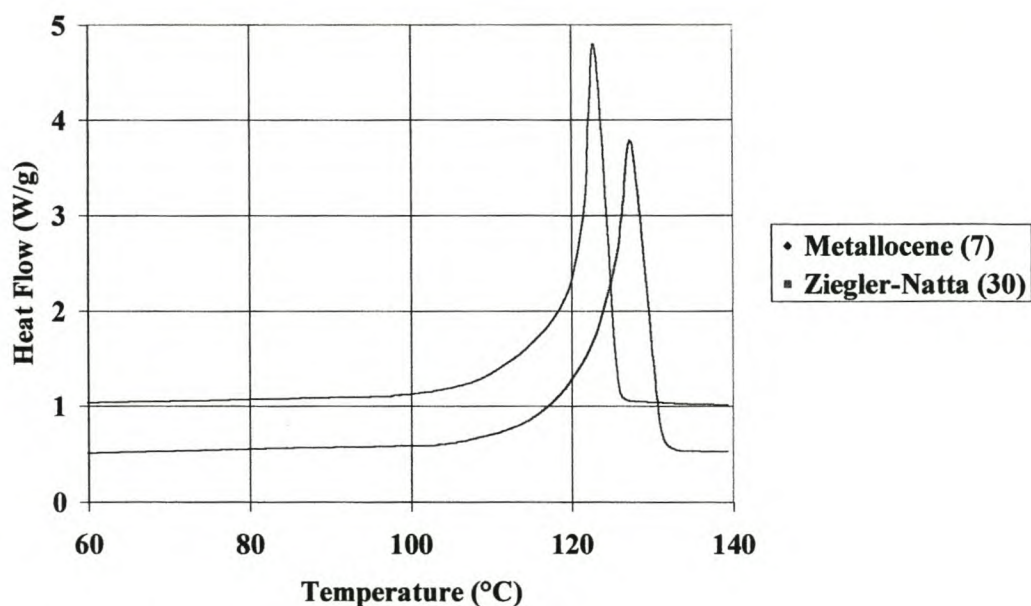


**Figure 7.18. Comparison of the Melting Curves of Metallocene- and Ziegler-Natta Catalyzed Ethylene / 1-Pentene / 1-Octene Terpolymers**

Samples 7 and 30, prepared using a metallocene and Ziegler-Natta catalyst respectively, have comparable total comonomer contents, densities and crystallinities. Their melting peaks are very similar in shape, but the melting peak temperatures are different (Figure 7.18).

For these two terpolymers, the difference in randomness is therefore clearly shown by the decreased melting temperature. This indicates that, even at these comonomer concentrations, clustering which seem unlikely, does exist. Some chains, produced by unprotected active sites, contain high amounts of comonomer which increases the possibility of clustering. Therefore, even if the comonomer distribution in these terpolymers are more random, as is indicated by their lower densities and melting temperatures, the effect is only mirrored by the chains containing high amounts of comonomer. No observable effect is expected from the primarily unbranched chains produced by the protected active sites.

#### 7.3.4 MICROSTRUCTURE

The depression of melting temperatures (of the high temperature peaks), observed when the co and the corresponding terpolymers containing similar total amounts of comonomer are compared, support the notion that the copolymerization of ethylene with 1-pentene (together with a third  $\alpha$ -olefin) resulted in a more random distribution of comonomer units along the chain. However, more direct evidence can be obtained by calculating the sequence lengths  $\tilde{n}_x$  of the different monomers from the NMR spectra of the terpolymers. Comparison of the sequence length with similar calculations done for the copolymers described in Chapter 6 was done. The equations:

$$\tilde{n}_E = (N_{EE} + 0.5N_{EC})/0.5 N_{EC} \quad (7.3)$$

$$\tilde{n}_C = (N_{CC} + 0.5N_{EC})/0.5 N_{EC} \quad (7.4)$$

were used. Here  $N_{EE}$  and  $N_{CC}$  are the intensities of the CH<sub>2</sub> carbons of ethylene or the comonomer centered dyads EEEE, EEEC, CEEC and CCCC, CCCE, ECCE



respectively and  $N_{EC}$  is the intensity of the  $CH_2$  carbons of the EECE, EECC, CECE, CECC dyads [13]. The calculated sequence lengths for the copolymers where the signal to noise ratio allowed accurate determination of the appropriate peaks, are shown in Table 7.8. For these calculations, the total intensity of all the  $CH_2$  carbons of the EECE, EECC, CECE, CECC dyads of both comonomers were used to determine a single value for  $N_{EC}$ . For all the comonomers the  $CH_2$  carbons, indicating clustered sequences, are downfield ( $< 40$  ppm) except for 1-butene containing terpolymers. It was thus not possible to determine 1-butene sequence lengths although the 1-pentene sequences could be estimated and are shown in brackets in Table 7.8. For the other terpolymers, where sequences were too short to determine the intensities of the  $CH_2$  carbons of the comonomer centered dyads CCCC, CCCE, ECCE accurately, a value of 1 was introduced to indicate isolated branches.

**Table 7.8. Comonomer Sequence Distribution of Ziegler-Natta Catalyzed Ethylene / 1-Pentene /  $\alpha$ -Olefin Terpolymers**

Sample Nr.	1-Pentene / 1-Butene (%)		$\bar{n}_E$	$\bar{n}_C$	Maximum Average Lamellar Thickness (Å)
8	3.0	2.4	33.2	-	85
9	1.9	1.7	65.6	-	167
10	4.0	5.0	16.5	(1.16)	42
11	4.0	2.0	19.6	(1.21)	50
12	0.7	6.8	17.1	-	43
	1-Pentene / 1-Hexene (%)				
15	2.4	1.1	64.1	1.0	163
17	0.6	1.0	247.6	1.0	631
18	3.0	0.3	56.7	1.0	144
19	1.0	5.2	41.2	1.18	105
22	2.4	2.0	29.5	1.0	75
	1-Pentene / 1-Heptene (%)				
23	4.9	1.1	31.6	1.0	80
24	3.8	3.4	20.3	1.05	52
	1-Pentene / 1-Octene (%)				
26	1.6	2.6	33.7	1.0	85
27	3.4	2.2	23.9	1.0	60
29	1.0	6.0	18.5	1.0	47
31	0.6	3.2	30.4	1.0	77
32	3.8	3.6	19.2	1.17	49
	1-Pentene / 1-Nonene (%)				
33	1.4	1.2	27.4	1.0	70

Similar to the calculations for the copolymers discussed in Chapter 6, the *average* maximum lamellar thicknesses for the terpolymers were also determined from the chain repeat distance  $c = 2.55 \text{ \AA}$ , taken from the polyethylene crystal [14,15], and the average ethylene sequence length  $\bar{n}_E$ .

In Figure 7.19, the ethylene sequence lengths of 1-butene and 1-octene containing terpolymers are compared with the corresponding copolymers. It can be seen that the ethylene / 1-pentene / 1-butene terpolymers have slightly shorter ethylene sequences lengths than the ethylene / 1-butene copolymers. This is in agreement with the discussion on density regarding the dilution and consequent decreased clustering for these terpolymers.

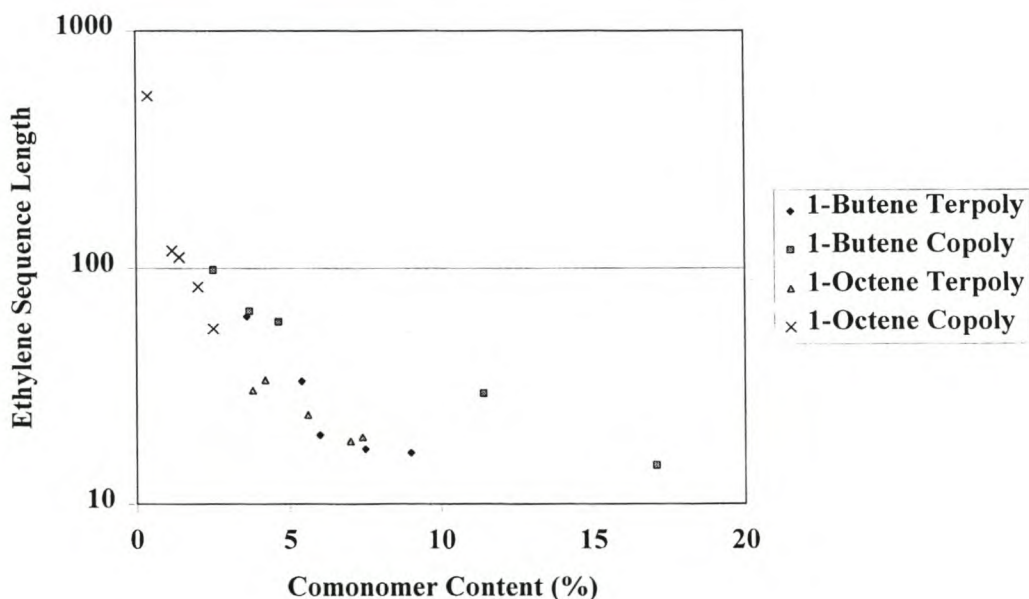


**Figure 7.19. Comparison Between Ethylene Sequence Length of 1-Butene and 1-Octene Containing Co- and Terpolymers**

A comparison of the ethylene sequence lengths of the copolymers (Table 7.4, Chapter 6) with those of the terpolymers (Table 7.9), revealed that sequence lengths become gradually shorter when higher  $\alpha$ -olefins are used although the differences are not drastic (Figure 7.19). From the discussion regarding the effect of the ratio between the different polymer chains present resulting from the different degrees of protection of different active sites, this is not unexpected. The terpolymers prepared with the

higher  $\alpha$ -olefins contain a larger fraction of ethylene / 1-pentene copolymer than those prepared using the lower  $\alpha$ -olefins. Randomness is thus only affected as a result of the progressively more random incorporation of the higher  $\alpha$ -olefins.

## 7.4 CONCLUSIONS

Polymer properties change in relatively large steps as different comonomers are introduced into the polymer chain. This may not be desirable. In order to erase these boundaries between different comonomers and to obtain a full range of properties, a third monomer can be introduced during polymerization to “dilute” the effect of the primary comonomer without substantially changing the polymerization process. Terpolymerization can therefore be employed for the production of different polymer grades which differ only slightly from the copolymer grades. Thus a smoother transition towards totally different grades of polymer using increasingly higher amounts of the third monomer is possible. A comprehensive study of all possible combinations of monomers is extremely time consuming. In order to illustrate the possibilities of this effect the presence of a third monomer on the properties of ethylene / 1-pentene copolymers was investigated.

It was expected that the introduction of a third  $\alpha$ -olefin during an ethylene / 1-pentene copolymerization reaction will produce a terpolymer with density and related properties similar to the mathematical average between those of the relevant copolymers. This was only observed for the terpolymers containing 1-heptene, 1-octene and 1-nonene. The 1-butene containing terpolymers have densities well *below* the expected values while the 1-hexene containing terpolymers have values very similar to that of the ethylene / 1-hexene copolymer densities, but still below the expected values. This divergence of properties was attributed to the different types of polymer chains produced which results from the different accessibility of the active sites present on a Ziegler-Natta catalyst. Larger comonomer molecules will be rejected by more active sites than the smaller molecules resulting in mainly three types of polymer chains: (a) ethylene homopolymer or low comonomer content copolymer, (b) ethylene / lower  $\alpha$ -olefin copolymer and (c) ethylene / lower  $\alpha$ -olefin / higher  $\alpha$ -olefin terpolymer. The resulting terpolymer will therefore display properties of a blend of these components. The ratio between these components in the final terpolymer depends, under similar comonomer feed concentrations, primarily on the size of the higher  $\alpha$ -olefin.

Properties related to density such as tensile strength and modulus all show the same trend. In particular the 1-butene and 1-hexene containing terpolymers show a synergistic effect and values for the terpolymers containing the higher  $\alpha$ -olefins are situated between the limits set by the relevant copolymers

The 1-butene and 1-hexene containing terpolymers seem to have reached an impact strength maximum at a total comonomer content lower than that of the 1-pentene copolymers. This also indicates an enhanced effect from the combined use of 1-pentene with these  $\alpha$ -olefins. No substantial difference between impact strengths of co- and terpolymers prepared with higher  $\alpha$ -olefins was observed.

The melting peaks of the samples prepared with the Ziegler-Natta catalyst are only modestly sensitive towards the amount of comonomer introduced. Melting temperatures decreased rapidly from about 135°C (homopolymer) after introduction of comonomer; thereafter they remained nearly constant. Comparison of the terpolymers prepared with the Ziegler-Natta catalyst with the copolymers shows that, in general, the melting temperatures of the terpolymers are slightly lower and broader melting range than those of the copolymers. The decreased melting temperatures are ascribed to the thinner lamellae caused by decreased length of crystallizable sequences. The decrease in melting temperature was, however, not as significant as for the metallocene-catalyzed terpolymers. This indicates that, although a higher degree of randomness was achieved by terpolymerization with the Ziegler-Natta catalyst, the latter polymers still contain a substantial amount of heterogeneity.

At increased crystallization times separation of the low and high temperature peaks was achieved. This was accomplished by decreased cooling rates from which higher melting temperatures and heats of fusion were obtained. The low-temperature peaks result mainly from thinner, less perfect lamellae i.e. shorter crystallizable sequences. From the areas under the low- and high temperature melting peaks it was observed that about 50% of the heat necessary to completely melt these terpolymers is consumed by the broad, low temperature peaks. In a metallocene-catalyzed polymer of similar total comonomer content, the low-temperature peak required about 65% of the total heat uptake.

Direct evidence of sequence lengths was obtained from calculations from  $^{13}\text{C}$  NMR spectra of the terpolymers. It was found that the crystallizable ethylene sequences of 1-butene containing terpolymers were shorter than those of the corresponding copolymers, which indicates that the introduction of a third comonomer resulted in an increase in randomness. Crystallizable sequence lengths became gradually shorter when higher  $\alpha$ -olefins were used in co- and terpolymers. Crystallizable sequences were shorter for the terpolymers.

## 7.5 REFERENCES

1. Tincul I., Joubert D.J., *Advances in Polyolefins II*, ACS, Napa, CA, Oct 24 – 27 (1999)
2. Grant D.M., Paul E.G., *J. Am. Chem. Soc.*, **86**, 2984 (1964)
3. Durand D.C., Morterol F.R.M.M., *EP 016 4215 A1*, BP Chemicals, London (1985)
4. Kissin Y.V., *Olefin Polymers (Polyethylene)* in *Encyclopedia of Chemical Technology*, Kroschwitz JI., Exec. Ed., John Wiley & Sons, New York, **17**, 724 (1995)
5. Bogdanov B.G., Michailov M., *Properties of Polyolefins* in *Handbook of Polyolefins – Synthesis and Properties*, Vasile C., Seymour R.B., Eds., Marcel Dekker Inc., New York, 295 (1993)
6. Fatou J.G., *Morphology and Crystallization in Polyolefins* in *Handbook of Polyolefins - Synthesis and Properties*, Vasile C., Seymour R.B., Eds., Marcel Dekker Inc., New York, 155 (1993)
7. Faucher J.A., Reding F.P., *Relationship Between Structure and Fundamental Properties* in *Crystalline Olefin Polymers Part I*, Ed. Raff R.A.V., Doak K.W., John Wiley & Sons, New York, 677 (1965)
8. Burfield D.R., Kashiva N., *Makromol. Chem.*, **186**, 2657 (1985)
9. Mandelkern L., Allou A.L., Gopalan M., *J. Phys. Chem.*, **72**, 1, 309 (1968)
10. Hingman R., Rieger J., Kersting M., *Macromolecules*, **28**, 3801 (1995)
11. Mandelkern L., *Crystallization and Melting* in *Comprehensive Polymer Science*, Sir Allen G, Chairman Ed. Board, Pergamon Press, Oxford, **2** (11), 363 (1989)
12. Mathot V.B.F., *The Crystallization and Melting Region* in *Calorimetry and Thermal Analysis of Polymers*, Mathot V.B.F., Ed., Carl Hanser Verlag, Munich, **9**, 231 (1994)
13. Herbert I., *Statistical Analysis of Copolymer Sequence Distribution* in *NMR Spectroscopy of Polymers*, Ibbett R.N., Ed., Blackie Acad. & Proff., London, (2), 50 (1993)

14. Vasile C., General Survey on the Properties of Polyolefins, in *Handbook of Polyolefins – Synthesis and Properties*, Vasile C., Seymour R.B., Eds., Marcel Dekker Inc., New York, 561 (1993)
15. Billmeyer F.W. Jr., *Textbook of Polymer Science*, John Wiley & Sons, New York, 141 (1962)



## CHAPTER 8

### PROPYLENE / $\alpha$ -OLEFIN RANDOM COPOLYMERS

#### 8.1 INTRODUCTION

The world production of polypropylene is 29 million tons with the copolymers taking a large share of this market. Process and catalyst developments are responsible for the production of an extremely versatile polymer with the polypropylene market showing continuous growth and diversification. However, the role of the comonomer has not always been acknowledged. In the polypropylene family, ethylene and 1-butene are employed as comonomers although 1-hexene has also been described and recommended [1]. Application of odd carbon number  $\alpha$ -olefins in the polypropylene family was, until recently, totally neglected. As was mentioned in Chapter 6, many linear (including odd carbon number  $\alpha$ -olefins) and branched  $\alpha$ -olefins useful as comonomers are produced in Sasol's Fischer-Tropsch oil-from-coal process, and can be isolated by a relatively cheap refinery operation. In previous presentations [2,3] the opportunities for using 1-pentene in the random copolymer market was presented. As an extension of this study, the application possibilities of the higher  $\alpha$ -olefins having uneven carbon numbers, was investigated.

## 8.2 EXPERIMENTAL

A 10-litre stainless steel automated autoclave was thoroughly flushed with nitrogen and 3 000 g of purified heptane added. The temperature was increased to 70°C and the catalyst system comprising 50 ml of a 10% solution of tri-ethyl aluminium (TEA) in heptane, 2 ml diphenyl dimethoxy silane and 1 g of a supported titanium chloride catalyst prepared as previously described (Chapter 5) was added, in this order, and stirred for 5 minutes. After this “ageing” period, propylene and comonomer were continuously introduced over a period of 25 minutes at a fixed ratio after which the monomer feeds were stopped and the reaction continued for a further 95 minutes. Molecular weight was regulated with hydrogen and the comonomer content by the propylene / comonomer ratio. The catalyst in the copolymer slurry was deactivated with iso-propanol, filtered, washed and dried.

The 1-pentene content of the copolymers was determined on a Perkin Elmer FT-IR 1720X instrument on 0.3 mm thick compression moulded film samples prepared on a Graseby Specac press at 180°C. A calibration curve was obtained from standard melt-blended samples of polypropylene with known poly(1-pentene) content. The moderately strong peak at 969 cm<sup>-1</sup> in the spectrum of PP arises from coupling vibrations, while the rocking of the CH<sub>3</sub> group at 734 cm<sup>-1</sup> was used in an in-house developed procedure to quantify the concentration of the propyl branch.

<sup>13</sup>C NMR analyses were done at 120°C on samples dissolved in *o*-dichlorobenzene on a Varian 400 MHz machine using a 90° pulse angle, a pulse width of 10, 25 000 scans and a 30 sec. delay. Composition was determined through the ratio between characteristic peaks of the different monomers making up the NMR spectrum of the copolymer as fully described in Chapter 4. Basically the ratio between the peak areas of the branching -CH and that of the backbone carbons was determined and expressed as a percentage. Assignments were done making use of the literature where possible, combined with DEPT analyses and checked against the chemical shift assignments predicted by the additivity rules described by Grant and Paul [4].

The molecular weights of the copolymers were determined on a Waters 150 CV GPC with a refractive index detector in 1,2,4-trichlorobenzene solution at 150°C. Each tray of samples included a polystyrene standard and the NBS 1475a standard in order to check the validity of data against the polystyrene calibration curve spanning the MW range of 1 000 to 3 100 000 g/mol.

Melt flow index (MFI) was determined according to ASTM D 1238, mechanical properties according to ASTM D 638 M and notched Izod impact strength according to ASTM 256.

Melting behavior was determined on a Perkin Elmer DSC-7 fitted with a TAC 7/PC instrument controller. The samples were heated from 50 to 200°C at 20°C/min, held at 200°C for 1 minute, cooled to 50°C at a rate of 20°C/min during which time the crystallization curve was recorded. At 50°C, the temperature was kept constant for 1 min after which the melting curve was recorded between 50 and 200°C at a heating rate of 10°C/min.

## 8.3 RESULTS AND DISCUSSION

Properties of polyolefins such as modulus, hardness, tensile strength at yield, impact strength and crystalline melting temperature depend on crystallinity [5]. As pointed out by Alamo *et al.* [6] the theory for melting of copolymers developed by Flory [7] does not imply that side groups are excluded from the crystal. Thus, if it is assumed that side groups larger than methyls are excluded from the polypropylene crystal, overall crystallinity will decrease and polymer properties will be affected. The larger the side group, the larger the disrupting effect on the crystal structure and the lower the amount of higher  $\alpha$ -olefins needed to achieve a certain level of crystallinity.

### 8.3.1 MECHANICAL PROPERTIES

In Table 8. 1 the properties of propylene copolymers prepared using different  $\alpha$ -olefins having uneven carbon numbers are presented.

**Table 8.1. Mechanical Properties of Propylene /  $\alpha$ -Olefin Copolymers**

Comonomer	MFI (dg/min)	Yield Strength (MPa)	Modulus (MPa)	Impact Strength (kJ/m <sup>2</sup> )	Hardness (Shore D)
<b>1-Pentene (%)</b>					
2.6	3.5	25.5	685	7.1	61
3.4	7	19.56	599	9.93	54
3.8	5	19.0	488	12.5	53
4.6	6.5	16.64	395	16.75	52
<b>1-Heptene (%)</b>					
0.8	11	23.1	885	6	61
2.0	13	18.2	745	7.5	58
2.8	10	15.1	546	19	56
4.0	5	12.6	445	46.5	50
<b>1-Nonene (%)</b>					
0.4	2.4	30.6	1014	6.3	65
1.8	2.3	20.7	937	16.0	61
2.1	3.3	20.1	800	18.0	60
3.0	2.2	16.5	546	46.9	56

### 8.3.1.1 Tensile Properties

Similar to that observed for polyethylene copolymers, it can be seen from Figure 8.1 that propylene copolymers also show a modulus vs. tensile strength dependence.

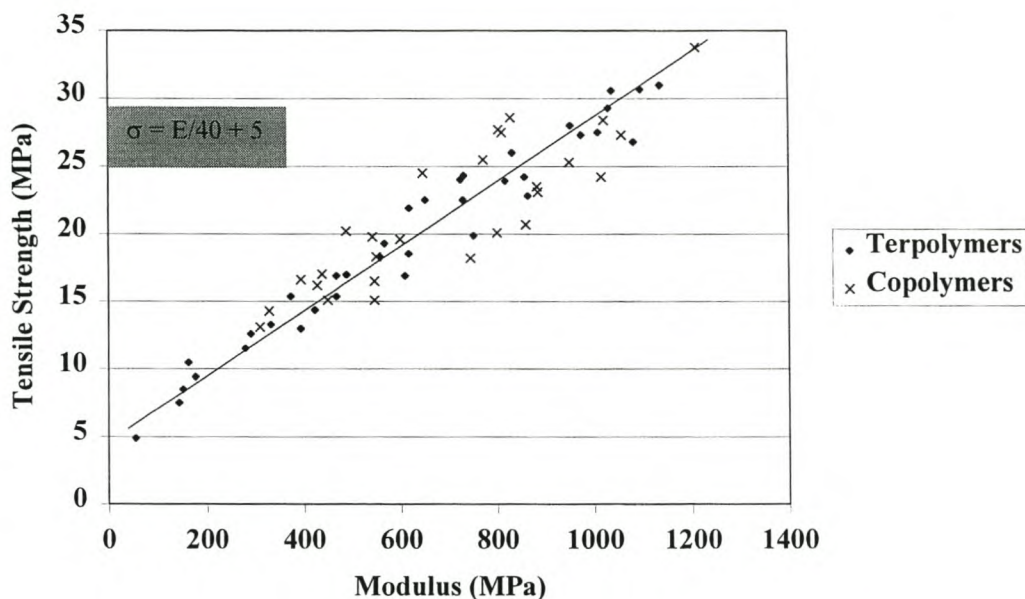


**Figure 8.1. Relationship Between Tensile Strength at Yield and Young's Modulus for Co- and Terpolymers**

The data points presented include propylene copolymers obtained using linear  $\alpha$ -olefins from 1-butene to 1-nonene, different catalysts as well as propylene / ethylene / 1-pentene terpolymers obtained with a  $MgCl_2$  supported catalyst. The scatter in the values are believed to result mainly from the different polymer molecular weights. Microstructure and tacticity may also have an effect on the values. Although the properties of some of these copolymers will not be discussed in this study, they were included to show that the tensile strength / modulus relationship trend in general holds for propylene copolymers.

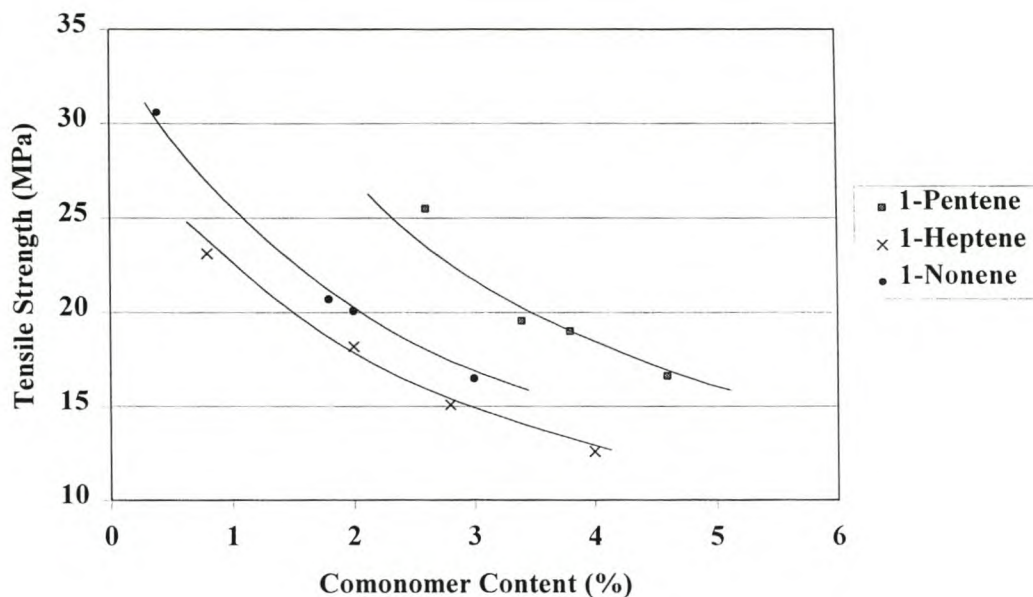


**Figure 8.2. Relationship Between Tensile Strength at Yield and Comonomer Type and Content**

It can be seen from Table 8.1 that, in general, a good agreement exists between tensile properties and comonomer content. As comonomer content increases, tensile properties decrease. This can more clearly be seen in Figure 8.2 where the tensile strengths of different copolymers are presented. However, the relationships describing each copolymer's dependence on comonomer content does not follow the logical trend expected and observed for the ethylene copolymers. The propylene / 1-heptene curve is situated *below* that of the propylene / 1-nonene copolymer. Inspection of the melt flow index results for the different copolymers suggest an apparent reason for this behavior. The 1-heptene copolymers have lower molecular weights and this has a significant effect on tensile properties [8,9]. As mentioned in the discussion of the ethylene copolymer properties, below a certain length, polymer chains can not act as tie-molecules. In addition, the longer molecules tend to crystallize first, resulting in separation based on molecular weight with the low molecular weight material concentrated in the amorphous interspherulitic region [10]. This same line of reasoning applies to the data point in the 1-pentene curve with the lowest MFI. Tensile strength of this polymer which seemingly does not fit the curve, but lies above it. In the light of the above it is believed that at comparable molecular

weights, different copolymers will follow the expected trend similar to that observed for the ethylene /  $\alpha$ -olefin copolymers described in Chapter 6.

### 8.3.1.2 Impact Strength

Impact strength depends on the amount of energy dissipated during fracture. Plasticizing the polypropylene matrix by the *random* introduction of the comonomer allows for increased viscous flow which consumes large amounts of energy [11]. During impact the chains will orient in the direction of the applied stress as a result of viscous flow, resulting in highly oriented, load bearing polymer at the crack tip [12]. Therefore, apart from the energy dissipated through viscous flow, the highly oriented polymer chains at the crack tip can arrest growth of a propagating crack, probably as a result of the higher modulus of the oriented strands as compared to that of the surrounding matrix [13].

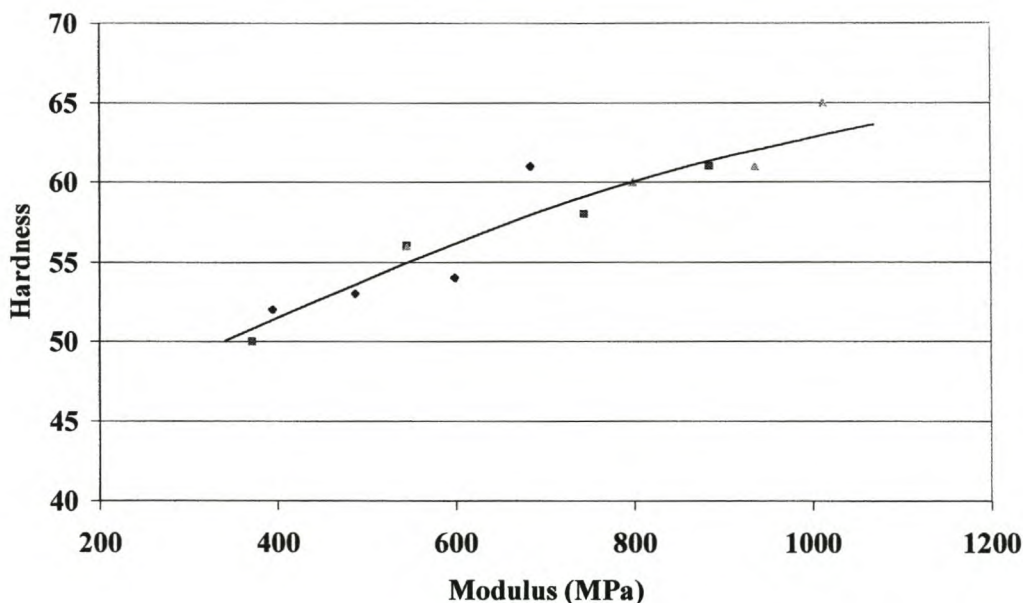


**Figure 8.3. Hardness vs. Modulus Showing Independence on Comonomer Type. 1-Pentene □, 1-Heptene ●, 1-Nonene △**

For random copolymers, introduction of comonomer results in plasticization of the copolymer matrix, thereby decreasing the modulus of the matrix. Figure 8.3 shows that for these random copolymers, a decrease in modulus directly results in a decrease

in hardness of the matrix, irrespective on the type of comonomer used. In Figure 8.4, impact strength was thus plotted against modulus, and this shows that impact strength is improved in the softer matrix.

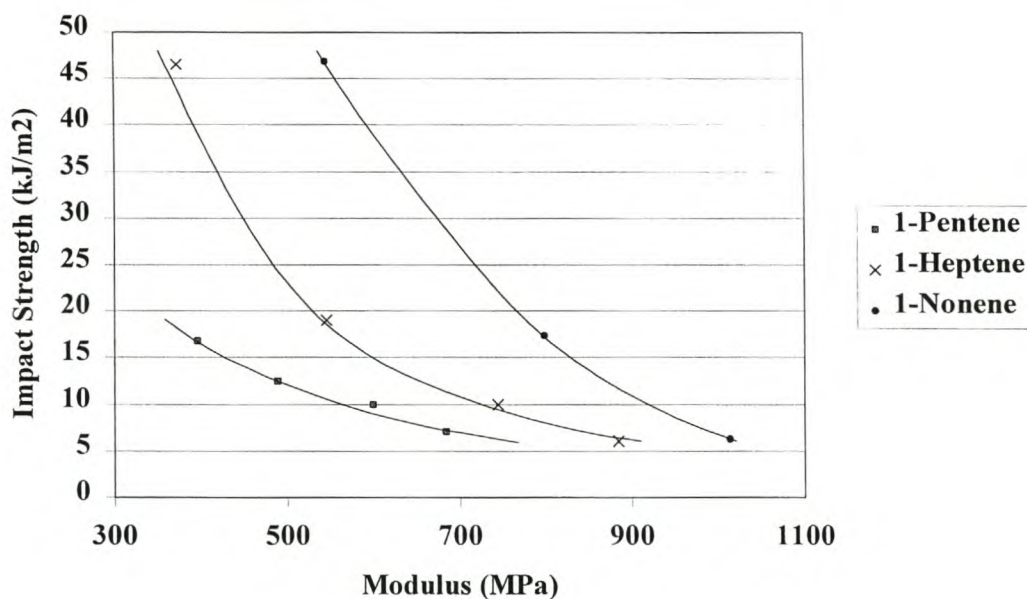


**Figure 8.4. Impact strength of Different Copolymers as a Function of Modulus**

For the same degree of orientation at the crack tip, the difference in modulus between the oriented polymer and a softer matrix is evidently larger. Therefore, in stead of continuing the growth of the crack, the softer matrix will yield to initiate a different crack resulting in improved efficiency in arresting the crack growth. Eventually, however, no more new cracks can be initiated (and arrested) in the softer matrix and the energy of the impact hammer is reduced by the *oriented polymer* and not by the soft matrix. This orientation results in high impact strength.

An increase in the length of the side chain improves the impact strength, an effect also observed for the ethylene copolymers. In Figure 8.5 the impact strength of the different copolymers are observed to be related to comonomer content. For the propylene copolymers, the impact strength does not start increasing immediately as was observed for the ethylene copolymers. Here the increase in impact strength is more gradual and follow an exponential increase with comonomer content in the range studied. A second difference from the impact curves of the ethylene



copolymers is that the maximum impact strengths (where the matrix becomes rubbery), were not reached in the range of comonomer contents investigated.

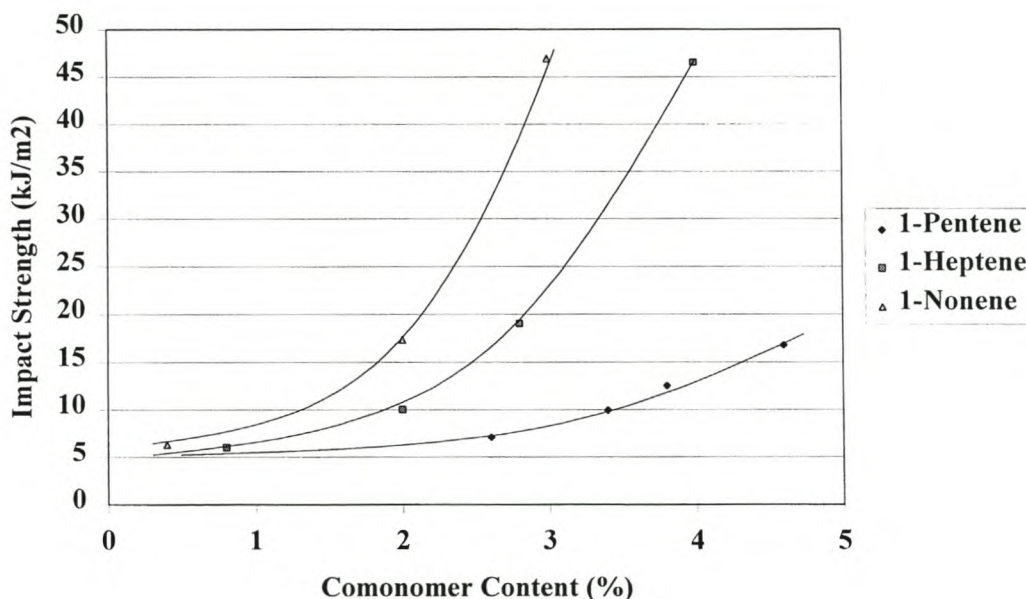


**Figure 8.5. Dependence of Impact Strength on Comonomer Type and Content**

However, it is clear that the higher  $\alpha$ -olefins are more effective at increasing impact strength. By comparing the length of the comonomer side chain with the amount of comonomer necessary to obtain a certain impact strength it should also be possible to determine whether the increased impact strength observed for the higher  $\alpha$ -olefins results from the size of the side chain. Based on 1-pentene, the relative effects of 1-heptene having a 5-carbon side chain and 1-nonene having a 7-carbon side chain should thus be 1-pentene : 1-heptene : 1-nonene = 1 : 1.67 : 2.33. The calculated and observed amounts of comonomer needed to obtain an impact strength of 15 kJ/m<sup>2</sup> are presented in Table 8.2.

**Table 8.2. Calculated vs. Observed Comonomer Content to Obtain an Impact Strength of 15 kJ/m<sup>2</sup>**

Comonomer	Relative Effect	Observed Content (%)	Calculated Content (%)	Difference
1-Pentene	1.0	4.3	4.3	0
1-Heptene	1.67	2.5	2.58	0.08
1-Nonene	2.33	1.8	1.88	0.08

From the small difference between observed and calculated comonomer content at 15 kJ/m<sup>2</sup> it can be seen that a close correlation exists between the size of the comonomer side chain and impact strength. This is an indication that for these copolymers, the comonomer size is primarily responsible for the observed difference in impact strength using different comonomers.

Similar to tensile strength, it is known that impact strength is also dependent on molecular weight [8,9]. Branching in copolymers reduces crystallinity and increases the tie-molecule concentration [6]. Low molecular weight material cannot act as tie molecules and gives a more brittle material. In Figures 8.4 and 8.5, the impact curves for the 1-heptene copolymer are, as expected, situated between those of the 1-pentene and 1-nonene copolymer curves. This seems to contradict the earlier observation that the 1-heptene copolymer tensile curve does not lie between those of the 1-nonene and 1-pentene curves where it was expected.

However, in a previous study, regarding the impact fracture behavior of propylene / 1-pentene copolymers [14], the effect of molecular weight on impact behavior was investigated. It was shown that the impact strength of propylene / 1-pentene copolymers having weight average and number average molecular weights of about 420 000 g/mole and 81 000 g/mole respectively, increased from 3.4 kJ/m<sup>2</sup> for the homopolymer to about 5.1 kJ/m<sup>2</sup> for a copolymer containing 2.9 mole % 1-pentene. For 1-pentene copolymers containing 2.3 ± 0.1% comonomer, impact strength increased from 4 to 9 kJ/m<sup>2</sup> when weight average molecular weight increased from 270 000 to 850 000 g/mole.

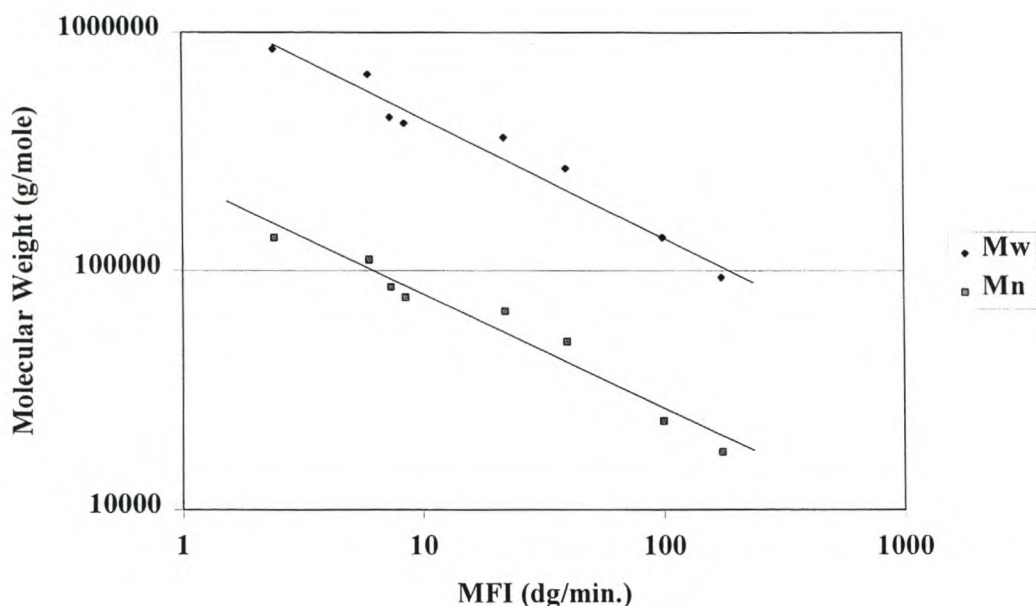


**Figure 8.6. Relationship Between Molecular Weight and Melt Flow Index**

In Figure 8.6, the relationship between MFI and molecular weight of the propylene / 1-pentene copolymers are presented in order to relate MFI with  $M_w$  and  $M_n$ . It can be seen that for these copolymers, a large change in molecular weight does not constitute a large change in impact strength and it is thus possible that the effect of molecular weight on the impact strength of the 1-heptene copolymers is not large enough to be observed.

### 8.3.2 THERMAL PROPERTIES

During crystallization under a standard set of conditions, homogeneous semi-crystalline polymers chain-fold to form lamellae with a distribution of thicknesses, which melt at different temperatures [15]. The thicknesses of the lamellae are directly related to the crystallization temperature or degree of supercooling [16]. A peak occurs in the melting curve at the temperature where crystallites of a specific size are the most abundant under the crystallization conditions applied. The presence of low levels of defects other than stereo errors, resulting from comonomer units in an otherwise regular chain, will hinder the extent to which crystallization will occur. The greater the number of disrupting units (branches) in a chain, the broader its

melting peak [17]. The melting peak height will decrease and the melting range will broaden. When the amount of uncrystallizable comonomer increases, the sequence lengths of the crystallizable units decreases. As the comonomer content increases above a critical value, the amount of thinner [18], lower melting crystallites increases [17] at the expense of the thicker, high-melting crystallites, resulting in a decrease in the melting temperature.

It is known that melting temperature does not depend directly on comonomer content but rather on sequence distribution [6]. The heterogeneous distribution of active sites in the Ziegler-Natta catalyst will generate heterogeneous copolymers because of differences in copolymerization characteristics of the different active sites [19]. This results in intermolecular and intramolecular heterogeneity as discussed for the ethylene copolymers. Chains produced from protected active sites have low comonomer content and those produced from open sites, which easily incorporate comonomer, have high comonomer content. These different chains depend on the difference in comonomer content, and thus crystallize at completely different temperatures, leading to different melting temperatures [17] resulting in multiple-peaked crystallization and melting curves.

In a heterogeneous mixture consisting of distinctly different components a variety of possible scenarios can occur. These include long crystallizable sequences of homopolymer or copolymer chains containing a small amount of comonomer, and copolymer chains containing large amounts of uncrystallizable comonomer. Thus, three basic phases may be observed during crystallization under set conditions. The thick, high-melting (mainly) homopolymer crystallites containing the longest and most crystallizable units will form according to its molecular weight- and sequence length distributions. This will enrich the melt (uncrystallized material) with high comonomer content chains and those having shorter sequences of crystalline material. This material will crystallize at lower temperatures to form the thinner, lower-melting crystallites. The cooling curve obtained from DSC will show a high temperature event during which the thicker crystallites formed and a lower temperature event where the less perfect, thinner crystallites formed, provided that two distinctly different crystallite size distributions were obtained during crystallization. On melting a double peaked DSC trace will be obtained, the high and low melting

temperatures of which correspond to the high and low temperature crystallization peaks.

In Table 8.3 the thermal properties of propylene copolymers prepared with 1-pentene, 1-heptene and 1-nonene are compared. Crystallinity was calculated from fusion enthalpy based on a value of 209 J/g for 100% crystalline material [20].

**Table 8.3. Thermal Properties of Propylene /  $\alpha$ -Olefin Copolymers**

<b>1-Pentene (%)</b>	<b>MFI (dg/min)</b>	<b>Melting Temp (°C)</b>	<b>Fusion Enthalpy (J/g)*</b>	<b>Crystallinity (%)</b>
0	7.4	166	101	48.3
2.6	3.5	146	55.5	26.5
3.4	7	145	53.5	25.6
3.8	5	145	54	25.8
4.6	6.5	142	32.5	15.5
<b>1-Heptene (%)</b>				
0.8	11	150	61	29.2
2.0	13	150	53	25.3
2.8	10	149	51	24.4
4.0	5	149	48	22.9
<b>1-Nonene (%)</b>				
0.4	2.4	152	63	30.1
1.8	2.3	151	60	28.7
2.1	3.3	150	60	28.7
3.0	2.2	149	57.5	27.5

\* Average of melting and crystallization

The melting temperatures of the different comonomers shown in Table 8.3 are relatively insensitive towards comonomer content, except for the initial large drop in melting temperature after introduction of a small amount of comonomer. The propylene homopolymer has a melting temperature of about 165°C and it can be seen from Table 8.3 that the introduction of only 0.4% 1-nonene or 0.8% 1-heptene resulted in a decrease in melting temperature to 152°C and 150°C respectively.

The melting temperatures of the different copolymers show a general decrease with increasing comonomer content (Figure 8.8). For the 1-pentene copolymers, the presence of a second melting peak was observed which made analysis of the melting peaks difficult. Double peaks were not observed in the melting curves of the 1-heptene and 1-nonene copolymers, but were present on the crystallization curves.

From Figure 8.7 it can be seen that the melting temperatures for the 1-nonene and 1-heptene copolymers are higher than those of the 1-pentene copolymers. It may be reasoned that 1-pentene can be incorporated easier than the higher  $\alpha$ -olefins. This, results in a larger amount of 1-pentene-containing copolymer chains, which melt at lower temperatures. The more bulky 1-heptene and 1-nonene are rejected by a larger amount of active sites and consequently, more chains are produced with low comonomer content. In these chains, lamellar thickness is less restricted, resulting in the persistence of the high temperature melting peak.

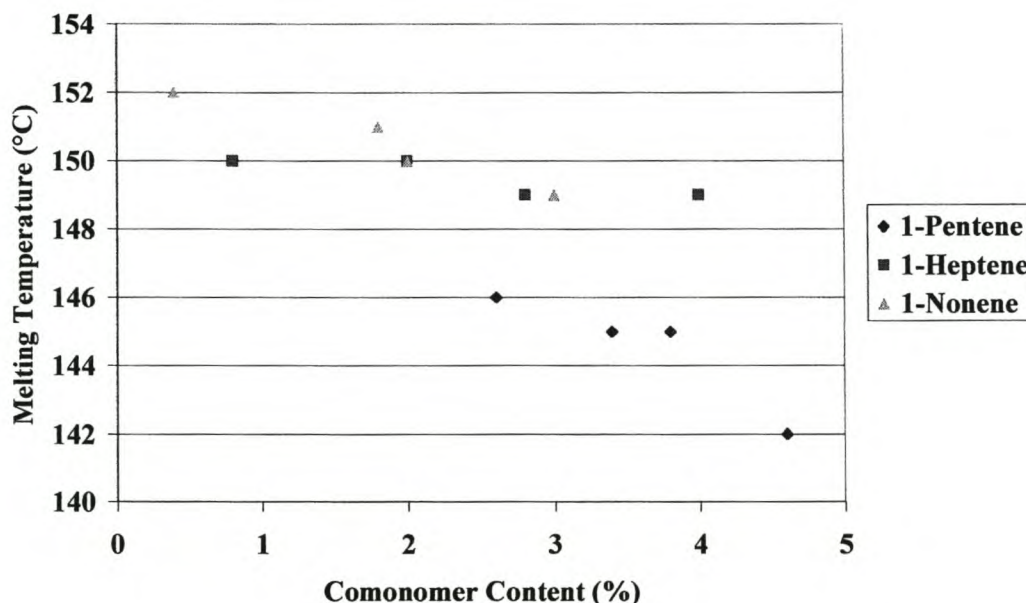


**Figure 8.7. Melting Temperatures of Different Propylene /  $\alpha$ -Olefin Copolymers**

In Figures 8.8, 8.9 and 8.10 the DSC melting and crystallization curves are presented. For the propylene / 1-pentene copolymers shown in Figure 8.8, double melting peaks are visible for the copolymer containing 2.6% 1-pentene. From the crystallization curve, the peaks at 105°C and 90°C, responsible for the dual melting peaks, can be observed. The crystallization curves, resulting from increased comonomer content (3.4%, 3.8%), show different states of transition from the high to the low temperature melting peaks as a result of decreased lamellar thicknesses. The crystallization curve of the copolymer with the highest comonomer content (4.6%) shows three peaks, the

center one which could be due to the emergence of lamellae having an intermediate thickness or perhaps result from overlap between the high and low temperature crystallization peaks. As comonomer content increases, fusion enthalpies can be seen to decrease which corresponds to the decrease in crystallinity shown in Table 8.3.

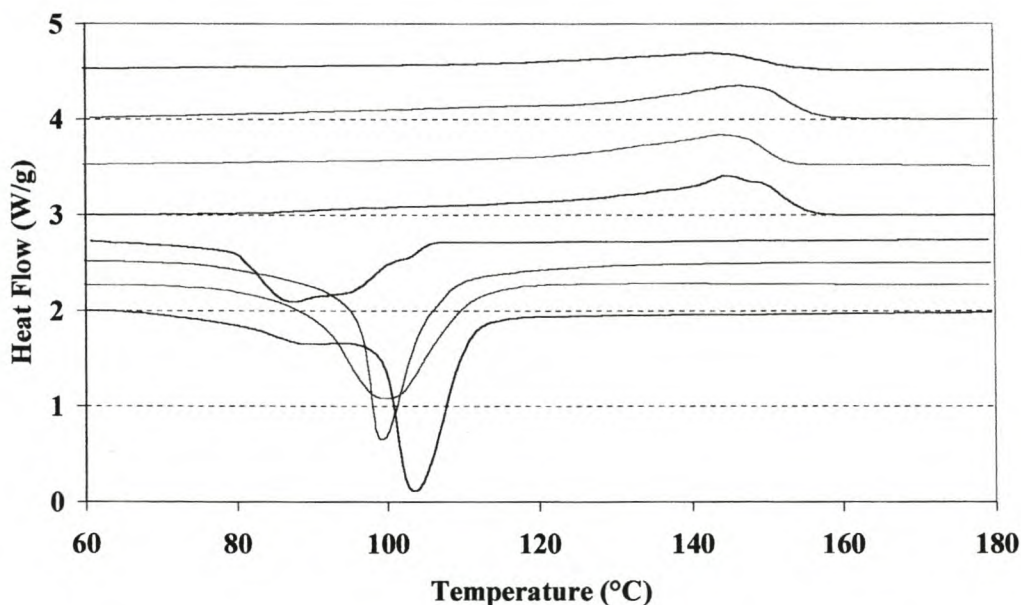


**Figure 8.8. Melting and Crystallization Curves for Propylene / 1-Pentene Copolymers. \_\_\_\_\_ 2.6%, \_\_\_\_\_ 3.4%, \_\_\_\_\_ 3.8%, \_\_\_\_\_ 4.6%**

Only very slight changes can be observed between the different propylene / 1-heptene copolymer melting curves shown in Figure 8.9. Increasing the 1-heptene content from 0.8 to 4% decreased the melting temperature by only 1°C, which indicates that this difference in comonomer content did not have a substantial influence on lamellar thickness. The average separation between comonomer units in the chain thus seemed to remain larger than the length of crystallizable propylene units necessary to produce the lamellar thickness prescribed by the crystallization conditions.

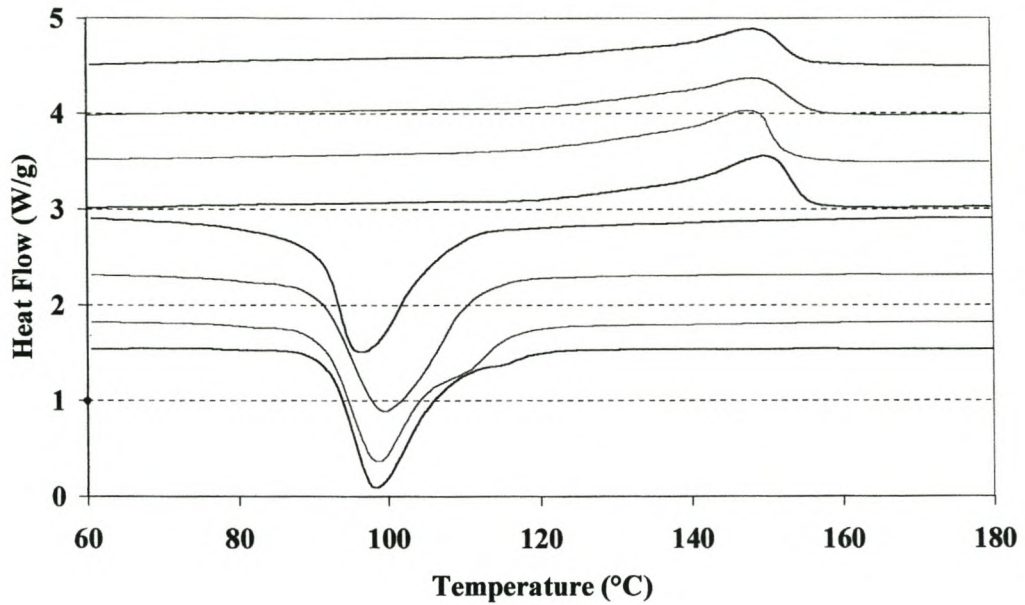


**Figure 8.9. Melting and Crystallization Curves for Propylene / 1-Heptene Copolymers. \_\_\_\_\_ 0.8%, \_\_\_\_\_ 1.0%, \_\_\_\_\_ 2.8%, \_\_\_\_\_ 4.0%**

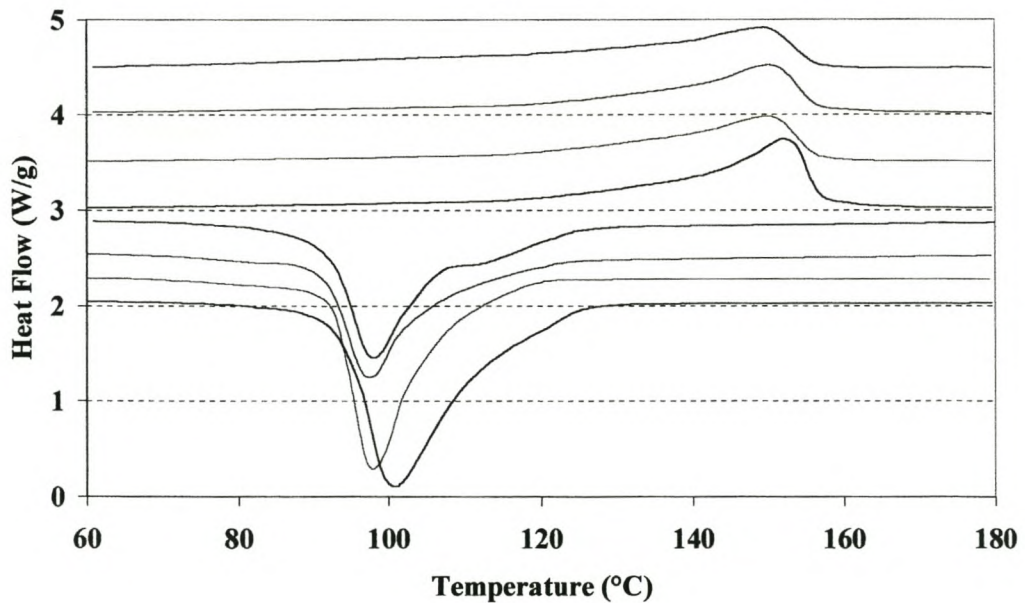


**Figure 8.10. Melting and Crystallization Curves for Propylene / 1-Nonene Copolymers. \_\_\_\_\_ 0.4%, \_\_\_\_\_ 1.8%, \_\_\_\_\_ 2.0%, \_\_\_\_\_ 3.0%**



For the 1-nonene copolymers shown in Figure 8.10, a substantial broadening of the melting curves can be seen as the comonomer content increases. For the low 1-nonene content copolymer, the crystallization peak is higher than that of the high comonomer content copolymer, although the latter also clearly shows a high temperature shoulder. The widely different crystallization temperatures of lamellae of different thickness is thus responsible for the broad melting range observed for the copolymers having high 1-nonene content.

By comparing the different copolymers, it can be seen that for the 1-heptene and 1-nonene copolymers, a high temperature crystallization event occurs between 110 and 120°C for most of these copolymers. The effect is more pronounced for 1-nonene copolymers. A similar event is not observed for the 1-pentene containing copolymers. By considering the active sites present on the Ziegler-Natta catalyst, it can once again be reasoned that a substantial amount of active sites are rejecting the more bulky comonomers, resulting in less-branched chains capable of easier crystallization. The thicker lamellae melt at higher temperatures and their co-existence with the lower-melting chains that contain a higher amount of comonomer, are deemed responsible for the broad melting peaks whilst maintaining the melting peak at a high temperature.

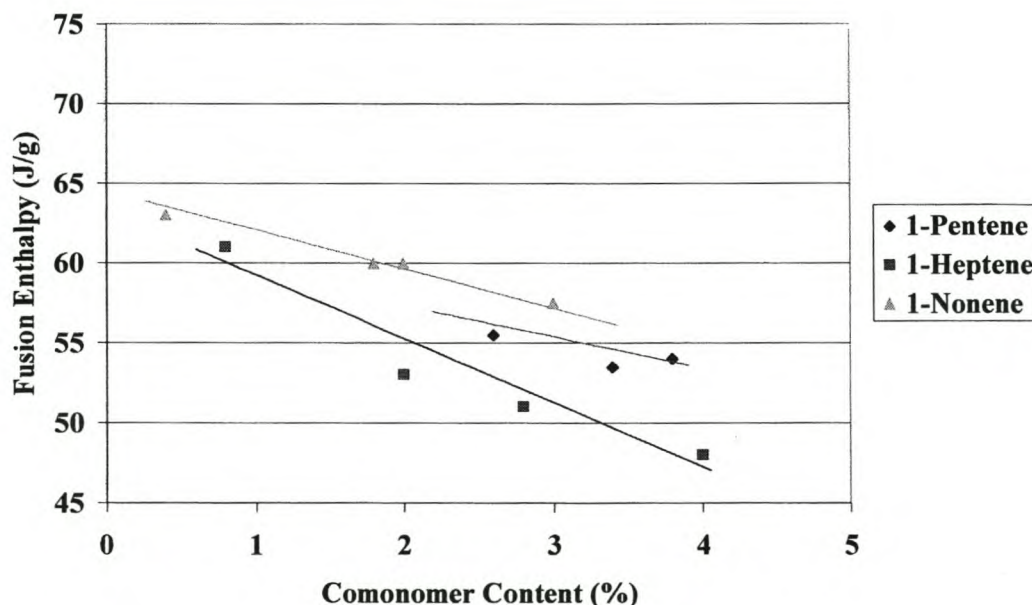


**Figure 8.11. Fusion Enthalpy as a Function of Comonomer Content**

It was expected that the fusion enthalpies of the different copolymers would follow a similar logical trend as that observed for the ethylene copolymers discussed in Chapter 6. From Figure 8.11, where fusion enthalpies of the different copolymers are plotted against comonomer content, it can be seen that within each series, a trend with regard to the fusion enthalpies exists. However, the trend between different copolymers are not as expected and it can be seen that the fusion enthalpies of the propylene / 1-nonene copolymers are higher than those of the propylene / 1-pentene copolymers.

Following the same argument as above, it is believed that the misfit of the fusion enthalpy curve of the 1-nonene copolymers, compared to those of the 1-pentene and 1-heptene copolymers may possibly be explained through the presence of a substantial amount of more crystalline polymer, containing low amounts of comonomer, which requires more heat to melt.

## 8.4 CONCLUSIONS

Process and catalyst developments are responsible for the production of an extremely versatile polymer. However, the role of the comonomer has not always been acknowledged. In the polypropylene family, ethylene and 1-butene are typically employed as comonomers. The possibility of using the higher  $\alpha$ -olefins containing uneven carbon numbers as comonomers in polypropylene, was investigated in this chapter.

Side groups larger than methyl groups disrupt polypropylene crystallization. This decrease in overall crystallinity will affect polymer properties. The larger the side group, the larger the disrupting effect in the crystal structure and consequently the effect on polymer properties. Thus, less of the higher  $\alpha$ -olefins will be needed to achieve a certain level of crystallinity. The new polymers showed a good agreement between tensile properties and comonomer type and content. The tensile curve of the 1-heptene copolymer was situated below that of the 1-nonene copolymer and this was ascribed to the lower molecular weight of the 1-heptene copolymers. It is thus believed that tensile strength of the copolymers should follow the same trend as that observed for the ethylene copolymers where the size of the branch and the resulting defect it causes in the crystal structure is the primary factor affecting tensile strength.

For impact strength, a close correlation between the size of the comonomer side chain and comonomer content was observed. It was shown that the effect of the heptyl branch derived from a 1-nonene unit was 2.3 times that of the propyl group derived from the 1-pentene unit.

It was observed that melting temperatures of the 1-pentene copolymers were generally lower than those of the higher  $\alpha$ -olefin copolymers. By comparing the melting and crystallization curves of the different copolymers it was observed that the crystallization peaks of the propylene / 1-pentene copolymer decreased with increasing 1-pentene content. For the higher  $\alpha$ -olefin copolymers, the crystallization peak temperatures did not decrease substantially. Considering the different accessibilities of active sites on a Ziegler-Natta catalyst, it is believed that the more

bulky  $\alpha$ -olefins were rejected by a substantial number of (protected) active sites. Polymer chains consisting mainly of propylene units were thus produced by these sites. These chains produce higher melting lamellae, which resulted in the maintainance of the melting temperatures observed for the copolymers containing 1-heptene and 1-nonene.

## 8.5 REFERENCES

1. Ficker H.K., Walker D.A., *Plastics and Rubber Processing and Application*, **14**, 103-118 (1990)
2. Tincul I., Potgieter I.H., *PP'96, MBS Conference*, Zurich, Switzerland, (1996)
3. Tincul I., Joubert D.J., *ESTAC 7, Hun. Chem. Soc.*, Balatonfüred, Aug. 30 – Sept 4, 291 (1998)
4. Grant D.M., Paul E.G., *J. Am. Chem. Soc.*, **86**, 2984 (1964)
5. Huff T., Busman C.J., Cavender J.V., *J. of Applied Polym. Sci.*, **8**, 825-837 (1964)
6. Alamo R., Domszy R., Mandelkern L., *J. Phys. Chem.* **88**, 6587 (1984)
7. Flory P.J., *J. Chem. Phys.*, **17**, 223 (1949)
8. Kissin Y.V., *Olefin Polymers (Polyethylene)* in *Encyclopedia of Chemical Technology*, Kroschwitz J.I., Exec. Ed., John Wiley & Sons, New York, **17**, 724 (1995)
9. Bogdanov B.G., Michailov M., *Properties of Polyolefins* in *Handbook of Polyolefins – Synthesis and Properties*, Vasile C., Seymour R.B., Eds., Marcel Dekker Inc., New York, 295 (1993)
10. Vaughan A.S., Bassett D.C., *Crystallization and Morphology* in *Comprehensive Polymer Science*, Sir Allen G, Chairman Ed. Board, Pergamon Press, Oxford, **2** (12), 415 (1989)
11. Berry J.P., *J. Polym. Sci.*, **50**, 107, 318 (1961)
12. Young R.J., *Strength and Toughness* in *Comprehensive Polymer Science*, Sir Allen G, Chairman Ed. Board, Pergamon Press, Oxford, **2** (15), 511 (1989)
13. Kambour P.P., *Crazing* in *Encyclopedia of Polymer Science and Engineering*, Kroschwitz J.I., John Wiley & Sons, New York, **4**, 299 (1988)
14. Tincul I., Joubert D.J., Potgieter A.H., *Am. Chem. Soc.*, (1998)
15. Hingman R., Rieger J., Kersting M., *Macromolecules*, **28**, 3801 (1995)
16. Mandelkern L., *Crystallization and Melting* in *Comprehensive Polymer Science*, Sir Allen G, Chairman Ed. Board, Pergamon Press, Oxford, **2** (11), 363 (1989)

17. Mathot V.B.F., *The Crystallization and Melting Region in Calorimetry and Thermal Analysis of Polymers*, Mathot V.B.F., Ed., Carl Hanser Verlag, Munich, **9**, 231 (1994)
18. Fatou J.G., *Crystallization Kinetics*, in *Encyclopedia of Polymer Science and Engineering*, Kroschwitz J.I., John Wiley & Sons, New York, Suppl. Vol., 231 (1988)
19. Sacchi M.C., Shan C., Forlini F., Tritto I., Locatelli P., *Makromol. Chem. Rapid Commun.*, **14**, 231 (1993)
20. Quirk R.P., Alsamarraie M.A.A., *Physical Properties of Poly(propylene)* in *Polymer Handbook*, Third Edition, Brandrup J., Immergut E.H., John Wiley & Sons, New York, V/27 (1989)

## CHAPTER 9

### PROPYLENE / 1-PENTENE BLOCK COPOLYMERS

#### 9.1 INTRODUCTION

Polypropylene (PP) is a very versatile polymer with many outstanding properties, which make it useful in fiber, tape, film, blow moulding, thermoforming and injection moulding applications. One drawback associated with PP is its low impact resistance at low temperatures. For some typical applications such as car bumpers and trimming, garden furniture, food containers etc., the polymer should be able to withstand rough handling. Random copolymers do have increased impact resistance when compared to the homopolymer but crystallinity is lower and consequently the melting and softening temperature, tensile strength, modulus, dimensional stability and hardness decrease. For the external automotive applications and furniture for example, stiffness over a wide temperature range is paramount. Bumpers and trimming in plastics are used because of the ease with which intricate designs for aesthetic, aerodynamic and energy absorbing purposes can be integrated with the rest of the bodywork and contribute to weight saving. Ideally, these parts should therefore have high impact strength, should not lose shape through creep and be as thin as possible. Food containers on the other hand are typically exposed to temperature extremes in a microwave oven where frozen foods are often heated, depending on sugar and fat content, to temperatures well above 100 °C. These containers should therefore be able to withstand low temperature impact as well as being dimensionally stable and not warp at elevated temperatures. These demands can not be simultaneously met by PP random copolymers.

In order to increase impact resistance of propylene polymers, propylene is typically copolymerized with ethylene in a two step cascade process where propylene is homopolymerized in one reactor, transferred to a second reactor and copolymerized

with ethylene to form the so-called block copolymers. These copolymers are not true block copolymers such as SBS rubbers or ABS high impact copolymer where each polymer chain consists of distinct blocks of the different monomers. Rather a reactor blend of polypropylene homopolymer, EPR copolymer, and a number of chains containing long runs of both propylene and EPR is produced. As a rule different polymers when added together do not mix, but separate out in their respective phases with very little, if any, adhesion between the phases. This phase separation is generally a disadvantage as a heterogeneous polymer will result, but actually gives a polymer with high impact strength and stiffness to meet the demands set above.

As was mentioned above, three different types of polymer are formed in the commercial block copolymerization of propylene with ethylene. The two main components - PP and EPR - phase separate, each through the exclusion of the other. PP associates with PP and EPR with EPR. The chains containing long runs of both propylene and EPR acts in a similar way as in an emulsifier molecule – the EPR part of the chain associates with the amorphous EPR phase and the propylene part with the semi-crystalline PP phase. This results in adhesion between the two incompatible phases. It should be clear that the ratio between these three phases is very important. To obtain a stiff matrix it is necessary to have the PP homopolymer as a continuous phase with the rubber globules homogeneously distributed therein. The PP/EPR blocky copolymer will preferentially be situated at the interface and its concentration will influence the rubber phase particle size and adhesion.

This adhesion between the two phases is extremely important [1] during an impact event, both during the time when stresses are building up in the matrix and when a crack is propagating through the matrix. During the build-up phase, the rubber particles with a modulus much lower than that of the PP matrix, act as stress concentrators that heats up the matrix in its immediate vicinity. This happens throughout the parts of the sample stressed beyond a critical value. This heating, localized around the equator of the rubber particles where stresses are highest, allow crazes (essentially small cracks bridged by oriented strands of polymer) to form through viscous flow of the PP chains with the crazes' long axis perpendicular to the direction of the applied stress (Figure 9.1). In this sense crazes are the defects where cracks are initiated [2].



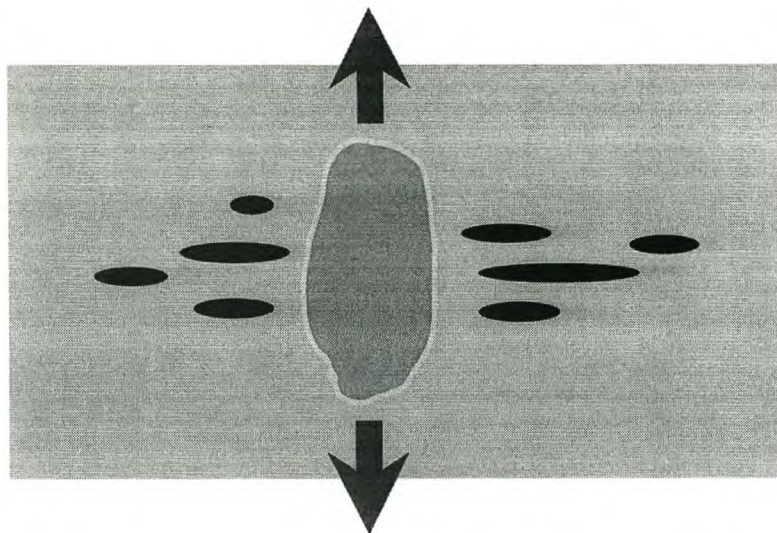


**Figure 9.1. Crazes Around a Vertically Stretched Rubber Particle.**

This process is accompanied by considerable whitening of the stressed sections in the sample [3] because these micrometer-sized entities reflect light. The viscous flow of the PP chains during craze initiation results in orientation of the chains in the direction of the applied stress, forming the craze. These oriented bundles of polymer strands in the craze, called microfibrils, are load-bearing [2] and therefore much more resistant to deformation than unoriented polymer chains in the matrix. During the process wherein the matrix deforms by elongation, the rubber particles also extract energy from the matrix in order to deform. It is thus clear that if no adhesion was present between the matrix and the rubber particles, the rubber particles would act as defects in the matrix and hence would not be able to contribute to the dissipation of energy. It should also be appreciated that a stiff rubber phase will need more energy to deform and therefore will assist the energy dissipation process. The rubber phase in propylene block copolymers is not cross-linked and resistance to deformation is derived from the flow properties of the chains. Because each chain is linked to many of its neighbors through entanglements, the longer the chain the more difficult it will disentangle and resist flow. By increasing the molecular weight in this phase, chain slippage through viscous flow can therefore be minimized. High molecular weight is also very important in the matrix polymer as chain slippage occurs in this phase as well. Although the matrix polymer is crystalline and consists of chain-folded lamellae that make up the spherulites, these spherulites can unravel and the chains line up and recrystallize to some extent in the direction of the applied stress to form the

load-bearing microfibrils. Low molecular weight polymer has a decreased tie-molecule content in the amorphous regions, resulting in low toughness because the crazed material can not form fibrils of sufficient toughness [4].

It should also be emphasized that the glass transition temperature of the rubber phase may never be higher than the temperature at which the polymer will be applied. Below the glass transition temperature of the rubber phase none of the described toughening mechanisms will apply, resulting in brittle failure of the product. When the stresses build up to levels where the microfibrils in a craze fail, a crack will start to propagate through the PP phase. More crazes are formed at the crack tip, which blunts the crack-tip by spreading the fracture energy over a larger volume in the matrix surrounding the crack-tip. This retards the crack propagation. When a crack grows into and through a rubber particle, the latter will stretch to a limit determined by the tensile properties of the rubber and the interface adhesive strength before cavitation (not debonding) occurs, all the while absorbing energy.

Another mechanism of dissipating energy is that of shear banding. When a stress is applied to a rigid matrix, stresses developed around stress concentrators such as rubber particles. These stresses are transmitted through the matrix to neighboring particles, which in turn transmit the stress to their immediate neighbors and so on. Because the stress field around a particle diminishes rapidly with distance, formation of shear bands depend strongly on the distance between particles. If the rubber particles are close enough for proper energy transfer to occur between them, the stress can be dispersed through a large volume of material and may account for up to 60 % of energy dissipation during fracture. These shear bands are regions of sheared polymer between neighboring rubber particles oriented at an angle of approximately 45° [1,2]. These shear bands, depending on the degree of orientation achieved, can stop the propagation of a craze, probably because their moduli in the loading direction are substantially increased relative to the surrounding unoriented matrix [2].

Each toughened system has a unique optimum rubber particle size and the toughening mechanism is only effective above the glass transition temperature of the rubber phase [5]. It should thus be clear from the broad description above that the development of

a new block copolymer is not as simple as the fairly straight-forward preparation of random copolymers where comonomer content is the primary concern determining properties. The ratios between the different phases, as well as their composition, are deemed more important at determining the properties of the block copolymers.

In order to determine the viability of replacing ethylene with 1-pentene in high impact block copolymers, a series of block copolymers was prepared in which the influence of molecular weight, homopolymer : copolymer ratios and comonomer content was studied.

## 9.2 EXPERIMENTAL

To a 1-litre stainless steel reactor, fitted with stirring and heating facilities and thoroughly flushed with nitrogen, was added 350 g of purified heptane which was heated to 80 °C. To the stirred solvent under a continuous nitrogen flow was added 10 ml of a 10 % solution of TEA in heptane and 2 ml of a 7 % solution of di-isopropyl dimethoxysilane in heptane. This mixture was stirred for 1 minute after which 0.1 g of a magnesium dichloride-supported titanium catalyst, prepared as described in Chapter 5, was added. Hydrogen was used as transfer agent for molecular weight manipulation. The reactor was sealed and the catalyst system stirred for 5 minutes during which time the polymerization sites were activated.

A specified amount of propylene was added at a rate of 20 g/min. and allowed to polymerize. After 30 minutes the reactor was depressurized and a further 0.1 g of the  $\text{TiCl}_4$  catalyst was added. Simultaneous flows of a fixed ratio of propylene and 1-pentene was started and kept constant until the specified amounts of materials were introduced. These components were left to copolymerize for a further 30 minutes after which the reactor was depressurized and the catalyst deactivated by the introduction of 100 ml iso-propanol. The slurry was filtered, washed with acetone, dried and the yield of block copolymer determined by weighing.

The 1-pentene content of the copolymers was determined on a Perkin Elmer FT-IR 1720X instrument on 0.3 mm thick compression moulded film samples prepared on a Graseby Specac press at 180°C. A calibration curve was obtained from standard melt-blended samples of polypropylene with known poly(1-pentene) content. The moderately strong peak at  $969\text{ cm}^{-1}$  in the spectrum of PP arises from coupling vibrations, while the rocking of the  $\text{CH}_3$  group at  $734\text{ cm}^{-1}$  was used in an in-house developed procedure to quantify the concentration of the propyl branch.

$^{13}\text{C}$  NMR analyses were done at 120°C on samples dissolved in *o*-dichlorobenzene on a Varian 400 MHz machine using a 90° pulse angle, a pulse width of 10, 25 000 scans and a 30 sec. delay. Composition was determined through the ratio between characteristic peaks of the different monomers making up the NMR spectrum of the

copolymer as fully described in Chapter 4. Basically the ratio between the peak areas of the branching -CH and that of the backbone carbons was determined and expressed as a percentage. Assignments were done making use of the literature where possible, combined with DEPT analyses and checked against the chemical shift assignments predicted by the additivity rules described by Grant and Paul [6].

Melt flow index (MFI) was determined according to ASTM D 1238, mechanical properties according to ASTM D 638 M and notched Izod impact strength according to ASTM 256.

Melting behavior was determined on a Perkin Elmer DSC-7 fitted with a TAC 7/PC instrument controller. The samples were heated from 50 to 200°C at 20°C/min, held at 200°C for 1 minute, cooled to 50°C at a rate of 20°C/min during which time the crystallization curve was recorded. At 50°C, the temperature was kept constant for 1 min after which the melting curve was recorded between 50 and 200°C at a heating rate of 10°C/min.

### 9.3 RESULTS AND DISCUSSION

Polymerization parameters for the preparation of the block copolymers investigated in this study are presented in Table 9.1.

**Table 9.1. Polymerization Parameters and Fundamental Properties of Propylene / 1-Pentene Block Copolymers**

Sample Number	C <sub>3</sub> (g)	C <sub>3</sub> : C <sub>5</sub> (g)	H <sub>2</sub> (mg)	Yield (g)	MFI (dg/min.)	1-Pentene (%)
1	100	0:50	20	83	70	12.5
2	50	50:50	20 + 20	150	69	13.8
3	50	50:50	20 + 20	121	110	21.1
4	50	75:25	20 + 20	131	130	8.8
5	50	25:75	20 + 20	132	158	51.8
6	40	55:55	20 + 20	94	112	14.2
7	40	30:80	20 + 20	85	175	36.5
8	80	40:30	20 + 20	104	110	13.4
9	60	45:45	20 + 20	88	80	18.9
10	60	70:20	20 + 20	102	98	5.2
11	60	20:70	20 + 20	83	112	37.2
12	50	50:50	-	39	2.2	3.1
13	50	75:25	-	65	1.2	2.6
14	50	25:75	-	35	4.5	16.5
15	40	55:55	-	50	5.0	8.2
16	40	30:80	-	32	1.1	6.5
17	80	40:30	-	37	1.5	2.9
18	60	45:45	-	37	1.7	5.8
19	60	70:20	-	76	1.0	1.9
20	60	20:70	-	34	0.6	8.3
21	50	25:75	-	30	1.1	16.3
22	40	30:80	-	46	2.1	8.8
23	60	45:45	-	54	1.8	3.7

Sample 1 was prepared by introducing all of the 1-pentene and all of the catalyst during the first half of the reaction. Then without venting, the full amount of propylene was introduced and the reaction left to continue for the full 60 minutes. Samples 2 to 11 were prepared by introducing half the amount of catalyst (0.1g) as well as 20 mg hydrogen followed by a specified amount of propylene and reacting for 30 minutes. After venting, the rest of the catalyst and another 20 mg hydrogen was added. This was followed by introduction of a specified mixture of propylene and 1-pentene and the reaction was left to continue for the full 60 minutes. Samples 12 to

20 were prepared in a similar way, but with the omission of the hydrogen addition step. Samples 21 to 23 were done by introducing 0.2 g of catalyst during the second part of the reaction in order to increase the total amount of copolymer prepared in the second phase.

The series of copolymers listed in Table 9.1 can be subdivided further according to the ratios of propylene and 1-pentene introduced during the two stages of the polymerization process. This resulted in subdivision of the polymers into low, medium and high 1-pentene content for the rubber phase as well as low, medium and high propylene for the rigid homopolymer matrix.

### 9.3.1 POLYMER YIELD - THE EFFECT OF HYDROGEN

The effect of hydrogen on the catalyst activity is immediately apparent. Contrary to what has sometimes been reported [7,8] a substantial increase in polymer yield as a result of an increased polymerization rate was observed in the presence of hydrogen. This was ascribed primarily to the regeneration of active sites following chain transfer with hydrogen at “dormant” 2,1-inserted sites [9,10,11] and the observation made in the literature that stereoregularity increased with hydrogen concentration [12]. This suggests that stereo-errors slow down the rate of chain propagation [13].

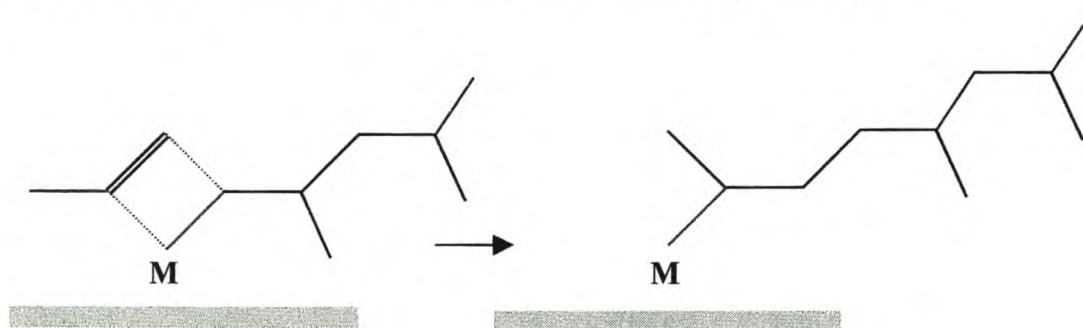


**Figure 9.2.** Active Site with Monomer Unit Co-ordinated and Subsequent Insertion such that a 2,1-Misinsertion will Occur, Leading to a Dormant, Sterically Hindered Site. The (\_\_\_\_), Metal/Carbon Bond (\_\_\_\_), inserted Monomer (\_\_\_\_)

It can be seen from Figure 9.2 that a regio-irregular 2,1-insertion between the metal center and the polymer chain renders the active site less accessible for another

(co)monomer molecule to co-ordinate with the metal before insertion. Hydrogen, being a small molecule can easily reach such a blocked active site and insert between the metal and the active polymer chain. This insertion detaches the chain from the metal center, leaving the site free to produce a new polymer chain. It was also suggested by Ross [14] that molecular hydrogen could create additional active centers, thus increasing the catalyst activity. This proposal was based on experimental data obtained using a  $\text{TiCl}_3 - \text{AlEt}_2\text{Cl}$  catalyst system.

### 9.3.2 POLYMER YIELD - THE EFFECT OF COMONOMER

The amount of comonomer introduced also has an effect on polymer yield. In Table 9.2 the yields from reactions in which equal amounts of homopolymer were produced are arranged according to the amount of 1-pentene introduced.

**Table 9.2. Effect of Introduced Comonomer on Copolymer Yield**

$\text{C}_3$ Introduced in First Phase (g)	Copolymer Yield (g)		
	Low 1-Pentene	Medium 1-Pentene	High 1-Pentene
50	131	120	132
40	-	94	85
60	102	88	83
50	65	39	35
40	-	50	32
60	76	37	34

Inspection reveals a general decrease in polymer yield with increased 1-pentene content. As was discussed in Chapter 5 it was observed during kinetic studies on *random* copolymerization of propylene with 1-pentene that catalyst activity increased at low 1-pentene concentrations and reached a maximum almost twice that of the homopolymer at 2.5 % 1-pentene content. At higher 1-pentene concentrations the activity dropped below that of the homopolymer. This phenomenon is known as the comonomer effect. The polymerization rate is enhanced by the introduction of small amounts of comonomer, which could arise from catalyst fragmentation, active site formation involving the comonomer, displacement of adsorbed complexes from active sites by the comonomer or by diffusion phenomena [15].



The contribution of the above to the process were not investigated, but it is believed that the results may best be explained through the comonomer diffusion model. As polymer forms around catalyst particles, the newly formed chains crystallize and diffusion of monomer to active sites becomes increasingly more difficult. It was previously observed that an increase in 1-pentene content in random propylene / 1-pentene copolymers leads to a decrease in density and copolymer crystallinity [16]. As diffusion occurs only through the amorphous material, decreased density will assist the diffusion of monomer to active sites, thereby increasing catalyst activity to levels higher than that displayed during propylene homopolymerization. There is however, a second effect acting concurrently with this rate enhancement effect which is derived from the reactivity ratios  $r_A$  and  $r_B$  of propylene and 1-pentene. 1-Pentene is between 2 and 5 times less active than propylene [17] so that an increase in 1-pentene content will reduce the overall activity from that displayed by pure propylene during homopolymerization purely by decreasing the statistical chances of polymerization of the more active propylene molecules. Maximum catalyst activity will therefore be reached at the 1-pentene concentration where the rate enhancement through increased monomer diffusion is more important than that of decreased activity displayed by the polymerization mixture at increased levels of 1-pentene.

The decay in propylene homopolymerization rate is mainly ascribed to chemical deactivation of active centers [18] and it was previously showed why monomer diffusion phenomena may be excluded [19,20]. However, by comparing the rates of decay observed during the propylene / 1-pentene copolymerization reaction, judged from the slopes of the rate / time curves shown in Figure 9.3 after maximum activity was reached, it can be seen that the low 1-pentene content copolymers exhibit a much faster decay than the high, 10% 1-pentene copolymer. This would be expected if monomer diffusion to the active sites becomes restricted. Less dense copolymer will allow easier diffusion of 1-pentene, resulting in longer-lasting activity.

As the block copolymers prepared in this study all contain 1-pentene at levels above 2.5 % (except for sample 19), the observed decrease in catalyst productivity was thus not unexpected.

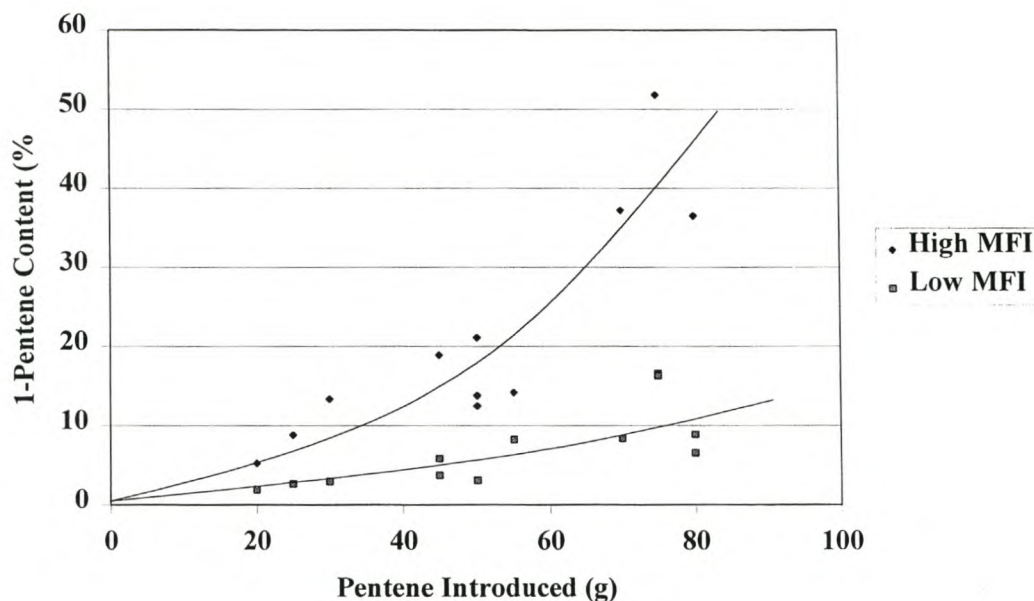


**Figure 9.3. Plot of 1-Pentene Introduced vs. Mole % 1-Pentene Found in the Copolymer. High Molecular Weight Polymers Contain Less 1-Pentene**

The ability of hydrogen to increase the catalyst productivity by “liberating” dormant active sites was described above. In Figure 9.3 it can be seen that the 1-pentene content of high MFI (low molecular weight) copolymers are higher than that of low MFI copolymers. From this observation it seems that in the presence of hydrogen, the active sites are also made more accessible for larger molecules such as 1-pentene. It is well-known that heterogeneous Ziegler-Natta catalysts contain mixtures of active sites which lead to different stereospecificities, molecular weights and copolymer composition [21]. This derives from the differences in geometry and electronic environments around the different active sites [15]. It is possible that molecular hydrogen creates additional active sites [14] since some of the sites polymerize 1-pentene at a higher rate than active sites produced in the absence of hydrogen.

### 9.3.3 MECHANICAL PROPERTIES

Results of the mechanical and thermal analyses are presented in Table 9.3.

**Table 9.3. Mechanical and Thermal Properties of Propylene / 1-Pentene Block Copolymers**

Sample Number	Tensile (MPa)	Elong. (%)	Modulus (MPa)	Impact (kJ.m <sup>-2</sup> )	Hard	$\Delta H_f$ (J/g)	T <sub>m</sub> <sup>High T</sup> (°C)	T <sub>m</sub> <sup>Low T</sup> (°C)
1	14.9	35.8	535	1.9	57	25	-	145
2	18.0	36.0	728	5.6	58	44	<b>161</b>	<b>153</b>
3	20.1	42.3	603	2.7	57	64	161	<b>157</b>
4	21.2	42.0	667	2.2	65	61	162	<b>155/-</b>
5	15.7	41.3	530	3.2	53	55	162	<b>157</b>
6	16.4	38.8	530	2.8	55	40	<b>162</b>	157/144
7	11.5	40.7	398	4.4	51	40	<b>163</b>	<b>158</b>
8	19.2	39.3	678	2.7	64	33	<b>163</b>	157/144
9	15.1	45.7	416	3.5	54	60	<b>161</b>	<b>156</b>
10	25.5	34.7	987	2.2	65	61	<b>162</b>	<b>156/145</b>
11	13.1	39.4	463	4.1	52	40	<b>163</b>	<b>159</b>
12	29.8	43.4	962	9.2	63	72	<b>157</b>	139
13	37.4	44.5	1058	6.6	66	81	154	<b>140</b>
14	20.9	46.8	675	27.7	55	48	<b>160</b>	-
15	22.3	43.0	751	7.9	55	42	159	<b>139</b>
16	27.5	44.8	852	10.8	62	65	<b>159</b>	141
17	35.7	49.5	898	8.7	69	75	<b>160</b>	-
18	23.7	51.6	581	13.1	57	28	160	<b>139</b>
19	36.2	48.6	875	4.5	70	74	<b>156</b>	144
20	27.8	57.6	603	12.0	65	57	<b>160</b>	-
21	21.8	54.5	573	11.9	57	44	<b>160</b>	142
22	20.3	51.0	544	9.2	56	39	<b>159</b>	142
23	26.2	49.1	681	6.2	61	59	<b>159</b>	142

\* Main peak in bold

Judged against comonomer content, no discrimination regarding tensile strength, elongation and Young's modulus could be observed between the copolymers in the low- and high molecular weight series. Impact strength, however, shows a substantial difference. The low molecular weight copolymers presented in the first series, even at high comonomer content, has low impact strength as compared to the high molecular weight copolymers listed in the second series. Tensile strength is generally lower, but compared to the random copolymers it seems that molecular weight has a much

greater influence on impact strength of these copolymers, probably due to the different strengthening mechanisms.

#### 9.3.4 THERMAL PROPERTIES

During crystallization under a certain set of conditions, homogeneous semi-crystalline polymers chain-fold to form lamellae with a distribution of thicknesses, which melt at different temperatures [22] to display a particularly shaped melting curve. The melting curve for real polymers is not sharp and this reflects the molecular weight distribution of a polymer [23]. The heat (energy) necessary to completely melt the crystalline material is directly related to the area under the DSC curve. The peak in the melting curve appears at the temperature where crystallites of a specific size are the most abundant under the crystallization conditions applied. The presence of low levels of defects other than stereo errors, resulting from comonomer units in an otherwise regular chain, will impede the extent to which crystallization will occur by decreasing the sequence length of crystallizable units that can only crystallize at lower temperatures. Comonomer units may also sometimes be incorporated in the lattice as a defect [23, 24]. Because the comonomer units hinder crystallization, the comonomer distribution leads to a crystallite size distribution which directly relates to the melting temperature distribution [25] *i.e.*, the more imperfections, the broader the melting peak. Although the melting peak height can be decreased and the melting range be broadened, the peak will still appear at the same temperature because below a certain maximum comonomer content, the average separation of co-units will be larger than the lamellar thickness prescribed by the crystallization conditions.

The description above applies to a real polymer system having intramolecular homogeneity such as found in truly random copolymers containing low levels of uncrystallizable comonomer units and long sequences of the crystallizable units. However, when the amount of uncrystallizable comonomer increases, the sequence lengths of the crystallizable units decreases. Because the crystal thickness is determined by the sequence length of the crystallizable units, as well as the crystallization conditions [23], thicker crystals become less abundant because less chains have sequences long enough to either span the high melting crystal thickness or to crystallize at the temperature where the thicker crystals are formed. Therefore,

as the comonomer content increases above a critical value, the amount of thinner [24], lower melting crystallites increase [25] at the expense of the thicker, high-melting crystallites, resulting in a decrease in the melting temperature.

Apart from the difference in their molecular weights, a homopolymer or random copolymer is considered homogeneous and, statistically, there are no differences within and between these polymer molecules. If the crystallizable sequence length distribution in these (co)polymers are single peaked, their DSC curves may be single peaked. Multiple peaked DSC curves may be an indication of heterogeneity within and between different molecules [25]. Multiple peaks are therefore an indication of distinctly different crystallite size distributions if recrystallization or transition to a different nucleation mechanism can be excluded. By crystallizing a heterogeneous mixture of molten polymer chains, molecular fractionation is known to occur whereby molecules of a particular length, amount of branching, or degree of regularity tend to become concentrated at specific locations within the overall structure [26]. Because branches are not easily incorporated into the crystal lattice, the average separation between adjacent branches sets an approximate upper limit for the lamellar thickness and consequently on the melting temperature. Chains containing these uncrystallizable branches will therefore be concentrated between lamellae and crystallizable sequences in the crystal lattice. In a heterogeneous mixture consisting of two distinctly different components such as long crystallizable sequences of homopolymer or copolymer chains containing a small amount of comonomer on the one hand and copolymer chains containing large amounts of uncrystallizable comonomer on the other, three basic phases may be observed during crystallization under set conditions. First, the thick, high-melting homopolymer crystallites containing the longest and most crystallizable units will form according to its molecular weight and sequence length distributions, concentrating the other components present in the melt in the interlamellar regions. This material will then crystallize to form the thinner, lower-melting crystallites from the shorter crystallizable sequences present in the copolymer. The material present in chain-folds and in the interlamellar regions, which could not crystallize at the lower temperature of the cooling cycle, even if it is crystallizable, forms part of the amorphous phase. The cooling curve obtained from a DSC scan will show a high temperature event when the thicker crystallites formed and a low temperature event where the less

perfect, thinner crystallites formed, provided that two substantially different crystallite size distributions were obtained during crystallization. On melting a double peaked DSC trace will be obtained, each peak of which correspond to the crystallization peaks.

The method followed for the preparation of the copolymers produced in this study generated a complex mixture of different homopolymers, random copolymers (containing different amounts of comonomer) and block copolymers with different sequence lengths of homopolymer and random copolymer. The composition of the copolymer can be related directly to the sequence and amounts of propylene and 1-pentene introduced during the polymerization reactions.

Sample 1 was prepared by first homopolymerizing 1-pentene and introducing propylene during a second phase to produce the propylene / 1-pentene copolymer. During the transition from 1-pentene to the propylene/1-pentene mixture, some poly(1-pentene) chains are attached to the active metal centers. When propylene is introduced, it is randomly incorporated into these chains together with 1-pentene until chain transfer occurs and the chain drops off the active metal center. These chains are the only true block copolymers formed during the reaction and the amount formed depends on the total amount of active sites participating in the reaction at the time the second monomer is introduced. The poly(1-pentene) phase does not show a melting peak under the conditions employed to obtain the DSC traces because it can not crystallize under these conditions. The chains that can crystallize are the propylene sequences in the propylene / 1-pentene copolymer present in the copolymer as well as those in the random copolymer which contain runs of crystallizable propylene units, the lengths of which are dependent on the 1-pentene content. The crystallizable sequence length distribution will determine crystal thickness distribution, and consequently the melting temperature distribution. For this specific copolymer a single melting peak at 145°C was obtained, indicating that a single crystallite size distribution was obtained. Heat of fusion is low because firstly, a large amount of material, i.e. the poly(1-pentene) homopolymer fraction, does not contribute to the energy uptake during melting and secondly, judged from the low melting peak temperature, the crystals that formed are thin and do not require much energy to melt.

As sample 1 consists mainly of non-rigid phases, tensile strength and modulus are low and due to the rubbery nature of the polymer, the value for impact strength is merely the energy necessary to bend the sample enough to let the impact hammer pass.

The rest of the copolymers were prepared by firstly homopolymerizing propylene and copolymerizing propylene with 1-pentene during the second phase of the reaction. Three types of polymer *viz.* (a) propylene homopolymer, (b) propylene homo-propylene/1-pentene random block copolymer and (c) propylene / 1-pentene random copolymer can be imagined to form under the procedure employed. Not surprisingly, these copolymers, being heterogeneous mixtures of the different polymers, exhibit multiple DSC peaks. Although the melting peaks were not always properly resolved, distinction could in most cases be made with a reasonable degree of accuracy. Even in cases where the low-temperature melting peak was very diffuse, the crystallization peaks were easily identifiable. In the low molecular weight series, up to three crystallization peaks could be identified in some of the samples, specifically in those containing low amounts of 1-pentene. The peak maxima for this series appear at approximately 162°C, 157°C and 145°C, indicating three distinctively different crystallite size distributions. The peak maxima may be attributed to the presence of propylene homopolymer, a random propylene / 1-pentene copolymer with propylene run lengths only slightly shorter than the polypropylene crystallite thickness and another propylene 1-pentene copolymer with even shorter propylene sequences. In the high molecular weight series, no more than two crystallization peaks (at about 160°C and 141°C) were observed, indicating the presence of (at least two) distinctly different crystallizable phases. These two melting temperatures were also observed for the propylene / 1-pentene random copolymers discussed in Chapter 8. In Chapter 8 it was shown that the propylene homopolymer had a melting temperature of 166°C, and for the copolymers, melting temperature rapidly decreased with increased 1-pentene content to values down to 142°C. The high and low melting peaks in the low molecular weight series differ by about the same amount as the corresponding peaks in the high molecular weight series, indicating approximately similar types of (co) polymer responsible for producing the different crystallite distributions. However, in the low molecular weight series a peak, about 4 to 5°C lower than observed for the propylene homopolymer peak is present in all the spectra. Close inspection of the

DSC crystallization and melting curves and comparison with 1-pentene content revealed that 1-pentene content alone did not affect the ratio between the 162°C and 157°C peak heights nearly as much as it did the 162°C / 145°C ratio. The position of this high temperature peak indicates that the lamellar thickness of the crystallites responsible for producing it is only slightly less than the lamellae of the propylene homopolymer. With hydrogen present it was seen that the polymer yield and 1-pentene content was higher than when no hydrogen was used. This finding can be explained by considering that additional active sites are produced in the presence of hydrogen [14]. In order to produce higher 1-pentene content copolymer chains it seems that, at least some of these sites are sufficiently open and thus assist 1-pentene incorporation.

A slightly higher melting temperature of the low molecular weight polypropylene homopolymer can be observed. According to Koika *et al.* [11], who investigated 1-butene polymerizations in the presence of hydrogen, this increase may be attributed to a decrease in stereo irregularities with increasing hydrogen content. This increase in stereospecificity was also observed by Chadwick *et al.* [13] during their investigation of propylene polymerization in the presence of hydrogen.

### **9.3.5 RELATIONSHIP BETWEEN IMPACT STRENGTH AND CRYSTALLIZATION CURVE PROFILE**

In both the low and high molecular weight series, a relationship between the ratio of the polypropylene and copolymer crystallization peaks and impact strength was observed. The highest impact strengths are displayed by copolymers having a single peaked DSC crystallization curve and a high 1-pentene content. By considering the amount and method of introduction of the monomers, the constituents of a high impact block copolymer which has this type of crystallization curve can be recognized. The single peak is derived mainly from crystallization of the homopolymer as well as low 1-pentene content copolymer while the high 1-pentene content propylene / 1-pentene rubber phase will not be seen in the DSC trace. The low temperature crystallization peak results from crystallizable propylene / 1-pentene



copolymer, which does not contribute to the rubber phase necessary to obtain high impact strength.

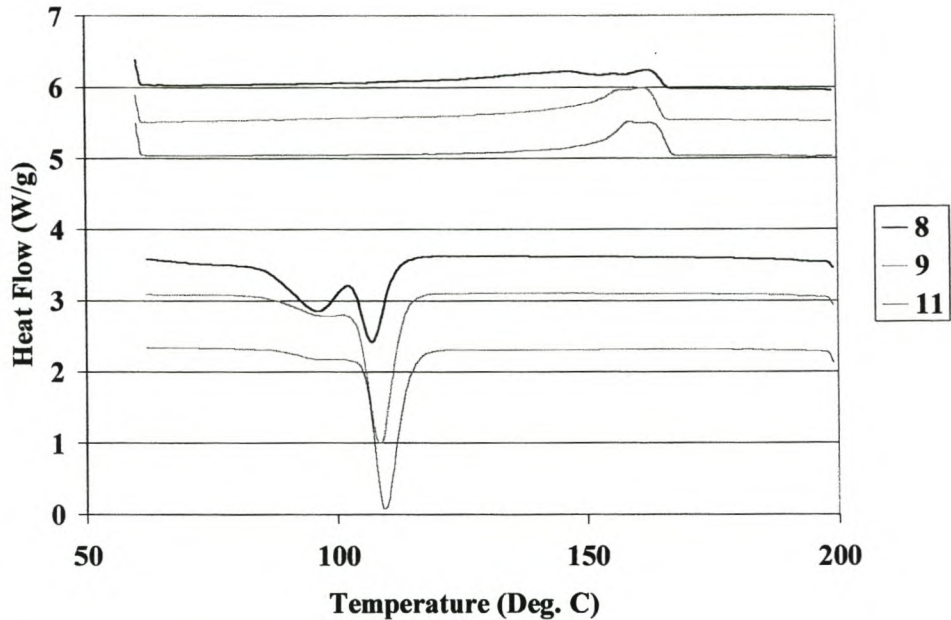


**Figure 9.4. Comparison of Melting- and Crystallization Curves of Low Molecular Weight Copolymers with Different Impact Properties**

This effect is illustrated in Figures 9.4 and 9.5 where melting and crystallization peaks (top and bottom sets respectively) of copolymers are arranged from low to high impact strength. In both series, the crystallization of the propylene / 1-pentene copolymer can clearly be observed for the low-impact samples (8 and 19) while the high impact copolymers (11 and 20) display only a very small low-temperature crystallization peak. It can thus be realized that the polymers having the highest impact strength contains a rubber phase having very little or no crystallinity.

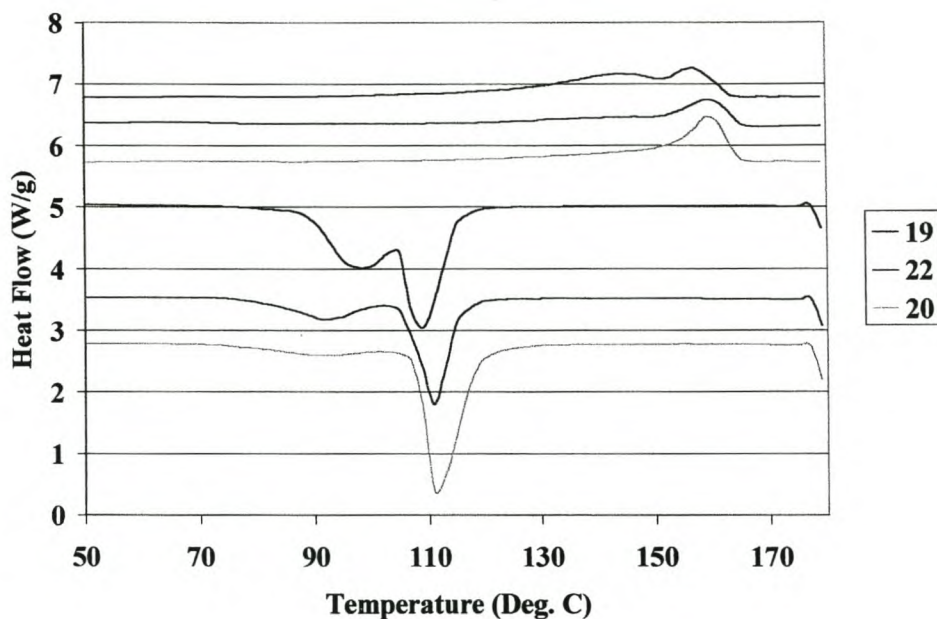


**Figure 9.5. Comparison of Melting- and Crystallization Curves of High Molecular Weight Copolymers with Different Impact Properties**

In general, it can thus be anticipated that an increase in 1-pentene content in the propylene / 1-pentene copolymer phase will result in increased rubberiness of this phase, with a consequent increase in impact strength. It was mentioned earlier, that each toughened system has a unique, optimum rubber particle size. There should therefore, exist a limit in 1-pentene content beyond which impact strength decreases. It is, however, not possible to determine this limit from the thermal properties of these copolymers.

Because the amount of crystalline material in the copolymers has an effect on the amount of heat necessary to melt the polymers, fusion enthalpy was investigated as a means of finding a correlation with the impact properties. No satisfactory correlation between mechanical properties and fusion enthalpy was, however, observed.

### 9.3.6 FRACTURE SURFACES OF PP/1-PENTENE BLOCK COPOLYMERS

In the high molecular weight series, the fracture surfaces of copolymers with different mechanical properties were investigated. In Figure 9.6, the break surface of sample 22 is shown. Impact strength of this polymer is relatively high, but the modulus is low. This soft matrix will therefore flow easily under stress as can be seen from photos (a) and (b) showing the fracture surfaces.

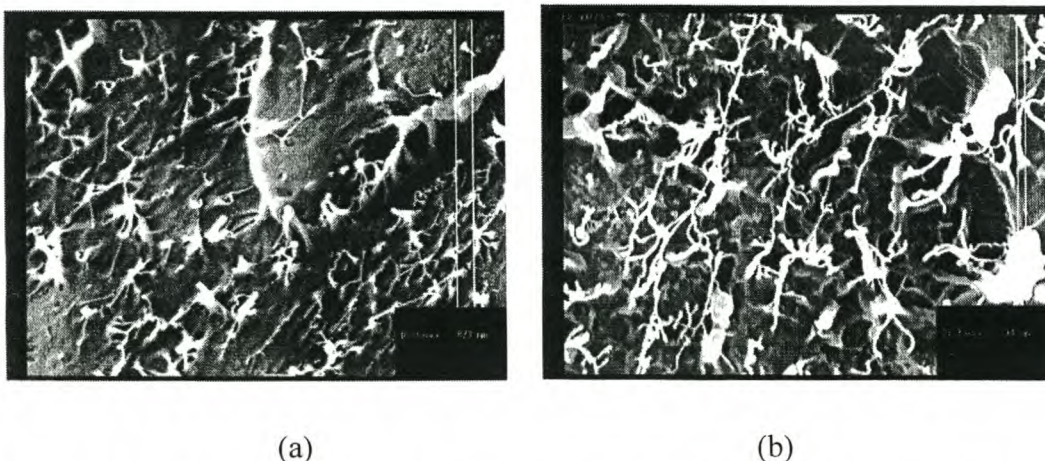


**Figure 9.6. Fracture Surface of Low Impact Strength Block Copolymer**

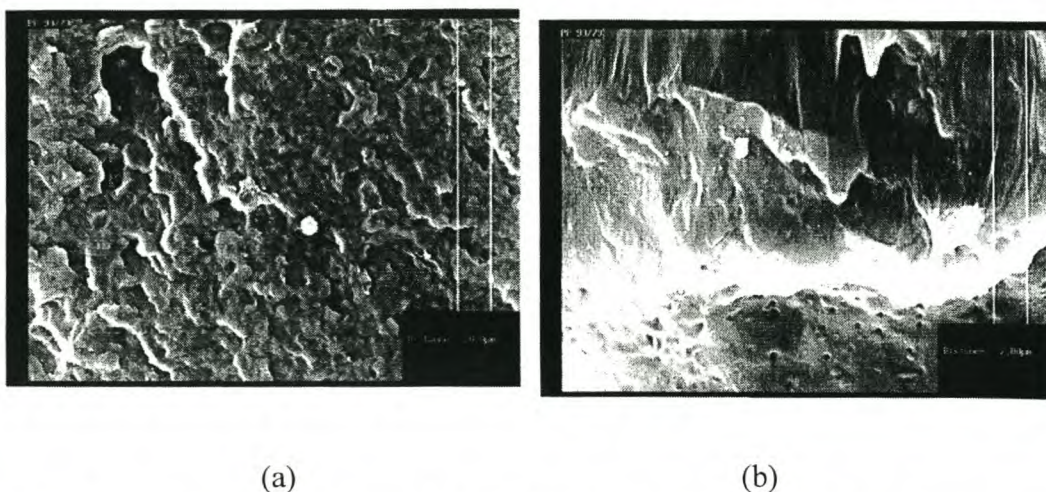
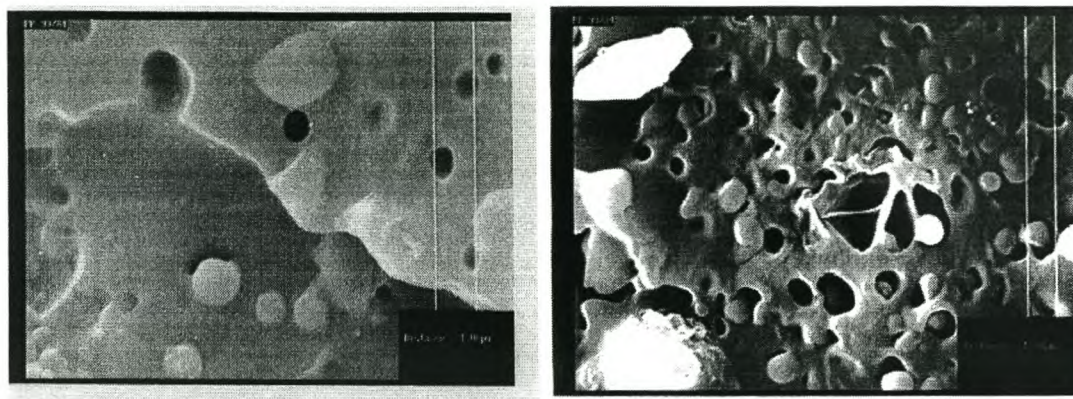


**Figure 9.7. Fracture Surface of Low Impact Strength Block Copolymer**

In Figure 9.7 typical features observed for sample 19 are shown. Impact strength and 1-pentene content of this copolymer is low and it can be seen from the smooth surfaces between the flaky features shown in photo (a) that this sample failed in a brittle manner. Some viscous flow was observed, but it was not as extensive as that of

the soft sample (Figure 9.6). It can further be seen from photo (b) that the rubber inclusions are spaced far apart and are less than 1  $\mu\text{m}$  across.



(a)

(b)

**Figure 9.8. Fracture Surface of High Impact Strength Block Copolymer**

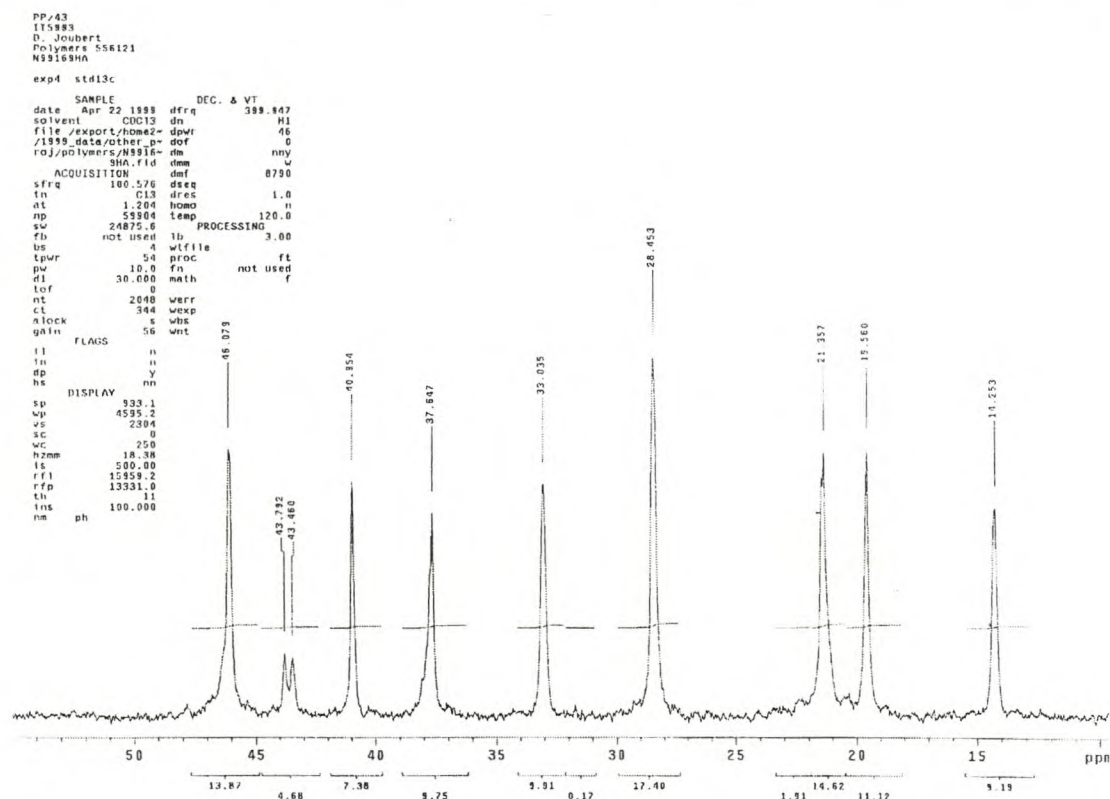
The fracture surface of a block copolymer having higher impact strength (sample 16) is shown in Figure 9.8. This picture shows very different features. The propylene / 1-pentene rubber particles can clearly be seen in the hard matrix. Particle sizes are very similar having diameter in the 1  $\mu\text{m}$  range. Some debonding between the rubber and the matrix can be observed although the strength of the interface seems to be sufficient as judged from the extensive deformation of the matrix [photo (b)] and only partial debonding of some of the rubber particles.

### 9.3.7 MICROSTRUCTURE

$^{13}\text{C}$  NMR analyses on some of the low molecular weight series was performed. A spectrum of sample 11 is shown in Figure 9.9 and peak assignments (using the Grant and Paul additivity rules [6]) are shown in Table 9.4 (see Chapter 4 for details). Peaks are numbered from left to right and to prevent confusion, split peaks such as the one at 43 to 44 ppm in Figure 9.9 are considered single.

**Table 9.4. Observed and Calculated Chemical Shifts of a Propylene / 1-Pentene Block Copolymer.**

Line	Carbon	Sequence	Observed	Calculated
1	CH <sub>2</sub>	5335, 3335, 3333	46.05	45.47
2	CH <sub>2</sub>	5353, 3355, 5355, 3353,	43.44	42.9, 42.96, 43.05
3	CH <sub>2</sub>	5555, 3553	40.93	40.39, 40.51
4	Branch CH <sub>2</sub>	353, 355, 555	38.08	38.08, 38.14, 38.2
5	CH	5	33.10	31.93
6	CH	3	28.43	28.11
7	CH <sub>3</sub>	333, 335, 535	21.39	22.2
8	Branch CH <sub>2</sub>	5	19.68	20.35
9	CH <sub>3</sub>	555	14.26	14.5

**Figure 9.9. NMR Spectrum of Propylene / 1-Pentene Block Copolymer**

From the reaction kinetics of propylene homopolymerization about 85% of the propylene introduced is converted to polymer in 30 minutes. From this, the amount of homopolymer in the block copolymer formed during the first phase of the reaction can be estimated. This amount was subtracted from the intensity of the -CH<sub>3</sub> peak situated at about 46 ppm. The number average sequence lengths for runs of propylene (3) and 1-pentene (5) in the copolymers formed during the second phase was

calculated as a function of the concentration of dyad sequence distributions according to equations 9.1 and 9.2 [27]:

$$\tilde{n}_3 = (2N_{33} + N_{35}) / N_{35} \quad (9.1)$$

$$\tilde{n}_5 = (2N_{55} + N_{35}) / N_{35} \quad (9.2)$$

where  $N_{33} = I_1$ ,  $N_{35} = I_2$  and  $N_{55} = I_3$  and  $I_x$  is the intensity of line x. In most cases, peaks were too wide to obtain resolution of the different peak sets such as CH<sub>2</sub> at the triad and tetrad level but this does not affect the calculation of sequence lengths. Number average sequence lengths for propylene and 1-pentene and the sequence length ratios ( $\tilde{n}_3 / \tilde{n}_5$ ) are shown (Table 9.5).

**Table 9.5. Propylene and 1-Pentene Sequence Lengths**

Sample Number	% PP Homopolymer	$\tilde{n}_3$ Propylene	$\tilde{n}_5$ 1-Pentene	$\tilde{n}_3 / \tilde{n}_5$
4	32.4	8.88	1.46	6.08
5	32.2	4.69	6.62	0.708
6	36.2	6.16	1.62	3.8
7	40.0	3.52	2.78	1.27
9	58.0	3.93	1.94	2.03
11	61.4	3.29	4.15	0.8

Although the disappearance of the low-temperature crystallization peaks on the DSC traces could be linked to the observed increase in impact strength, the effect could not be quantified. However, impact strength, tensile strength, hardness and modulus was found to be related to this sequence length ratio ( $\tilde{n}_3 / \tilde{n}_5$ ) which can be quantified. In Figure 9.10 such a correlation between the monomer sequence length ratios and impact strength is depicted. It can be seen that an optimum sequence length ratio between propylene and 1-pentene of about 1.2 exist and that long propylene or 1-pentene sequences result in low impact strength.

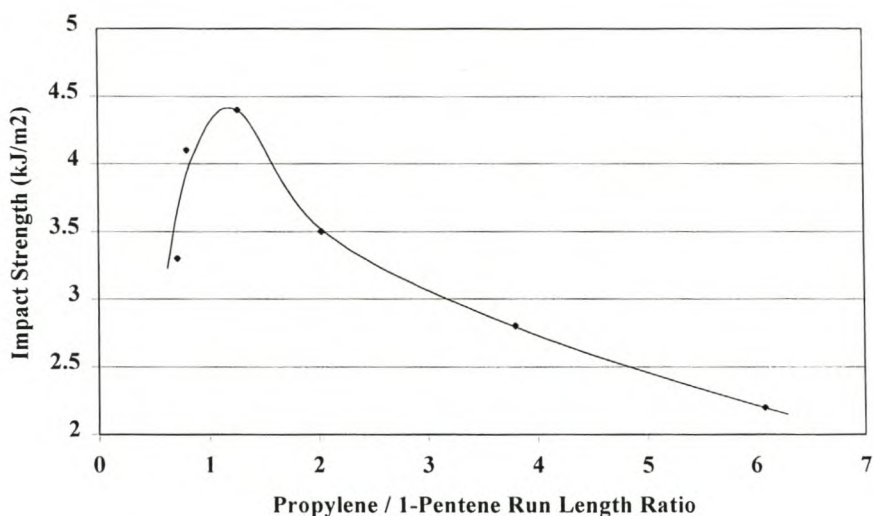


**Figure 9.10. Dependence of Impact Strength on the Number Average Propylene : 1-Pentene Sequence Length Ratio.**

Modulus, tensile strength and hardness exhibit this same dependence on the sequence length ratio, but as expected, they go through a minimum at a ratio of about 1.2. In Table 9.6 the mechanical properties of some of the copolymers are related to the propylene / 1-pentene sequence length ratio.

**Table 9.6. Mechanical Properties as Related to Propylene / 1-Pentene Sequence Length Ratio**

Sample Number	$\bar{n}_3 / \bar{n}_5$	Impact Strength (kJ/m <sup>2</sup> )	Modulus (MPa)	Tensile Strength (MPa)	Hardness
4	6.08	2.2	667	21.2	65
5	0.708	3.2	530	15.7	53
6	3.8	2.8	530	16.4	55
7	1.27	4.4	398	11.5	51
9	2.03	3.5	416	15.1	54
11	0.8	4.1	463	13.1	52

For the random copolymers, all properties could be related to comonomer content. For the block copolymers, however, even though a general trend with 1-pentene content exists, total 1-pentene content was found to be of lesser importance.

## 9.4 CONCLUSIONS

An increase in catalyst activity resulting from the presence of hydrogen was observed. In addition, it was found that the amount of 1-pentene incorporated in the copolymer, as well as the copolymer yields, were higher in the presence of hydrogen than when the reaction was carried out in its absence.

Although a general increase in impact strength with increased 1-pentene content was observed, the properties of block copolymers were not related directly to overall 1-pentene content as can be done with random copolymers. This is mainly associated with the heterogeneity of the copolymer which consists of propylene homopolymer, propylene / 1-pentene copolymer and true block copolymer containing propylene as first block and propylene / 1-pentene random copolymer as second block. Mechanical properties are related to the ratio and microstructure of these different phases.

By using DSC it was possible to identify different crystalline phases due to the differences in their crystallization kinetics. A connection between the low-temperature crystallization peak and impact strength was observed. It was found that the presence of the low-temperature peak resulting from crystallizable propylene / 1-pentene copolymer was undesirable if high impact strength is required. A decrease in the size of this peak at increasing 1-pentene content shows that the propylene / 1-pentene phase is less crystalline and thus more rubbery. This rubbery copolymer is incompatible with the crystalline matrix and therefore is separated as a different phase, which is necessary for the preparation of high impact block copolymers. It was however, not possible to quantify the extent to which the intensity of this peak affected mechanical properties. The possibility of using heat of fusion was investigated but no satisfactory relationship was found.

The microstructure of these copolymers can best be analyzed by means of  $^{13}\text{C}$  NMR spectroscopy. These copolymers were prepared in two steps, the first of which was the preparation of the polypropylene homopolymer. By determining the amount of polypropylene formed during the first phase, the amount of propylene / 1-pentene copolymer can be determined from the total yield by difference. This amount of



copolymer was used to determine the number average sequence lengths of propylene and 1-pentene units in the chains. It was found that the ratio between the propylene and 1-pentene sequence lengths could be related quantitatively to impact strength, modulus, hardness and tensile strength of the polymers investigated. The correlation between mechanical properties and sequence length discovered for the propylene / 1-pentene block copolymers now makes it possible to quantify the effect of microstructure on mechanical properties for these copolymers.

## 9.5 REFERENCES

1. Young R.J., *Strength and Toughness in Comprehensive Polymer Science*, Sir Allen G, Chairman Ed. Board, Pergamon Press, Oxford, **2** (15), 511 (1989)
2. Kambour P.P., *Crazing in Encyclopedia of Polymer Science and Engineering*, Kroschwitz J.I., John Wiley & Sons, New York, **4**, 299 (1988)
3. Kulich D.M., Kelley P.D., Pace J.E., *Acrylonitrile-Butadiene-Styrene Polymers in Encyclopedia of Polymer Science and Engineering*, Kroschwitz J.I., John Wiley & Sons, New York, **1**, 388 (1988)
4. Channell A.D., Clutton E.Q., *Polymer*, **33**, 19, 4112 (1992)
5. Seymour R.B., *Origin and Early Development of Rubber-Toughened Plastics in Rubber-Toughened Plastics*, Riew C.K., Ed., Am. Chem. Soc., Washington, (1), 3 (1989)
6. Grant D.M., Paul E.G., *J. Am. Chem. Soc.*, **86**, 2984 (1964)
7. Haward R.N., Roper A.N., Fletcher K.L., *Polymer*, **14**, 365 (1973)
8. Tait P.J.T., Watkins N.D., *Monalkene Polymerization: Mechanisms*, in *Comprehensive Polymer Science*, Sir Allen G, Chairman Ed. Board, Pergamon Press, Oxford, **4** (2), 533 (1989)
9. Chadwick J.C., Miedema A., Sudmeijer O., *Macromol. Chem. Phys.*, **195**, 167 (1994)
10. Chadwick J.C., Kessel G.M.M., Sudmeijer O., *Macromol. Chem. Phys.*, **196**, 1431 (1995)
11. Koika M., Mizuno A., Tsutsui T., Kashiwa N., *1-Butene Polymerization with Ethylene bis(1-Indenyl) Zirconium Dichloride and MAO Catalyst System*, Am. Chem. Soc., **5**, 72 (1992)
12. Busico V., Cipullo R., Chadwick J.C., Modder J.F., *Macromolecules*, **27**, 7538 (1994)
13. Chadwick J.C., Morini G., Albizzati E., Balbontin G., Mingozi I., Cristofori A., Sudmeijer O., Kessel G.M.M., *Macromol. Chem. Phys.*, **197** (8), 2501 (1996)
14. Ross J.F., *J. Polym. Sci.*, **22**, 2255 (1984)

15. Tait P.J.T., Berry I.G., *Monalkene Polymerization: Copolymerization*, in *Comprehensive Polymer Science*, Sir Allen G, Chairman Ed. Board, Pergamon Press, Oxford, **4** (4), 575 (1989)
16. Tincul I., Joubert D.J., A.H. Potgieter *American Chemical Society, 1998 fall Meeting Proceedings*, Boston, 22 August (1998)
17. Kissin Y.V., *Principal Kinetic Parameters for Olefin Homo- and Copolymerization in Isospecific Polymerization of Olefins with Heterogeneous Ziegler-Natta Catalysts*, Springer-Verlag, New York, (I-5), 67 (1985)
18. Barbe P.C., Cecchin G., Noristi L., *The Catalytic System Ti-Complex/MgCl<sub>2</sub> in Adv. Polym. Sci.*, Springer-Verlag, Berlin, 1, (1987)
19. Keii T., *Makromol. Chem.*, **183**, 2285 (1982)
20. Goodall B.L., *MMI Press Symp. Ser.*, **4**, 355 (1983)
21. Krentsel B.A., Kissin Y.V., Kleiner V.J., Stotskaya L.L., *Copolymers of Ethylene and Higher  $\alpha$ -Olefins in Polymers and Copolymers of Higher  $\alpha$ -Olefins*, Carl Hanser Verlag, Munich, (8), 243 (1997)
22. Hingman R., Rieger J., Kersting M., *Macromolecules*, **28**, 3801 (1995)
23. Mandelkern L., *Crystallization and Melting in Comprehensive Polymer Science*, Sir Allen G, Chairman Ed. Board, Pergamon Press, Oxford, **2** (11), 363 (1989)
24. Fatou J.G., *Crystallization Kinetics*, in *Encyclopedia of Polymer Science and Engineering*, Kroschwitz J.I., John Wiley & Sons, New York, Suppl. Vol., 231 (1988)
25. Mathot V.B.F., *The Crystallization and Melting Region in Calorimetry and Thermal Analysis of Polymers*, Mathot V.B.F., Ed., Carl Hanser Verlag, Munich, **9**, 231 (1994)
26. Vaughan A.S., Bassett D.C., *Crystallization and Morphology in Comprehensive Polymer Science*, Sir Allen G, Chairman Ed. Board, Pergamon Press, Oxford, **2** (12), 415 (1989)
27. Herbert I.R., *Statistical Analysis of Copolymer Sequence Distribution in NMR Spectroscopy of Polymers*, Ibbett R.N., Ed., Chapman & Hall, London, (2), 50 (1993)